

Drought-Induced Mortality in *Pinus halepensis* Planted Forests: A Study on Several Spatial Scales

**Thesis submitted in partial fulfillment of the requirements
for the degree of "DOCTOR OF PHILOSOPHY"**

by

Michael Dorman

**Submitted to the Senate of
Ben-Gurion University of the Negev**

November 2014

Beer-Sheva

Drought-Induced Mortality in *Pinus halepensis* Planted Forests: A Study on Several Spatial Scales

**Thesis submitted in partial fulfillment of the requirements
for the degree of "DOCTOR OF PHILOSOPHY"**

by

Michael Dorman

**Submitted to the Senate of
Ben-Gurion University of the Negev**

November 2014

Beer-Sheva

Drought-Induced Mortality in *Pinus halepensis* Planted Forests: A Study on Several Spatial Scales

**Thesis submitted in partial fulfillment of the requirements
for the degree of "DOCTOR OF PHILOSOPHY"**

by

Michael Dorman

Submitted to the Senate of

Ben-Gurion University of the Negev

Approved by the supervisors _____

Approved by the Dean of the Kreitman School of Advanced
Graduate Studies _____

November 2014

Beer-Sheva

This work was carried out under the supervision of:

Prof. Tal Svoray and Prof. Avi Perevolotsky

In the Department of Geography and Environmental Development,

Faculty of Humanities and Social Sciences

Declaration

I, Michael Dorman, whose signature appears below, hereby declare that I have written this Thesis by myself, except for the help and guidance offered by my Thesis Advisors.

The scientific materials included in this Thesis are products of my own research, culled from the period during which I was a research student.

Date: _____ Student's name: _____

Signature: _____

Acknowledgements

First and foremost, I would like to sincerely thank my supervisors – Tal Svoray and Avi Perevolotsky. Their help, guidance and advice have been indispensable for completing the study, as well as shaped my understanding and point of view in the fields of GIS, remote sensing and forest ecology. I wish to thank Dimitrios Sarris, for introducing me to the fascinating world of dendrochronology and sharing his expertise, from basic concepts to field work methodology. I would like to thank Yitzhak Moshe for providing most valuable observations and guidance concerning tree mortality in southern Israel, based on his vast field experience.

I would like to acknowledge Ira Mor, Yagil Osem, Efrat Sheffer, Gil Siaki, Shmuel Sprintsin, Ronen Talmor, Israel Tauber and Chanoch Zoref for providing helpful information regarding Israel's planted forests, and Gabriel Schiller – for the fruitful discussions on the subject of forestry in Israel and general advice. I thank Natalya Panov for assistance with satellite imagery processing, and Chris Briggs, Shaul Krakover and Hillary Voet for advice regarding statistical analysis. I thank David Brand and the Jewish National Fund (JNF), who willingly provided forest GIS layers and purchased the necessary equipment and software for the dendrochronological analysis. I thank Talia Horovitz and the Israel Meteorological Service for providing climatic data for the study. I express my gratitude to Ezra Ben-Moshe, Arnon Cooper, Or Livni, Yosi Moshe, Yoni Waitz and Adam Wattenberg for their help and company during field work. Many thanks go to the fellow students at the GIS lab at Ben-Gurion University of the Negev – Shai, Inbar, Ofir, Leilah, Dudi, Hodaya and Galia – for their good friendship and support.

This study was supported by a grant from the Chief Scientist of the Israeli Ministry of Agriculture and Rural Development and the JNF. The financial support from the Faculty of Humanities and Social Sciences at the Ben-Gurion University of

the Negev and the René Karshon Foundation are also acknowledged.

Last but not least, I thank my wife Hila for the unconditional support and encouragement.

Table of Contents

1 Abstract *X*

 1.1 Introduction *X*

 1.2 Methods *XI*

 1.3 Results *XII*

 1.4 Discussion *XIV*

2 General introduction *I*

 2.1 Climate change and forest mortality *I*

 2.2 Main directions in current research *2*

 2.3 The research approach and its potential advantages *3*

 2.4 The relation between chapters *6*

3 Results *9*

 3.1 Temporal characteristics of forest response to consecutive droughts along a climatic gradient *9*

 3.2 Interplay between the effects of local and regional environmental factors on forest performance *19*

 3.3 Influential time-scales of climatic effects and modulating effects of competition on tree growth *31*

 3.4 Determinants of local-scale variation in tree mortality in a semi-arid region: observations on several scales *79*

4 Concluding discussion *144*

 4.1 Observing forest response to drought – from patterns to processes *144*

4.2 Environmental determinants of forest mortality	146
5 References	148
6 Supplementary material	154
6.1 Supplementary material for Section 3.1	154
6.2 Supplementary material for Section 3.2	160
6.3 Supplementary material for Section 3.3	163
6.4 Supplementary material for Section 3.4	173
6.5 Additional figures regarding missing tree rings	185

1 Abstract

1.1 Introduction

Forest ecosystems function under increasing stress due to global climate changes that may lead to large-scale tree mortality. However, factors determining when and where mortality events will occur within the wider landscape are poorly understood. For example, the following aspects of forest response to drought are associated with substantial uncertainty:

- (a) Response to consecutive droughts along climatic gradients
- (b) Time-scales of climatic conditions effect on tree growth, and their spatiotemporal variation with respect to water balance
- (c) Local environmental influences, in particular those of competition intensity, on tree growth and mortality risk

Observational studies are thus necessary for documenting forest decline events, understanding their determinants, and developing sustainable management plans. A central obstacle towards achieving these goals, however, is the fact that mortality is often patchy across a range of spatial scales and is usually characterized by long-term temporal dynamics. Research must therefore integrate various methods and sources of information, from several scientific disciplines, to capture as many relevant informative patterns as possible; however this has rarely been done.

The improvement of the present study, over previous efforts in the above-mentioned directions, was twofold. *First*, the forests studied here (planted *Pinus halepensis* in Israel) are located along a wide climatic gradient, yet comprise a relatively homogeneous man-made ecosystem (even-aged monoculture), reducing the

confounding effects of species composition on drought response and isolating the climatic gradient effect. In addition, the forests have recently experienced an unprecedented sequence of drought periods, resulting in substantial mortality. *Second*, a multi-perspective approach was applied to provide a more comprehensive view of patterns associated with forest decline. Forest performance was simultaneously observed on three distinct scales, by integrating: (1) Normalized Difference Vegetation Index (NDVI) time-series, from satellite remote sensing; (2) individual dead trees point-pattern, from a high-resolution aerial photograph; and (3) Basal Area Increment (BAI) time-series, from dendrochronological sampling.

1.2 Methods

On a regional scale, time-series of spatially interpolated rainfall data and remote sensing images were used to estimate the environmental settings to which the forests are exposed and their corresponding performance responses. Forest canopy state was evaluated using NDVI values, obtained from Landsat satellite images for 1994–2011. To widen the study perspective, forest performance was sampled all along the climatic gradient in the planted *P. halepensis* forests in Israel (~250 to ~750 mm of average annual rainfall). Topographic aspect data were used to investigate the interaction between local and regional environmental factors that affect forest performance during drought.

To evaluate the temporal characteristics of climatic effects on tree growth, as well as the modulating effects of tree-to-tree competition on drought response, tree rings were sampled in three regions along the rainfall gradient (~300, ~500 and ~700 mm). Regional tree growth chronologies were constructed and examined with respect to detailed climatic data for 1983–2012. In addition, competition intensity was evaluated for each sampled tree, to examine the modulating effect of competition on growth decline during drought (2011) and subsequent recovery (2012).

On a local scale, an assessment of mortality and its determinants was executed in two

representative *P. halepensis* planted forests from a dry environment (~300 mm). A mapped dead trees point-pattern was derived from a high-resolution aerial photograph from 2012, while environmental conditions were characterized in a spatially explicit manner using a Digital Elevation Model, historical aerial photographs and Israel Forest Service data. NDVI data from Landsat for 1994–2012 and tree growth data from tree ring sampling provided complementary information.

1.3 Results

The main study questions *and the respective results* were as following:

- (a) How did forest performance response to two consecutive drought periods vary along the climatic gradient (Section 3.1)? *Three response types were identified:*
 - a. *Stable performance with low correlation to the rainfall pattern in the humid region (>500 mm)*
 - b. *Moderate performance decline with strong correlation to rainfall in the intermediate region (350–500 mm)*
 - c. *Steep performance decline with intermediate correlation to rainfall in the arid region (<350 mm)*
- (b) Did the response to a second drought period differ from that of the first drought period, and how did this difference vary along the climatic gradient (Section 3.1)? *The forests' response to the first drought was homogeneously negative along the climatic gradient. The response to the second drought differed among regions, being negative in the arid and intermediate regions (<500 mm) and close to zero in the humid region.*
- (c) How does annual rainfall relate to the difference in performance between northern and southern aspects in a given year, and how does the effect vary

along the rainfall gradient (Section 3.2)? *The effect of aspect on forest performance was linearly associated with rainfall in the arid region, but not in the intermediate and humid regions.*

- (d) How does the length of the climatic integration period, to which trees are most responsive, vary in space, i.e., at different positions along the climatic gradient, and in time, i.e., during a relatively wet compared with an extremely dry period (Section 3.3)? *Influential time scales of rainfall effect on growth were annual under relatively dry conditions (<500 mm) in both space and time, and multi-annual under more humid conditions.*
- (e) To what extent does competition, between trees within a stand, modulate growth decline during a drought year and growth recovery in the following wet year, and how do these effects change along the climatic gradient (Section 3.3)? *No profound difference in the nature of competition effect among regions was detected. Competition appeared to set an upper limit to growth, while the lower limit was unaffected by competition intensity, and thus growth variation among individual trees increased as competition intensity decreased.*
- (f) What was the spatial pattern (i.e., clustered, random or regular) of dead tree occurrence within the forest following a severe drought (Section 3.4)? *Dead trees were clustered across the whole range of spatial scales.*
- (g) How did biotic (age, density) and abiotic (topographic aspect, soil depth) conditions influence tree mortality risk (Section 3.4)? *Mortality risk was significantly higher in older-aged sparse stands, on southern aspects and on deeper soils. However, the locations of mortality patches within "high-risk" areas could not be fully explained by studied environmental factors.*
- (h) In what way is the forested area divided into distinct zones characterized by unique past performance trajectories? Are these associated with environmental conditions and with tree mortality risk (Section 3.4)? *Two different parts of*

the forest were affected during the two drought periods. However, differences among regions with distinct performance trajectories over time could be only partially elucidated by differences in the physical and biotic characteristics of the areas they occupy.

1.4 Discussion

The highest sensitivity to drought was observed in forests occupying the dry part of the studied climatic gradient (<350 mm). In addition to the observed forest greenness decline and substantial mortality, trees growing in that region immediately (same-year) and strongly (90% of growth rate variation explained by annual rainfall) responded to annual rainfall amount reduction. The pattern suggested that no "buffering", in terms of water availability for the trees, takes place in such dry settings. This result was in agreement with previous studies conducted in the region, which have shown that the majority of annual rainfall is lost to the atmosphere during the same year, likely resulting in a very limited potential for carried-over moisture over multi-annual time scales.

The mild response to drought at the humid edge of the climatic gradient, as well as a weaker and more lagged relation between tree growth and rainfall amounts, suggest that *P. halepensis* forests are relatively insensitive to drought in that region. Divergence was thus observed along the climatic gradient, both in long-term forest greenness trend (<540 mm – decrease; >540 mm – increase) and in time-scale of dominant response to rainfall variation (<500 mm – annual; >500 mm – multi-annual). These thresholds identify the transition zone southwards of which planted *P. halepensis* forests are probably not sustainable, given the climatic conditions and management practices experienced during 1983-2012.

On a local spatial scale, higher mortality was observed under locally drier conditions (south-facing aspects) coinciding with higher moisture demands (older forest stands). It was also demonstrated that although forest performance becomes most highly

homogeneous during drought, trees located in the locally drier habitats still reach the lowest absolute performance levels (and experience higher mortality rates), supporting a nonlinear (i.e. threshold-related) tree mortality risk behavior. Counter intuitively, deeper soils have been identified as a risk-factor to drought-induced mortality. That is supposedly due to the fact that under prolonged drought they impose limited root access to the bedrock layers, where residual moisture may sustain tree survival after the entire soil profile dries out. In addition, competition intensity had no negative effects on either tree survival or growth rate of inferior trees. This result, in combination with the patchy spatial pattern of mortality, suggests a potential role to self-amplifying mechanisms in tree mortality, and casts doubt on the generally held view that forest thinning should necessarily reduce tree mortality risk.

This PhD study has demonstrated that the integration of several data sources (satellite remote sensing, aerial photography and dendrochronology) can provide a more complete understanding of the spatiotemporal variation in drought-induced damage to forests. While inferences based on the different methods were generally in agreement, the differences were informatively related to the different levels of organization that each method addresses, making them complementary. For example, dendrochronological methods account only for the portion of population present at the time of sampling, thus potentially overestimating forest resilience, while satellite remote sensing may aggregate the reflectance of large forest canopy "portions", thus limiting the attribution of decline to either demographic (e.g. mortality) or structural (e.g. defoliation) processes. It is therefore suggested that evaluation of forest ecosystem resilience should ultimately be based on an integration of several metrics, each suited for detecting transitions at a different level of organization.

2 General introduction

2.1 Climate change and forest mortality

According to the recent report of the Intergovernmental Panel on Climate Change (Stocker *et al.*, 2013), unequivocal significant warming trends have been observed over most of the earth's surface during 1901-2012. Observed trends in precipitation amounts were associated with higher spatial variability and lower confidence. Nevertheless, in the Mediterranean region (the focus of this study) precipitation declines have generally been observed (Hoerling *et al.*, 2012). These climatic changes already have profound impacts on the biosphere (Walther *et al.*, 2002; Parmesan, 2006; Penuelas *et al.*, 2013), and the impacts are expected to increase as climatic change intensifies.

One of the biological responses to global warming is the apparent increase in drought-induced mortality in forests around the world in recent decades (Allen *et al.*, 2010). For example, an extreme drought during 2000-2002 in Southwestern USA triggered the death of about 350 million *Pinus edulis* trees over an area of 12,000 km² (Hicke & Zeppel, 2013). In Spain, significant mortality proportion increases have been observed for 15 out of 16 forest tree species when comparing the 1989-1996 and the 1997-2007 forest inventory surveys (Carnicer *et al.*, 2011). Since forests provide numerous ecosystem services contributing to our sustained existence on earth (Gamfeldt *et al.*, 2013), to say nothing of the value of forest biodiversity in its own right, these trends have drawn increased attention from the scientific community in recent years (Matyas, 2010; Birdsey & Pan, 2011; McDowell *et al.*, 2013a).

2.2 Main directions in current research

Three major directions of research can be identified within the recent literature dealing with large-scale drought-induced forest mortality. *First*, the way spatial (Williams *et al.*, 2010) and temporal (Williams *et al.*, 2013) variation in forest mortality is related to variation in environmental conditions (primarily in climate, physical environment and forest structure) is being investigated, based on observations of past forest mortality events. This type of observations is essential (Allen *et al.*, 2010) to identify significant environmental factors and their interdependence, both poorly understood at present. In addition to the value of basic ecological knowledge, understanding the environmental thresholds triggering extensive forest mortality is necessary to predict spatial patterns and timing of future forest mortality events.

For example, speaking of the above-mentioned forest mortality event in Southwestern USA, mortality was highly variable in space – in some locations mortality rate exceeded 90%, while in other locations only a few dying trees were observed (Breshears *et al.*, 2005). However, despite the fact that this particular forest mortality event (Breshears *et al.*, 2005, 2009; Floyd *et al.*, 2009), as well as the ecological and physiological properties of the tree species involved (McDowell *et al.*, 2008; Adams *et al.*, 2009; Gaylord *et al.*, 2013), have received a relatively large share of attention from the scientific community, the sources of local-scale spatial variation in mortality rates remained unresolved (Clifford *et al.*, 2013; Hicke & Zeppel, 2013).

Second, the physiological processes that forest trees undergo during drought-induced mortality are being investigated (McDowell *et al.*, 2011), not only to gain basic physiological insight of this complex phenomenon, but also to help identify the genetic and/or physiological basis for differences in drought resistance among individual trees, ecotypes or species (Breshears *et al.*, 2009). Three main mechanisms involved in tree mortality have been identified thus far: embolism (Hoffmann *et al.*, 2011), carbon starvation (Galiano *et al.*, 2011) and weakening of defenses against insect attacks (Jactel *et al.*, 2012). However, key questions remain regarding the interdependencies of those mechanisms (McDowell *et al.*, 2011), as well as their

relative importance in different species and environmental conditions (Anderegg *et al.*, 2012). This information is necessary for advancing towards mechanistic models of tree mortality (McDowell *et al.*, 2008, 2013b) as well as for making informed species/provenances selection decisions in afforestation (Klein *et al.*, 2013).

Third, in addition to understanding the ecological settings and physiological mechanisms of forest mortality, there is a necessity to understand and quantify the consequences of large-scale forest mortality for various aspects of ecosystem functioning. The latter includes, for example, effects on community structure (Mueller *et al.*, 2005), radiation fluxes (Royer *et al.*, 2011), water fluxes (Adams *et al.*, 2012) and regional climate (Anderson *et al.*, 2010a; Rotenberg & Yakir, 2010). Quantifying the impacts of forest mortality is essential for monitoring and management of valued resources, such as of the various ecosystem services forests provide.

The purpose of this PhD study was to address several of the significant knowledge gaps within the scope of the *first* research direction. The general question of the study was when and where (i.e. under which environmental conditions) a significant change in forest state takes place in response to drought. More specifically, three unresolved issues were emphasized: (1) Variation in forest response to consecutive droughts along a climatic gradient (Sections 3.1 and 3.2); (2) Influential time-scales of climatic conditions effect on tree growth, and their spatiotemporal variation with respect to the climatic water balance (Section 3.3); and (3) Local environmental impacts, in particular those of competition intensity, on tree growth and mortality risk (Sections 3.2, 3.3 and 3.4). The exact study questions are briefly listed in Section 1, and further developed in the respective sub-sections of Section 3.

2.3 The research approach and its potential advantages

This PhD study has several contributions to the current knowledge on the subject. These can be divided in two categories: the studied system (which is research-independent) and the employed methods (which are research-dependent).

The studied system, *Pinus halepensis* planted forests in Israel, was particularly suitable to address the study questions for several reasons. *First*, the climatic gradient in Israel is wide, encompassing a large portion of the moisture conditions within which the species in question can survive. Of particular importance are those forests located in the arid region (Schiller & Atzmon, 2009), where the climate is drier and more seasonally-affected than that encountered across the natural distribution of the species (de Luis *et al.*, 2013). The gradient is also steep, thus similar temporal sequences of wet/dry periods are experienced in its different portions. Comparison of responses to specific drought events among forests located under contrasting climatic regimes is thus made possible (Sections 3.1, 3.2 and 3.3).

Second, the planted forests are a relatively homogeneous ecosystem, since they are mostly composed of even-aged monoculture stands with limited understory development (Osem *et al.*, 2009, 2013). Contrariwise, in natural ecosystems variation in forest structure and community composition along climatic gradients limits our ability to attribute differences in response along a climatic gradient to the climatic effects alone. Planted forests are much closer to being an (unintended) transplant experiment, where the "forest structure" and "species composition" variables are kept relatively constant, so that drought response of the given tree species can be evaluated under different environmental conditions.

Third, the second half of the studied period (1998-2012) was unprecedentedly dry, encompassing two drought periods affecting the whole studied area (Sections 3.1 and 3.3). As a result, increased mortality of *P. halepensis* was noted in the planted forests of Israel (Schiller *et al.*, 2005, 2009; Klein *et al.*, 2014), although the spatial and temporal patterns had not been quantified previously to the present study.

A set of methods which has not, or has rarely been, employed in previous studies was used to observe forest state changes over time. Briefly, on a regional scale (Sections 3.1 and 3.2), time series of satellite images were combined with spatially and temporally explicit climatic information (Anderson *et al.*, 2010b), obtained using spatial interpolation of annual rainfall data from meteorological stations. Tree ring

analysis (Section 3.3) was combined with comprehensive estimates of competition intensity (Linares *et al.*, 2010a) and climatic conditions on several time scales (Pasho *et al.*, 2011), in distinct regions along a climatic gradient, and over relatively dry and wet periods. On a local scale (Section 3.4), individual dead trees were mapped over a relatively large area using a high-resolution aerial photograph. This is in contrast with most previous studies on spatial pattern of tree mortality which usually covered a small (Linares *et al.*, 2010b) / discontinuous (Michaelian *et al.*, 2011) area, aggregated individual trees (Clifford *et al.*, 2011; Garrity *et al.*, 2013), or addressed inconsistent time frames (Gomez-Aparicio *et al.*, 2011; Coll *et al.*, 2013).

In addition, the simultaneous observation of forest response to drought on three distinct scales (see Section 2.4) constitutes a central methodological unique feature of the present study. One of the difficulties associated with observation of forest mortality is that while the functional ecological unit (Levin, 1992) of the process is obviously a single tree, mortality often occurs over very large geographical areas and long (multi-annual) temporal scales (Bigler *et al.*, 2007). A trade-off thus inevitably exists between "directness" of observation and the spatiotemporal extent which can be feasibly covered. For that reason it has been acknowledged that combining observations at several scales is essential to link individual tree responses with entire forest mortality patterns (Breshears *et al.*, 2009; McDowell *et al.*, 2013a). Nevertheless, most previous studies on forest mortality have been conducted either on a small spatial scale, using physiological measurements and tree ring analysis (McDowell *et al.*, 2010; Sarris *et al.*, 2013), or on a large spatial scale using remote sensing (Lloyd *et al.*, 2011; Berner *et al.*, 2013), national forest inventories (Gomez-Aparicio *et al.*, 2011; Coll *et al.*, 2013) or surveys (Gitlin *et al.*, 2006; Koepke *et al.*, 2010). This has resulted in a gap between the hypothesized physiological and structural processes involved in individual tree mortality, and the regional-scale spatial patterns of forest mortality and their associated climatic factors. The fact that methodologies associated with either domain often belong to very distinct disciplines also contributed to the separation. For example, only recently have tree-ring analyses and satellite remote sensing been combined to gain more comprehensive insight of

forest response to climate change (Beck *et al.*, 2011; Lloyd *et al.*, 2011; Berner *et al.*, 2013; Kharuk *et al.*, 2013; Mathisen *et al.*, 2014), however this was done usually without addressing local site characteristics such as tree density.

2.4 The relation between chapters

The results regarding three individual spatiotemporal domains (Figure 1), with the associated study questions, methods and measured variables are reported in separate chapters. For simplicity, the division (Table 1) is hereby labeled according to the method of forest state assessment: satellite remote sensing (Sections 3.1 and 3.2), tree-ring analysis (Section 3.3) and aerial photography (Section 3.4). Eventually the three points of view on forest response to drought are integrated, to provide a broader perspective on the studied phenomenon (Section 4). The way such integration takes place in practice, and its potential benefits, is also addressed (Section 3.4).

It is worth mentioning that the research summarized in Sections 3.1, 3.2, 3.3 and 3.4 was conducted roughly in chronological order. Therefore each of these sections also relies on the material from the previous one(s).

Table 1 – Overview of independent methods for estimating forest state used in this study.

Method	Satellite remote sensing	Tree-ring analysis	Aerial photography
Sections	3.1, 3.2	3.3	3.4
Forest state estimate	Normalized Difference Vegetation Index (NDVI)	Basal Area Increment (BAI)	Mortality proportion
Measurement unit	30×30 m pixel	Individual tree	Individual tree
Spatial scale and extent	Regional Continuous, ~100 km ²	Local Discrete, ~300 trees	Local Continuous, ~6.6 km ²
Temporal extent	14-17 years	30 years	1 year
Environmental factors considered	Rainfall amount Topographic aspect	Rainfall amount Temperature Competition intensity	Topographic aspect Soil depth Tree age Tree density

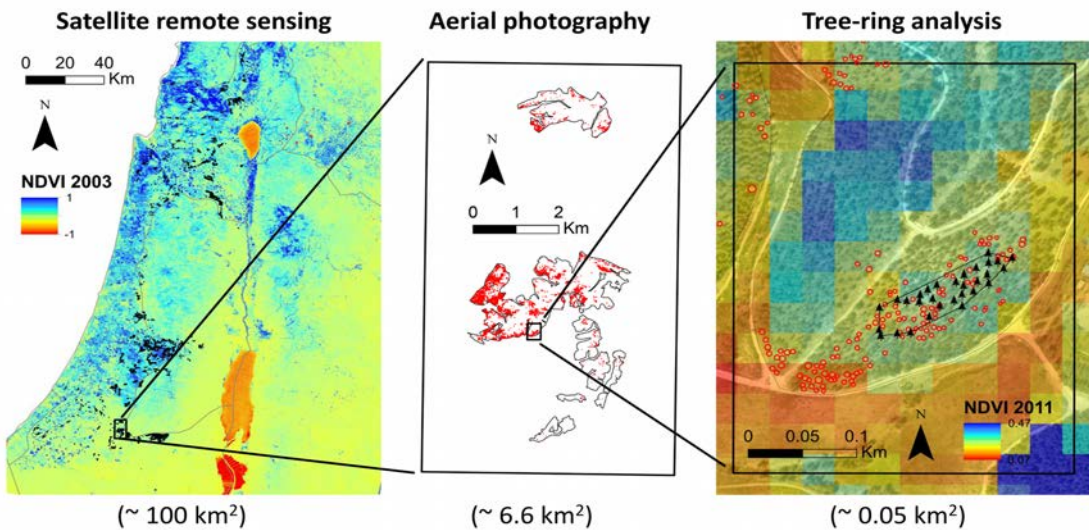


Figure 1 – Illustration of the spatial scales associated with each of the three independent methods of observation (Table 1). The *left* panel shows a Normalized Difference Vegetation Index (NDVI) image of the studied area for 2003, with the locations of *Pinus halepensis* planted forests marked in black. The *middle* panel shows the locations of dead *P. halepensis* trees identified on a high-resolution aerial photograph in Dvira (top) and Lahav (bottom) forests. The *right* panel shows the location of one (out of 10) tree-ring sampling sites; locations of sampled trees are marked by black symbols, locations of dead trees (in red, based on the aerial photographs) and NDVI values (in semi-transparent red-blue, based on a satellite image from 2011) are also shown for comparison.

3 Results

3.1 Temporal characteristics of forest response to consecutive droughts along a climatic gradient

In this chapter, the long-term forest functioning trend and the sensitivity to climatic variation were examined in the planted *Pinus halepensis* forests in Israel. Regional assessment of responses to climate change was made possible using remote sensing in combination with spatially and temporally explicit climatic data. In the semi-arid region (<350 mm) forest performance consistently declined, suggesting accumulated drought damage.

The results of this study are described in Dorman *et al.* (2013a) (see below).

Supplementary material for this chapter appears in Section 6.1.



Forest performance during two consecutive drought periods: Diverging long-term trends and short-term responses along a climatic gradient

Michael Dorman ^{a,*}, Tal Svoray ^a, Avi Perevolotsky ^b, Dimitrios Sarris ^{c,d,e}

^a Department of Geography and Environmental Development, Ben-Gurion University of the Negev, Beer-Sheva 84105, Israel

^b Department of Agronomy and Natural Resources, Agricultural Research Organization, Volcani Ctr, Bet Dagan 50250, Israel

^c Faculty of Pure & Applied Sciences, Open University of Cyprus, 2252 Latsia, Nicosia, Cyprus

^d Department of Biological Sciences, University of Cyprus, 1678 Nicosia, Cyprus

^e Division of Plant Biology, Department of Biology, University of Patras, 265 00 Patras, Greece



ARTICLE INFO

Article history:

Received 25 May 2013

Received in revised form 5 August 2013

Accepted 5 August 2013

Available online 5 September 2013

Keywords:

Drought response

Landsat

Normalized Difference Vegetation Index (NDVI)

Pinus halepensis

Spatial interpolation

ABSTRACT

Forest decline, attributed to increased aridity under global climate change, has been observed with rising frequency worldwide. One of the knowledge gaps making its spatially explicit prediction difficult is the identification of the climatic settings that generate a significant change in the forest state. A relatively rare sequence of unfavourable climatic events – a short extreme drought followed by a prolonged moderate drought within one decade – has allowed us to examine how rainfall amount affects forest performance.

Large-scale monitoring, at high spatial and temporal resolutions, is required to study climatic effects on forest performance. Therefore, time-series of spatially interpolated rainfall maps, remote sensing images and tree growth data were used to estimate the environmental settings to which the forests are exposed, and the corresponding forest performance responses. Performance was estimated from Normalized Difference Vegetation Index (NDVI) values obtained from 32 Landsat satellite images for 1994–2011. To widen the study perspective we sampled forest performance along a rainfall gradient (250–750 mm) in the planted *Pinus halepensis* forests in Israel.

Performance response was not spatially homogeneous. Three response types could be identified along the rainfall gradient: stable performance with low correlation to rainfall pattern in the humid region (>500 mm), moderate performance decline with high correlation to rainfall in the intermediate region (350–500 mm), and steep performance decline with intermediate correlation to rainfall in the arid region (<350 mm). The response to the second drought differed among regions, unlike the response to the first drought, which was homogeneous.

The observed diverging performance trend along the climatic gradient can be attributed to the varied importance of water availability as a limiting factor. The reduced effect of rainfall on performance deviations, the steep performance decline, and the difference between responses to the first and second droughts at the most arid locations, imply to higher importance of multi-annual accumulated and carried-over drought stress effects at these locations.

© 2013 Elsevier B.V. All rights reserved.

1. Introduction

Large-scale forest decline, i.e. defoliation, reduced tree growth rate and increased mortality, attributed to increasing aridity under global climate change, have been observed with rising frequency worldwide (Allen et al., 2010). For example, widespread mortality of *Pinus edulis*, *Pinus ponderosa*, and other species was recorded in south-western USA in 2002–2003, following an extreme drought (Breshears et al., 2005; Shaw et al., 2005). This event was

considered an ecosystem “crash” (Breshears et al., 2011; Breshears and Allen, 2002), since in semiarid environments it can take more than a century for tree cover to fully re-establish. The magnitude of these ecosystem functional changes, generated by forest mortality, could be revealed by remote sensing with multispectral sensors (Breshears et al., 2005; Huang et al., 2010; Rich et al., 2008; Yuhas and Scuderi, 2009).

The increased forest mortality raises concerns regarding the fate of forest cover and sustainability of stands if climate becomes drier. However, forest decline and mortality are not well understood processes, either on the individual tree level (McDowell et al., 2011) or on the whole-forest level (Allen et al., 2010). In particular, it is asserted that the link between forest decline and causal

* Corresponding author. Tel.: +972 86479054.

E-mail address: michael.dorman@mail.huji.ac.il (M. Dorman).

climatic drivers should be systematically examined to evaluate forest sensitivity to climatic changes in various environmental settings (Allen et al., 2010).

In water-limited ecosystems, decline in forest performance is generally expected to be greater at the arid edge of a species distribution, where water availability constraint on vegetation is highest (Allen et al., 2010; Babst et al., 2013; Linares et al., 2009). However, studies of forests arid distribution limits received smaller amount of attention among forest-related ecological studies until now (Hampe and Petit, 2005; Matyas, 2010; but see Vicente-Serrano, 2007). For example, Carnicer et al. (2011) studied crown defoliation rates in European forests. The authors have found that a significant increase in defoliation rates occurred during 1987–2007 only in southern Europe, in contrast to the stable state observed in northern and central Europe over the same period. A divergent trend between the arid forest border and more humid locations with *Pinus halepensis* forests was also recently reported from Spain (Vicente-Serrano et al., 2010c).

Both abovementioned studies (Carnicer et al., 2011; Vicente-Serrano et al., 2010c) examined long-term performance trends with respect to the location along climatic gradients (i.e., average rainfall amount), but not to the temporally explicit trajectory of annual rainfall at each location. However, the way in which climatic events, such as droughts, translate into short-term deviations of forest performance from their long-term trend holds information on forest resilience when facing climatic deviations. For example, a significant long-term trend may indicate steady growth in areas which are not water-limited (in the case of a positive trend) or steady decline in locations irreversibly damaged by drought (in the case of a negative trend). No significant long-term performance changes, accompanied by short-term deviations of performance in response to rainfall amount variation, however, may indicate limits of a species distribution. Those are the locations where the role of rainfall as a limiting factor to performance is strongest, although no pronounced growth or decline has yet been observed. Drying trends have been observed around the Mediterranean (e.g. Kafle and Bruins, 2009; Sarris et al., 2007), while global climate change models predict further desertification in the region (Giorgi and Lionello, 2008). Therefore, it is particularly important to acknowledge how sequences of climatic deviations, such as recurrent drought, affect forest performance (Girard et al., 2012; Sanchez-Salguero et al., 2012; Sarris et al., 2011).

In forest science, remote sensing is a modern and efficient tool to obtain high temporal and spatial resolution data on vegetation performance and physiology (Pettorelli et al., 2005; Zhu et al., 2012). Indices summarizing reflectance patterns obtained from multispectral sensors (such as TM and ETM+ on Landsat satellites) were developed for these purposes. The most commonly used index in ecological studies, the Normalized Difference Vegetation Index (NDVI) (Rouse et al., 1973; Tucker, 1979), is used to quantify green biomass (Pettorelli et al., 2005; Wang et al., 2011). NDVI was used to assess forest structural and physiological responses to climatic change in numerous studies, including studies on *P. halepensis* forests (Lloret et al., 2007; Vicente-Serrano et al., 2010c; Volcani et al., 2005) as well as on forests in other ecosystems (Verbyla, 2008). In the present study, NDVI is a measure of forest performance, reflecting green biomass quantity and state (Pettorelli et al., 2005; Wang et al., 2011), of the forested area in a given location, at a given year.

P. halepensis grows naturally in the Mediterranean region, mainly in the western part but a few isolated populations have been located in the eastern part, including Israel (Schiller, 2000). Its natural distribution is limited by minimum annual precipitation of 450 mm (Liphschitz and Biger, 2001; Schiller, 2000). However *P. halepensis* was planted under a wide range of climatic conditions in Israel, including regions with annual rainfall ranging between 200

and 850 mm, thus extending beyond the climatic envelope of the species' natural distribution. Planted forests cover about 8% of the Mediterranean climatic zone in Israel (Osem et al., 2008) and are dominated (~75%) by conifers, of which *P. halepensis* is the most common species (Perevolotsky and Sheffer, 2009). The majority of the forests are monocultures of even-aged trees (Osem et al., 2009), planted during a relatively short time period (1961–1970; Israel Forest Service GIS layer, 2011).

Recently, increased mortality of *P. halepensis* in the planted forests of Israel was reported in the southernmost locations (Schiller et al., 2005, 2009; Ungar et al., 2013), following a sequence of two drought periods: a short extreme drought (1998–2000) and a prolonged moderate drought (2005–2011). This has provided a unique opportunity to examine forest performance response to recurrent drought events.

In the present study we examine the response of *P. halepensis* forests planted along a rainfall gradient of 250–750 mm in Israel, to two consecutive drought periods during 1994–2011, as related to annual rainfall amount.

The principal questions that this study aims to tackle are:

1. How did forest performance response to two consecutive drought periods vary along a wide rainfall gradient, extending from the arid forest border towards the more humid Mediterranean zone?
2. Did the response to a second drought period differ from that of the first drought period, and how did this difference vary along the rainfall gradient?

2. Materials and methods

2.1. Study area

The study area encompasses 46 forests (see Figs. S1 and S2 in Supporting information) located in central and northern Israel, amounting to a total sampled area of 31.7 km². The forests are spread across a climatic gradient extending from semi-arid to Mediterranean conditions, i.e., annual rainfall ranging from 236 to 746 mm. The climate in the region is characterized by winter rains occurring mainly between December and March, and a relatively long, dry, hot summer (Osem et al., 2009).

Three forests along the rainfall gradient were chosen for dendrochronological sampling (Fig. S2). All sites were located on southern aspects and were of comparable age (planting year of 1969, 1965 and 1960 for the arid, intermediate and humid sites, respectively). Since growth declines with age (Sarris et al., 2007, 2011), the slight age increase towards the humid edge of the gradient in fact makes the comparison more conservative. The sites are hereafter referred to as "arid site", "intermediate site" and "humid site". Note that we do not refer to climatic regions; these labels are used to enable easier reference to relative position along the rainfall gradient (the same applies when referring to "arid", "intermediate" and "humid" parts of the rainfall gradient, see below).

2.2. Remote sensing data

To estimate forest structural responses on a large spatial scale, 30 Landsat-5 TM and 2 Landsat-7 ETM+ images from the period 1994–2011 were used. Two adjacent Landsat scenes (path 174, rows 37 and 38) from the same date were merged to cover the area of interest; sample sizes were 15 and 17 images for the northern and southern parts of the area, respectively. Images were selected from a relatively short time period during the end of the dry season (8 September–16 October) for two reasons (Vicente-Serrano et al., 2010c). First, during the dry season there is lower variation in

water availability for the trees, therefore there is lower seasonal variation in the vegetation activity signal. Second, herbaceous vegetation is completely dry during the summer; therefore a higher proportion of the spectral signal can be attributed to *P. halepensis* trees.

Images were geometrically corrected in the AutoSync Workstation module of Erdas Imagine 2011 software (ERDAS, 2011), by using a 5th-order polynomial geometric model. The images from 2003 were chosen as the reference set for all other images in the series. Root Mean Square Error (RMSE) was <0.5 pixel length in all cases. Radiometric calibration was performed based on up-to-date coefficients (Chander et al., 2009). Atmospheric correction was applied with the Dark Object Subtraction 4 method (Song et al., 2001). A Dark Object Subtraction method was chosen because supplementary atmospheric data (such as Aerosol Optical Depth) are not available for the older images, which necessitated application of an image-based method. Manually prepared cloud masks were used in order to exclude cloud and cloud shadow areas from the analysis.

The NDVI was calculated as:

$$\text{NDVI} = \frac{\rho_{\text{IR}} - \rho_R}{\rho_{\text{IR}} + \rho_R} \quad (1)$$

in which ρ_{IR} is the reflectivity in the near-infrared region (Landsat band 4), and ρ_R is the reflectivity in the red region (Landsat band 3) of the electromagnetic spectrum. Image processing, spatial interpolation and statistical analyses were applied by using R software (R Development Core Team, 2012). Atmospheric correction of Landsat images was done with the “landsat” package (Goslee, 2011).

Images were aggregated from 30-m to 90-m resolution by using a mean function, to reduce the amount of data as well as to reduce position errors stemming from geometric correction inaccuracy. A polygonal layer of Israeli planted forests (obtained from the Israeli forest service, KKL) was used to delineate areas within a given forest containing >80% *P. halepensis*. Mean NDVI values time series of each forest was then extracted from 90-m pixels completely within those areas of interest.

2.3. Rainfall data

Annual rainfall grids with 1000-m resolution were produced by applying spatial interpolation to data from 96 meteorological stations (Fig. 1a), for 26 rainfall seasons (1985–2011). Two interpolation methods were evaluated for this task: Ordinary Kriging, and Universal Kriging (Carrera-Hernandez and Gaskin, 2007; Di Piazza et al., 2011; Vicente-Serrano et al., 2003) with all possible combinations of three covariates – elevation (Goovaerts, 2000), distance from the Mediterranean Sea, and latitude. Prediction accuracy was compared by using the mean RMSE obtained from Leave-One-Out cross validation. Universal Kriging with elevation as a covariate yielded the lowest average RMSE (58.2 mm) among the 26 years, therefore this method was chosen for preparing the rainfall maps (Table S1). Since interpolation accuracy decreases with distance, only those forests within 15 km of the nearest meteorological station were considered for analysis. Spatial interpolation of rainfall data was done with the “gstat” package (Pebesma, 2004) in R.

A monthly time series of Standardized Precipitation-Evapotranspiration Index (SPEI; Vicente-Serrano et al., 2010a, 2010b) was obtained (Fig. 1b) in order to provide a broader perspective on the increased aridity in the region within the temporal window that is relevant for the studied planted forests (1960–2011). The SPEI is a site-specific drought indicator of deviations from the average water balance (precipitation minus potential evapotranspiration). Different SPEI time series may be calculated for different time scales, representing the cumulative water balance over the previous n months (Vicente-Serrano et al., 2013). A 12-months

integration period was chosen since a stronger response of *P. halepensis* to cumulative droughts over 11-months was detected in a previous study (Pasho et al., 2011). The data were downloaded from the Global SPEI database, available at a 0.5° spatial resolution and monthly time resolution (<http://www.sac.csic.es/spei/>), for a grid cell located at the center of the studied area (32°15'N, 35°15'E).

2.4. Dendrochronological methods

Sampling took place during autumn 2011–spring 2012. In each of the three sites (Fig. S2), 30 living unsuppressed trees were selected. GPS receiver was used to record the coordinates of all sampled trees. Two wood cores were extracted from opposite sides of each tree at breast height using an increment borer. Cores were sanded using increasingly fine sanding paper until tree rings were clearly visible under a binocular microscope. Tree Ring Width (TRW) was measured to an accuracy of 0.01 mm using a LINTAB 6 measuring device (Rinnotech, Heidelberg, Germany). Among the two cores from a given tree, the core having better agreement with the site's mean series was chosen according to the “Gleichläufigkeit”, a classical time-series agreement test based on sign test (Eckstein and Bauch, 1969). This step was performed using the TSAP software (Rinnotech, Heidelberg, Germany). Its purpose was to remove unrepresentative cores having mechanical damage or growth irregularities while retaining the sample of 30 individual trees. The final 90 TRW series were used in order to calculate the mean and standard error of TRW per site per year (Fig. 4).

2.5. Statistical methods

The research questions were examined by fitting linear regression models to the data, and by using model selection procedures (Johnson and Omland, 2004); presence of a given predictor in the best model was interpreted as support for the hypothesis underlying that predictor (i.e. presence of a performance temporal trend and/or an association between performance and annual rainfall amount, see below). Model selection was based on the small-sample unbiased Akaike Information Criterion (AICc) (Johnson and Omland, 2004), which is a modified version of the Akaike Information Criterion (AIC) (Akaike, 1974) containing an additional bias-correction term for small sample sizes. For simplicity, AICc is hereafter referred to as AIC.

The effect of rainfall on NDVI was evaluated by selecting one of four models: the one described in Eq. (2) and the three simplified nested models each of which lacked one or both of the predictors, t and Rain_t .

$$\text{NDVI}_t = \beta_0 + \beta_1 * t + \beta_2 * \text{Rain}_t + \varepsilon \quad (2)$$

in which NDVI_t is the value of NDVI in year t , Rain_t is the rainfall amount during the previous year; i.e., NDVI_t is an NDVI value obtained in September–October of year t , and Rain_t is the rainfall amount during the previous wet season, i.e., October–April of years $t-1$ to t , and ε is the error term.

The model-fitting procedure was performed separately for the NDVI time series of each forest. Forest samples included 46 locations (see Fig. S2), which were selected according to three criteria: (1) forest size is at least 10 (90 × 90 m) pixels, i.e., at least 90 Landsat pixels; (2) at least 14 years of observation remaining after removal of years in which more than 10% of the data were missing because of cloudiness; (3) four forests were removed from the analysis because they had experienced fires during the studied period – one known to have occurred in 1995 (Levin and Saaroni, 1999) and three others more recently, as verified by reference to aerial photographs of these locations from 2010.

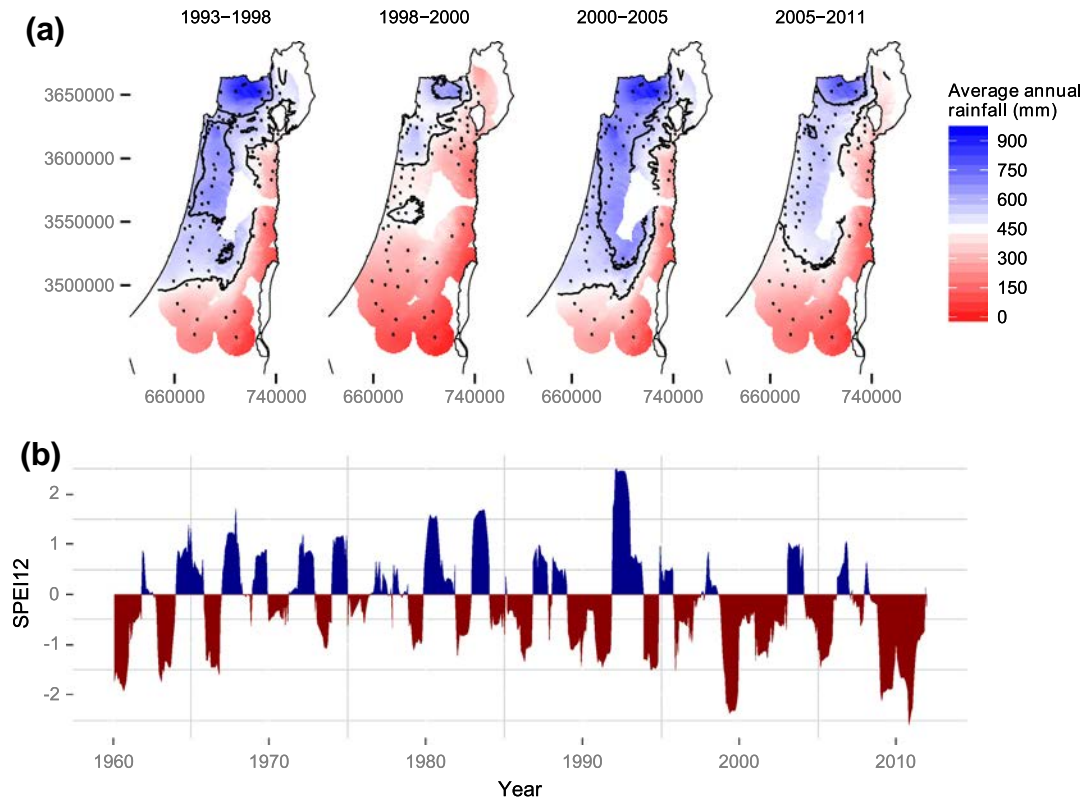


Fig. 1. (a) Maps of average annual rainfall during four consecutive periods: 1993/94–1997/98 (5 rain seasons), 1998/99–1999/00 (2 rain seasons), 2000/01–2004/05 (5 rain seasons) and 2005/06–2010/11 (6 rain seasons). Whereas the first (1993–1998) and third (2000–2005) periods had average rainfall distribution, the second period (1998–2000) encompassed a short but extreme drought and the fourth (2005–2011) – a prolonged moderate drought. Lines show the 450 mm and the 600 mm isohyets. Values were obtained by spatial interpolation of data from 96 meteorological stations (shown as black points) by using Universal Kriging with elevation as a covariate. Universal Transverse Mercator (UTM) zone 36 N coordinates (m) are shown on the axes. (b) A cumulative Standardized Precipitation-Evapotranspiration Index (SPEI) over the previous 12-months period as function of month, during 1960–2011, in the central part of the studied area. The SPEI is a standardized variable; values above zero (blue) denote water surplus, values below zero (red) denote water deficit. (For interpretation of the references to color in this figure legend, the reader is referred to the web version of this article.)

Rainfall amounts for each forest were standardized to mean of zero and standard deviation of 1, according to the 26 years of observation, i.e., standardized anomaly values were calculated (Anderson et al., 2010), to enable comparison among forests (Schielzeth, 2010).

An example of the input data and of the model selection procedure on two of the 46 forests can be found in Fig. S3.

3. Results

Rainfall maps of four consecutive periods between 1993 and 2011 (Fig. 1a) show that the studied period began with five average years (1993–1998). Two extremely dry years followed (1998–2000). The next five years (2000–2005) returned to average conditions, and were followed by six years of moderate drought (2005–2011). The two drought periods (1998–2000 and 2005–2011) represent a relatively rare sequence of unfavourable climatic events. For example, the rainfall record for 1963–2011 at the Bet Dagan station (central Israel; see Fig. S4) shows that the last 14-year period (1998–2011) was particularly dry in that it included 12 below-average rainfall years (all except for 2002 and 2003), including the driest year on the record (1999). The SPEI time series (Fig. 1b) for 1960–2011 also showed that the two recent drought periods (1998–2000 and 2005–2011) encompassed the most extreme conditions the forests have experienced since they were planted.

The temporal trend of NDVI and the effect of rainfall on NDVI were examined at the 46 forest locations. Fitted coefficients of the two terms in Eq. (2) are plotted for each location on a map (Fig. 2a and b) and also on a graph, as functions of average rainfall

at the location (Fig. 2d and e). Adjusted R^2 values of the respective models are shown on a map (Fig. 2c) and also on a graph (Fig. 2f).

Fig. 2a shows the temporal trend of NDVI, which is expressed in the fitted values of the coefficient β_1 from Eq. (2). It appears that NDVI decreased in the arid region, while increasing or remaining constant in the humid region (e.g. Fig. S3), even though the whole studied area was affected by drought (Fig. 1a). Fig. 2d shows the NDVI trend from Fig. 2a as a function of the average rainfall in the 46 locations. This allows quantitative assessment of the relation between the temporal trend of NDVI and the average rainfall along the climatic gradient in Israel. The average annual rainfall that yielded an estimated zero trend was 543 mm. In other words, during the examined period, direction and magnitude of the NDVI trend were related to position along the rainfall gradient; the NDVI trend during 1994–2011 was characterized by a transition from decreasing to increasing at 543 mm. Naturally, this pattern led to an increase in NDVI contrast along the rainfall gradient during 1994–2011 (Fig. 3e).

Fig. 2b shows the estimated effects of previous-year rainfall on NDVI at the 46 locations, which is the fitted value of the coefficient β_2 from Eq. (2). The fitted coefficients were positive in all cases where this variable appeared in the lowest AIC model, meaning that effect of previous year rainfall on NDVI was either positive or absent. However, the strength of this relationship differed between the more humid and more arid parts of the studied climatic gradient. Fig. 2e shows the effect of rainfall depicted in Fig. 2b as a function of the average rainfall in the 46 locations; the effect of rainfall on NDVI appears to be stronger in the more arid locations than in the more humid ones. However, unlike the relation between the trend of NDVI and the climatic gradient (Fig. 2d), the

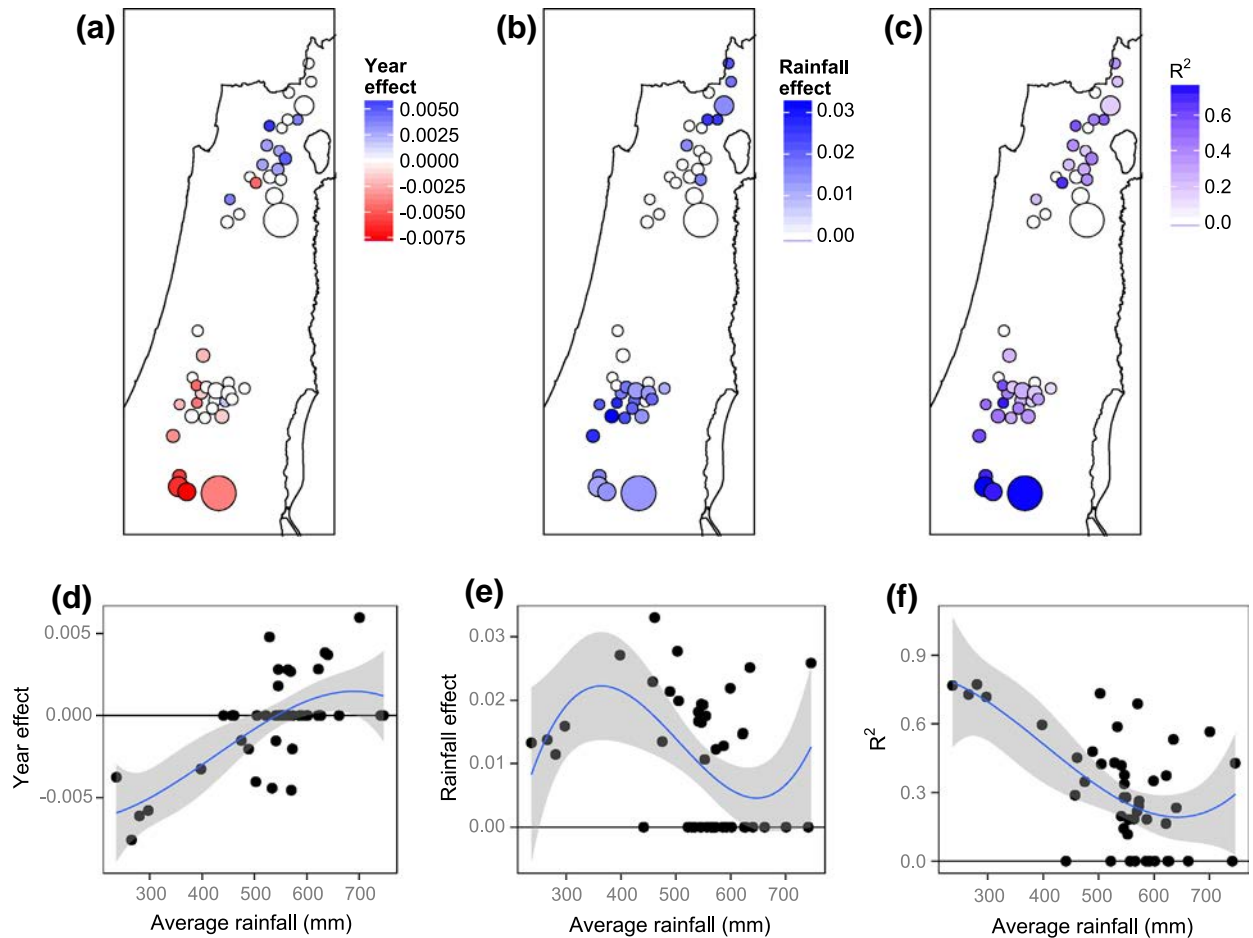


Fig. 2. Maps of the coefficients and adjusted R^2 from the lowest AIC Linear models describing NDVI as function of year and of rainfall in 46 forests in Israel (Eq. (2)): (a and d) – Year effect β_1 , (b and e) – Rainfall effect β_2 , and (c and f) – Adjusted R^2 . Coefficient values are shown in geographical space (a–c) and as functions of average rainfall at the location (d–f). Third-order polynomial regression-fitted lines with 95% confidence interval are shown (d–f); all were significant – (d) $p < 0.001$ and adjusted $R^2 = 0.43$, (e) $p < 0.05$ and adjusted $R^2 = 0.13$, (f) $p < 0.001$ and adjusted $R^2 = 0.34$. Average rainfall values are based on the period 1985–2011. Symbol size in (a–c) is proportional to forest size, ranging between 11 and 656 pixels of (90 × 90) m. (For interpretation of the references to color in this figure legend, the reader is referred to the web version of this article.)

relation between the effect of rainfall and the climatic gradient seems distinctly non-linear (Fig. 2e). The effect of annual rainfall on NDVI was strongest around 400 mm, and decreased towards the arid forest border (below 350 mm) as well as towards the humid region (above 500 mm; Fig. 2e).

Fig. 2c shows adjusted R^2 values of the fitted models at each location. A higher proportion of NDVI variation is attributed to trend and rainfall effects at the arid region (up to R^2 of 0.77 in both of the largest forests in that region, Fig. 2c), than towards the humid region, where the strength of this relationship gradually decreases (Fig. 2f). Locations with $R^2 = 0$ begin to appear at 440 mm annual rainfall, but become common above 500 mm. At these locations the lowest AIC model did not include any terms except for the intercept, indicating that NDVI was relatively stable in the long-term and not affected by annual rainfall in the short-term.

Fig. 3 summarizes the NDVI change (ΔNDVI) between the beginning and end of each of the four periods defined in Fig. 1a. Instead of evaluating the ΔNDVI (namely $\text{NDVI}_{t2} - \text{NDVI}_{t1}$) values in each of 46 forests, the NDVI_{t1} and NDVI_{t2} values were plotted as a function of average rainfall, and a smoothing was applied to visualize the “ NDVI_{t1} – rainfall” and “ NDVI_{t2} – rainfall” relations. The area between the two smoothing lines thus expresses the average ΔNDVI as a function of average rainfall during a given period.

The differing responses of the intermediate and arid (<500 mm) as opposed to humid (>500 mm) parts of the rainfall gradient are apparent. At the arid end, ΔNDVI was negative at all periods except

for 2000–2005 (Fig. 3c). However, the increase during 2000–2005 was not sufficient even to compensate for the decrease that occurred during the previous period – 1998–2000 (Fig. 3b) – which was an extreme drought. As a result, the NDVI decrease during 1998–2000, combined with the NDVI decreases of 1994–1998 (Fig. 3a) and 2005–2011 (Fig. 3d), resulted in a negative ΔNDVI for the whole studied period in the more arid region (Fig. 3e).

In the humid region, however, ΔNDVI was negative only during the extreme drought of 1998–2000 (Fig. 3b), and close to zero during the moderate drought of 2005–2011 (Fig. 3d). During the other two periods – 1994–1998 (Fig. 3a) and 2000–2005 (Fig. 3c) – ΔNDVI was positive, resulting in an overall positive ΔNDVI for the humid region for the whole studied period (Fig. 3e).

Another notable feature is that the responses of the two parts of the rainfall gradient to the second moderate drought of 2005–2011 (Fig. 3d) differed, in contrast to their similar responses to the first extreme drought period of 1998–2000 (Fig. 3b). Whereas the responses to the first drought were negative with similar magnitude in both parts (Fig. 3b), the response to the second drought was negative in the arid and intermediate regions but close to zero in the humid region (Fig. 3d).

The three sites where wood cores were sampled differed in their growth patterns (Fig. 4). In an arid site, the lowest TRW value was reached by the end of the second drought, in 2011 (0.22 mm). However, in the intermediate site the lowest TRW was observed during the first drought, in 1999 (0.75 mm), while in 2011 TRW

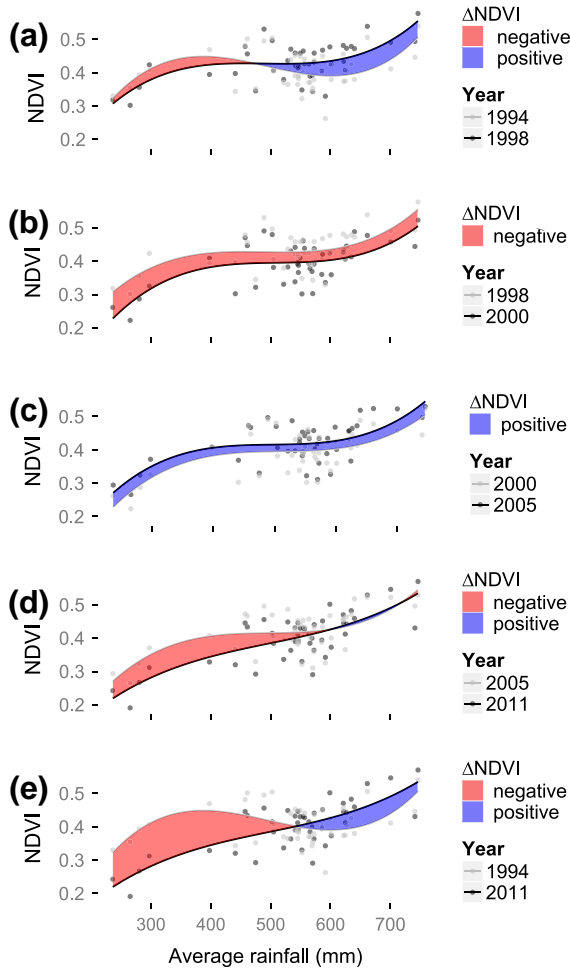


Fig. 3. NDVI differences between beginning and end of four consecutive periods (shown in Fig. 1) and between the beginning and end of the whole studied period, in 46 forests: (a) 1994–1998, (b) 1998–2000, (c) 2000–2005, (d) 2005–2011 and (e) 1994–2011. Third-order polynomial regression-fitted lines are shown – all were significant: $p < 0.01$ and adjusted $R^2 = 0.21$ (1994); $p < 0.001$ and adjusted $R^2 = 0.39$ (1998); $p < 0.001$ and adjusted $R^2 = 0.42$ (2000); $p < 0.001$ and adjusted $R^2 = 0.42$ (2005); $p < 0.001$ and adjusted $R^2 = 0.57$ (2011). Positive and negative differences between fitted lines are filled with blue and red colors, respectively. (For interpretation of the references to color in this figure legend, the reader is referred to the web version of this article.)

was higher (1.09 mm). In the humid site neither the 1999 nor 2011 TRW were particularly low (1.74 and 1.59 mm, respectively), while the lowest TRW was observed in 1992 (1.22 mm).

4. Discussion

The contrasting long-term trend of NDVI along a rainfall gradient in planted *P. halepensis* forests (Fig. 2a and d) may be attributed to the effects of water availability decrease on tree growth under differing water balance conditions. The effect of drought may be stronger in more arid regions, where the forest is more strongly dependent on water availability and weaker in humid regions, which are less water-limited. Evidence for such a divergent trend of *P. halepensis* performance was recently recorded in a few studies, which covered smaller ranges of rainfall variation than those in the present study. Vicente-Serrano et al. (2010c) found a divergent NDVI trend in *P. halepensis* forests in Spain between 391 and 626 mm of annual rainfall; Schiller et al. (2005) and Sanchez-Salguero et al. (2010) demonstrated *P. halepensis* performance decline at locations closer to its arid range limit; Vila et al.

(2008) and Linares et al. (2011) reported performance improvement at more humid locations. These findings suggest a decline in performance at the arid forest limit coupled with a performance improvement at the humid part of the gradient. Our results – increasing difference in NDVI along the rainfall gradient (Fig. 3e) – also support this conclusion. This phenomenon is probably related to relative dryness that occurred in the Mediterranean region during the last several decades.

The observed increasing contrast in performance expresses a northward shift of the optimal habitat for a planted *P. halepensis* forest. In the arid part of the gradient, NDVI values decreased, reflecting decrease in green biomass, which may be caused either by increased tree mortality (Schiller et al., 2005, 2009; Ungar et al., 2013) or by defoliation. The latter, too, may eventually lead to increased mortality, since defoliation is detrimental to the trees' carbon budget (Galiano et al., 2011; Girard et al., 2012). We therefore hypothesize that the observed pattern reflects increased defoliation and tree mortality rates in the arid part of *P. halepensis* forests in Israel. Our own field observations as well as observations of others (regional foresters, pers. comm.) give the impression that both drought periods were accompanied by episodes of increased mortality, especially towards the arid forest border. It seems that the present planted *P. halepensis* forests in the semi-arid regions of Israel are not fully adapted to withstand climatic deviations such as the sequence of two consecutive drought periods experienced during 1993–2011 (Fig. 1).

In addition to the divergent performance trend, the two regions (intermediate and arid compared to humid) differed in their responses to the second drought period, which was characterized by a negative trend in NDVI in the arid and intermediate regions and a stable state in the humid region (Fig. 3d). This contrasts with the responses to the first drought period, when all forests responded negatively (Fig. 3b). Two hypotheses may be offered to explain this difference. First, the second drought was relatively moderate (Fig. 1a), therefore, unlike the first extreme drought, rainfall may still have been sufficient to maintain a stable quantity of green biomass in the humid region, even though growth was halted – hence, the zero ΔNDVI (Fig. 3d). In the dry region, however, water availability may already have been low enough to induce drought damage such as defoliation, lower leaf production and tree mortality – hence the negative ΔNDVI (Fig. 3d).

The second hypothesis is related to the recovery from the damage caused by the first, extreme drought (Fig. 3b). This recovery could be quicker in the humid region, since both soil water storage and tree physiological status were probably not as close to limiting levels as in the arid region. However, in the arid region, the drought stress experienced during 1998–2000 could have led to vulnerable physiological state so that many of the trees had not yet recovered by 2005, and therefore exhibited greater and more apparent drought damage during the second drought period of 2005–2011.

Lagging responses to drought were previously observed, for example, in the Rocky Mountains of northern Colorado (USA), where following an early-season drought event, mortality risk of *Picea engelmannii* increased over the subsequent 5 years and mortality risk of *Abies lasiocarpa* increased over the subsequent 11 years (Bigler et al., 2007). "Memory effects" (Schwinning et al., 2004) were previously observed in many water-limited ecosystems (Potts et al., 2006; Richard et al., 2008; Sarris et al., 2007). We hypothesize that critical physiological thresholds of *P. halepensis* were passed (Girard et al., 2012) in the dry region during the extreme drought of 1998–2000, and the resulting damage was carried over to the moderate drought of 2005–2011, and added to the higher impact of drought in the arid region.

Dendrochronological analysis of three sites along the rainfall gradient revealed a pattern that matches our remote sensing findings (Fig. 4). In the arid site the second drought led to very limited

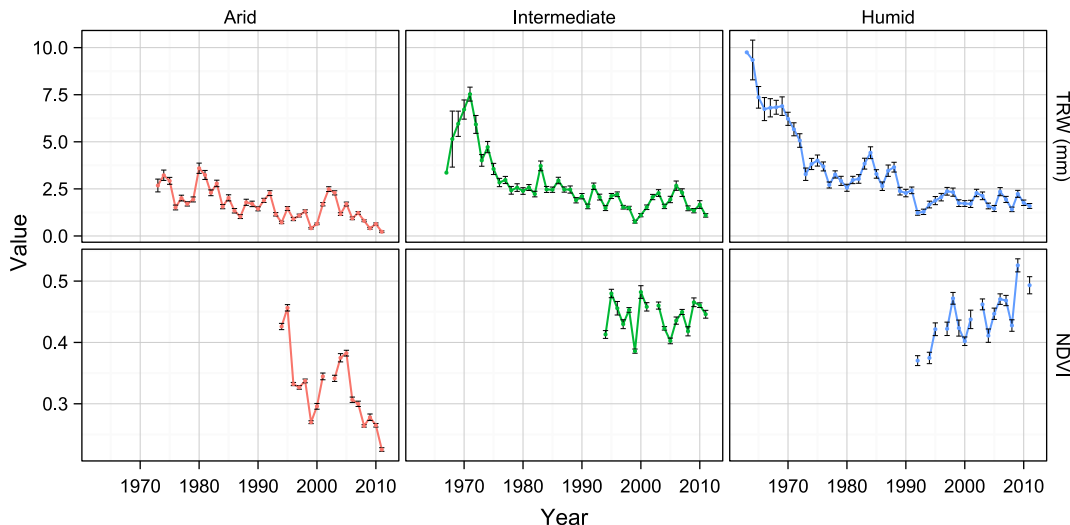


Fig. 4. Tree Ring Width (TRW; upper panel) and NDVI (lower panel) values as function of year, obtained for three sites along the rainfall gradient. Average values \pm one standard error are shown for both TRW ($n = 30$ trees for each site) and for NDVI ($n = 10, 11$ and 11 pixels of (30×30) m for the arid, intermediate and humid sites, respectively).

growth in 2011. In the intermediate site the narrowest tree-rings were found during the first drought, while the second drought effect was smaller. In the humid site both droughts did not have a noticeable effect on tree growth. In fact, the lowest TRW in the humid site was observed in 1992, which was an unusually wet and cold year, probably due to growth inhibition under low temperatures or snow damage (while growth increased in the arid and intermediate sites in that year, likely due to high water availability). Dendrochronological data provides further evidence for the diverging performance trend along the rainfall gradient. In addition, the fact that in the arid site the lowest TRW value was reached in the last year of the second drought supports the hypothesis of accumulated drought damage.

We hypothesize that the non-linear pattern (Fig. 2e) of performance deviations as related to annual rainfall may be attributed to the interplay between the threshold of climatic limitation on forest performance and the degree of temporal autocorrelation of performance. An analogous framework was previously offered to explain tree-ring width variation among trees in a given site (Fritts et al., 1965); it encompasses two complementary hypotheses. First, the correlation between resource availability, e.g., soil moisture, as determined mainly by rainfall amount, and tree performance, e.g., tree-ring width, becomes stronger as the resource becomes more limiting to the physiological processes of the tree. Thus, in progressing from humid locations towards arid locations, the sensitivity of forest performance to rainfall increases (Fritts et al., 1965). For example, Knutson and Pyke (2008) show that correlations between *Juniperus occidentalis* and *P. ponderosa* growth with climate were stronger at low-elevation (drier) sites than at high-elevation sites in southern Oregon, USA.

The second hypothesis suggests that a decrease in sensitivity of performance to rainfall at the most arid locations could result from increasing temporal autocorrelation at those extreme locations (Fritts et al., 1965) because trees may rely on soil water that accumulated during longer periods than one year (Sarris et al., 2007). In other words, the correlation with previous-year rainfall may weaken because tree performance becomes influenced by a sequence of past rainy seasons and not only by the most recent one.

Taken together, the long-term performance trends (Fig. 2a and d) and the short-term performance deviations correlation with rainfall (Fig. 2b and e) help to identify three zones, characterized by differing responses of *P. halepensis* forests to climate. The arid

zone (<350 mm) was characterized by the most negative long-term performance trend, and performance deviations were moderately correlated with rainfall. We hypothesize that this area experienced severe drought damage, which was also carried over to subsequent years, causing a declining pattern of performance and lower responsiveness to annual rainfall amount. It may be expected that additional drought periods in the near future will lead to further mortality and decline in those forests.

The intermediate zone (350–500 mm) was characterized by moderate to zero performance declines, along with high correlation of short-term performance deviations with annual rainfall. We hypothesize that this area currently contains the limit to sustainable distribution of planted *P. halepensis* forests, because it showed only moderate decline during the whole study period, and because its higher correlation between performance deviations and annual rainfall suggests increased resilience in face of climatic deviations. In this case a recovery during the years following drought may be expected.

The humid zone (>500 mm) was characterized by a trend of moderately increasing performance along with a small effect of rainfall on short-term performance deviations. We hypothesize that this area is where the role of water availability as a limiting factor to *P. halepensis* becomes weaker (Zavala et al., 2000). It may be therefore expected that these forests will not be severely affected by future drought periods of the same magnitude as experienced during 1994–2011.

The present study, using remotely sensed NDVI and precipitation records interpolation, enabled considering a broad spatial extent while still working within a single system (i.e. single-species planted forests) along a climatic gradient. The spatio-temporal data on coupled forest performance and rainfall amount trajectories was transformed into continuous descriptors depicting forest performance trends and sensitivity to rainfall amount, thus allowing identification of thresholds in a non-linear system. The observed diverging performance trend in *P. halepensis* along the climatic gradient (i.e. stable performance at the humid end vs. steep decline at the arid edge) may be attributed to the varied importance of water availability as a limiting factor. Moreover, in the most arid region (<350 mm), reduced effect of rainfall on performance deviations, steep performance decline, and differing responses to the first and second droughts were detected. It is proposed that the latter phenomena imply higher importance of

multi-annual accumulated and carried-over drought stress effects at these extreme locations. The present approach may be beneficial in both management-monitoring (e.g. identifying forests deviating from the general climate-performance relation) and scientific aspects of forest and climatic change research (e.g. studying the spatial pattern of climate-performance relation and its environmental determinants).

Acknowledgements

We thank David Brand, Israel Tauber, Ronen Talmor, Efrat Shefer and Shmuel Sprintsin for providing helpful information and Resources. The Israeli Forest Service (KKL) willingly provided forests GIS layers and purchased the equipment and software for the dendrochronological analysis. We thank Talia Horovitz and the Israel Meteorological Service for providing the rainfall data. We thank Arnon Cooper, Or Livni, Adam Wattenberg and Yoni Waitz for assistance in field work. This study is supported by a grant from the Chief Scientist of the Israeli Ministry of Agriculture and Rural Development and the Jewish National Fund.

Appendix A. Supplementary material

Supplementary data associated with this article can be found, in the online version, at <http://dx.doi.org/10.1016/j.foreco.2013.08.009>.

References

- Akaike, H., 1974. A new look at the statistical model identification. *IEEE Trans. Autom. Control* AC19, 716–723.
- Allen, C.D., Macalady, A.K., Chenchouni, H., Bachelet, D., McDowell, N., Vennetier, M., Kitzberger, T., Rigling, A., Breshears, D.D., Hogg, E.H., Gonzalez, P., Fensham, R., Zhang, Z., Castro, J., Demidova, N., Lim, J.H., Allard, G., Running, S.W., Semerci, A., Cobb, N., 2010. A global overview of drought and heat-induced tree mortality reveals emerging climate change risks for forests. *For. Ecol. Manage.* 259, 660–684.
- Anderson, L.O., Malhi, Y., Aragao, L.E.O.C., Ladle, R., Arai, E., Barbier, N., Phillips, O., 2010. Remote sensing detection of droughts in Amazonian forest canopies. *New Phytol.* 187, 733–750.
- Babst, F., Poultre, B., Trouet, V., Tan, K., Neuwirth, B., Wilson, R., Carrer, M., Grabner, M., Tegel, W., Levanic, T., 2013. Site-and species-specific responses of forest growth to climate across the European continent. *Glob. Ecol. Biogeogr.* 22, 706–717.
- Bigler, C., Gavin, D.G., Gunning, C., Veblen, T.T., 2007. Drought induces lagged tree mortality in a subalpine forest in the Rocky Mountains. *Oikos* 116, 1983–1994.
- Breshears, D.D., Allen, C.D., 2002. The importance of rapid, disturbance-induced losses in carbon management and sequestration. *Glob. Ecol. Biogeogr.* 11, 1–5.
- Breshears, D.D., Cobb, N.S., Rich, P.M., Price, K.P., Allen, C.D., Balice, R.G., Romme, W.H., Kastens, J.H., Floyd, M.L., Belnap, J., Anderson, J.J., Myers, O.B., Meyer, C.W., 2005. Regional vegetation die-off in response to global-change-type drought. *Proc. Nat. Acad. Sci. USA* 102, 15144–15148.
- Breshears, D.D., Lopez-Hoffman, L., Graumlich, L.J., 2011. When ecosystem services crash: preparing for big, fast, patchy climate change. *Ambio* 40, 256–263.
- Carnicer, J., Coll, M., Ninyerola, M., Pons, X., Sanchez, G., Penuelas, J., 2011. Widespread crown condition decline, food web disruption, and amplified tree mortality with increased climate change-type drought. *Proc. Nat. Acad. Sci. USA* 108, 1474–1478.
- Carrera-Hernandez, J.J., Gaskin, S.J., 2007. Spatio temporal analysis of daily precipitation and temperature in the Basin of Mexico. *J. Hydrol.* 336, 231–249.
- Chander, G., Markham, B.L., Helder, D.L., 2009. Summary of current radiometric calibration coefficients for Landsat MSS, TM, ETM+, and EO-1 ALI sensors. *Rem. Sens. Environ.* 113, 893–903.
- Di Piazza, A., Lo Conti, F., Noto, L.V., Viola, F., La Loggia, G., 2011. Comparative analysis of different techniques for spatial interpolation of rainfall data to create a serially complete monthly time series of precipitation for Sicily, Italy. *Int. J. Appl. Earth Obs. Geoinf.* 13, 396–408.
- Eckstein, D., Bauch, J., 1969. Beitrag zur rationalisierung eines dendrochronologischen verfahrens und zur analyse seiner aussagesicherheit. *Forstwiss. Centralbl.* 88, 230–250.
- Fritts, H.C., Smith, D.G., Cardis, J.W., Budelsky, C.A., 1965. Tree-ring characteristics along a vegetation gradient in northern Arizona. *Ecology* 46, 393–401.
- Galiano, L., Martinez-Vilalta, J., Lloret, F., 2011. Carbon reserves and canopy defoliation determine the recovery of Scots pine 4 yr after a drought episode. *New Phytol.* 190, 750–759.
- Giorgi, F., Lionello, P., 2008. Climate change projections for the Mediterranean region. *Glob. Planet. Change* 63, 90–104.
- Girard, F., Vennetier, M., Guibal, F., Corona, C., Ouarmim, S., Herrero, A., 2012. *Pinus halepensis* Mill. crown development and fruiting declined with repeated drought in Mediterranean France. *Eur. J. For. Res.* 131, 919–931.
- Goovaerts, P., 2000. Geostatistical approaches for incorporating elevation into the spatial interpolation of rainfall. *J. Hydrol.* 228, 113–129.
- Goslee, S.C., 2011. Analyzing remote sensing data in R: the landsat package. *J. Stat. Softw.* 43, 1–25.
- Hampe, A., Petit, R.J., 2005. Conserving biodiversity under climate change: the rear edge matters. *Ecol. Lett.* 8, 461–467.
- Huang, C.Y., Asner, G.P., Barger, N.N., Neff, J.C., Floyd, M.L., 2010. Regional aboveground live carbon losses due to drought-induced tree dieback in pinon-juniper ecosystems. *Rem. Sens. Environ.* 114, 1471–1479.
- Johnson, J.B., Omland, K.S., 2004. Model selection in ecology and evolution. *Tr. Ecol. Evol.* 19, 101–108.
- Kafle, H.K., Bruins, H.J., 2009. Climatic trends in Israel 1970–2002: warmer and increasing aridity inland. *Clim. Change* 96, 63–77.
- Knutson, K.C., Pyke, D.A., 2008. Western juniper and ponderosa pine ecotonal climate-growth relationships across landscape gradients in southern Oregon. *Can. J. For. Res. – Rev. Can. Rech. For.* 38, 3021–3032.
- Levin, N., Saaroni, H., 1999. Fire weather in Israel—synoptic climatological analysis. *GeoJournal* 47, 523–538.
- Linares, J.C., Camarero, J.J., Carreira, J.A., 2009. Interacting effects of changes in climate and forest cover on mortality and growth of the southernmost European fir forests. *Glob. Ecol. Biogeogr.* 18, 485–497.
- Linares, J.C., Delgado-Huertas, A., Carreira, J.A., 2011. Climatic trends and different drought adaptive capacity and vulnerability in a mixed *Abies pinsapo*–*Pinus halepensis* forest. *Clim. Change* 105, 67–90.
- Liphschitz, N., Biger, G., 2001. Past distribution of Aleppo pine (*Pinus halepensis*) in the mountains of Israel (Palestine). *Holocene* 11, 427–436.
- Lloret, F., Lobo, A., Estevan, H., Maisongrande, P., Vayreda, J., Terradas, J., 2007. Woody plant richness and NDVI response to drought events in Catalonia (northeastern Spain) forests. *Ecology* 88, 2270–2279.
- Matyas, C., 2010. Forecasts needed for retreating forests. *Nature* 464, 1271.
- McDowell, N.G., Beerling, D.J., Breshears, D.D., Fisher, R.A., Raffa, K.F., Stitt, M., 2011. The interdependence of mechanisms underlying climate-driven vegetation mortality. *Tr. Ecol. Evol.* 26, 523–532.
- Osem, Y., Ginsberg, P., Tauber, I., Atzmon, N., Perevolotsky, A., 2008. Sustainable management of Mediterranean planted coniferous forests: an Israeli definition. *J. For.* 106, 38–46.
- Osem, Y., Zangy, E., Bney-Moshe, E., Moshe, Y., Karni, N., Nisan, Y., 2009. The potential of transforming simple structured pine plantations into mixed Mediterranean forests through natural regeneration along a rainfall gradient. *For. Ecol. Manage.* 259, 14–23.
- Pasho, E., Camarero, J.J., de Luis, M., Vicente-Serrano, S.M., 2011. Impacts of drought at different time scales on forest growth across a wide climatic gradient in north-eastern Spain. *Agric. For. Meteorol.* 151, 1800–1811.
- Pebesma, E.J., 2004. Multivariable geostatistics in S: the gstat package. *Comput. Geosci.* 30, 683–691.
- Perevolotsky, A., Sheffer, E., 2009. Forest management in Israel – the ecological alternative. *Isr. J. Plant Sci.* 57, 35–48.
- Pettorelli, N., Vik, J.O., Mysterud, A., Gaillard, J.-M., Tucker, C.J., Stenseth, N.C., 2005. Using the satellite-derived NDVI to assess ecological responses to environmental change. *Tr. Ecol. Evol.* 20, 503–510.
- Potts, D.L., Huxman, T.E., Cable, J.M., English, N.B., Ignace, D.D., Elts, J.A., Mason, M.J., Weltzin, J.F., Williams, D.G., 2006. Antecedent moisture and seasonal precipitation influence the response of canopy-scale carbon and water exchange to rainfall pulses in a semi-arid grassland. *New Phytol.* 170, 849–860.
- R Development Core Team, 2012. R: A language and environment for statistical computing. In: R Foundation for Statistical Computing, Vienna, Austria. ISBN 3-900051-07-0, <<http://www.R-project.org/>>.
- Rich, P.M., Breshears, D.D., White, A.B., 2008. Phenology of mixed woody-herbaceous ecosystems following extreme events: net and differential responses. *Ecology* 89, 342–352.
- Richard, Y., Martiny, N., Fauchereau, N., Reason, C., Rouault, M., Vigaud, N., Tracol, Y., 2008. Interannual memory effects for spring NDVI in semi-arid South Africa. *Geophys. Res. Lett.* 35, 1–6.
- Rouse, J.W., Haas, R.H., Schell, J.A., Deering, D.W., 1973. Monitoring vegetation systems in the Great Plains with ERTS. In: 3rd ERTS Symposium, NASA SP-351 I, pp. 309–317.
- Sanchez-Salguero, R., Navarro-Cerrillo, R.M., Camarero, J.J., Fernandez-Concio, A., 2010. Drought-induced growth decline of Aleppo and maritime pine forests in south-eastern Spain. *For. Syst.* 19, 458–469.
- Sanchez-Salguero, R., Navarro-Cerrillo, R.M., Julio Camarero, J.J., Fernandez-Concio, A., 2012. Selective drought-induced decline of pine species in southeastern Spain. *Clim. Change* 113, 767–785.
- Sarris, D., Christodoulakis, D., Korner, C., 2007. Recent decline in precipitation and tree growth in the eastern Mediterranean. *Glob. Change Biol.* 13, 1187–1200.
- Sarris, D., Christodoulakis, D., Korner, C., 2011. Impact of recent climatic change on growth of low elevation eastern Mediterranean forest trees. *Clim. Change* 106, 203–223.
- Schielzeth, H., 2010. Simple means to improve the interpretability of regression coefficients. *Meth. Ecol. Evol.* 1, 103–113.
- Schiller, G., 2000. Ecophysiology of *Pinus halepensis* Mill. and *P. brutia* Ten. In: Nee'man, G.T.L. (Ed.), *Ecology, Biogeography and Management of Pinus Halepensis and P. Brutia Forest Ecosystems in the Mediterranean Basin*. Backhuys Publishers, Leiden, The Netherlands, pp. 51–65.

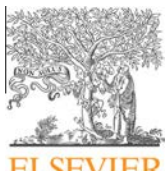
- Schiller, G., Ungar, E.D., Genizi, A., 2005. Is tree fate written in its tree rings? Characterization of trees in Kramim forest following the 1998/99 dry winter. *Yaar*, 18–25 (In Hebrew).
- Schiller, G., Ungar, E.D., Cohen, S., Moshe, Y., Atzmon, N., 2009. Aspect effect on transpiration of *Pinus halepensis* in Yatir forest. *Yaar* 11, 14–19 (In Hebrew).
- Schwinning, S., Sala, O.E., Loik, M.E., Ehleringer, J.R., 2004. Thresholds, memory, and seasonality: understanding pulse dynamics in arid/semi-arid ecosystems. *Oecologia* 141, 191–193.
- Shaw, J.D., Steed, B.E., DeBlander, L.T., 2005. Forest Inventory and Analysis (FIA) annual inventory answers the question: what is happening to pinyon-juniper woodlands? *J. For.* 103, 280–285.
- Song, C., Woodcock, C.E., Seto, K.C., Lenney, M.P., Macomber, S.A., 2001. Classification and change detection using Landsat TM data: when and how to correct atmospheric effects? *Rem. Sens. Environ.* 75, 230–244.
- Tucker, C.J., 1979. Red and photographic infrared linear combinations for monitoring vegetation. *Rem. Sens. Environ.* 8, 127–150.
- Ungar, E.D., Rotenberg, E., Raz-Yaseef, N., Cohen, S., Yakir, D., Schiller, G., 2013. Transpiration and annual water balance of Aleppo pine in a semiarid region: implications for forest management. *For. Ecol. Manage.* 298, 39–51.
- Verbyla, D., 2008. The greening and browning of Alaska based on 1982–2003 satellite data. *Glob. Ecol. Biogeogr.* 17, 547–555.
- Vicente-Serrano, S.M., 2007. Evaluating the impact of drought using remote sensing in a Mediterranean, semi-arid region. *Nat. Hazard.* 40, 173–208.
- Vicente-Serrano, S.M., Saz-Sánchez, M.A., Cuadrat, J.M., 2003. Comparative analysis of interpolation methods in the middle Ebro Valley (Spain): application to annual precipitation and temperature. *Clim. Res.* 24, 161–180.
- Vicente-Serrano, S.M., Beguería, S., Lopez-Moreno, J.I., 2010a. A multiscalar drought index sensitive to global warming: the standardized precipitation evapotranspiration index. *J. Clim.* 23, 1696–1718.
- Vicente-Serrano, S.M., Beguería, S., Lopez-Moreno, J.I., Angulo, M., El Kenawy, A., 2010b. A new global 0.5° Gridded Dataset (1901–2006) of a multiscalar drought index: comparison with current drought index datasets based on the palmer drought severity index. *J. Hydrometeorol.* 11, 1033–1043.
- Vicente-Serrano, S.M., Lasanta, T., Gracia, C., 2010c. Aridification determines changes in forest growth in *Pinus halepensis* forests under semiarid Mediterranean climate conditions. *Agric. For. Meteorol.* 150, 614–628.
- Vicente-Serrano, S.M., Gouveia, C., Camarero, J.J., Beguería, S., Trigo, R., López-Moreno, J.I., Azorín-Molina, C., Pasho, E., Lorenzo-Lacruz, J., Revuelto, J., Morán-Tejeda, E., Sanchez-Lorenzo, A., 2013. Response of vegetation to drought time-scales across global land biomes. *Proc. Nat. Acad. Sci. USA* 110, 52–57.
- Vila, B., Vennetier, M., Ripert, C., Chandioux, O., Liang, E., Guibal, F., Torre, F., 2008. Has global change induced divergent trends in radial growth of *Pinus sylvestris* and *Pinus halepensis* at their bioclimatic limit? The example of the Sainte-Baume forest (south-east France). *Ann. For. Sci.* 65, 709p701–709p709.
- Volcani, A., Karniel, A., Svoray, T., 2005. The use of remote sensing and GIS for spatio-temporal analysis of the physiological state of a semi-arid forest with respect to drought years. *For. Ecol. Manage.* 215, 239–250.
- Wang, X., Piao, S., Ciais, P., Li, J., Friedlingstein, P., Koven, C., Chen, A., 2011. Spring temperature change and its implication in the change of vegetation growth in North America from 1982 to 2006. *Proc. Nat. Acad. Sci. USA* 108, 1240–1245.
- Yuhas, A.N., Scuderi, L.A., 2009. MODIS-derived NDVI characterisation of drought-induced evergreen Dieoff in Western North America. *Geogr. Res.* 47, 34–45.
- Zavala, M.A., Espelta, J.M., Retana, J., 2000. Constraints and trade-offs in Mediterranean plant communities: the case of holm oak-Aleppo pine forests. *Bot. Rev.* 66, 119–149.
- Zhu, W., Tian, H., Xu, X., Pan, Y., Chen, G., Lin, W., 2012. Extension of the growing season due to delayed autumn over mid and high latitudes in North America during 1982–2006. *Glob. Ecol. Biogeogr.* 21, 260–271.

3.2 Interplay between the effects of local and regional environmental factors on forest performance

This chapter addresses the knowledge gap regarding the relative importance of local vs. regional environmental conditions in determining forest response to drought. It was found that the difference between contrasting habitats – north- and south-facing aspects – linearly diminishes when rainfall amount is reduced. However, south-facing aspects still reach a lower absolute level of performance, which can explain the significantly higher tree mortality.

The results of this study are described in Dorman *et al.* (2013b) (see below).

Supplementary material for this chapter appears in Section 6.2.



Homogenization in forest performance across an environmental gradient – The interplay between rainfall and topographic aspect



Michael Dorman ^{a,*}, Tal Svoray ^a, Avi Peregolotsky ^b

^a Department of Geography and Environmental Development, Ben-Gurion University of the Negev, Beer-Sheva 84105, Israel

^b Department of Agronomy and Natural Resources, Agricultural Research Organization, Volcani Ctr, Bet Dagan 50250, Israel

ARTICLE INFO

Article history:

Received 25 May 2013

Received in revised form 12 August 2013

Accepted 14 August 2013

Available online 13 September 2013

Keywords:

Aerial photography

Landsat

Tree mortality

Normalized Difference Vegetation Index (NDVI)

Pinus halepensis

Solar radiation

ABSTRACT

This study aimed to investigate the interaction between local and regional environmental factors that affect forest performance during drought periods. In previous studies, contradictory results regarding the effect of aspect on forests performance, under different settings, were reported. However, each study focused on a different forest ecosystem at a different time frame, making synthesis inadequate. Monoculture planted *Pinus halepensis* forests in Israel, covering a broad climatic gradient (200–850 mm annual rainfall), form a suitable study system to address this question.

We used remote sensing and GIS methods to observe a large number of afforested stands over a wide area at high resolution. Normalized Difference Vegetation Index (NDVI), obtained from Landsat satellite images for 14 years between 1994 and 2011, served as an inclusive measure of forest performance. Data on the examined environmental factors were obtained from spatially interpolated annual rainfall maps and a topographic aspects map. The effects of aspect on NDVI were evaluated separately for three regions along the rainfall gradient: arid (200–350 mm), intermediate (350–500 mm), and humid (500–850 mm).

During the studied period, NDVI declined in the arid region but remained constant in the intermediate and humid regions. NDVI was positively related to annual rainfall in all three regions. The effect of aspect on NDVI was positively associated with rainfall in the arid region, but not in the intermediate and humid regions. In other words, forest performance homogenization across local habitats occurred in the arid region under drought stress. Relatively wet years were characterized by high NDVI values (~0.4), with large differences (~0.025) between northern and southern aspects, whereas dry years were characterized by low NDVI values (~0.3) and small differences (~0.01).

The present study supports the concept that under severe drought stress forest performance becomes more homogeneous across local habitats, both temporally (in drought years) and spatially (towards the arid forest boundary). Performance homogenization may occur when low soil water levels are reached, and climatic conditions become the dominant limiting factor. When water availability is high enough, differential performance responses among local habitats are maintained. We evaluated the trends and relations among local and regional environmental factors on performance, and assessed their relative effect sizes. Such an evaluation is essential to link local and global studies aimed at predicting the fate of forests facing global climate change.

© 2013 Elsevier B.V. All rights reserved.

1. Introduction

Large-scale decline and mortality of forests are occurring with increasing frequency worldwide, and interest in various aspects of this phenomenon is similarly increasing. These aspects range from the physiological mechanisms involved in the process (Anderegg et al., 2012; Chaot et al., 2012), to the global carbon budget (Ma et al., 2012) and implications for ecosystem functioning (Anderegg et al., 2013a; Royer et al., 2011). However, one of the

main knowledge gaps in this field concerns the factors determining spatial and temporal patterns of forest mortality, at both regional and local spatial scales (Allen et al., 2010).

On the regional scale, mortality events are often reported from the arid edge of the climatic water-availability gradient (Matyas, 2010; Michaelian et al., 2011; Sanchez-Salguero et al., 2012). However, the effects of local site characteristics, e.g., soil, elevation, topographic aspect, slope and topographic position, in determining forest responses to drought, are not well understood, and contradictory results have been obtained from different studies (see below). Moreover, the interplay between local and regional factors is often ignored, because most studies deal with natural

* Corresponding author. Tel.: +972 86479054.

E-mail address: michael.dorman@mail.huji.ac.il (M. Dorman).

ecosystems in which changes in the forest community occur along regional, i.e., climatic, gradients. This makes comparison between the effects of local-scale factors in different locations inadequate. In the present study, we aimed to investigate quantitatively the interaction between local and regional environmental effects on forest performance during drought, and considered that the most suitable pair of factors for this purpose comprised rainfall gradient (a regional factor) and topographic aspect (a local factor).

Topographic aspect is one of the important local environmental factors affecting vegetation performance (Nevo, 2012; Svoray and Karnieli, 2011; Vicente-Serrano et al., 2012). Aspect affects water availability for plants, since in the northern hemisphere south-facing slopes receive more solar radiation than north-facing ones. This results in more rapid soil moisture loss (Pigott and Pigott, 1993) by means of “direct and indirect influences on solar radiation, surface temperature, evaporation, soil moisture, and precipitation of an area” (Huang and Anderegg, 2012). In water-limited ecosystems this results in higher productivity on northern aspects than on southern aspects (e.g., Coble et al., 2001).

During a drought event the effects of local site quality on forest performance characteristics, such as trunk growth rate and green biomass production or mortality, are not straightforward. In some cases, higher forest mortality rates following drought were observed on southern aspects (Gitlin et al., 2006; Huang and Anderegg, 2012; Worrall et al., 2008). This is intuitively expected, as a consequence of reduced water availability and consequently narrower safety margins to buffer the physiological drought-tolerance limit. In other cases, however, increased mortality was observed on northern aspects (Guarin and Taylor, 2005). This pattern was attributed to higher tree density, which led to more intense competition for water and/or increased probability of insect outbreaks during drought. Finally, in some cases no significant effect of aspect on tree mortality was observed (Brouwers et al., 2013; Martinez-Vilalta and Pinol, 2002; Suarez et al., 2004).

A promising approach to clarifying the contradictions in the patterns of aspect-mortality relations involves taking into account the spatial nonstationarity of this relationship, especially along climatic gradients. In general, it is expected that aspect effect becomes more important as the role of water availability for vegetation development becomes more influential, for instance, in the transition from mesic to xeric environments along an aridity gradient (Sternberg and Shoshany, 2001).

Indeed, the effect of topographic aspect on performance of *Pinus halepensis* was shown to vary according to location along the rainfall gradient. Topographic aspect had a large negative effect – i.e., southern aspects had lower performance – at two arid sites with annual rainfall of 280 and 303 mm (Schiller, 1972), and a minor effect at a more humid site, with 414 mm (Olarieta et al., 2000). At even more humid sites, with 480–740 mm of annual rainfall, the effect was reversed to positive: *P. halepensis* was more abundant on southern aspects, and was gradually replaced by *Quercus ilex*, initially on northern aspects and then also on southern aspects (Zavala et al., 2000). However, an opposite pattern was observed in the temporal domain: Volcani et al. (2005) showed that in Yatir Forest (southern Israel; 236 mm average annual rainfall during 1985–2011) spatial variation in the Normalized Difference Vegetation Index (NDVI) was associated with aspect in a wet year (360 mm), but became insignificant during drought (157 mm). Similarly, in a study of *Pinus sylvestris* forests in an inner-alpine valley Vacchiano et al. (2012) showed that Enhanced Vegetation Index (EVI) values obtained from the Moderate Resolution Imaging Spectroradiometer (MODIS) were not correlated with radiation amount following a drought year, whereas they were correlated in several other years.

The NDVI is the most commonly used remote sensing index in ecological studies (Rouse et al., 1973; Tucker, 1979); in the present

study it served as a measure of forest performance, reflecting the quantity and state of the green biomass (Pettorelli et al., 2005; Wang et al., 2011) in a given location in a given year. The inter-annual variation in NDVI values of *P. halepensis* forests was found to be related to drought intensity in previous studies (Lloret et al., 2007; Vicente-Serrano et al., 2010; Volcani et al., 2005).

P. halepensis grows naturally in the Mediterranean region; its natural distribution is limited by a minimum temperature of -10°C and minimum annual precipitation of 450 mm (Liphschitz and Biger, 2001; Schiller, 2000). Planted forests cover about 8% of the Mediterranean climatic zone in Israel (Osem et al., 2008), and are dominated (~75%) by conifers, of which *P. halepensis* is the most common species (Perevolotsky and Sheffer, 2009). The 25–75% quartile range of planting years in the forests examined in the present study is 1961–1970 (Israel Forest Service GIS layer, 2011), during which *P. halepensis* was planted in a wide range of climatic conditions – from annual rainfall of 850 mm in northern Israel down to 200 mm in the south – which extended beyond the lower limit of precipitation in its natural distribution (Osem et al., 2008). Recently, increased mortality of *P. halepensis* was observed in the planted forests of Israel, following the droughts of 1998–2000 and 2005–2011 (Dorman et al., 2013; Schiller et al., 2005, 2009; Ungar et al., 2013), and similar observations were made elsewhere in the Mediterranean region (Girard et al., 2011, 2012; Sarris et al., 2007; Vicente-Serrano et al., 2010).

In Israel's arid Yatir Forest, the effect of aspect on the NDVI was lower in a drought year than in a wet one (Volcani et al., 2005). In the present study, by focusing on aspect and annual rainfall as examples of local and regional environmental factors, respectively, we aimed to investigate the balance between the two determinants of forest performance. Specifically, we investigated several aspects of the spatio-temporal characteristics of the effects of topographic aspect on forest performance:

1. Spatial scope – What is the spatial scope of the phenomenon (i.e. reduction of aspect effect on performance in drought years)? Is it confined to relatively arid regions or does it occur in more mesic regions as well?
2. Resilience and temporal pattern – How long does the difference in performance between northern and southern aspects remains diminished following drought? Is the previous state recovered after wet year/s?
3. Relationship to climatic condition – How does annual rainfall relate to the difference in performance between northern and southern aspects in a given year? Does the diminished difference among habitats characterize extreme drought years only – i.e., is there a “threshold” rainfall amount? – or does the difference change linearly with the annual rainfall?

2. Materials and methods

2.1. Study area

The study area encompassed all *P. halepensis* forests located in central and northern Israel and aged above 24 years at 1994 (Fig. 1a). The forests extend across a climatic gradient from semi-arid to Mediterranean conditions, i.e., annual rainfall ranging from 200 to 850 mm. The climate in the region is characterized by winter rains occurring mainly during December through March, and a relatively long, dry, hot summer (Osem et al., 2009).

Lahav forest, the second largest forest in the arid part of the study area (200–350 mm), was chosen for tree mortality examination (see Section 2.5). This forest received an average of 280 mm during the period 1985–2011.

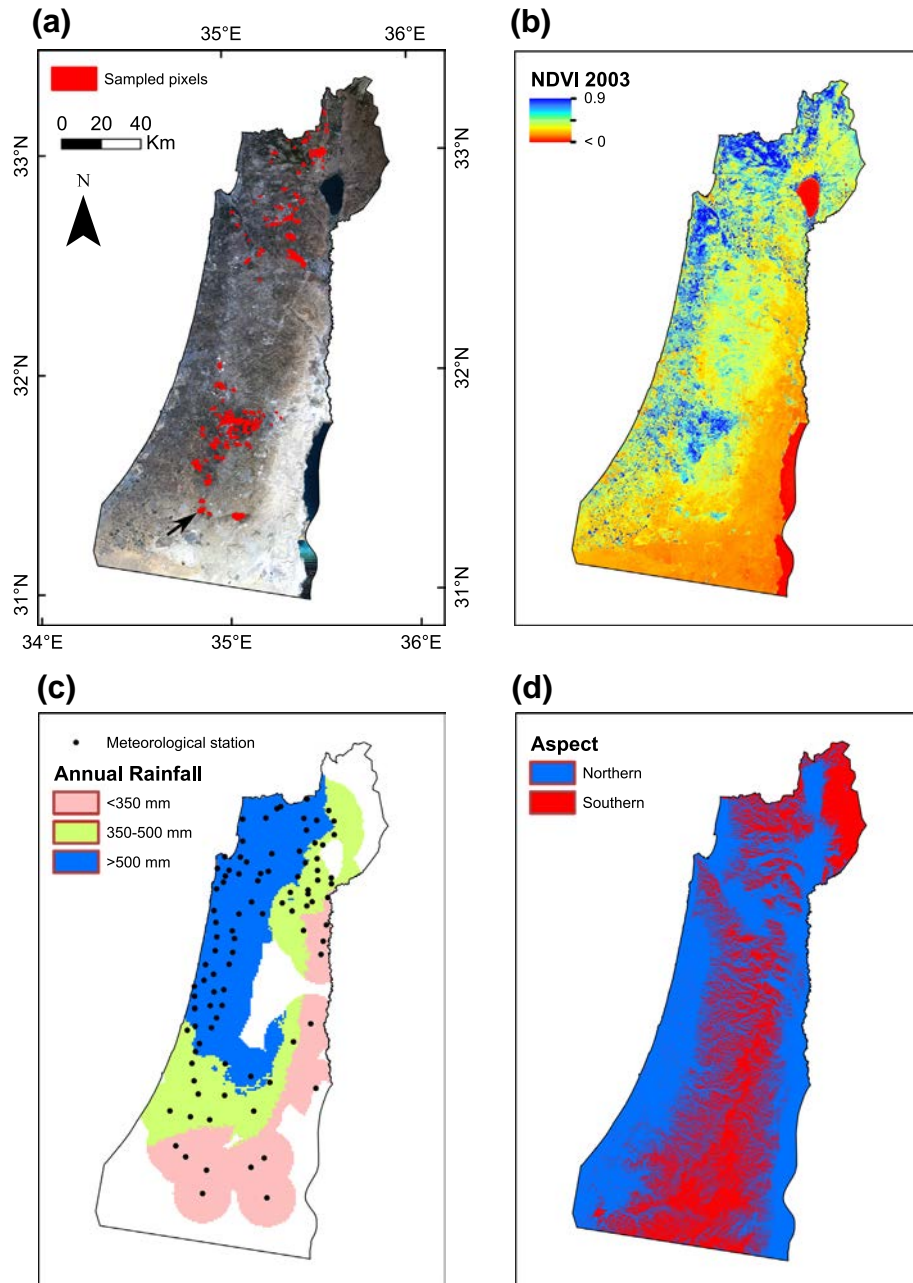


Fig. 1. (a) NDVI sampling locations (4020 pixels, each covering 90×90 m) in planted *P. halepensis* forests in Israel. Symbol size is exaggerated in order to make locations visible. The background is an RGB image prepared from a pair of Landsat-5 satellite images obtained on 11th September 2003. A black arrow marks the location of Lahav forest (see Fig. 5). (b) NDVI image of the studied area, calculated by using a pair of Landsat-5 satellite images obtained on 11th September 2003. NDVI values used in this study were extracted into the 4020 pixels (Fig. 1a) from this image and 13 others, obtained for 14 different years during 1985–2011. (c) Average annual rainfall during 1985–2011, classified into three categories – 200–350, 350–500, and 500–850 mm – and locations of 96 meteorological stations that provide data used in this study. (d) Estimated radiation amount, classified into two categories: above (“southern aspect”) and below/equal to (“northern aspect”) the median encountered among sampling locations. Note that the term “aspect” is not used here in its narrow sense, but as a label for locations differing in their radiation load due to topographic position. Radiation was estimated according to a 25-m DEM layer of Israel. (For interpretation of the references to color in this figure legend, the reader is referred to the web version of this article.)

2.2. Remote-sensing data

To estimate forest structural responses on a large spatial scale, 26 Landsat-5 TM and two Landsat-7 ETM+ images from the period 1994–2011 were used. Two adjacent Landsat scenes (path 174, rows 37 and 38), both from the same date, were merged to cover the area of interest, yielding a sample of 14 images of the whole study area for years 1994–1995, 1997–2000, 2003–2009, and 2011. The images were selected from a relatively short time window (8th September–16th October) at the end of the dry season,

when there was less than 10% cloud cover over the studied area. This was not found possible in the other four years of the study (1996, 2001, 2002 and 2010). There were two reasons for the choice of this seasonal time window. First, during the dry season there is less variation in water availability for the trees and, therefore, there is less within-season variation in the vegetation activity signal. Second, herbaceous vegetation is completely dry during the summer, therefore a higher proportion of the spectral signal can be attributed to *P. halepensis* trees (Vicente-Serrano et al., 2010).

Images were geometrically corrected in the AutoSync Workstation module of Erdas Imagine 2011 software (ERDAS, Atlanta, GA, USA), by using a 5th-order polynomial geometric model. The images from 2003 were chosen as the reference set for all other images in the series. The Root Mean Square Error (RMSE) was <0.5 pixel length in all cases. Radiometric calibration was based on up-to-date coefficients (Chander et al., 2009). Atmospheric correction was applied with the Dark Object Subtraction 4 method (Song et al., 2001), which was chosen because supplementary atmospheric data, such as Aerosol Optical Depth, were not available for the older images, which necessitated application of an image-based method. Manually prepared cloud masks were used to exclude clouds and cloud shadow areas from the analysis.

NDVI was calculated as:

$$\text{NDVI} = \frac{\rho_{\text{IR}} - \rho_R}{\rho_{\text{IR}} + \rho_R} \quad (1)$$

in which ρ_{IR} is the reflectivity in the near-infrared region (Landsat band 4) and ρ_R is the reflectivity in the red region (Landsat band 3) of the electromagnetic spectrum. Image processing, spatial interpolation and statistical analyses were applied by using R software (R Development Core Team, 2012). Atmospheric correction of Landsat images was done with the “landsat” package (Goslee, 2011).

The NDVI data were extracted for 4020 pixels of 90×90 m located in planted forests across Israel (Fig. 1a). NDVI values (Fig. 1b) were extracted into each 90×90 m pixel by averaging pixel values from the overlaid nine 30×30 m Landsat pixels, thus reducing the amount of data as well as the effect of geographic registration errors among satellite images. Each pixel was completely within a forest polygon planted with over 80% *P. halepensis* (according to a GIS layer obtained from the Israel Forest Service). Pixels within clouded areas in any of the 14 Landsat images were excluded, i.e., all 4020 pixels were assigned with 14 NDVI values.

2.3. Rainfall data

Annual rainfall maps with 1000-m resolution were produced by applying spatial interpolation to point data from 96 meteorological stations, for 26 rainfall seasons (1985–2011). Two geostatistical interpolation methods were evaluated for this task: Ordinary Kriging and Universal Kriging (Carrera-Hernandez and Gaskin, 2007; Di Piazza et al., 2011; Vicente-Serrano et al., 2003). Universal Kriging was examined with the seven possible combinations of three covariates that were considered to affect average rainfall amount in the studied area: elevation (Goovaerts, 2000), distance from the Mediterranean Sea, and latitude. Thus, eight interpolation procedures were evaluated, and their prediction accuracies were compared by using the mean RMSE obtained from leave-one-out cross validation. Universal Kriging with elevation as a covariate yielded the lowest average RMSE (58.2 mm) among the 26 years, therefore this method was chosen for preparing the rainfall maps. Since interpolation accuracy decreases with distance, only the area within 15 km of the nearest meteorological station was considered for analysis (Fig. 1c). Spatial interpolation of rainfall data was done with the “gstat” package (Pebesma, 2004) in R.

Maps of annual rainfall amount were used for two purposes: (1) to delineate three regions along the rainfall gradient (Fig. 1c); and (2) to extract average annual rainfall time series (Fig. 2c) for each region in order to evaluate the relationship between annual rainfall and aspect effect on NDVI (Table 2, Fig. 3).

2.4. Radiation data

A GIS-based method (Fu and Rich, 2002), implemented in ArcGIS 10.0 software (ESRI, 2012), was used to estimate integrated annual incoming amount of solar radiation over each pixel in a 25-m

resolution Digital Elevation Model (DEM) layer of Israel (Hall and Cleave, 1988). The model calculates an upward-looking hemispherical viewshed based on topography, and then uses it to calculate incoming direct and diffuse radiation from each sky direction, taking into account latitude, date and time. Thus it “accounts for atmospheric effects, site latitude and elevation, steepness (slope) and compass direction (aspect), daily and seasonal shifts of the sun angle, and effects of shadows cast by surrounding topography” (ESRI, 2012). The calculation is repeated for each pixel, producing an annual incoming solar radiation map for the entire studied area.

The 4020 examined pixels were classified as “Southern” or “Northern” aspects, according to whether the radiation amount they receive was above the median encountered among those 4020 pixels, or below/equal to it (Figs. 1c and S1). Thus we use the terms “Northern aspect” and “Southern aspect” not in their narrow sense (slopes facing the north or the south, respectively), but as a label helping the classification of our studied area into two distinct categories differing in their radiation load, while the latter was consistently evaluated based on the surrounding topography for each location.

2.5. Aerial photography

An aerial photograph of Lahav forest was used in order to contrast remote sensing findings with field information on tree mortality. A high resolution (0.25 m) RGB aerial photograph of the forest was obtained in winter 2011/2012. The photograph displays the last of two major forest mortality events that occurred in the arid region during the studied period of 1994–2011 (Shmuel Sprintsin, Israel Forest Service, personal communication), following the drought of 2005–2011 (Dorman et al., 2013; Ungar et al., 2013). The previous mortality event occurred following the drought of 1998–2000 (Schiller et al., 2005, 2009).

The studied area within Lahav forest (2.72 km^2) was selected following the same criteria applied in the regional examination (>80% *P. halepensis* aged above 24 in 1994; see Sections 2.1 and 2.2). Dead trees were identified and marked by manual interpretation of the photograph, where they were clearly distinguishable due to their gray/reddish color, compared to the green living trees (Fig. S1).

The sampled area was covered with a 30-m grid coinciding with the Landsat pixels. Each pixel was classified into northern and southern aspects according to same procedure as in the regional examination (see Section 2.4). The numbers of dead trees and annual NDVI values were also recorded for each pixel. Due to very low cloudiness in Lahav forest during Landsat image acquisition, NDVI values for Lahav forest were available for 17 years (instead of 14 years that were used in the regional examination) – all years between 1994 and 2011 except for 2002 (Fig. S2). Non-forest areas (roads, buildings, etc.) were digitized and pixels where >25% of the area was non-forest were removed from the analysis. For the remaining pixels (92.7%) the number of dead trees per 30 m^2 was calculated taking into account the proportion of forested area within the pixel.

2.6. Statistical methods

The effects of aspect on NDVI in different years and regions were evaluated by fitting Mixed Effects linear models to the data. Mixed Effects linear models were chosen because they allow incorporation of structures of correlation among observations, in our case – in space (Brown et al., 2011; Zuur et al., 2009). Otherwise, violation of independence among observations would occur (Zuur et al., 2009), because pixels that are close to each other have more similar NDVI values than those further apart. A spherical spatial correlation structure among observations was used (Pinheiro and

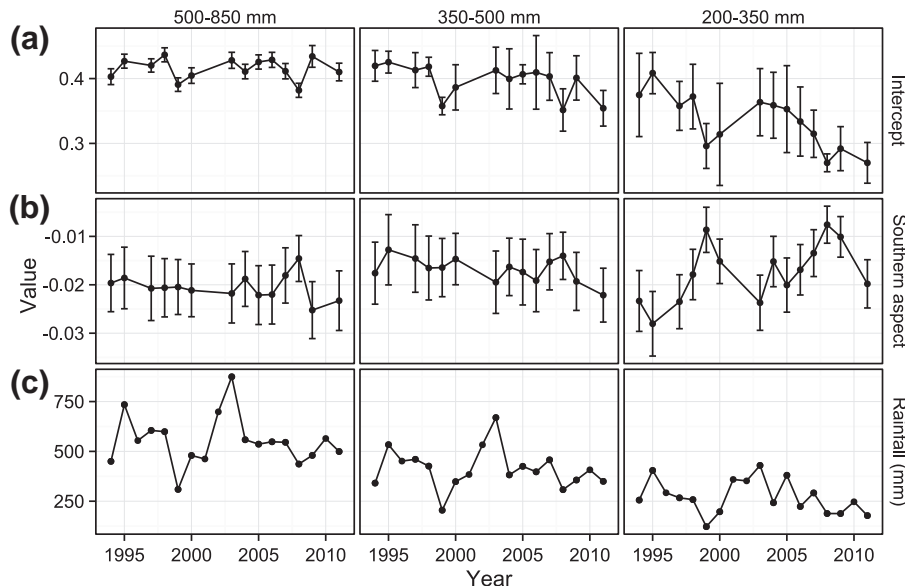


Fig. 2. Coefficients of fixed effects (Table 1) from the Mixed Effects linear models describing mean NDVI in 14 years between 1994–2011 in three climatic regions (humid, intermediate and arid): (a) intercept and (b) aspect (dummy variable for “southern aspect”). Estimates with upper and lower limits of the 95% confidence intervals are shown. (c) Average annual rainfall amount during 1994–2011 for each of the three climatic regions. Note that lines between points do not indicate continuous variation.

Bates, 2000; Zuur et al., 2009), which represented the spatially auto-correlated random effects on NDVI. Effect sizes of the examined factors were assessed according to the fixed effects estimates, with 95% confidence intervals. Mixed Effects models were fitted by using package “nlme” (Pinheiro and Bates, 2000) in R.

The effect of aspect on NDVI was examined by evaluating the model described in

$$\text{NDVI} = \beta_0 + \beta_1 * \text{Aspect} + \varepsilon \quad (2)$$

in which NDVI is the NDVI value of a given (90×90)-m pixel, Aspect is the dummy variable that represents southern aspects, i.e., the aspect dummy variable had the values of “1” and “0” in southern and northern aspect pixels, respectively, and ε is the error term.

The model described by Eq. (2) for NDVI data of each of the 14 years was evaluated separately for each of three regions: arid, 200–350 mm; intermediate, 350–500 mm; and humid, 500–850 mm. Note that “arid”, “intermediate” and “humid” do not refer to climatic regions; they are labels to enable easier reference to relative position along the rainfall gradient. An estimate and a 95% confidence interval for the intercept (β_0 in Eq. (2)) and aspect effect (β_1 in Eq. (2)) were obtained from each of the 42 (i.e., 14 years \times 3 regions) models (Fig. 2 and 3, Table 1). The coefficients with 95% confidence intervals were not standardized, and therefore were interpreted at their original scale (Schielzeth, 2010). In other words, β_0 estimates express NDVI values at northern aspects; β_1 estimates express the NDVI reduction in southern aspects compared to northern aspects. The 42 models were then used to show predicted NDVI values in northern and southern aspects in the three regions, during the examined time period (Fig. 4).

The effect of aspect on the frequency of dead trees, in Lahav forest, was evaluated using a Poisson Generalized Linear Model (GLM). The independent variable was the aspect dummy variable (southern vs. southern); the dependent variable was dead trees count; the sampling units were the 2440 30-m² cells. Since overdispersion was detected, the standard errors were corrected using a quasi-GLM model (Zuur et al., 2009, p. 226).

3. Results

The results of fitting the models (Eq. (2)) are summarized in Table 1. The estimates of intercept and aspect effects, for each climatic zone, are also plotted in Fig. 2a and 2b, respectively. The use of a Mixed Effects linear model, instead of a linear model, was favorable, according to the Akaike Information Criterion (AIC; Akaike, 1974; Zuur et al., 2009). Values of the AIC for the Mixed Effects linear models (Column “AIC” in Table 1) were better than those for the analogous linear models (Column “AIC (linear)” in Table 1) in all 42 cases, with differences ranging between 687 and 2165 AIC units.

Estimates for the intercept show differing temporal trends among the three climatic regions (Fig. 2a). The range of intercept estimates values observed over time increased with progress from the humid region (500–850 mm), through the intermediate region (350–500 mm), and towards the arid region (200–350 mm). Ranges of intercept estimates in the three respective regions were 0.38–0.44 (average = 0.42), 0.35–0.43 (average = 0.40), and 0.27–0.41 (average = 0.33). In the intermediate region, and even more so in the arid region, the final (2011) intercept estimate was significantly lower than the initial (1994) estimate, according to confidence intervals (Fig. 2a), which suggests that the NDVI declines in these two regions were moderate and steep, respectively. Linear regressions of intercept estimates as functions of time (year) were used to examine this trend. In the humid and intermediate regions no significant temporal decline of the intercept estimate was observed (slope = -0.0001 , $p > 0.1$; and slope = -0.0023 , $p > 0.05$, respectively). In the arid region, however, the intercept estimate declined significantly ($p < 0.01$) by 0.0057 NDVI units per year. This apparent divergence among climatic regions, in forest stand performance following the two drought periods of 1998–2000 and 2005–2011 was discussed elsewhere (Dorman et al., 2013) and will not be further addressed here.

Estimates of aspect effects were negative across all regions and years, and always differed significantly from zero, according to confidence intervals (Fig. 2b). This means that lower NDVI values were observed on southern aspects (Fig. 1c), as could be expected. Aspect effect estimates were lower than intercept estimates by an order of magnitude (Fig. 2 and 4) and ranged from -0.025 to

Table 1

Estimates and standard errors (SE) for the fixed effects of Mixed Effects linear models. Each row corresponds to one of the 42 evaluated models that describe NDVI as a function of aspect in three regions (humid, intermediate and arid) and in 14 years (1994–1995, 1997–2000, 2003–2009, and 2011). *P*-values are not shown since they were <0.001 in all cases. The AIC value of each model is presented under “AIC”. For comparison purposes, AIC values of the analogous linear models (i.e., ordinary linear regression) based on the same data, are presented under “AIC (linear)”.

Region	Year	Intercept		Aspect (southern)		AIC	AIC (linear)
		Estimate	SE	Estimate	SE		
Humid	1994	0.40	0.006	−0.020	0.003	−6105	−4052
Humid	1995	0.43	0.005	−0.019	0.003	−5866	−4344
Humid	1997	0.42	0.005	−0.021	0.003	−5731	−4150
Humid	1998	0.44	0.006	−0.021	0.003	−6061	−4290
Humid	1999	0.39	0.005	−0.020	0.003	−6273	−4507
Humid	2000	0.40	0.006	−0.021	0.003	−6399	−4436
Humid	2003	0.43	0.006	−0.022	0.003	−5999	−3851
Humid	2004	0.41	0.006	−0.019	0.003	−6269	−4165
Humid	2005	0.43	0.006	−0.022	0.003	−6027	−4257
Humid	2006	0.43	0.006	−0.022	0.003	−6012	−4286
Humid	2007	0.41	0.006	−0.018	0.003	−6236	−4368
Humid	2008	0.38	0.006	−0.015	0.002	−6896	−4754
Humid	2009	0.43	0.009	−0.025	0.003	−6076	−3960
Humid	2011	0.41	0.007	−0.023	0.003	−5953	−3814
Intermediate	1994	0.42	0.012	−0.018	0.003	−4353	−2546
Intermediate	1995	0.43	0.009	−0.013	0.004	−4089	−2760
Intermediate	1997	0.41	0.014	−0.015	0.004	−4144	−2740
Intermediate	1998	0.42	0.007	−0.017	0.003	−4312	−3168
Intermediate	1999	0.36	0.007	−0.016	0.003	−4534	−3308
Intermediate	2000	0.39	0.018	−0.015	0.003	−4773	−2608
Intermediate	2003	0.41	0.018	−0.019	0.003	−4329	−2590
Intermediate	2004	0.40	0.024	−0.016	0.003	−4510	−2714
Intermediate	2005	0.41	0.008	−0.017	0.003	−4250	−2839
Intermediate	2006	0.41	0.029	−0.019	0.003	−4318	−2853
Intermediate	2007	0.40	0.019	−0.015	0.003	−4560	−2744
Intermediate	2008	0.35	0.017	−0.014	0.002	−4971	−3097
Intermediate	2009	0.40	0.017	−0.019	0.003	−4497	−2871
Intermediate	2011	0.35	0.014	−0.022	0.003	−4676	−2924
Arid	1994	0.37	0.033	−0.023	0.003	−3642	−2830
Arid	1995	0.41	0.016	−0.028	0.003	−3529	−2842
Arid	1997	0.36	0.019	−0.023	0.003	−3890	−3152
Arid	1998	0.37	0.025	−0.018	0.003	−4027	−3175
Arid	1999	0.30	0.018	−0.009	0.002	−4249	−3253
Arid	2000	0.31	0.040	−0.015	0.002	−4252	−2695
Arid	2003	0.36	0.026	−0.024	0.003	−3823	−2702
Arid	2004	0.36	0.026	−0.015	0.003	−3998	−2980
Arid	2005	0.35	0.034	−0.020	0.003	−3858	−2819
Arid	2006	0.33	0.027	−0.017	0.003	−4000	−3041
Arid	2007	0.31	0.019	−0.013	0.002	−4145	−3123
Arid	2008	0.27	0.007	−0.008	0.002	−4621	−3607
Arid	2009	0.29	0.017	−0.010	0.002	−4421	−3166
Arid	2011	0.27	0.016	−0.020	0.003	−4066	−3103

Table 2

Estimates, standard errors (SE), *p*-values and adjusted R^2 values for linear regression models describing the relationships depicted in Fig. 3, i.e., of the intercept and aspect effects as functions of rainfall amount.

Region	Intercept – rainfall relation (Fig. 3a)				Aspect effect – rainfall relation (Fig. 3b)			
	Estimate	SE	<i>p</i> -value	Adj. R^2	Estimate	SE	<i>p</i> -value	Adj. R^2
Humid	7.59×10^{-5}	2.71×10^{-5}	0.0162	0.34	-1.29×10^{-6}	5.46×10^{-6}	0.8180	−0.08
Intermediate	1.48×10^{-4}	5.02×10^{-5}	0.0121	0.37	1.61×10^{-7}	6.72×10^{-6}	0.9810	−0.08
Arid	3.40×10^{-4}	9.23×10^{-5}	0.0031	0.49	-4.92×10^{-5}	1.35×10^{-5}	0.0033	0.49

−0.015 (average = −0.021), −0.022 to −0.013 (average = −0.017), and −0.028 to −0.008 (average = −0.017), in the humid, intermediate and arid regions, respectively. Again, the range of observed values was widest in the arid region, suggesting that variation among northern and southern aspects was also highest in this region. Negative correlations were found between the estimates of intercept and aspect, among years, in the humid (Pearson's correlation coefficient (P) = −0.61, $p < 0.05$) and arid (P = −0.77, $p < 0.01$) regions, but not in the intermediate region (P = 0.15, $p > 0.1$). It is apparent that in the arid region, temporal changes in aspect effect estimates

mirrored those of the intercept (compare panels “a” and “b” for the “200–350 mm” region in Fig. 2). However, according to linear regression, the aspect estimate in the arid region did not change significantly with time (slope = 0.00058, $p > 0.05$), unlike the decreasing intercept estimate in that region. In other words, it seems that in the arid region temporal fluctuations in NDVI were accompanied by fluctuations in the effect of aspect, whereas the former (but not the latter) also persistently decreased with advancing time. Also in the intermediate and humid regions, no significant changes in the aspect estimate over time were observed

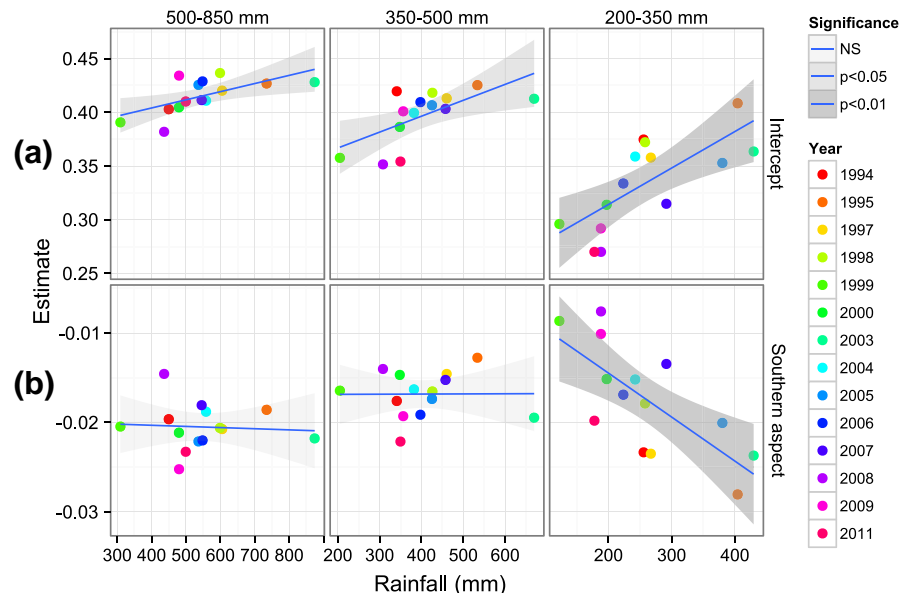


Fig. 3. (a) Intercept and (b) aspect effect estimates (Table 1; Fig. 2a and b) as functions of annual rainfall (Fig. 2c) among years, in three examined regions. The predicted linear regression line of the estimate as a function of rainfall (Table 2) is shown in blue, with the 95% confidence interval surrounding the line shaded in gray. Transparency of the confidence interval band corresponds to significance of the linear regression slope. Note that the ranges of x-axis values are not the same among panels. (For interpretation of the references to color in this figure legend, the reader is referred to the web version of this article.)

(slope = -0.00024 , $p > 0.05$ and slope = -0.0001 , $p > 0.1$, respectively).

The relationships between the estimates of the intercept (Fig. 2a) and aspect (Fig. 2b) effects of a certain year with annual rainfall of that year (Fig. 2c) are shown in Fig. 3, and the statistics of these relationships are summarized in Table 2. The intercept estimates had a significant positive relationship with annual rainfall (Fig. 3a, Table 2) in all three regions, which means that the temporal fluctuations of NDVI (Fig. 2a) coincided with those of annual rainfall (Fig. 2c). The estimates of aspect effect, however, were not significantly correlated with rainfall in the humid and intermediate regions (Fig. 3b, Table 2). Only in the arid region was a significant negative relationship, which appears to be linear, found between rainfall and the effect of aspect on NDVI (Fig. 3b, Table 2). In other words, no “threshold” amount of rainfall was identified that would prompt NDVI homogenization among northern and southern aspects. Instead, a gradual reduc-

tion of the aspect effect was observed among years with decreasing annual rainfall. It appears that, in the arid region, relatively wet years were characterized by high NDVI values (~ 0.4) and large differences (~ 0.025) between northern and southern aspects. Relatively dry years, however, were characterized by low NDVI values (~ 0.3) and small differences (~ 0.01) between northern and southern aspects.

A total of 4220 dead trees were identified on the aerial photograph within the 2.72 km^2 sampled in Lahav forest (Fig. 5). Based on an estimate of trees density in 2011 in each of the forest polygons (Shmuel Sprintsin, Israel Forest Service, personal communication), this translates to $\sim 3.5\%$ mortality. However, the frequency of dead trees was more than three times higher on the southern aspects compared to the northern aspects (2.50 and 0.68 trees per 30 m^2 pixel, on average, respectively; Figs. 5, 6 and S1). The difference among aspects was statistically significant according to a GLM of dead trees count as a function of aspect ($p < 0.001$). The

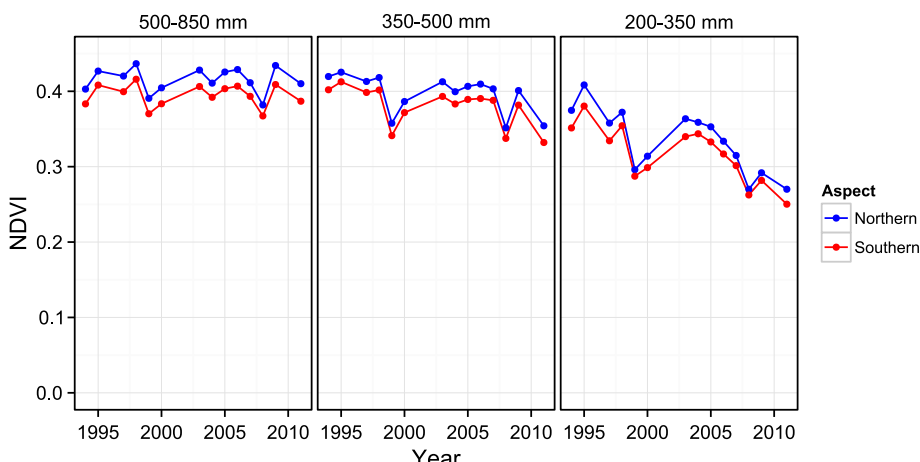


Fig. 4. Predicted NDVI values in 14 years during 1994–2011, based on the 42 Mixed Effects linear models described in Table 1. Note that lines between points do not indicate continuous variation, and also that differences between northern and southern aspect locations were significant in all cases (according to confidence intervals, Table 1 and Fig. 2b). (For interpretation of the references to color in this figure legend, the reader is referred to the web version of this article.)

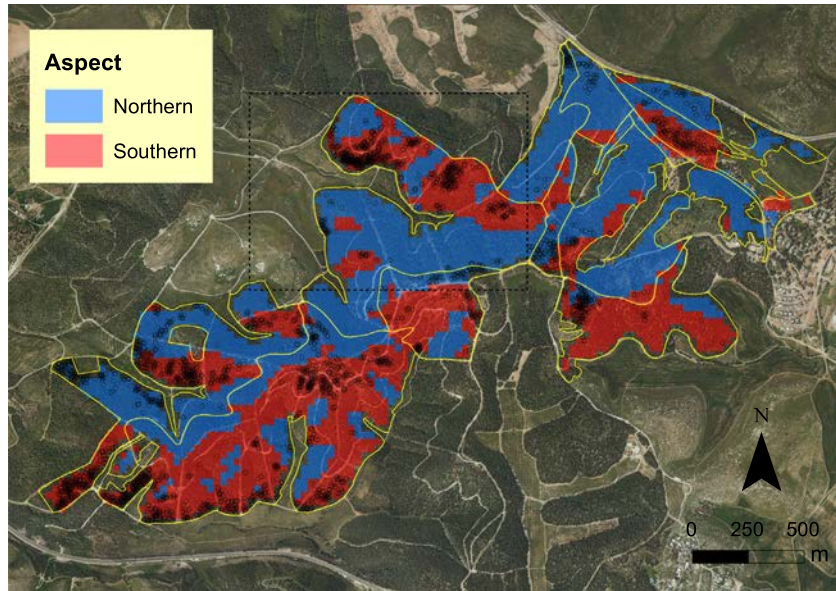


Fig. 5. Trees mortality in Lahav forest following the 2005–2011 drought. Black circles mark the locations of dead trees, manually identified on an aerial photograph from winter 2011/2012. Semi-transparent blue and red colors mark northern and southern aspects, respectively. See Fig. S1 for a zoom-in view and ground photographs of the area marked by a black dashed rectangle. (For interpretation of the references to color in this figure legend, the reader is referred to the web version of this article.)

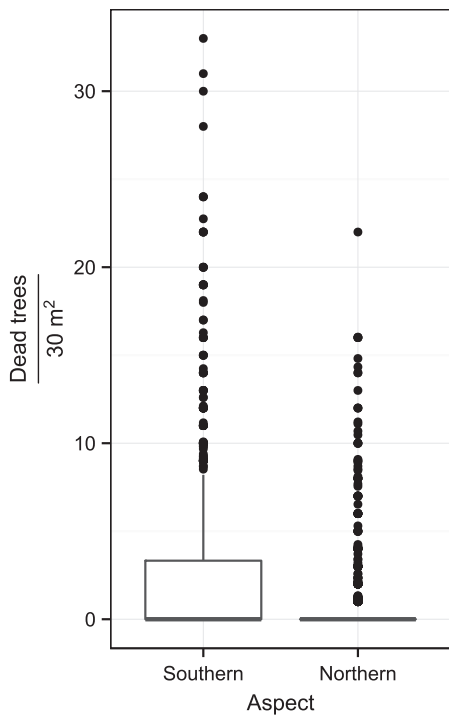


Fig. 6. Box and whiskers plot of dead trees count, among 30 m^2 pixels on southern and northern aspects in Lahav forest (Fig. 5). The upper and lower “hinges” correspond to the 25% and 75% quartiles. The upper whiskers extend from the hinge to the highest value that is within 1.5 of the 25–75% inter-quartile range. Data beyond the end of the whiskers are outliers and plotted as points.

concentration of dead trees on southern aspects was also evident from ground-view (Fig. S1).

4. Discussion

In the arid region, the effect of aspect was relatively stable in the long term, but was characterized by temporary deviations

whose magnitude was proportional to the annual rainfall amount (Fig. 3b). The average effect of aspect in the arid region was -0.017 , meaning that, within a forest, when moving from northern to southern aspects, NDVI decreased, on average, by 0.017 units, which is $\sim 5\%$ of the average NDVI in that region. However, the effect of aspect was not constant in time; it was related to the varying annual rainfall. Dry years were characterized by a significant weakening of the aspect effect, down to -0.008 ($\sim 2\%$ of the average NDVI), while wet years were characterized by a significant increase, to as much as -0.028 ($\sim 8\%$ of the average NDVI; Fig. 2b).

It may be assumed that during drought years, soil water availability becomes so limiting that the advantage of northern aspects is annulled. In other words, possibly because of very low levels of physiological activity (Schiller and Atzmon, 2009) throughout the forest in drought years, trees in all local habitats are affected. This may be manifested in reduced needle production, i.e., shorter and fewer needles, and/or defoliation (Baquedano and Castillo, 2006; Borghetti et al., 1998; Körner et al., 2005), resulting in uniformly low NDVI values across diverse habitats. In wet years, however, the advantage of the northern aspects may be realized. In such years the soil water content may be high enough to allow, for example, prolonged physiological activity on the northern aspects in spring and early summer (Klein et al., 2005; Schiller and Cohen, 1995). The contrast between northern and southern aspects will then appear, because cessation of physiological activity is reached faster in the latter.

An analogous hypothesis was suggested to explain why forest mortality patterns differed among different temporal phases of a drought event. Mortality was hypothesized to be higher in locations with high tree density, where competition for soil water is more intense, in the earlier phases of a mortality event (Negron and Wilson, 2003), and more homogeneous among differing density levels in the later phases of that event (Floyd et al., 2009; Ganey and Vojta, 2011). It was hypothesized that, in the case of an extreme drought, density dependence might operate in the earlier phases of mortality events, when trees in less competitive environments could obtain sufficient moisture, whereas those faced with competition could not. Later, under persistent drought stress, density dependence might be masked because the environmental

conditions would be so stressful that competition was no longer important, and mortality would occur at all density levels (Floyd et al., 2009; Ganey and Vojta, 2011).

The low responsiveness of the aspect effect to annual rainfall in the intermediate and humid regions (Table 2, Fig. 3b) might be attributed to the less extreme limitation on tree performance in those regions than in the arid region. Examination of the x-axis in Fig. 3 shows that in the intermediate and humid regions annual rainfall levels during the 14 examined years were only once lower than 300 and 400 mm, respectively, whereas in the arid region 11 out of the examined 14 years received less than 300 mm of rainfall. In contrast to this obvious difference in rainfall regimes, the performance difference among regions was not very high at the beginning of the studied period. In 1994–1995, average estimated NDVI values were 0.42, 0.43 and 0.39 in the humid, intermediate and arid regions, respectively (Fig. 2a). Thus, fluctuations in the performance difference between northern and southern aspects (Fig. 2b), and the accompanying decline in the performance “base level” (Fig. 2a) in the arid region, may both be viewed as manifestations of the decline exhibited by *P. halepensis* forests in the arid region during the examined 18-year period of 1994–2011 (Dorman et al., 2013).

It may be hypothesized that, in the arid region, damage caused to the forest under very low water availability was causing homogenization of performance in drought years, possibly because of low needle production in all habitats. Irreversible damage that led to mortality through, e.g., defoliation and depletion of carbon-reserves (Galiano et al., 2011; Sanchez-Salguero et al., 2012), or through accumulated hydraulic damage (Anderegg et al., 2013b), could have reduced potential productivity in subsequent years. In contrast, in the intermediate and humid regions, invariable differences between northern and southern aspects (Fig. 2b) and stable performance “base levels” (Fig. 2a) were observed. These two patterns may express the preservation of high enough soil water levels to maintain a persistent advantage of improved local habitats and to avoid irreversible drought damage, respectively.

The abovementioned two hypotheses, regarding variation in aspect effect in the temporal and spatial domains, are analogous. Performance homogenization among local habitats occurred in the arid region during drought, supposedly when very low levels of soil water availability were reached, and regional climatic conditions became the dominant limiting factor. However, performance differences among local habitats were maintained in all years in the intermediate and humid regions, and in the arid region in wet years only, since water availability was high enough to allow differential performance responses among local habitats.

In light of the proposed explanation, higher sensitivity to drought, i.e., a higher ratio between performance figures during normal vs. drought periods, may be expected in locally improved habitats (Fig. 4). In agreement with the latter, Knutson and Pyke (2008), in southern Oregon, USA, reported a significant negative association between growth rates in wet and dry years ratio, on the one hand, and radiation amount, on the other hand, in both *Pinus ponderosa* and *Juniperus occidentalis*. However, they regarded the finding as contradictory to the expectation that locations with increased radiation stress would be more sensitive to climatic changes. In the present study we observed the opposite: inferior local habitats, such as southern aspects, might exhibit lower drought sensitivity of performance traits such as NDVI. This is because drought impact becomes the major limiting factor, and homogenization of performance occurs across all habitats. Contrariwise, during wet years the potential for advantageous performance is exploited in the improved habitats. However, from the demographic point of view indeed the opposite pattern of sensitivity was observed: mortality was higher in the inferior habitats (Huang and Anderegg, 2012) in a representative forest within the

arid region. It appears that although improved habitats exhibit relatively steeper performance declines following drought, inferior habitats nevertheless fall to lower absolute performance levels (Figs. 4 and S2), and thus may be the first in which trees exceed critical physiological thresholds and mortality occurs (Figs. 5 and S1).

The difference in performance between northern and southern aspects was significant in all cases, in addition to significant temporal fluctuations caused by rainfall variation in the arid region (Fig. 2b). However, these fluctuations were quite small, compared with the “background” long-term changes of average forest performance (Figs. 2a and 4). For example, the average rate of performance decline in the arid region (-0.0057 NDVI units year $^{-1}$) was only one third of the average difference in performance between northern and southern aspects (0.017 NDVI units). Thus, during this 18-year study period, the performance “base level” in the arid region forests declined by a value six times the average performance difference between northern and southern aspects. This simple calculation demonstrates the importance of providing effect size information, i.e., the mean value with its confidence interval (Cohen, 1994; Nakagawa and Cuthill, 2007). The latter enables evaluation of the relative importance of the studied environmental effect in the context of other effects that characterize the studied system. In that respect the present study adds to the previous study focusing only on effect significance (Volcani et al., 2005).

In summary, the present findings support the concept that under severe drought forest performance becomes more homogeneous across local habitats, both temporally (in drought years) and spatially (towards the arid forest boundary). In these settings, the role of climate as a limiting factor to performance increases, whereas the roles of local factors, such as topographic aspect, become masked. It was also demonstrated that the local differences in performance between locally improved and locally inferior locations remained well conserved in the long term, even while the region suffered from regional performance reduction resulting from recurrent drought. The ability to observe a homogeneous forest ecosystem, in terms of species composition and structure, with high resolution over a wide area, was made possible by using remote sensing. Such an examination enabled a detailed evaluation of the trends and relationships among local and regional environmental factors, as they affect performance, as well as assessment of the relative importance of their effects. In addition to the basic ecological insight, such an evaluation is essential for relating local and global studies that aim at predicting the fate of forests in face of global climate change.

Acknowledgements

We thank Israel Tauber, Ronen Talmor, Efrat Sheffer and Shmuel Sprintsin for providing GIS layers of the planted forests, and the Israeli Forest Service (KKL) for permission to use these data. We thank Talia Horovitz and the Israel Meteorological Service for providing the rainfall data. This study was supported by a grant from the Chief Scientist of the Israeli Ministry of Agriculture and Rural Development, and the Jewish National Fund. We thank two anonymous reviewers for useful comments on a previous version of the manuscript.

Appendix A. Supplementary material

Supplementary data associated with this article can be found, in the online version, at <http://dx.doi.org/10.1016/j.foreco.2013.08.026>.

References

- Akaike, H., 1974. A new look at the statistical model identification. In: IEEE Trans. Auto. Cont. AC19, pp. 716–723.
- Allen, C.D., Macalady, A.K., Chenchouni, H., Bachelet, D., McDowell, N., Vennetier, M., Kitzberger, T., Rigling, A., Breshears, D.D., Hogg, E.H., Gonzalez, P., Fensham, R., Zhang, Z., Castro, J., Demidova, N., Lim, J.H., Allard, G., Running, S.W., Semerci, A., Cobb, N., 2010. A global overview of drought and heat-induced tree mortality reveals emerging climate change risks for forests. *For. Ecol. Manage.* 259, 660–684.
- Anderegg, W.R.L., Berry, J.A., Smith, D.D., Sperry, J.S., Anderegg, L.D.L., Field, C.B., 2012. The roles of hydraulic and carbon stress in a widespread climate-induced forest die-off. *Proc. Natl. Acad. Sci. USA* 109, 233–237.
- Anderegg, W.R.L., Kane, J.M., Anderegg, L.D.L., 2013a. Consequences of widespread tree mortality triggered by drought and temperature stress. *Nat. Clim. Change* 3, 30–36.
- Anderegg, W.R.L., Plavcova, L., Anderegg, L.D.L., Hacke, U.G., Berry, J.A., Field, C.B., 2013b. Drought's legacy: multiyear hydraulic deterioration underlies widespread aspen forest die-off and portends increased future risk. *Global Change Biol.* 19, 1188–1196.
- Baquedano, F.J., Castillo, F.J., 2006. Comparative ecophysiological effects of drought on seedlings of the Mediterranean water-saver *Pinus halepensis* and water-spenders *Quercus coccifera* and *Quercus ilex*. *Trees – Struct. Funct.* 20, 689–700.
- Borghetti, M., Cinnirella, S., Magnani, F., Saracino, A., 1998. Impact of long-term drought on xylem embolism and growth in *Pinus halepensis* Mill. *Trees (Berlin)* 12, 187–195.
- Brouwers, N.C., Mercer, J., Lyons, T., Poot, P., Veneklaas, E., Hardy, G., 2013. Climate and landscape drivers of tree decline in a Mediterranean ecoregion. *Ecol. Evol.* 3, 67–79.
- Brown, C.J., Schoeman, D.S., Sydeman, W.J., Brander, K., Buckley, L.B., Burrows, M., Duarte, C.M., Moore, P.J., Pandolfi, J.M., Poloczanska, E., Venables, W., Richardson, A.J., 2011. Quantitative approaches in climate change ecology. *Global Change Biol.* 17, 3697–3713.
- Carrera-Hernandez, J.J., Gaskin, S.J., 2007. Spatio-temporal analysis of daily precipitation and temperature in the Basin of Mexico. *J. Hydrol.* 336, 231–249.
- Chander, G., Markham, B.L., Helder, D.L., 2009. Summary of current radiometric calibration coefficients for Landsat MSS, TM, ETM+, and EO-1 ALI sensors. *Rem. Sens. Environ.* 113, 893–903.
- Choat, B., Jansen, S., Brodrribb, T.J., Cochard, H., Delzon, S., Bhaskar, R., Bucci, S.J., Feild, T.S., Gleason, S.M., Hacke, U.G., Jacobsen, A.L., Lens, F., Maherli, H., Martinez-Vilalta, J., Mayr, S., Mencuccini, M., Mitchell, P.J., Nardini, A., Pittermann, J., Pratt, R.B., Sperry, J.S., Westoby, M., Wright, I.J., Zanne, A.E., 2012. Global convergence in the vulnerability of forests to drought. *Nature* 491, 752–755.
- Coble, D.W., Milner, K.S., Marshall, J.D., 2001. Above- and below-ground production of trees and other vegetation on contrasting aspects in western Montana: a case study. *For. Ecol. Manage.* 142, 231–241.
- Cohen, J., 1994. The Earth is round (*p*-less-than-.05). *Am. Psychol.* 49, 997–1003.
- Di Piazza, A., Lo Conti, F., Noto, L.V., Viola, F., La Loggia, G., 2011. Comparative analysis of different techniques for spatial interpolation of rainfall data to create a serially complete monthly time series of precipitation for Sicily, Italy. *Int. J. Appl. Earth Obs. Geoinf.* 13, 396–408.
- Dorman, M., Svoray, T., Perevolotsky, A., Sarris, D., 2013. Forest performance during two consecutive drought periods: diverging long-term trends and short-term responses along a climatic gradient. *Forest Ecol. Manage.* 310, 1–9.
- ESRI Inc., 2012. ArcMap Version 10.0 (Redlands, CA: ESRI).
- Floyd, M.L., Clifford, M., Cobb, N.S., Hanna, D., Delph, R., Ford, P., Turner, D., 2009. Relationship of stand characteristics to drought-induced mortality in three Southwestern pinon-juniper woodlands. *Ecol. Appl.* 19, 1223–1230.
- Fu, P.D., Rich, P.M., 2002. A geometric solar radiation model with applications in agriculture and forestry. *Comput. Electron. Agric.* 37, 25–35.
- Galiano, L., Martinez-Vilalta, J., Lloret, F., 2011. Carbon reserves and canopy defoliation determine the recovery of Scots pine 4 yr after a drought episode. *New Phytol.* 190, 750–759.
- Ganey, J.L., Vojta, S.C., 2011. Tree mortality in drought-stressed mixed-conifer and ponderosa pine forests, Arizona, USA. *For. Ecol. Manage.* 261, 162–168.
- Girard, F., Vennetier, M., Ouarmim, S., Caraglio, Y., Misson, L., 2011. Polycyclism, a fundamental tree growth process, decline with recent climate change: the example of *Pinus halepensis* Mill. in Mediterranean France. *Trees – Struct. Funct.* 25, 311–322.
- Girard, F., Vennetier, M., Guibal, F., Corona, C., Ouarmim, S., Herrero, A., 2012. *Pinus halepensis* Mill. crown development and fruiting declined with repeated drought in Mediterranean France. *Eur. J. For. Res.* 131, 919–931.
- Gitlin, A.R., Stultz, C.M., Bowker, M.A., Stumpf, S., Paxton, K.L., Kennedy, K., Munoz, A., Bailey, J.K., Whitham, T.G., 2006. Mortality gradients within and among dominant plant populations as barometers of ecosystem change during extreme drought. *Conserv. Biol.* 20, 1477–1486.
- Goovaerts, P., 2000. Geostatistical approaches for incorporating elevation into the spatial interpolation of rainfall. *J. Hydrol.* 228, 113–129.
- Goslee, S.C., 2011. Analyzing remote sensing data in R: the landsat Package. *J. Stat. Softw.* 43, 1–25.
- Guarin, A., Taylor, A.H., 2005. Drought triggered tree mortality in mixed conifer forests in Yosemite National Park, California, USA. *For. Ecol. Manage.* 218, 229–244.
- Hall, J.K., Cleave, R.L., 1988. The DTM project. *Geol. Surv. Isr.* 6, 1–7.
- Huang, C.-Y., Anderegg, W.R.L., 2012. Large drought-induced aboveground live biomass losses in southern Rocky Mountain aspen forests. *Global Change Biol.* 18, 1016–1027.
- Klein, T., Hemming, D., Lin, T.B., Grunzweig, J.M., Maseyk, K., Rotenberg, E., Yakir, D., 2005. Association between tree-ring and needle delta C-13 and leaf gas exchange in *Pinus halepensis* under semi-arid conditions. *Oecologia* 144, 45–54.
- Knutson, K.C., Pyke, D.A., 2008. Western juniper and ponderosa pine ecotonal climate-growth relationships across landscape gradients in southern Oregon. *Can. J. For. Res. – Rev Can. Rech. For.* 38, 3021–3032.
- Korner, C., Sarris, D., Christodoulakis, D., 2005. Long-term increase in climatic dryness in the East-Mediterranean as evidenced for the island of Samos. *Reg. Environ. Change* 5, 27–36.
- Liphschitz, N., Biger, G., 2001. Past distribution of Aleppo pine (*Pinus halepensis*) in the mountains of Israel (Palestine). *Holocene* 11, 427–436.
- Lloret, F., Lobo, A., Estevan, H., Maisongrande, P., Vayreda, J., Terradas, J., 2007. Woody plant richness and NDVI response to drought events in Catalonian (northeastern Spain) forests. *Ecology* 88, 2270–2279.
- Ma, Z., Peng, C., Zhu, Q., Chen, H., Yu, G., Li, W., Zhou, X., Wang, W., Zhang, W., 2012. Regional drought-induced reduction in the biomass carbon sink of Canada's boreal forests. *Proc. Natl. Acad. Sci. USA* 109, 24232427.
- Martinez-Vilalta, J., Pinol, J., 2002. Drought – induced mortality and hydraulic architecture in pine populations of the NE Iberian Peninsula. *For. Ecol. Manage.* 161, 247.
- Matyas, C., 2010. Forecasts needed for retreating forests. *Nature* 464, 1271.
- Michaelian, M., Hogg, E.H., Hall, R.J., Arsenault, E., 2011. Massive mortality of aspen following severe drought along the southern edge of the Canadian boreal forest. *Global Change Biol.* 17, 2084–2094.
- Nakagawa, S., Cuthill, I.C., 2007. Effect size, confidence interval and statistical significance: a practical guide for biologists. *Biol. Rev.* 82, 591–605.
- Negrón, J.F., Wilson, J.L., 2003. Attributes associated with probability of infestation by the pinon IPS, IPS confusus (Coleoptera: Scolytidae), in pinon pine, *Pinus edulis*. *West. N. Am. Nat.* 63, 440–451.
- Nevo, E., 2012. "Evolution Canyon", a potential microscale monitor of global warming across life. *Proc. Natl. Acad. Sci. USA* 109, 2960–2965.
- Olarieta, J.R., Uson, A., Rodriguez, R., Rosa, M., Blanco, R., Antunez, M., 2000. Land requirements for *Pinus halepensis* Mill. growth in a plantation in Huesca, Spain. *Soil Use Manage.* 16, 88–92.
- Osem, Y., Ginsberg, P., Tauber, I., Atzman, N., Perevolotsky, A., 2008. Sustainable management of Mediterranean planted coniferous forests: an Israeli definition. *J. For.* 106, 38–46.
- Osem, Y., Zangy, E., Bney-Moshe, E., Moshe, Y., Karni, N., Nisan, Y., 2009. The potential of transforming simple structured pine plantations into mixed Mediterranean forests through natural regeneration along a rainfall gradient. *For. Ecol. Manage.* 259, 14–23.
- Pebesma, E.J., 2004. Multivariable geostatistics in S: the gstat package. *Comput. Geosci.* 30, 683–691.
- Perevolotsky, A., Sheffer, E., 2009. Forest management in Israel – the ecological alternative. *Isr. J. Plant Sci.* 57, 35–48.
- Pettorelli, N., Vik, J.O., Mysterud, A., Gaillard, J.-M., Tucker, C.J., Stenseth, N.C., 2005. Using the satellite-derived NDVI to assess ecological responses to environmental change. *Trends Ecol. Evol.* 20, 503–510.
- Pigott, C.D., Pigott, S., 1993. Water as a determinant of the distribution of trees at the boundary of the Mediterranean zone. *J. Ecol.* 81, 557–566.
- Pinheiro, J.C., Bates, D.M., 2000. *Mixed-Effects Models in S and S-PLUS*. Springer Verlag, New York.
- R Development Core Team, 2012. R: A Language and Environment for Statistical Computing. R Foundation for Statistical Computing, Vienna, Austria, ISBN 3-900051-07-0, <<http://www.R-project.org/>>.
- Rouse, J.W., Haas, R.H., Schell, J.A., Deering, D.W., 1973. Monitoring vegetation systems in the Great Plains with ERTS. In: 3rd ERTS Symposium, NASA SP-351 I, pp. 309–317.
- Royer, P.D., Cobb, N.S., Clifford, M.J., Huang, C.-Y., Breshears, D.D., Adams, H.D., Camilo Villegas, J., 2011. Extreme climatic event-triggered overstorey vegetation loss increases understorey solar input regionally: primary and secondary ecological implications. *J. Ecol.* 99, 714–723.
- Sanchez-Salguero, R., Navarro-Cerrillo, R.M., Swetnam, T.W., Zavala, M.A., 2012. Is drought the main decline factor at the rear edge of Europe? The case of southern Iberian pine plantations. *For. Ecol. Manage.* 271, 158–169.
- Sarris, D., Christodoulakis, D., Korner, C., 2007. Recent decline in precipitation and tree growth in the eastern Mediterranean. *Global Change Biol.* 13, 1187–1200.
- Schieltz, H., 2010. Simple means to improve the interpretability of regression coefficients. *Meth. Ecol. Evol.* 1, 103–113.
- Schiller, G., 1972. Ecological Factors Affecting the Growth of Aleppo Pine in the Southern Judean Hills. Agricultural Research Organization, Forest Division, Ilanot, Leaflet No. 44 (in Hebrew).
- Schiller, G., 2000. *Ecophysiology of Pinus halepensis Mill. and P-brutia Ten.* In: Ne'eman, G.T.L. (Ed.), *Ecology, Biogeography and Management of Pinus Halepensis and P. Brutia Forest Ecosystems in the Mediterranean Basin*. Backhuys Publishers, Leiden, The Netherlands, pp. 51–65.
- Schiller, G., Atzman, N., 2009. Performance of Aleppo pine (*Pinus halepensis*) provenances grown at the edge of the Negev desert: a review. *J. Arid Environ.* 73, 1051–1057.
- Schiller, G., Cohen, Y., 1995. Water regime of a pine forest under a Mediterranean climate. *Agric. For. Meteorol.* 74, 181–193.

- Schiller, G., Ungar, E.D., Genizi, A., 2005. Is tree fate written in its tree rings? Characterization of trees in Kramim forest following the 1998/99 dry winter. *Yaar*, 18–25 (in Hebrew).
- Schiller, G., Ungar, E.D., Cohen, S., Moshe, Y., Atzmon, N., 2009. Aspect effect on transpiration of *Pinus halepensis* in Yatir forest. *Yaar* 11, 14–19 (in Hebrew).
- Song, C., Woodcock, C.E., Seto, K.C., Lenney, M.P., Macomber, S.A., 2001. Classification and change detection using Landsat TM data: when and how to correct atmospheric effects? *Rem. Sens. Environ.* 75, 230–244.
- Sternberg, M., Shoshany, M., 2001. Influence of slope aspect on Mediterranean woody formations: comparison of a semiarid and an arid site in Israel. *Ecol. Res.* 16, 335–345.
- Suarez, M.L., Ghermandi, L., Kitzberger, T., 2004. Factors predisposing episodic drought-induced tree mortality in Nothofagus – site, climatic sensitivity and growth trends. *J. Ecol.* 92, 954–966.
- Svoray, T., Karniel, A., 2011. Rainfall, topography and primary production relationships in a semiarid ecosystem. *Ecohydrology* 4, 56–66.
- Tucker, C.J., 1979. Red and photographic infrared linear combinations for monitoring vegetation. *Rem. Sens. Environ.* 8, 127–150.
- Ungar, E.D., Rotenberg, E., Raz-Yaseef, N., Cohen, S., Yakir, D., Schiller, G., 2013. Transpiration and annual water balance of Aleppo pine in a semiarid region: implications for forest management. *For. Ecol. Manage.* 298, 39–51.
- Vacchiano, G., Garbarino, M., Borgogno Mondino, E., Motta, R., 2012. Evidences of drought stress as a predisposing factor to Scots pine decline in Valle d'Aosta (Italy). *Eur. J. For. Res.* 131, 989–1000.
- Vicente-Serrano, S.M., Saz-Sánchez, M.A., Cuadrat, J.M., 2003. Comparative analysis of interpolation methods in the middle Ebro Valley (Spain): application to annual precipitation and temperature. *Clim. Res.* 24, 161–180.
- Vicente-Serrano, S.M., Lasanta, T., Gracia, C., 2010. Aridification determines changes in forest growth in *Pinus halepensis* forests under semiarid Mediterranean climate conditions. *Agric. For. Meteorol.* 150, 614–628.
- Vicente-Serrano, S.M., Zouber, A., Lasanta, T., Pueyo, Y., 2012. Dryness is accelerating degradation of vulnerable shrublands in semiarid Mediterranean environments. *Ecol. Monogr.* 82, 407–428.
- Volcani, A., Karniel, A., Svoray, T., 2005. The use of remote sensing and GIS for spatio-temporal analysis of the physiological state of a semi-arid forest with respect to drought years. *For. Ecol. Manage.* 215, 239–250.
- Wang, X., Piao, S., Ciais, P., Li, J., Friedlingstein, P., Koven, C., Chen, A., 2011. Spring temperature change and its implication in the change of vegetation growth in North America from 1982 to 2006. *Proc. Natl. Acad. Sci. USA* 108, 1240–1245.
- Worrall, J.J., Egeland, L., Eager, T., Mask, R.A., Johnson, E.W., Kemp, P.A., Shepperd, W.D., 2008. Rapid mortality of *Populus tremuloides* in southwestern Colorado, USA. *For. Ecol. Manage.* 255, 686–696.
- Zavala, M.A., Espelta, J.M., Retana, J., 2000. Constraints and trade-offs in Mediterranean plant communities: the case of holm oak-Aleppo pine forests. *Bot. Rev.* 66, 119–149.
- Zuur, A.F., Ieno, E.N., Walker, N.J., Saveliev, A.A., Smith, G.M., 2009. Mixed Effects Models and Extensions in Ecology with R. Springer-Verlag, New-York.

3.3 Influential time-scales of climatic effects and modulating effects of competition on tree growth

Using tree-ring analysis, in this chapter the variation in climate and competition effects on tree growth along a climatic gradient was examined. The immediate response to rainfall amount decline, and lack of competition effect on the slowest-growing trees, in the dry region (~300 mm), suggest no buffering against extreme drought conditions and limited potential benefit of thinning to increase forest resilience (contrary to the generally held view).

The results of this study are described in Dorman *et al.* (2015a) (see below).

Supplementary material for this chapter appears in Section 6.3.

The effect of rainfall and competition intensity on forest response to drought: lessons learned from a dry extreme

Michael Dorman · Avi Pervolotsky · Dimitrios Sarris ·
Tal Svoray

Received: 24 February 2014 / Accepted: 13 January 2015 / Published online: 6 February 2015
© Springer-Verlag Berlin Heidelberg 2015

Abstract We investigated forest responses to global warming by observing: (1) planted *Pinus halepensis* forests, (2) an aridity gradient—with annual precipitation (P) ranging from ~300 to ~700 mm, and (3) periods of wet and dry climate that included the driest period during at least the last 110 years. We examined: (1) how the length of climatic integration periods to which trees are most responsive varies in space and time, (2) the extent to which competition modulates growth decline during drought (2011) and subsequent recovery (2012) years. The temporal scale of rainfall that was most influential

on growth shortened in progressing southward, and in the drier than in the wetter period. Long-term underground water storage, as reflected in the relationship of growth to multiple-year rainfall, remained significant up to the point where $P \approx 500$ mm. Under drier conditions ($P < 500$ mm) in both space and time, influential rainfall scales shortened, probably reflecting a diminishing role of water storage. These drier locations are the first from which the species would be likely to retreat if global warming intensified. Competition appeared to set an upper limit to growth, while growth variation among individual trees increased as competition-intensity decreased. That upper limit increased in 2012 compared with 2011. The observed insensitivity of slow-growing trees to competition implies that mortality risk may be density independent, when even any potential for higher soil moisture availability in open stands is lost to evapotranspiration before it can benefit tree growth.

Communicated by Russell K Monson.

Electronic supplementary material The online version of this article (doi:[10.1007/s00442-015-3229-2](https://doi.org/10.1007/s00442-015-3229-2)) contains supplementary material, which is available to authorized users.

M. Dorman (✉) · T. Svoray
Department of Geography and Environmental Development,
Ben-Gurion University of the Negev, 84105 Beer-Sheva, Israel
e-mail: michael.dorman@mail.huji.ac.il

A. Pervolotsky
Department of Agronomy and Natural Resources, Agricultural
Research Organization, Volcani Center, 50250 Bet Dagan, Israel

D. Sarris
Faculty of Pure and Applied Sciences, Open University
of Cyprus, Latsia, 2252 Nicosia, Cyprus

D. Sarris
Department of Biological Sciences, University of Cyprus,
1678 Nicosia, Cyprus

D. Sarris
Division of Plant Biology, Department of Biology, University
of Patras, 26500 Patras, Greece

Keywords Aleppo pine · Basal area increment · *Pinus halepensis* · Standardized precipitation-evapotranspiration index · Tree rings

Introduction

Extreme climatic events, superimposed on persistent warming and drying of the weather, have become more frequent in the Mediterranean region (Hoerling et al. 2012). Climatic projections associated with global warming scenarios indicate a similar trend (Giorgi and Lionello 2008), with aridity expected to shift northwards and/or to higher altitudes (Jump et al. 2009). Water availability is the main limiting factor for vegetation in the Mediterranean region (Pigott and Pigott 1993), therefore this trend has profound

implications for functioning of vegetation: increased incidence of performance decline and mortality events in forests have already been reported, both in this region (Korner et al. 2005; Carnicer et al. 2011; Sanchez-Salguero et al. 2012) and worldwide (Allen et al. 2010), in the last few decades. Knowledge of the spatial and temporal determinants of responses of the main forest tree species to climatic changes is, therefore, important for predicting and, possibly, alleviating forest decline.

It is well known that, in many cases, radial growth of trees integrates the effects of previous year(s) climatic and ecological conditions (Fritts 1976), which are expressed in temporally autocorrelated series of tree-ring widths. Such integration may result from buffered and/or accumulative behavior of the temporal variation in the resources the tree utilizes; behavior expressed in: the physiological [e.g., carbon balance (Niinemets 2010)] and structural [e.g., foliage amount (Galiano et al. 2011); xylem integrity (Brodrribb et al. 2010)] state of the tree itself, or of its immediate environment [e.g., soil/bedrock water storage (Breshears et al. 2009)]. Regarding the latter, moisture stored in deep soil layers and in bedrock can play an important role in the survival of vegetation in dry climates (Raz-Yaseef et al. 2010; Schwinnig 2010). Such moisture domains are within reach of tree roots (Zwieniecki and Newton 1995), relatively safe from evaporative loss (Newman et al. 1997), and may be quantitatively substantial (Querejeta et al. 2007; Breshears et al. 2009; Schwinnig 2010). Thus, they potentially may serve as a moisture resource for trees, which fluctuates over multi-annual periods.

The dominant low-elevation conifer in the Mediterranean is *Pinus halepensis* s.l. (Schiller 2000). Diverging trends of performance were recently observed among *P. halepensis* forests in relatively humid (Linares et al. 2011) and arid (Sarris et al. 2011) parts of its distribution, as well as along climatic gradients (Vicente-Serrano et al. 2010b; Dorman et al. 2013b). Differences among responses to drought events may be, at least partially, due to differing time scales over which vegetation is sensitive to drought stress (Pasho et al. 2011; Levesque et al. 2013; Vicente-Serrano et al. 2013). Characterization of the dominant time scales over which drought influences forest performance could, therefore, be critical for early detection of forest decline and mortality events.

Indeed, under past exposures to drought intensification, growth of *P. halepensis* s.l. in Greece has been found to shift from seasonal to multi-annual influences of previous rainfall (Sarris et al. 2007), as occurred during the extremely dry decades in the region at the end of the twentieth century (Sarris et al. 2011). It has been hypothesized that dependence on longer rainfall-integration periods expressed increasing utilization of deep moisture pools by the drought-stressed trees (Sarris et al. 2007), and this hypothesis was supported by interpretations of carbon and oxygen isotope signals in tree rings (Sarris et al. 2013).

Such effects have also been noticed for other low-elevation conifers in the central Mediterranean region, e.g., *Pinus pinea* (Mazza and Manetti 2013).

Pinus halepensis s.l. populations in Israel include a large portion of the moisture conditions within which the species can survive: from relatively moist conditions (~800 mm annual rainfall) in the north to very dry (~250 mm) in the south. The southernmost populations are of special interest (Grunzweig et al. 2003; Maseyk et al. 2008a, b) since they are very close to the species' survival limits and beyond the limit of its natural distribution. *P. halepensis* is considered the most drought resistant of the Mediterranean pines (Schiller 2000), thanks to physiological adjustments associated with drought avoidance (Klein et al. 2011). Nevertheless, its populations in southern Israel recently exhibited high mortality rates, reaching even 90 % in some locations (Dorman et al. 2013a). Thus, they were ideal for testing the hypothesis that multi-annual accumulated rainfall drives growth under severe drought stress, possibly related to forest die-back caused by depletion of deeper-ground moisture pools.

In addition to effects of climate, forest performance is affected by structural attributes such as tree density. Competition intensity is generally negatively related to growth (Linares et al. 2010), although not in all cases (e.g., Julio Camarero et al. 2011; Granda et al. 2013). Density may significantly interact with climatic conditions and with location along a climatic gradient, which suggests enhanced detrimental effects of high density in drought years (Sanchez-Salguero et al. 2013) and at the dry edges of forest distributions (Gomez-Aparicio et al. 2011; Coll et al. 2013). However, the density at which further thinning would not increase water availability for the remaining trees remains unknown (Ungar et al. 2013).

Extreme drought events may present important tipping points in forest ecosystems (Penuelas et al. 2001; Breda and Badeau 2008). Thus, improved understanding of the sources of variability in the effect of density on tree response to drought requires bridging the gap between regional (Carnicer et al. 2011; Gomez-Aparicio et al. 2011) and more local studies (Pasho et al. 2012; Sanchez-Salguero et al. 2013). Whereas in the former, multivariate effects have been characterized along wide climatic gradients on the basis of forest inventory data, studies in the latter enable analysis of growth responses to specific climatic events by means of a dendro-ecological approach based on annual resolution radial growth trajectories.

It is presumed that thinning could reduce between-tree competition for soil water (McDowell et al. 2006) and thus enhance the trees' adaptive capacity to withstand drought stress (Breda and Badeau 2008; Kerhoulas et al. 2013; Sanchez-Salguero et al. 2013). Recognizing the maximal benefit from thinning, in terms of drought resistance and resilience, for a given tree species in different environmental

Table 1 Geographical and structural characteristics of the ten study sites

Site ^a	T. (C.)	Latitude/longitude	Elev.	Planted	DBH ^b	Height ^b	Density ^b	Mortality ^b
S0	25 (50)	31.38N/34.86E	438	1961	19.4 ± 0.3	10.2 ± 0.3	188.3 ± 11.5	78
S1	30 (60)	31.38N/34.86E	469	1967	20.6 ± 0.3	12.1 ± 0.2	311.7 ± 16.3	2
S2	28 (56)	31.37N/34.85E	409	1969	12.6 ± 0.2	8.4 ± 0.1	373.0 ± 12.6	25
S3	27 (54)	31.42N/34.85E	372	1968	16.0 ± 0.3	11.3 ± 0.2	527.2 ± 13.6	1
C1	29 (58)	31.82N/35.01E	337	1965	22.0 ± 0.6	15.7 ± 0.3	384.6 ± 22.2	2
C2	30 (60)	31.80N/34.99E	328	1962	21.3 ± 0.3	13.5 ± 0.4	336.5 ± 10.6	1
C3	26 (52)	31.78N/34.98E	378	1964	31.2 ± 0.6	16.7 ± 0.4	202.3 ± 14.1	8
N1	25 (50)	33.01N/35.54E	384	1960	35.1 ± 0.9	23.2 ± 0.5	187.3 ± 14.0	2
N2	29 (58)	32.99N/35.48E	678	1960	31.3 ± 1.2	17.5 ± 0.4	278.5 ± 23.1	1
N3	26 (52)	32.95N/35.49E	604	1967	39.6 ± 0.6	19.9 ± 0.4	167.4 ± 10.5	0

T. Sample size of trees, C. sample size of cores, Elev. elevation (m)

^a Sample for site S0 included living and dead trees; samples for the other nine sites included living trees only

^b Averages ± SE (except for mortality) among either the sampled (“focal”) trees [diameter at breast height (DBH; cm), tree height (Height; m)] or those in the 8-m-radius circles around them [density (trees ha⁻¹), mortality (%)]

settings, is essential for sustainable forest management (Ungar et al. 2013; Olivar et al. 2014). The climatic gradient in Israel is steep, but, nevertheless is synchronized with respect to the temporal sequences of climatic deviations, and homogeneous with respect to forest structure in planted *P. halepensis* forests. It therefore provides an excellent opportunity to compare the modulating effects of competition on decline and recovery following a specific drought event, among different positions along this climatic gradient.

In the present study, dendro-ecological methods and quasi-manipulation experiments based on natural variation (i.e., comparison between wet and dry climatic periods) were used to fill in key pieces missing from the puzzle of how semi-arid forests respond to extreme drought, and how competition intensity modulates this response. Our specific study questions were:

1. How does the length of the climatic integration period to which trees are most responsive vary in space, i.e., at different positions along a steep climatic gradient, and in time, i.e., during a relatively wet compared with an extremely dry period?
2. To what extent does competition between trees within a stand modulate growth decline during a drought year and growth recovery in the following wet year, and how do these effects change along a steep climatic gradient?

Materials and methods

Study sites

Nine sites, located in three regions (three sites per region)—south (S1–S3), center (C1–C3) and north (N1–N3)—along

a rainfall gradient with southwardly increasing aridity, were chosen for dendrochronological sampling (Table 1; Figs. S1, S2). An additional site (S0), which exhibited the highest tree mortality levels (78 %) encountered during preliminary field trips, was also sampled in order to contrast the growth rates observed in the nine main sites with those observed under apparently extreme conditions. For site selection, the following criteria were applied: (1) planted forest comprising >80 % *P. halepensis*; (2) planting year during the 1960s; (3) south-facing aspect; (4) similar lithology; and (5) pairwise proximity (i.e., <10-km spacing between each pair of adjacent sites within a region). All ten eventually chosen sites were located on chalk bedrock, the prevailing rock type within Israeli planted forests. Species composition and planting dates were obtained from the Israeli Forest Service geographic information system layer. Aspect data were based on a 25-m digital elevation model layer of Israel (Hall and Cleave 1988). Rock type data were based on 1:50,000 geological maps (Geological Survey of Israel).

Climate data

Daily data of precipitation (*P*), minimum temperature (*T*_{min}), and maximum temperature (*T*_{max}) were obtained from three meteorological stations (Table 2; Figs. S1, S3). Two additional stations (Fig. S1) were used to interpolate missing daily *T*_{min} and *T*_{max} values in regions S and C, where they involved, respectively, 6 and 5 % of days (Fig. S4). This procedure was our only means of obtaining complete time series of *P*, *T*_{min} and *T*_{max} for the three studied regions. Values were interpolated by using linear regression models (Sarris et al. 2014), based on days when both “predictor” and “predicted” stations operated, i.e., ~17,000 and ~15,000 days in regions S and C,

Table 2 Characteristics of the main three meteorological stations used to monitor climatic conditions in the studied regions and average conditions for 1966–2012

Variable	Season	South ^a	Center ^a	North
Latitude/longitude		31.38N/34.87E	31.72N/34.98E	32.98N/35.51E
Elevation (m)		460	353	930
Distance ^b		1.1, 1.1, 2.9, 5.0	10.7, 8.6, 5.6	4.5, 2.5, 4.0
<i>P</i> (mm)	Fall	43.8	76.6	109.6
	Winter	194.7	338.7	446.9
	Spring	60.5	98.8	135.3
	Summer	0.3	0.0	1.3
	Annual	299.3	514.1	693.0
<i>T</i> _{min.} (°C)	Fall	15.8	17.4	14.4
	Winter	8.0	10.0	5.0
	Spring	11.9	13.3	10.5
	Summer	18.4	20.0	18.3
	Annual	13.5	15.1	12.1
<i>T</i> _{max.} (°C)	Fall	26.8	27.7	22.9
	Winter	16.2	17.3	10.7
	Spring	24.0	24.4	19.5
	Summer	31.7	31.9	29.3
	Annual	24.7	25.3	20.6

P Precipitation, *T* Temperature, *min.* minimum, *max.* maximum

^a Missing daily temperature values for the south and central stations (5–6 %) were interpolated based on two additional stations. See Fig. S1 for station locations, Figs. S4, S5 and text for details

^b Distance (km) from the meteorological station to sites 0–3 (*South*) or sites 1–3 (*Center* and *North*), respectively (Fig. S1)

respectively (Fig. S5). The agreement within station pairs was very high (Fig. S4), with *R*²-values of 0.99 and 0.96 for *T*_{max.}, and 0.88 and 0.89 for *T*_{min.}, in S and C, respectively (Fig. S5).

Potential evapotranspiration (PET) was estimated on the basis of *T*_{min.}, *T*_{max.} and latitude, according to Hargreaves (1994). Monthly *P* and PET values were then used to calculate the standardized precipitation-evapotranspiration index (SPEI) (Vicente-Serrano et al. 2010a), which is a site-specific drought indicator that expresses standardized deviations from the average monthly water balance (*P*–PET); it offers several advantages: (1) the standardization process permits comparison in time and space (Vicente-Serrano et al. 2010a), (2) inclusion of temperature data in the SPEI formulation takes into account the role of warming-induced drought stress (Adams et al. 2009), and (3) the multi-scalar nature of droughts may be expressed by calculating SPEI for different time scales (Pasho et al. 2011). Thus, the SPEI served the following purposes in the present study: (1) it delineated drought periods; and (2) it served as an inclusive indicator of drought severity, encompassing its two main components, i.e., *P* and PET. A 12-month integration period, i.e., SPEI12 (Fig. 1), was chosen for (1) in the light of a previous study in which a stronger response of *P. halepensis* to cumulative droughts over 11 months was detected (Pasho et al. 2011).

The main analysis of climatic conditions (Tables 2, S1; Figs. 1d–f, S3) was based on 47 hydrological seasons (1965/1966–2011/2012), which is the longest period over

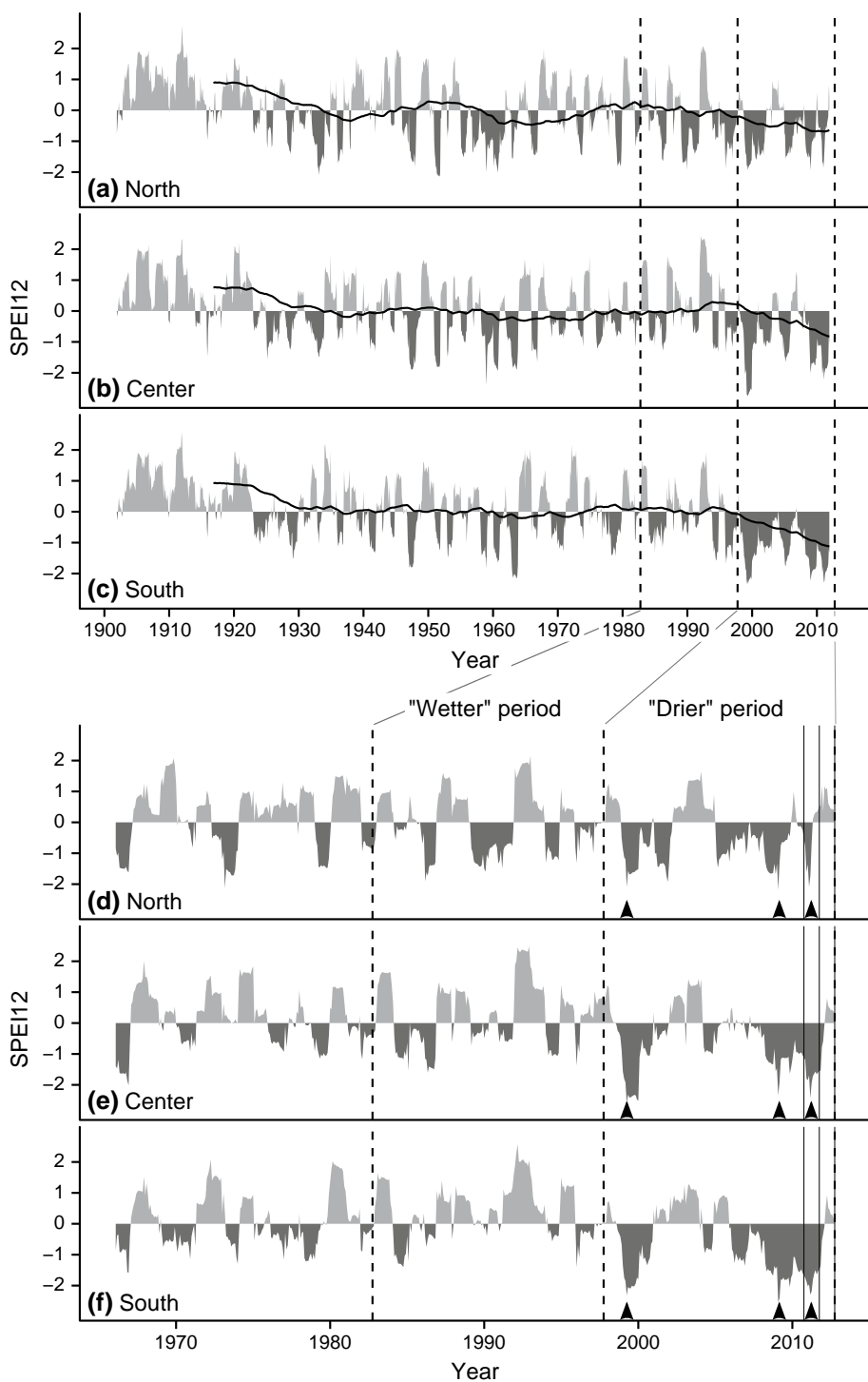
which *P*, *T*_{min.} and *T*_{max.} data were available from meteorological stations in all three studied regions. In order to provide a broader perspective on the analyzed time frame, we also evaluated SPEI12 evolution over a 110-year period (Fig. 1a–c). The data were downloaded from the global SPEI data base (<http://sac.csic.es/spei/>), which covers the period 1901–2011, for three 0.5° grid cells (north—32°45'N, 35°45'E; center—31°45'N, 34°45'E; and south—31°15'N, 34°45'E).

Field measurements and sampling

Field measurements and dendrochronological sampling took place from autumn 2012 up to and including spring 2013. In each of the nine main sites (S1–3, C1–3, N1–3), 30 “focal” trees were randomly selected from among the living, unsuppressed, i.e., not overshadowed by their neighbours, individuals. In site S0 there were few living trees (Table 1); therefore 27 focal trees were selected, of which eight were alive and 19 dead. Two wood cores were extracted at breast height from opposite sides of each focal tree, by using an increment borer.

All trees located within 8 m (Linares et al. 2010) from a focal tree were considered “neighbours.” We recorded the diameter at breast height (DBH) of each focal tree and its neighbors(s), the distance of each neighbor from its respective focal tree, and the height of each focal tree. Woody species other than *P. halepensis* or regenerated *P. halepensis* individuals were very rare in all sites (Fig. S2) (Osem et al. 2009, 2013).

Fig. 1 A cumulative standardized precipitation-evapotranspiration index (SPEI) over the previous 12-month period ($SPEI_{12}$) as a function of month, based on two data sources, **a–c** 0.5° pixels from the global SPEI database for 1901–2011 (see <http://sac.csic.es/spei/>) and **d–f** local meteorological stations' data for 1966–2012 (see Fig. S1; Table 2), in three regions: **a, d** north, **b, e** center and **c, f** south. The SPEI is a standardized variable; values above zero denote water surplus, values below zero denote water deficit. **a–c** A 15-year moving average of $SPEI_{12}$ (positioned at the end of each consecutive 15-year period) is shown as a black solid line. **d–f** The 2011 and 2012 seasons are marked with vertical lines; extreme drought conditions ($SPEI_{12} < -2$) during the studied period (1983–2012) are marked with arrows



Competition index

The intensity of competition around each focal tree was expressed as a distance- and size-dependent competition index (CI) (Linares et al. 2010). The CI of a focal tree (f) is the sum of N quotients (N = the number of neighbours) between the ratio DBH_n/DBH_f and $dist_{fn}$, where DBH_n and DBH_f are DBH values of the neighbor and focal trees,

respectively, and $dist_{fn}$ is the distance from the focal tree to the corresponding neighbor tree, as follows:

$$CI = \sum_{n=1}^N \frac{DBH_n/DBH_f}{dist_{fn}}$$

The effect of CI on tree growth was examined for the last 2 years—2011 and 2012—which happened to form

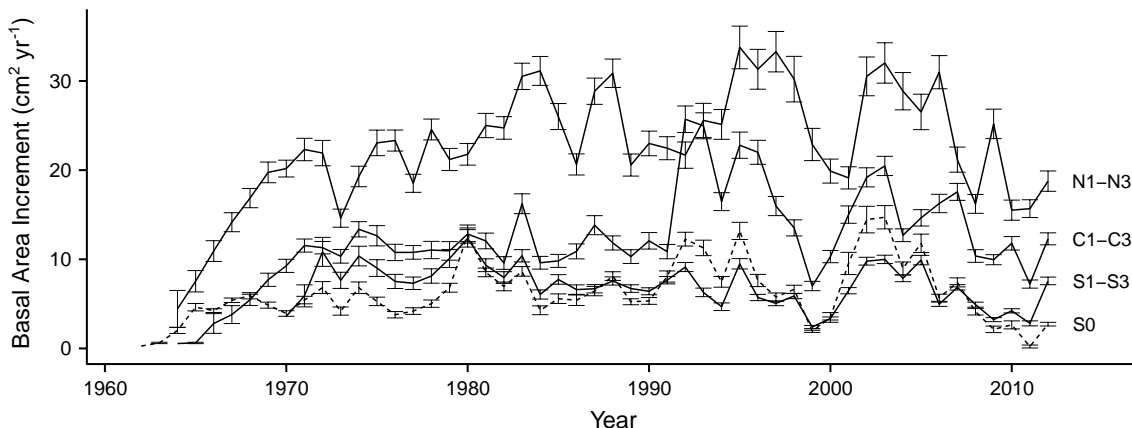


Fig. 2 Basal area increment (BAI) of *Pinus halepensis* as function of year (yr) in the three regions, and in the high-mortality site in the southern region (S0). Values are averages \pm SE, based on 80, 85, and

85 trees for the north (N1–N3), center (C1–C3) and south (S1–S3) regions, respectively, and on 25 trees for the S0 site

a sequence of a drought and a wet year, respectively (see “Results”), enabling us to explicitly address the effects of competition on drought-induced growth decline and subsequent recovery.

Dendrochronological methods

Cores were sanded with increasingly fine sandpaper until tree rings were clearly visible under a binocular microscope. Tree ring width (TRW) was measured to an accuracy of 0.01 mm with a LINTAB 6 measuring device (Rinntech, Heidelberg). In 47 cores (7.9 %) a missing ring could be confidently “interpolated” on the basis of cautious cross-dating against the second core from the same tree (Fig. S6) and the site chronology. These interpolated rings were given the value of 0 mm. In 24 cores (4.0 %) the existence of a missing ring was inferred, but its position could not be unambiguously determined, or the core could not be cross-dated because of tree damage. All 34 cores (5.7 %) from the 17 trees of which at least one core belonged to the latter group were excluded from the analysis. For the remaining 280 trees, average TRW series were calculated based on the two intact cores per tree (Weber et al. 2008).

The last year of growth was 2012, except for the dead trees from site S0, for which the latest year used was that in which a tree ring was present on both cores of the given tree. About half (48 %) of the 54 cores collected in site S0 thus ended at one of the years in the last sequence of drought years (2008–2011) (Fig. 1d–f); the rest ended either earlier (1998–2007; 28 %) or later (2012; 24 %).

To exclude trees having uncharacteristic growth pattern because of damage, agreement of each tree’s TRW series with the corresponding site mean series was evaluated according to the Gleichläufigkeit (Glk) value and its significance. The Glk is a classic time-series agreement

measure based on a sign test—a test that measures the year-to-year agreement between the interval trends of two chronologies, based on the sign of year-to-year growth change and expressed as a percentage (Eckstein and Bauch 1969). Only five trees did not have significant ($p < 0.05$) agreement with their site mean series; these trees were discarded from the analysis. Thus, the final sample (Table 1) consisted of 275 average TRW series from individual trees, i.e., from 92.6 % of the sampled trees.

Detrending by fitting flexible curves (e.g., splines) to the TRW series, followed by removal of autocorrelation from the residual series by means of autoregressive modeling, is a frequently adopted practice in tree ring research (e.g., Pasho et al. 2011), which is intended to emphasize the high-frequency, i.e., year-to-year, component of growth variation. However, it also removes an uncontrolled amount of low-frequency variability (Frank et al. 2007), which is exactly the kind of variability we would expect when growth processes integrate climatic conditions over several years. We thus decided to retain any climate-related low-frequency signals in our tree ring data (Sarris et al. 2014). Therefore, we chose to remove only the trend of decreasing ring width with increasing tree age and size (Biondi and Qeadan 2008), by converting TRW to basal area increment (BAI) values (Fig. 2). The BAI is considered biologically more meaningful than TRW because, by definition, it may express change in resistance to drought of the tree hydraulic system (Brodrribb et al. 2010), and it was shown to outperform TRW for evaluating overall tree growth (Biondi and Qeadan 2008), as related to tree mortality (Bigler and Bugmann 2004) and competition intensity (Weber et al. 2008). BAI was extensively used as the primary indicator of trees physiological state in studies examining trees responses to competition (e.g., Linares et al. 2010) and/or

to drought (e.g., Jump et al. 2006), while more refined traits of annual tree rings, e.g., earlywood and latewood widths (Pasho et al. 2012) or isotopic composition (e.g., Levesque

Table 3 Effects of four climatic variables, at seasonal to annual scales, on average basal area increment (BAI) per region, for the period 1983–2012

Variable	Scale	South	Center	North
<i>P</i>	Fall	0.26 (+)		
	Winter	0.45 (+)	0.41 (+)	
	Spring ^a			0.19 (+)
	Annual	0.71 (+)	0.56 (+)	0.18 (+)
SPEI	Fall			
	Winter	0.50 (+)	0.41 (+)	
	Spring ^a			0.20 (+)
	Annual	0.70 (+)	0.58 (+)	0.22 (+)
<i>T</i> _{min}	Fall	0.14 (−)		
	Winter	0.28 (−)	0.25 (−)	
	Spring		0.26 (−)	0.24 (−)
	Summer			0.14 (−)
<i>T</i> _{max}	Annual	0.25 (−)	0.23 (−)	0.21 (−)
	Fall	0.19 (−)		
	Winter	0.35 (−)	0.35 (−)	
	Spring	0.14 (−)	0.33 (−)	0.17 (−)
Summer				
	Annual	0.33 (−)	0.36 (−)	0.17 (−)

Values are R^2 of linear regressions with the sign of the slope estimate in parentheses, positive (+) or negative (−). Cells where the effects were not significant ($p > 0.05$) are left blank. For other abbreviations, see Tables 1 and 2

^a The effects of summer *P* and the standardized precipitation-evapotranspiration index (SPEI) were not examined because *P* is negligible in that season (Table 2), therefore the effect of *P* is meaningless and that of SPEI is reduced to the effect of *T*_{min} and *T*_{max}.

et al. 2013), are used to obtain supplementary physiological information. The BAI was calculated as follows:

$$\text{BAI}_t = \pi(R_t^2 - R_{t-1}^2)$$

where R_t and R_{t-1} , respectively, are the stem radii at breast height at the end and at the beginning of annual ring formation. The radius was derived by summing all TRW values, from the pith outwards. If the pith was not reached by the borer, the calculated distance from the pith to the first measured ring, based on each site average, was added at the beginning of the series and removed after calculation of the BAI series (Martin-Benito et al. 2011). Finally, regional average BAI chronologies from the last 30 years (1983–2012), when growth patterns had already stabilized after the establishment phase (Fig. 2), were used for analysis of climatic effects on forest growth in each region.

Statistical analysis

Climatic trends (Table S1; Fig. S3) and effects of climatic conditions on BAI (Table 3; Figs. 3, S7, S8) were evaluated at various time scales by using linear regression; more specifically, by using the estimates and *p*-values of the terms in a given model, and the fractions of variance explained by that model (R^2). Quantile regression (Cade and Noon 2003) was used to examine the effect of CI on BAI (Table 4; Fig. 4), where a non-homogeneous relationship was detected (see “Results”).

Statistical analyses were done with the R software (R Development Core Team 2013). The quantreg package (Koenker 2013) was used for fitting quantile regression models; the SPEI package (Beguería and Vicente-Serrano 2013) for calculating PET and SPEI, and the dplR package (Bunn 2008) for calculating Glk.

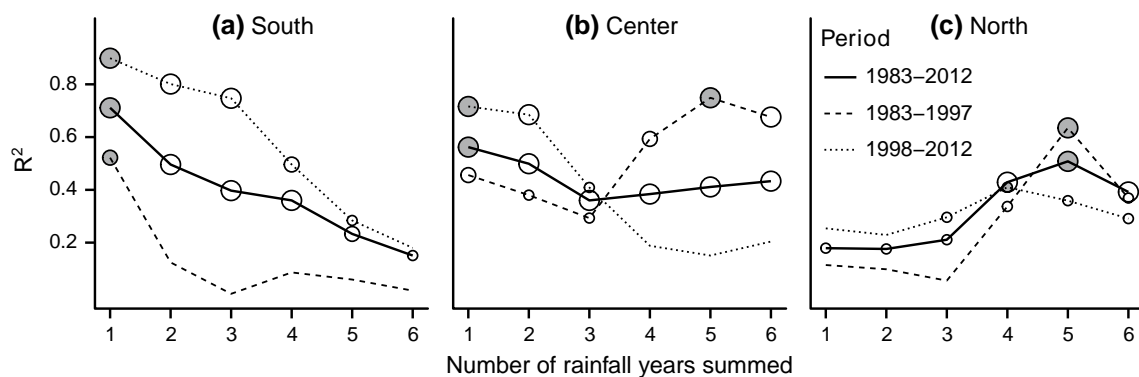


Fig. 3 R^2 -values from linear regression of tree growth (BAI) as function of rainfall amount, for different rainfall integration time-scales (1–6 years) and for three periods (1983–1997, 1998–2012, and 1983–2012), in each of the three regions: **a** south, **b** center and **c** north. Rainfall effects on BAI were positive in all cases. Significant effects

of rainfall are marked with empty circles, with circle size proportional to significance level [$p < 0.001$ (large), $p < 0.01$ (intermediate), $p < 0.05$ (small)]. The integration period that produced the highest R^2 in each region/period combination is marked with a filled circle

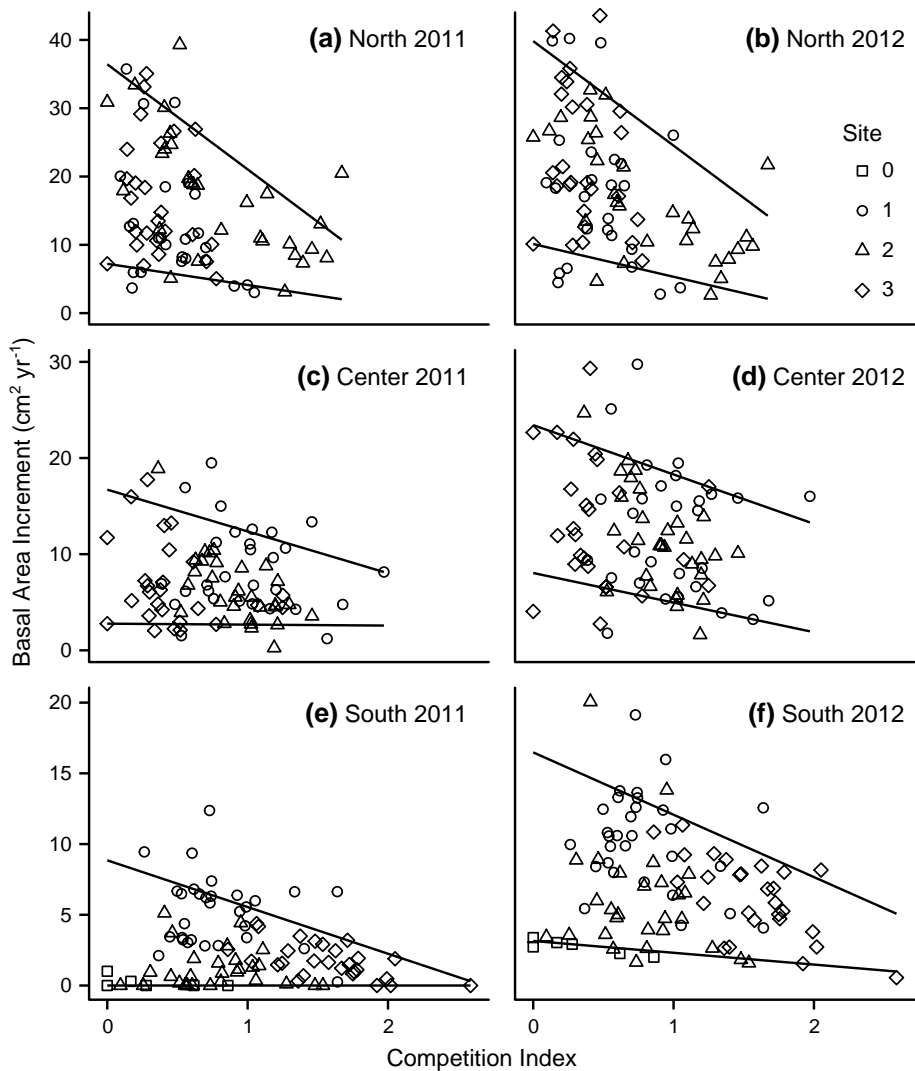
Table 4 Summaries of quantile regression models (10 and 90 % quantiles, i.e., $\tau = 0.1$ and 0.9, respectively) for BAI as function of the competition index (CI), for 2 years in three regions

Estimates, SE and significance of the intercept and slope terms were obtained from 12 quantile regression models. The respective 12 fitted lines are shown in Fig. 4

Significant ($p < 0.05$) effects are marked in bold

Term	τ	Region	2011			2012		
			Value	SE	p	Value	SE	p
Intercept	0.1	North	7.22	2.47	0.005	10.12	3.02	0.001
		Center	2.77	1.38	0.047	8.04	2.32	0.001
		South	0	0.66	1	3.15	1.12	0.006
	0.9	North	36.43	3.18	<0.001	39.82	3.11	<0.001
		Center	16.71	2.23	<0.001	23.42	2.34	<0.001
		South	8.85	1.19	<0.001	16.48	1.87	<0.001
	CI	0.1	North	-3.1	3.19	0.335	-4.8	3.69
		Center	-0.1	1.45	0.946	-3.08	2.51	0.224
		South	0	0.52	1	-0.83	0.89	0.353
	0.9	North	-15.39	3.66	<0.001	-15.3	3.98	<0.001
		Center	-4.35	2.17	0.049	-5.13	2.51	0.044
		South	-3.3	0.86	<0.001	-4.41	1.44	0.003

Fig. 4 BAI as a function of competition index, separately for three regions, **a**, **b** north, **c**, **d** center and **e**, **f** south, and 2 years, **a**, **c**, **e** the dry year 2011, and **b**, **d**, **f** the wet year 2012. Each point represents an individual tree. Quantile regression lines are drawn for each combination of region, year, and quantile (10 and 90 %). **a–f** Lower line 10 % Quantile, upper line 90 % quantile. See Table 4 for statistics of the 12 respective models. Note that y-axis' ranges differ among panels



Results

Climatic trends

Based on the global SPEI database, the most recent 15-year period has been the driest all three regions have experienced during the last 110 years (Fig. 1a–c). Meteorological station data show that three instances of extreme drought conditions ($\text{SPEI12} < -2$) have been observed during the last 30 years (1983–2012), and that they occurred in the same years (1999, 2009, and 2011) in all three regions (Fig. 1d–f). Notably, these years were concentrated into the second (“drier”) half (1998–2012) of the studied period. However, the durations of extreme droughts differed between regions: in the north, each lasted only 1 month, i.e., 1 month satisfied the criterion $\text{SPEI12} < -2$, whereas longer extremely dry periods were observed in the center (10, 1, and 1 months) and south (7, 3, and 3 months in 1999, 2009 and 2011, respectively).

Annual and seasonal rainfall amounts did not show significant temporal trends, except for a decrease in spring rainfall ($p < 0.05$) in the central and northern regions (Table S1; Fig. S3). Temperature (T_{\min} and T_{\max}), however, significantly increased in all three regions, at annual ($p < 0.001$) (Fig. S3) and, in most cases, also seasonal (Table S1) scales. In all regions the steepest rate of temperature increase was observed in summer. For example, the estimated warming rates in the south were 0.051 and 0.054 °C year⁻¹ (Table S1), summing over 47 years to increases of 2.4 and 2.5 °C in T_{\min} and T_{\max} , respectively.

Missing rings

The percentages of cores having at least one missing ring were higher in the south than in the center and north (Table S2). Almost all identified missing rings were associated with the year 2011 (Table S2), and the lowest growth rate among all combinations of sites and years was observed in the high-mortality site S0 in 2011. Six living trees from that site were the only ones for which the 2011 tree ring could be dated on both sampled cores; four of them had a ring missing from the 2011 position, the other two had BAI of 0.30 and 1.00 cm² year⁻¹, giving an average BAI of only 0.22 cm² for that year (Fig. 2). This observation expresses the potentially devastating impact of the 2011 drought on tree growth processes, as well as the association of low growth rates with high mortality risk.

Climate–growth relationships at seasonal to annual scales

In all cases with significant ($p < 0.05$) effects of climatic variables on BAI, the effects of P and SPEI were positive, whereas the effects of T_{\min} and T_{\max} were negative

(Table 3). Annual P had a stronger effect on BAI than seasonal P in the south and center, whereas in the north the effect of annual P was slightly lower than that of spring P . The temperature terms accounted for variation in BAI to similar, relatively small degrees (14–36 %) in all regions, whereas rainfall accounted for it to higher, more variable, degrees (18–71 %).

The importance of the total annual rainfall was further demonstrated by comparing the effects of total rainfall among all possible 12-month annual integration periods. Rainfall totals in the seven 12-month periods that include November–April (which is when ~ 95 % of rainfall occurs, in all three regions) had the highest and relatively constant influence on BAI (Fig. S7). The period November–October was chosen for all subsequent analyses, because, on “average,” it produced slightly higher R^2 -values, among regions (0.48 vs. 0.47–0.48; Fig. S7); however, it was noted that each of the seven alternative periods produced essentially identical results.

In the south and center, either annual P or annual SPEI had the closest fits to the average BAI pattern, whereas in the north T_{\min} had the same effect magnitude as P and SPEI (Table 3). The R^2 -values for the effects of annual P and SPEI were very similar—differing by 0.01–0.04 R^2 “units,” with a similar “average” R^2 of 0.48–0.50 in the three regions. This suggests that use of the more complex SPEI (which is based on P , T_{\min} , T_{\max} , and latitude) offered no advantage over the use of P alone. In accordance with the principle of parsimony (Johnson and Omland 2004), we chose to proceed with the simpler variable (i.e., P) that accounted for the same amount of variation in tree growth.

Multi-annual rainfall effect on growth

When the whole studied period (1983–2012) was examined, multiple-year rainfall was found to have less influence on tree growth than shorter integration periods with progression from north to south (Figs. 3, S8), in contrast to what could be expected based on previous studies (see “Introduction”). Annual rainfall had the highest effect on BAI in the south and center, whereas in the north the most influential scale was 5 years (Figs. 3, S8). Furthermore, in parallel with the lengthening of the influential rainfall integration period, the percentage of BAI variation accounted for by rainfall amount decreased in absolute terms (Fig. 3) in progressing from the south (71 %; 1 year) through the center (56 %; 1 year) to the north (51 %; 5 years).

The responses to climate also differed when the “wetter” (1983–1997) and “drier” (1998–2012) halves (Fig. 1d–f) of the studied period were compared (Fig. 3). In the south, annual rainfall was most influential in both periods, but its effect was higher in the drier period ($R^2 = 0.90$) than in the wetter one ($R^2 = 0.52$). In the center, 5-year rainfall was

most influential in the wetter period ($R^2 = 0.75$), whereas annual rainfall became most influential in the drier period ($R^2 = 0.72$). In the north, the most influential scales were 5 ($R^2 = 0.64$) and 4 ($R^2 = 0.41$) years in the wetter and drier periods, respectively. Thus, a drastic transition in the rainfall-integration periods that accounted for growth was only observed in the center, as the climate shifted to drier conditions.

Competition effect on growth

A heteroscedastic (i.e., heterogeneous statistical variances) pattern was evident in the relationship between CI and BAI, characterized by decreasing variation in BAI among sampled trees, with increasing CI (Fig. 4). Within a given moisture regime, competition appeared to set the upper limit that growth could reach, whereas BAI variation decreased as CI increased. Consequently, we were interested in statistically testing whether the likelihood of observing extreme values of growth (very high or very low BAI) was related to competition. We used quantile regression to separately assess the effects of competition on the lower and upper parts of the BAI distribution (Cade and Noon 2003), specifically the upper and lower deciles, i.e., the 10 and 90 % quantiles (Table 4; Fig. 4).

The slopes, i.e., CI effects (Table 4) of the 10 % quantile regressions were not significantly different from zero in all regions and both years ($p > 0.1$), but the intercepts of the 10 % quantile regressions were significantly ($p < 0.05$) different from zero in all cases except for 2011 in the south ($p > 0.1$). In other words, the “lower level” that BAI reached was constant, consistently uninfluenced by competition. That lower level of BAI was generally higher than zero, except for 2011 in the south (Fig. 4e).

As for the 90 % quantile regressions, both the slope and intercept terms were significantly ($p < 0.05$) different from zero in all cases, and all slopes were negative (Table 4; Fig. 4). In other words, CI had a negative effect on the “upper level” that BAI reached, in all regions and both years. Interestingly, the effect was strongest in the north, where the 90 % quantile of BAI decreased by $15 \text{ cm}^2 \text{ year}^{-1}$ per unit CI, compared with $3\text{--}5 \text{ cm}^2 \text{ year}^{-1}$ in the south and center (Table 4).

The upper limit of BAI variation increased during the wet year 2012 compared with the very dry one of 2011 in all three regions (Table 4; Fig. 4), and the change was more pronounced towards drier areas. From 2011 to 2012, the estimated 90 % BAI quantile at zero competition (i.e., the intercept term in the 90 % quantile regression model) increased from 8.9 to $16.5 \text{ cm}^2 \text{ year}^{-1}$ in the south, compared with an increase from 16.7 to $23.4 \text{ cm}^2 \text{ year}^{-1}$ in the center, and from 36.4 to $39.8 \text{ cm}^2 \text{ year}^{-1}$ in the north (Table 4).

The implication of these results is that the range of observed BAI values decreased as CI increased. The clearest example of this phenomenon was observed during the drought year 2011 in the south, where the 10 and 90 % regression lines meet at CI of 2.7, at BAI of 0, and cross the x -axis at BAI of 0 and $8.9 \text{ cm}^2 \text{ year}^{-1}$, respectively (Table 4; Fig. 4e). In other words, zero growth was expected in all trees experiencing intense competition ($\text{CI} > 2.7$), whereas under minimal competition pressure ($\text{CI} = 0$) BAI values varying between 0 and $8.9 \text{ cm}^2 \text{ year}^{-1}$ could be expected.

Discussion

Rainfall effect at the annual to multi-annual scales

The limiting effect of storage capacity on vegetation is expected to be maximized in regions where $P \approx \text{PET}$, on an annual scale, since the water budget is mainly limited by energy in wetter regions and by precipitation in drier regions (Milly 1994; Schwinnig 2010). Although the entire studied area falls into the $P < \text{PET}$ category, the average annual water balance ($P - \text{PET}$) was most negative in the south, at $-1,096 \text{ mm}$, compared with -858 mm in the center and -470 mm in the north (during 1983–2012). Therefore the potential importance of multi-annual rainfall is theoretically expected to increase from south to north, as indeed has been observed in the present study (see below).

The importance of the single-year integration period of rainfall in explaining tree growth in the southern region (Maseyk et al. 2011), which is extremely dry for *P. halepensis*, could be associated with the very negative water balance, which leads to loss of most of the annual rainfall during the same year (Raz-Yaseef et al. 2012; Ungar et al. 2013). It was previously shown that the proportion of annual rainfall transpired by a planted *P. halepensis* stand increases with progress from a relatively humid to a relatively arid region. In a region having 280-mm average annual rainfall—Yatir Forest, adjacent to our southern sites—transpiration of the *P. halepensis* trees amounted to 80 % of annual rainfall (Schiller and Cohen 1998), compared with 69 % in a 700-mm year^{-1} region (Ramat Hanadiv) (Schiller and Cohen 1995). Subsequent studies in Yatir Forest found lower proportions: 49–66 % in 2004–2006 (Klein et al. 2013; Ungar et al. 2013); 37 % in 2007 (Raz-Yaseef et al. 2010) and 57 % in 2010 (Klein et al. 2014). The reduction is attributed to thinning from 600 to 300 trees ha^{-1} , which took place in 1994 (Ungar et al. 2013). However, it was also found that surface runoff and deep drainage were negligible (Raz-Yaseef et al. 2010). Therefore, most of the “remaining” rainfall water is lost to the atmosphere each year through interception or through

evapotranspiration from the soil and the herbaceous understory vegetation (Ungar et al. 2013). Thus, the potential for water to be stored and carried over from one year to the next is expected to be low in that region.

In the more humid regions, i.e., center and north, the potential for water to accumulate in deep soil/bedrock layers may be higher, as suggested by the effect of multi-annual accumulated rainfall on tree growth. The shorter influential rainfall-integration periods in the “drier” half of the studied period than in its “wetter” half, are also in accordance with the latter expectation. The higher drought stress during the drier period could result in depletion of water accumulated in deeper layers from previous years, leading to trees’ dependence on shorter rainfall-integration periods. Thus, as could be expected, the transition from longer to shorter integration periods was most pronounced in the central region (Fig. 3), which experiences moderate dryness. In the south, single-year rainfall was already the most influential factor from the beginning of the studied period; therefore drought only increased the impact of the loss of annual rainfall. In the north, rainfall reduction may have had a relatively minor effect, compared with that in the other regions, because the water balance in this region is the least negative (Fig. S3), and recent droughts were the mildest (Fig. 1).

Our estimate for the threshold of the transition towards dependence on annual rainfall was $P \approx 500$ mm (or $P - PET \approx -850$ mm), because the dramatic shift in the influential integration periods (from 5 years to annual; Fig. 3b) was observed in the center, where P decreased from 563 to 438 mm (or $P - PET$ from -788 to -895 mm) between 1983–1997 and 1998–2012. In the north and south, average P (and $P - PET$) values were outside of that range in both periods (higher and lower, respectively) and, indeed, no prominent changes in the lengths of influential rainfall-integration periods were observed in these two regions. The region-dependent disruption of carry-over effects may be a valuable target for future research (Granda et al. 2013), since the shortening of time scales at which climatic influences on tree growth occur implies that more immediate response to drought would be expected; the latter needs to be incorporated into predictions of forest responses to drought (Vicente-Serrano et al. 2013).

Sarris et al. (2007) have shown that on the island of Samos (Greece), which experienced gradual rainfall decline, *P. halepensis* s.l. depended on 4–6 years of rainfall during 1994–2000, when average annual precipitation was 659 mm; during the previous wetter period, shorter integration periods were more influential. These results are in accordance with our present findings, in light of the hypothesis regarding the dependence of the importance of storage capacity on the annual water balance. During 1994–2000 Samos received rainfall amounts similar to those of

northern Israel (659 and 693 mm, respectively), and similar integration periods (4–6 and 4–5 years, respectively) were found to have the most influence on tree growth in both cases. The earlier period in Samos was wetter (842 mm in 1951–1977), therefore it could be that the importance of storage and, therefore, of multi-annual rainfall was again reduced, because the limiting effect of water availability on tree growth was weaker (Schwinning 2010). This is in agreement with findings for another tree species growing in a relatively humid environment (Levesque et al. 2013), where greater utilization of water from deeper soil layers was indicated at a relatively xeric site (701-mm annual rainfall) than at a relatively mesic one (1,184 mm).

In light of our present findings, together with those from Greece (Sarris et al. 2007, 2011, 2013), we suggest that along the aridity gradient in eastern Mediterranean *P. halepensis* forests, influential drought scales are multi-annual under intermediate water-balance conditions, and that they contract towards annual scales under either drier or wetter conditions, in space (along climatic gradients) and in time (under alternating wetter and drier climatic conditions). By artificially extending the geographical range of the species, the planted forests may, therefore, provide a valuable demonstration of the processes that will occur at the xeric limit of the natural distribution of *P. halepensis* s.l. in the future, under global climate change.

Effect of competition

The non-homogeneous variability of competition effect on tree growth was in accordance with the concept of multiple limiting factors operating in the studied system (Cade and Noon 2003). In other words, the degree of responsiveness to competition varied among trees from different “portions” of the BAI variation; whereas the fast-growing trees were sensitive to competition, and therefore more likely to occur in low-competition neighborhoods, the slow-growing trees were insensitive, and therefore equally likely to occur under all competition intensities (Fig. 4). The insensitivity to competition of the slowest growing trees, as well as the lack of association between tree density and mortality among sites (Table 1), thus indicate that mortality risk may be density independent, contrariwise to the traditional assumption (e.g., Linares et al. 2010).

The *P. halepensis* forests in Israel were mostly planted on shallow soil, because areas of deeper soil were utilized for agriculture. For example, average soil depths in Lahav (where sites S0–S2 are located) and Yatir (~15 km to the east) forests are 30–35 cm (Schiller 1972). Under such conditions, the differences in tree growth and performance are significantly affected by the differences in storage capacity of the subsoil materials (Schiller 1982), which can be substantial (Schwinning 2010, 2013). For

example, the development of *P. halepensis* was similarly good on marl and chalk (which our study sites are located on) in a 200- to 300-mm-rainfall area to that on limestone or dolomite in a 500- to 600-mm area, probably because of the contributions to water retention of the higher porosity and lower permeability of the former (Schiller 1982).

We hypothesize that the structure of the soil/bedrock complex, in addition to modifying water storage, may change the nature of competition for water. When soil water storage is mainly limited to shallow soil/bedrock interfaces, trees' zones of influence may be much less under their own control, i.e., with a fixed water-harvesting area surrounding each tree, but instead may be determined by the frequency of suitable bedrock fissures (Schwinning 2010, 2013). It is even possible for pathways for roots through rocks to be so scarce that roots of different individuals will rarely come into close contact except in the soil horizon (Schwinning 2013). Further research is necessary to examine whether slow growth and insensitivity to competition, at both the individual-tree and site levels, may characterize locations of low-capacity and/or fragmented water pools in deep soil layers.

It is important to note that the present study addressed only unsuppressed trees; therefore, the range of competition intensities (Fig. 4) does not include the most extreme competition conditions. However, extrapolation of our results shows that the probability of observing high growth rates in suppressed trees was very low, regardless of local habitat quality; with regard to the drought year 2011 in the south as an extreme example, zero growth was expected in all trees at CI > 2.7 (Fig. 4e). The association of lower growth rates with increased mortality risk was established in numerous studies (e.g., Suarez et al. 2004; Bigler et al. 2007). It was also shown that tree ring production may stop some years before actual tree death, as defined by lack of green foliage (Cherubini et al. 2002). Very narrow or missing tree rings, therefore, express the most extreme degrees of stress along that continuum, likely indicating high mortality risk for those individual trees (Sarris et al. 2007; Novak et al. 2011).

Author contribution statement MD, AP, DS and TS have conceived and designed the study, MD and DS conducted fieldwork and tree-ring measurements, MD wrote the manuscript.

Acknowledgments We thank David Brand, Israel Tauber, Ronen Talmor, Efrat Sheffer, and Shmuel Sprintsin for providing helpful information and resources. The Israeli Forest Service (KKL) willingly provided forest geographic information system layers and purchased the equipment and software for the dendrochronological analysis. We thank Arnon Cooper, Or Livni, Adam Wattenberg, Yoni Waitz, Ezra Ben-Moshe, and Yosi Moshe for assistance in field work. This study

is supported by grants from the Chief Scientist of the Israeli Ministry of Agriculture and Rural Development, and the Jewish National Fund. M. D. acknowledges financial support from the René Karshon Foundation. D. S. acknowledges financial support from the Short Scientific Visit programme of the European Forest Institute (Mediterranean Office)—EFIMED.

References

- Adams HD, Guardiola-Claramonte M, Barron-Gafford GA et al (2009) Temperature sensitivity of drought-induced tree mortality portends increased regional die-off under global-change-type drought. Proc Natl Acad Sci USA 106:7063–7066
- Allen CD, Macalady AK, Chenchouni H et al (2010) A global overview of drought- and heat-induced tree mortality reveals emerging climate change risks for forests. For Ecol Manage 259:660–684
- Beguería S, Vicente-Serrano SM (2013) SPEI: calculation of the standardised precipitation-evapotranspiration index. R package version 1.4. <http://CRAN.R-project.org/package=SPEI>
- Bigler C, Bugmann H (2004) Predicting the time of tree death using dendrochronological data. Ecol Appl 14:902–914
- Bigler C, Gavin DG, Gunning C, Veblen TT (2007) Drought induces lagged tree mortality in a subalpine forest in the Rocky Mountains. Oikos 116:1983–1994
- Biondi F, Qeadan F (2008) A theory-driven approach to tree-ring standardization: defining the biological trend from expected basal area increment. Tree Ring Res 64:81–96
- Breda N, Badeau V (2008) Forest tree responses to extreme drought and some biotic events: towards a selection according to hazard tolerance? Comptes Rendus Geosci 340:651–662
- Breshears DD, Myers OB, Barnes FJ (2009) Horizontal heterogeneity in the frequency of plant-available water with woodland intercanopy-canopy vegetation patch type rivals that occurring vertically by soil depth. Ecohydrology 2:503–519
- Brodrribb TJ, Bowman D, Nichols S, Delzon S, Burlett R (2010) Xylem function and growth rate interact to determine recovery rates after exposure to extreme water deficit. New Phytol 188:533–542
- Bunn AG (2008) A dendrochronology program library in R (dplR). Dendrochronologia 26:115–124
- Cade BS, Noon BR (2003) A gentle introduction to quantile regression for ecologists. Front Ecol Environ 1:412–420
- Carnicer J, Coll M, Ninyerola M, Pons X, Sanchez G, Penuelas J (2011) Widespread crown condition decline, food web disruption, and amplified tree mortality with increased climate change-type drought. Proc Natl Acad Sci USA 108:1474–1478
- Cherubini P, Fontana G, Rigling D, Dobbertin M, Brang P, Innes JL (2002) Tree-life history prior to death: two fungal root pathogens affect tree-ring growth differently. J Ecol 90:839–850
- Coll M, Penuelas J, Ninyerola M, Pons X, Carnicer J (2013) Multivariate effect gradients driving forest demographic responses in the Iberian Peninsula. For Ecol Manage 303:195–209
- Dorman M, Svoray T, Perevolotsky A (2013a) Homogenization in forest performance across an environmental gradient—the interplay between rainfall and topographic aspect. For Ecol Manage 310:256–266
- Dorman M, Svoray T, Perevolotsky A, Sarris D (2013b) Forest performance during two consecutive drought periods: diverging long-term trends and short-term responses along a climatic gradient. For Ecol Manage 310:1–9
- Eckstein D, Bauch J (1969) Beitrag zur Rationalisierung eines dendrochronologischen Verfahrens und zur Analyse seiner Aussagesicherheit. Forstwissenschaftl Centralbl 88:230–250

- Frank D, Buentgen U, Boehm R, Maugeri M, Esper J (2007) Warmer early instrumental measurements versus colder reconstructed temperatures: shooting at a moving target. *Quat Sci Rev* 26:3298–3310
- Fritts HC (1976) Tree rings and climate. Academic Press, London
- Galiano L, Martinez-Vilalta J, Lloret F (2011) Carbon reserves and canopy defoliation determine the recovery of Scots pine 4 yr after a drought episode. *New Phytol* 190:750–759
- Giorgi F, Lionello P (2008) Climate change projections for the Mediterranean region. *Glob Planet Change* 63:90–104
- Gomez-Aparicio L, Garcia-Valdes R, Ruiz-Benito P, Zavala MA (2011) Disentangling the relative importance of climate, size and competition on tree growth in Iberian forests: implications for forest management under global change. *Glob Change Biol* 17:2400–2414
- Granda E, Julio Camarero J, Gimeno TE, Martinez-Fernandez J, Valladares F (2013) Intensity and timing of warming and drought differentially affect growth patterns of co-occurring Mediterranean tree species. *Eur J For Res* 132:469–480
- Grunzweig JM, Lin T, Rotenberg E, Schwartz A, Yakir D (2003) Carbon sequestration in arid-land forest. *Glob Change Biol* 9:791–799
- Hall JK, Cleave RL (1988) The DTM project. *Geol Surv Isr* 6:1–7
- Hargreaves GH (1994) Defining and using reference evapotranspiration. *J Irrig Drain Eng ASCE* 120:1132–1139
- Hoerling M, Eischeid J, Perlitz J, Quan X, Zhang T, Pegion P (2012) On the increased frequency of Mediterranean drought. *J Clim* 25:2146–2161
- Johnson JB, Omland KS (2004) Model selection in ecology and evolution. *Trends Ecol Evol* 19:101–108
- Julio Camarero J, Bigler C, Carlos Linares J, Gil-Pelegrin E (2011) Synergistic effects of past historical logging and drought on the decline of Pyrenean silver fir forests. *For Ecol Manage* 262:759–769
- Jump AS, Hunt JM, Penuelas J (2006) Rapid climate change-related growth decline at the southern range edge of *Fagus sylvatica*. *Glob Change Biol* 12:2163–2174
- Jump AS, Matyas C, Penuelas J (2009) The altitude-for-latitude disparity in the range retractions of woody species. *Trends Ecol Evol* 24:694–701
- Kerhoulas LP, Kolb TE, Hurteau MD, Koch GW (2013) Managing climate change adaptation in forests: a case study from the U.S. Southwest. *J Appl Ecol* 50:1311–1320
- Klein T, Cohen S, Yakir D (2011) Hydraulic adjustments underlying drought resistance of *Pinus halepensis*. *Tree Physiol* 31:637–648
- Klein T, Shprunger I, Fikler B, Elbaz G, Cohen S, Yakir D (2013) Relationships between stomatal regulation, water use, and water-use efficiency of two coexisting key Mediterranean tree species. *For Ecol Manage* 302:34–42
- Klein T, Rotenberg E, Cohen-Hilaleh E, et al. (2014) Quantifying transpirable soil water and its relations to tree water use dynamics in a water-limited pine forest. *Ecohydrology* 7:409–419
- Koenker R (2013) quantreg: quantile regression. R package version 5.05. <http://CRAN.R-project.org/package=quantreg>
- Korner C, Sarris D, Christodoulakis D (2005) Long-term increase in climatic dryness in the East-Mediterranean as evidenced for the island of Samos. *Reg Environ Change* 5:27–36
- Levesque M, Saurer M, Siegwolf R, Eilmann B, Brang P, Bugmann H, Rigling A (2013) Drought response of five conifer species under contrasting water availability suggests high vulnerability of Norway spruce and European larch. *Glob Change Biol* 19:3184–3199
- Linares JC, Camarero JJ, Carreira JA (2010) Competition modulates the adaptation capacity of forests to climatic stress: insights from recent growth decline and death in relict stands of the Mediterranean fir *Abies pinsapo*. *J Ecol* 98:592–603
- Linares JC, Delgado-Huertas A, Carreira JA (2011) Climatic trends and different drought adaptive capacity and vulnerability in a mixed *Abies pinsapo*–*Pinus halepensis* forest. *Clim Change* 105:67–90
- Martin-Benito D, Kint V, Del Rio M, Muys B, Canellas I (2011) Growth responses of West-Mediterranean *Pinus nigra* to climate change are modulated by competition and productivity: past trends and future perspectives. *For Ecol Manage* 262:1030–1040
- Maseyk K, Grunzweig JM, Rotenberg E, Yakir D (2008a) Respiration acclimation contributes to high carbon-use efficiency in a seasonally dry pine forest. *Glob Change Biol* 14:1553–1567
- Maseyk KS, Lin T, Rotenberg E, Gruenzweig JM, Schwartz A, Yakir D (2008b) Physiology–phenology interactions in a productive semi-arid pine forest. *New Phytol* 178:603–616
- Maseyk K, Hemming D, Angert A, Leavitt SW, Yakir D (2011) Increase in water-use efficiency and underlying processes in pine forests across a precipitation gradient in the dry Mediterranean region over the past 30 years. *Oecologia* 167:573–585
- Mazza G, Manetti MC (2013) Growth rate and climate responses of *Pinus pinea* L. in Italian coastal stands over the last century. *Clim Change* 121:713–725
- McDowell NG, Adams HD, Bailey JD, Hess M, Kolb TE (2006) Homeostatic maintenance of Ponderosa pine gas exchange in response to stand density changes. *Ecol Appl* 16:1164–1182
- Milly PCD (1994) Climate, soil water storage, and the average annual water balance. *Water Resour Res* 30:2143–2156
- Newman BD, Campbell AR, Wilcox BP (1997) Tracer-based studies of soil water movement in semi-arid forests of New Mexico. *J Hydrol* 196:251–270
- Niinemets U (2010) Responses of forest trees to single and multiple environmental stresses from seedlings to mature plants: past stress history, stress interactions, tolerance and acclimation. *For Ecol Manage* 260:1623–1639
- Novak K, De Luis M, Cufar K, Raventos J (2011) Frequency and variability of missing tree rings along the stems of *Pinus halepensis* and *Pinus pinea* from a semiarid site in SE Spain. *J Arid Environ* 75:494–498
- Olivar J, Bogino S, Rathgeber C, Bonnesoeur V, Bravo F (2014) Thinning has a positive effect on growth dynamics and growth–climate relationships in Aleppo pine (*Pinus halepensis*) trees of different crown classes. *Ann For Sci* 71:395–404
- Osem Y, Zang Y, Bney-Moshe E, Moshe Y, Karni N, Nisan Y (2009) The potential of transforming simple structured pine plantations into mixed Mediterranean forests through natural regeneration along a rainfall gradient. *For Ecol Manage* 259:14–23
- Osem Y, Yavlovich H, Zecharia N, Atzmon N, Moshe Y, Schiller G (2013) Fire-free natural regeneration in water limited *Pinus halepensis* forests: a silvicultural approach. *Eur J For Res* 132:679–690
- Pasho E, Julio Camarero J, De Luis M, Vicente-Serrano SM (2011) Impacts of drought at different time scales on forest growth across a wide climatic gradient in north-eastern Spain. *Agric For Meteorol* 151:1800–1811
- Pasho E, Julio Camarero J, Vicente-Serrano SM (2012) Climatic impacts and drought control of radial growth and seasonal wood formation in *Pinus halepensis*. *Trees Struct Funct* 26:1875–1886
- Penuelas J, Lloret F, Montoya R (2001) Severe drought effects on Mediterranean woody flora in Spain. *For Sci* 47:214–218
- Pigott CD, Pigott S (1993) Water as a determinant of the distribution of trees at the boundary of the Mediterranean zone. *J Ecol* 81:557–566
- Querejeta JI, Estrada-Medina H, Allen MF, Jimenez-Osorio JJ (2007) Water source partitioning among trees growing on shallow karst soils in a seasonally dry tropical climate. *Oecologia* 152:26–36
- Raz-Yaseef N, Yakir D, Rotenberg E, Schiller G, Cohen S (2010) Ecohydrology of a semi-arid forest: partitioning among water balance components and its implications for predicted precipitation changes. *Ecohydrology* 3:143–154

- Raz-Yaseef N, Yakir D, Schiller G, Cohen S (2012) Dynamics of evapotranspiration partitioning in a semi-arid forest as affected by temporal rainfall patterns. *Agric For Meteorol* 157:77–85
- R Development Core Team (2013) R: a language and environment for statistical computing. R Foundation for Statistical Computing, Vienna. <http://www.R-project.org/>
- Sanchez-Salguero R, Navarro-Cerrillo RM, Julio Camarero J, Fernandez-Cancio A (2012) Selective drought-induced decline of pine species in southeastern Spain. *Clim Change* 113:767–785
- Sanchez-Salguero R, Camarero JJ, Dobbertin M, et al. (2013) Contrasting vulnerability and resilience to drought-induced decline of densely planted vs. natural rear-edge *Pinus nigra* forests. *For Ecol Manage* 310:956–967
- Sarris D, Christodoulakis D, Körner C (2007) Recent decline in precipitation and tree growth in the eastern Mediterranean. *Glob Change Biol* 13:1187–1200
- Sarris D, Christodoulakis D, Körner C (2011) Impact of recent climatic change on growth of low elevation eastern Mediterranean forest trees. *Clim Change* 106:203–223
- Sarris D, Siegwolf R, Körner C (2013) Inter- and intra-annual stable carbon and oxygen isotope signals in response to drought in Mediterranean pines. *Agric For Meteorol* 168:59–68
- Sarris D, Christopoulou A, Angelonidi E, Koutsias N, Fulé P, Ariontsou M (2014) Increasing extremes of heat and drought associated with recent severe wildfires in southern Greece. *Reg Environ Change* 14:1257–1268
- Schiller G (1972) Ecological factors affecting the growth of Aleppo pine in the southern Judean Hills (in Hebrew). Leaflet no. 44. Agricultural Research Organization, Forest Division, Ilanot
- Schiller G (1982) Significance of bedrock as a site factor for Aleppo pine. *For Ecol Manage* 4:213–223
- Schiller G (2000) Ecophysiology of *Pinus halepensis* Mill. and *P. brutia* Ten. In: Ne'eman G, Trabaud L (eds) Ecology, biogeography and management of *Pinus halepensis* and *P. brutia* forest ecosystems in the Mediterranean Basin. Backhuys, Leiden, pp 51–65
- Schiller G, Cohen Y (1995) Water regime of a pine forest under a Mediterranean climate. *Agric For Meteorol* 74:181–193
- Schiller G, Cohen Y (1998) Water balance of *Pinus halepensis* Mill. afforestation in an arid region. *For Ecol Manage* 105:121–128
- Schwinning S (2010) The ecohydrology of roots in rocks. *Ecohydrology* 3:238–245
- Schwinning S (2013) Do we need new rhizosphere models for rock-dominated landscapes? *Plant Soil* 362:25–31
- Suarez ML, Ghermandi L, Kitzberger T (2004) Factors predisposing episodic drought-induced tree mortality in *Nothofagus*—site, climatic sensitivity and growth trends. *J Ecol* 92:954–966
- Ungar ED, Rotenberg E, Raz-Yaseef N, Cohen S, Yakir D, Schiller G (2013) Transpiration and annual water balance of Aleppo pine in a semiarid region: implications for forest management. *For Ecol Manage* 298:39–51
- Vicente-Serrano SM, Beguería S, Lopez-Moreno JI (2010a) A multiscalar drought index sensitive to global warming: the standardized precipitation evapotranspiration index. *J Clim* 23:1696–1718
- Vicente-Serrano SM, Lasanta T, Gracia C (2010b) Aridification determines changes in forest growth in *Pinus halepensis* forests under semiarid Mediterranean climate conditions. *Agric For Meteorol* 150:614–628
- Vicente-Serrano SM, Gouveia C, Julio Camarero J, et al (2013) Response of vegetation to drought time-scales across global land biomes. *Proc Natl Acad Sci USA* 110:52–57
- Weber P, Bugmann H, Fonti P, Rigling A (2008) Using a retrospective dynamic competition index to reconstruct forest succession. *For Ecol Manage* 254:96–106
- Zwieniecki MA, Newton M (1995) Roots growing in rock fissures: their morphological adaptation. *Plant Soil* 172:181–187

3.4 Determinants of local-scale variation in tree mortality in a semi-arid region: observations on several scales

In this chapter, the spatial pattern of drought-induced tree mortality in a semi-arid region was examined, for the first time, simultaneously on three distinct scales, using satellite remote sensing, aerial photography and tree-ring analysis. Results quantitatively supported previous observations, pointing at risk factors for tree mortality (such as deep soil). In addition, the relative strengths of methods to monitor forest response to drought, and the way they can be combined, were clarified.

The results of this study are described in Dorman *et al.* (2015b) (see below).

Supplementary material for this chapter appears in Section 6.4.

What determines tree mortality in dry environments? a multi-perspective approach

MICHAEL DORMAN,^{1,7} TAL SVORAY,¹ AVI PEREVOLOTSKY,² YITZHAK MOSHE,³ AND DIMITRIOS SARRIS^{4,5,6}

¹Department of Geography and Environmental Development, Ben-Gurion University of the Negev, Beer-Sheva 84105 Israel

²Department of Agronomy and Natural Resources, Agricultural Research Organization, Volcani Center, Bet Dagan 50250 Israel

³Keren Kayemeth LeIsrael, Southern Region, Gilat Afforestation and Soil Conservation, Gilat Doar-Na Hanegev 85410 Israel

⁴Faculty of Pure and Applied Sciences, Open University of Cyprus, 2252 Latsia, Nicosia, Cyprus

⁵Department of Biological Sciences, University of Cyprus, 1678 Nicosia, Cyprus

⁶Division of Plant Biology, Department of Biology, University of Patras, 265 00 Patras, Greece

Abstract. Forest ecosystems function under increasing pressure due to global climate changes, while factors determining when and where mortality events will take place within the wider landscape are poorly understood. Observational studies are essential for documenting forest decline events, understanding their determinants, and developing sustainable management plans. A central obstacle towards achieving this goal is that mortality is often patchy across a range of spatial scales, and characterized by long-term temporal dynamics. Research must therefore integrate different methods, from several scientific disciplines, to capture as many relevant informative patterns as possible.

We performed a landscape-scale assessment of mortality and its determinants in two representative *Pinus halepensis* planted forests from a dry environment (~300 mm), recently experiencing an unprecedented sequence of two severe drought periods. Three data sources were integrated to analyze the spatiotemporal variation in forest performance: (1) Normalized Difference Vegetation Index (NDVI) time-series, from 18 Landsat satellite images; (2) individual dead trees point-pattern, based on a high-resolution aerial photograph; and (3) Basal Area Increment (BAI) time-series, from dendrochronological sampling in three sites.

Mortality risk was higher in older-aged sparse stands, on southern aspects, and on deeper soils. However, mortality was patchy across all spatial scales, and the locations of patches within “high-risk” areas could not be fully explained by the examined environmental factors. Moreover, the analysis of past forest performance based on NDVI and tree rings has indicated that the areas affected by each of the two recent droughts do not coincide.

The association of mortality with lower tree densities did not support the notion that thinning semiarid forests will increase survival probability of the remaining trees when facing extreme drought. Unique information was obtained when merging dendrochronological and remotely sensed performance indicators, in contrast to potential bias when using a single approach. For example, dendrochronological data suggested highly resilient tree growth, since it was based only on the “surviving” portion of the population, thus failing to identify past demographic changes evident through remote sensing. We therefore suggest that evaluation of forest resilience should be based on several metrics, each suited for detecting transitions at a different level of organization.

Key words: *aerial photography; Aleppo pine; dendrochronology; drought; Landsat; Pinus halepensis; remote sensing; semiarid; tree rings.*

INTRODUCTION

Drought-induced forest mortality

Changes in climate are taking place at an increasing rate across the globe, and are likely to continue into the future (Mora et al. 2013). The uncertainty of how forest ecosystems will respond to projected climatic changes is an on-going challenge. For instance, the physiological mechanisms through which drought drives tree mortal-

ity are a rapidly growing research interest (McDowell et al. 2008, 2011, Anderegg et al. 2012). However, mechanistic understanding of tree mortality processes is yet insufficient for prediction of timing, or spatial pattern, of tree die-off events (McDowell et al. 2011, 2013a). Therefore, observational studies are essential for documenting the decline events that are already underway (Allen et al. 2010), understanding their determinants, and developing forest management plans to ensure that forest ecosystems services are sustained (Anderegg et al. 2013a). Particularly, factors and processes determining when and where mortality events will take place within the wider landscape are poorly

Manuscript received 12 April 2014; revised 30 July 2014; accepted 2 October 2014. Corresponding Editor: W. J. D. van Leeuwen.

⁷ E-mail: michael.dorman@mail.huji.ac.il

understood (Allen et al. 2010, Dwyer et al. 2010, Brouwers et al. 2013a, Clifford et al. 2013).

A multi-perspective observation approach; motivation

Mortality processes are often patchy across a range of spatial scales (Breshears et al. 2011, Michaelian et al. 2011, Macfarlane et al. 2013) and are characterized by long-term temporal dynamics (Bigler et al. 2007, Galiano et al. 2011, Anderegg et al. 2013b). Research therefore must necessarily integrate several scientific disciplines and their respective methods (Hicke and Zeppel 2013, McDowell et al. 2013b) to capture as many relevant informative patterns as possible, such as lagged drought effects on mortality (Bigler et al. 2007) or spatial clustering of dead trees (Liu et al. 2007). In particular, for better understanding the spatial pattern of mortality at regional scales, it is necessary to integrate explicit measurements of ecosystem functioning indicators in the field (Breshears et al. 2009b) with remotely sensed data. The latter are essential to fill data gaps, both in terms of extensive spatial coverage and the ability to look back in time (Rich et al. 2008, Garrity et al. 2013).

The Normalized Difference Vegetation Index (NDVI) is a measure of vegetation greenness and moisture content (Tucker 1979, Pettorelli et al. 2005, Stimson et al. 2005) that is often used as an inclusive measure of forest physiological performance in response to environmental change (Volcani et al. 2005, Dorman et al. 2013b). However, the highest spatial resolution of currently available long-term data (30 m, in Landsat) is insufficient to interpret change in terms of structural and demographic processes the forest goes through (Macfarlane et al. 2013). Therefore, it is necessary to complement remotely sensed greenness trends with measurements of individual tree performance (e.g., radial growth rate) and demographic processes (e.g., mortality rate).

On the one hand, high-resolution aerial photographs, where individual trees are detectable, may provide spatially extensive information on population density changes and mortality rates (Shimazaki et al. 2011, le Polain de Waroux and Lambin 2012, Dorman et al. 2013a, Baguskas et al. 2014), although for sparse and irregularly spaced points in time. On the other hand, the information recorded in tree rings can be dated to construct annual-resolution time series, expressing physiological state of individual sampled trees, although usually covering a limited spatial extent (but see Rozas and Olano 2013). Thus, each of the above-mentioned approaches contributes a unique piece of information, essential for addressing the complex problem at hand. Many previous efforts to examine environmental determinants of forests' response to drought have, however, used a single approach (e.g., satellite remote sensing [Volcani et al. 2005, Yuhas and Scuderi 2009, Vacchiano et al. 2012], aerial photography [Allen and Breshears 1998, Fensham et al. 2005, Clifford et al.

2011], and field or dendrochronological measurements [Suarez et al. 2004, Gitlin et al. 2006, Vila-Cabrera et al. 2013]). Recently, several studies have successfully combined dendrochronological methods with remote sensing to provide a more comprehensive perspective on forest mortality dynamics (Lopatin et al. 2006, Linares et al. 2009a, Babst et al. 2010, Beck et al. 2011, Berner et al. 2011, Lloyd et al. 2011, Kharuk et al. 2013).

*The case study; *Pinus halepensis*-planted forests in a semiarid region*

Pinus halepensis is considered the most drought-tolerant of the Mediterranean pine species (Schiller 2000). Planted forests of this species in the semiarid region of Israel, established primarily for their aesthetic values and used for recreation (Perevolotsky and Sheffer 2009), represent one of the most extreme environments in which the species occurs (Schiller and Atzmon 2009, de Luis et al. 2013). Following an unprecedented sequence of drought periods (1998–2000 and 2005–2011), a steep decline in NDVI (Dorman et al. 2013b), as well as increased mortality (Schiller et al. 2005, Dorman et al. 2013a, Klein et al. 2014), were observed in the planted *P. halepensis* forests occupying the dry edge of the Mediterranean region in Israel (<350 mm of annual rainfall). The latter is one of several analogous observations made in *P. halepensis* s.l. forests around the Mediterranean (Sarris et al. 2007, Vicente-Serrano et al. 2010, Girard et al. 2011, 2012), as well as at the dry edges of distribution of other tree species (Linares et al. 2009a, Matyas 2010, Vila-Cabrera et al. 2011). However, the extent, spatial pattern, and association of mortality with environmental conditions have not been systematically investigated.

Due to the harsh climate, natural regeneration is negligible in the *P. halepensis* planted forests that receive <400 mm of rainfall (Osem et al. 2009, 2013), making forest mortality irreversible without replanting. Analogously, mortality is considered “irreversible” in natural semiarid forests, where it may take decades for a pre-drought extent of mature canopy overstory to develop (Breshears et al. 2011). Understanding the spatial pattern of mortality is therefore crucial for preparing management guidelines designed for these forests, and semiarid forest ecosystems elsewhere, which are expected to experience increasing drought stress under global climate change. Moreover, thanks to the relative homogeneity and the artificial “placement” (by means of planting) of the studied system beyond the natural distribution limit of the species (~450 mm of rainfall [Schiller 2000, Liphshitz and Biger 2001]), it may serve as an (unintended) experiment demonstrating trends and processes that may occur at natural forest xeric limits in the future.

A high-resolution aerial photograph of the drought-affected area was taken in winter 2011/2012, immediately following the peak of a drought period (2005–2011). Identification of individual dead trees in the

photograph, the feasibility of which has been previously demonstrated (Dorman et al. 2013a), has been used to systematically map mortality pattern in two representative forests. Forest age (Dorman et al. 2012), topographic aspect (Dorman et al. 2013a), past (pre-plantation) cultivation indicative of deeper soil (Y. Moshe, *personal observation*), and tree density were examined concerning tree mortality. The last parameter is of particular importance in forest management, since thinning is considered the main tool for enhancing forests' adaptive capacity to withstand drought stress (Linares et al. 2009b, Kerhoulas et al. 2013, Sánchez-Salguero et al. 2013). A series of Landsat satellite images and dendro-ecological field data provided complementary information for characterizing the spatiotemporal variation in forest performance.

Aim and study questions

The aim of this paper was to perform a landscape-scale assessment of *P. halepensis* mortality pattern and its determinants in a dry environment using a multi-perspective approach. From the applied point of view of forest management, the results of the study are ultimately intended to provide knowledge for projecting future impacts of climate change on semiarid planted forests, and for how (and to what extent) the effects may be alleviated. The specific study questions were:

- 1) What was the spatial pattern (i.e., clustered, random, or regular) of dead trees occurrence within the forests following a severe drought?
- 2) How did biotic (age, density) and abiotic (topographic aspect, soil depth) conditions influence tree mortality risk?
- 3) In what way is the forested area divided into distinctive zones characterized by unique past performance trajectories? Are these associated with environmental conditions and with tree mortality risk?

MATERIALS AND METHODS

Study area

The studied area included all 6.6 km² of *P. halepensis*-planted stands in Lahav and Dvira forests (Fig. 1; Israel Forest Service). The climate is semiarid (average annual rainfall of ~300 mm; Fig. 2), and highly seasonal (five consecutive months with <2.5 mm rainfall depth). The forests are located almost exclusively on Brown Lithosol and Colluvial-Alluvial Loess (93% of area) and on Light Brown Loess Soils and Brown Lithosol (7%) (Dan et al. 1970). From personal observations and communication with foresters it was apparent that: (a) dead trees are removed within a short time, and (b) the routine forest management includes thinning once every 12–15 years.

Three sites were randomly selected within the area of Lahav and Dvira forests (Fig. 1) for dendrochronological sampling for tree growth. All sites were located on

south-facing slopes, and were of similar age (43–45 years old in 2012).

Mapping forest mortality and environmental conditions

Forest mortality and trees density were measured using a high-resolution (0.25 m) orthophoto from the winter of 2011/2012. Dead trees were identified and marked by visual interpretation of the aerial photograph, where they were clearly distinguishable due to their gray/reddish color, compared with the green living trees (Appendix A: Figs. A1, A2; see also Fig. S1 in Dorman et al. 2013a). To measure total (dead + living trees) tree density (Appendix A: Fig. A3), and subsequently mortality fraction (dead trees/total number of trees), the living trees were counted as well, within a subset of the forest area. That subset consisted of a randomly selected 10% of the 6070 grid cells (coinciding with Landsat pixels, see *Materials and methods: Satellite remote sensing*) covering the whole forest area. Forest age in 2012 (Appendix A: Fig. A3) was calculated based on planting dates GIS layer (acquired from the Israel Forest Service).

The area was classified to north- and south-facing topographic aspects (Appendix A: Fig. A3) using the 25-m resolution Digital Elevation Model (DEM) layer of Israel (Hall and Cleave 1988). Classification was based on incoming solar radiation estimate (Fu and Rich 2002, Dorman et al. 2013a). Thus, we use the terms “northern” and “southern” aspects not in their narrow sense (slopes facing the north or the south, respectively), but as labels for the classification of the studied area into two distinct categories differing in their radiation load.

Historical aerial photographs were used to delineate previously cultivated fields (i.e., traditional rain-fed cereal plots) indicative of deep soils. The fields could be identified by their bright and “smooth” texture with sharp, straight boundaries (Appendix A: Fig. A3), compared with the rocky terrain which is unsuitable for cultivation and used mainly for grazing. Ten images of the Lahav and Dvira forests (Appendix A: Fig. A4), taken during winter–spring 1945, were geo-referenced to the 2012 images based on position of invariant features such as rock outcrops. Geo-referencing was performed using a second-order polynomial model and >20 control points for each image. Geo-referencing Root Mean Square Error (RMSE) was between 2.4 and 4.6 m (Appendix A: Table A1). A given 30 × 30 m² pixel was considered as “deep soil” if >90% of its area was covered by fields.

Satellite remote sensing

Eighteen Landsat satellite images (16 from Landsat-5 TM, 2 from Landsat-7 ETM+; Appendix B: Table B1), from the period 1994–2012 (one image per year, except for 2002), were used to calculate NDVI time-series for the 6070 pixels of 30 × 30 m² that are completely within forest polygons (Appendix B: Fig. B1). All images were acquired during a relatively short time period at the end

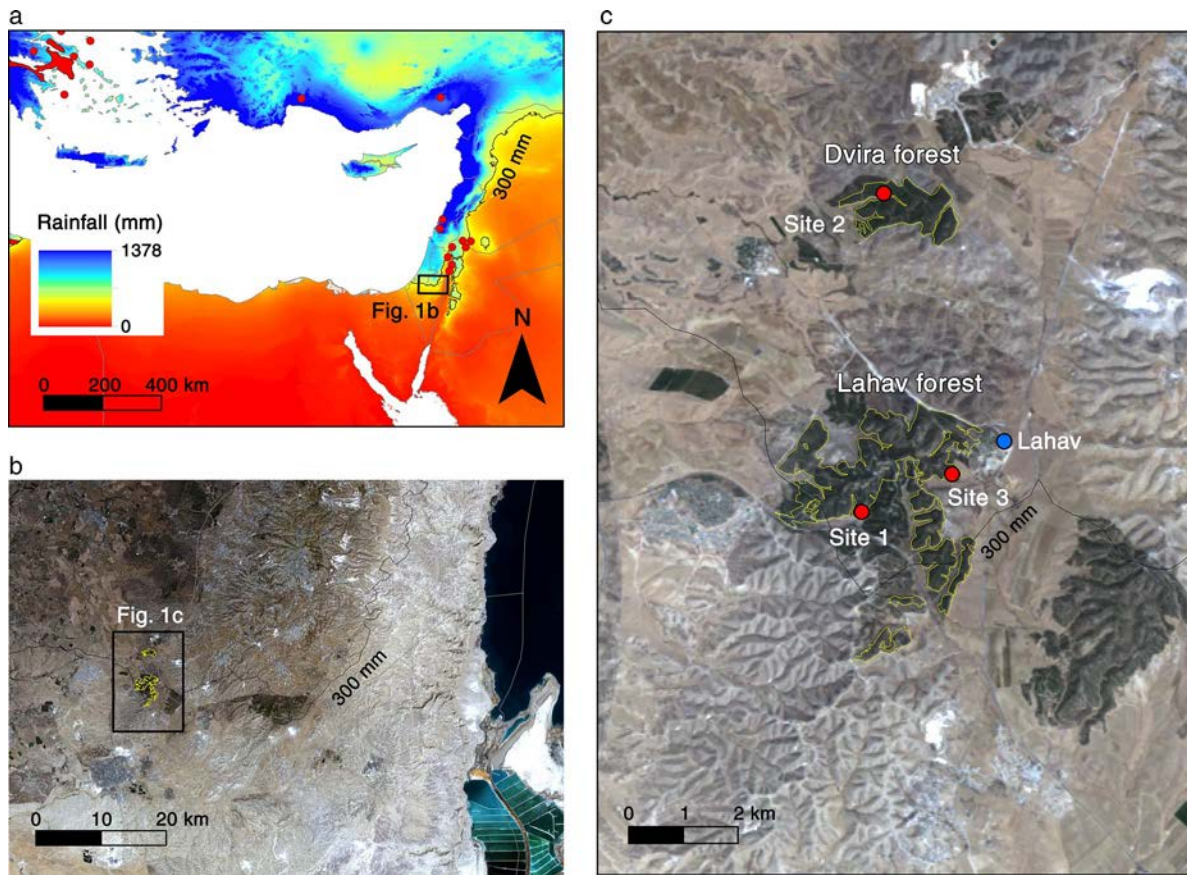


FIG. 1. Location of the study area within the semiarid climatic zone, bordering the more humid Mediterranean climate to the north and the more arid Negev desert to the south. In (a), average annual rainfall amounts for the period 1950–2000 (data from <http://www.worldclim.org/>) are shown as background colors and natural distribution range of *Pinus halepensis* is shown in red (data from <http://www.euforgen.org/distribution-maps>). Lahav and Dvira forests locations, respectively to the 300-mm rainfall line, are shown in (b) and (c), where the background is an RGB Landsat-5 satellite image from 2003. The blue data point in panel (c) marks the location of “Lahav” meteorological station (Fig. 2); the red data points mark the locations of dendrochronological sampling sites.

of the dry season (8 September–16 October), when annual vegetation is completely dry (Appendix A: Fig. A1; [Svoray and Karnieli 2011, Shafran-Nathan et al. 2013]) and soil water content is most temporally stable (Raz-Yaseef et al. 2012). Since perennial vegetation (other than the *P. halepensis* trees) and natural regeneration of *P. halepensis* in this area are negligible due to aridity (Appendix A: Fig. A1) (Osem et al. 2009, 2013), the NDVI signal can be fully attributed to the greenness and water content of the planted *P. halepensis* tree canopy. Images were subjected to geo-referencing, followed by radiometric and atmospheric calibration, using standard methods (see Dorman et al. 2013b for details).

Since 2003, Landsat-7 ETM+ has been operating without the Scan Line Corrector (SLC), which compensates for the forward motion of the satellite during image acquisition. Data collected at the SLC-off mode have gaps in a systematic wedge-shaped pattern; however, spatial and spectral qualities of the remaining

portions of the imagery are not diminished (Wulder et al. 2008, Chen et al. 2011). The issue applies only to our 2012 Landsat-7 ETM+ image, which does not cover ~22% of studied area due to the SLC-off mode (Appendix B: Fig. B1). To eliminate any potential bias due to the incomplete NDVI coverage for 2012, only the period 1994–2011 was considered for spatiotemporal analysis of NDVI data (see *Materials and methods: Statistical methods*). However, since the 2012 image did cover the three dendrochronological sampling sites, it could still be used in the comparison between remote sensing and tree rings inferences regarding drought response (see Fig. 8).

Non-forest areas (roads, buildings, etc.) were manually digitized, and pixels where >10% of the area was non-forest were excluded from the analysis. The final sample sizes were 4839 pixels of $30 \times 30 \text{ m}^2$ for spatiotemporal clustering of NDVI, and 471 pixels for evaluation of environmental effects on mortality.

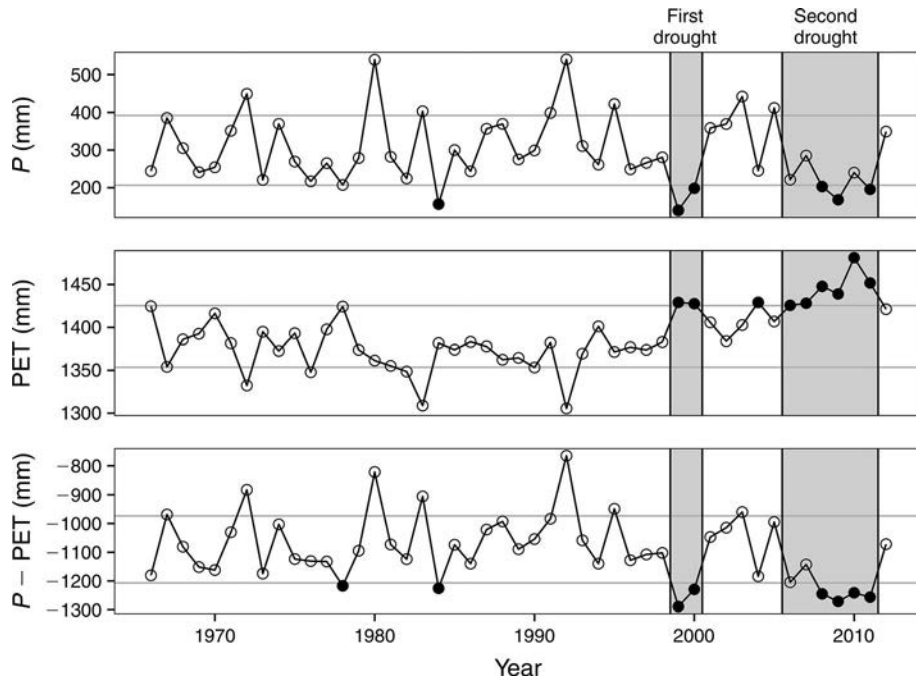


FIG. 2. Annual precipitation (P), potential evapotranspiration (PET), and water balance ($P - PET$) in Lahav during 47 years (1966–2012). Horizontal lines mark the range of the average ± 1 SD for each variable. Values outside of this range towards drought conditions (low P , high T, low $P - PET$), are marked in black.

Dendrochronological methods

Dendrochronological sampling was conducted during autumn 2011–spring 2012. In each of the three sites, 30 living, unsuppressed, i.e., not overshadowed by their neighbors, trees were randomly selected. Two wood cores were extracted from opposite sides of each tree at breast height using an increment borer. Cores were sanded using increasingly fine sanding paper until tree rings were clearly visible under a binocular microscope. Tree ring width (TRW) was measured to an accuracy of 0.01 mm using a LINTAB 6 measuring device (Rinnotech, Heidelberg, Germany). Five trees with damaged cores or undatable missing rings were removed from the analysis. Finally, TRW values were converted to basal area increment (BAI) values (Biondi and Qeadan 2008), and average BAI chronologies were calculated per site. Structural characteristics of the sites (tree dimensions, density, and mortality) are provided in Appendix C.

Climate data

To characterize climatic conditions in the studied area, precipitation (P), minimum temperature (T_{\min}), and maximum temperature (T_{\max}) daily data for the period 1966–2012 were obtained from the standard meteorological station “Lahav” bordering Lahav forest (Fig. 1). Missing values (6%) of T_{\min} and T_{\max} were filled based on data from “Beer-Sheva” station (16 km to the south from “Lahav”) using linear regression. The agreement between the data series from the stations was very high, producing R^2 values of 0.99 for T_{\max} , and

0.88 for T_{\min} , based on ~ 17000 days when both stations operated. Potential evapotranspiration (PET) was estimated based on T_{\min} , T_{\max} , and latitude using the Hargreaves method (Fig. 2) (Hargreaves 1994).

Annual rainfall amount was elected as the most important climatic variable affecting forest growth in the studied region, following a previous systematic examination (Dorman et al., *in press*). It was therefore used to evaluate the degree to which climatic conditions determine NDVI and tree growth rates.

Statistical methods

Two main issues of interest in the analysis of spatial point patterns concern the distribution of events (dead trees, in our case; Appendix A: Fig. A2) in space, and the existence of possible interactions between them (Bivand et al. 2008). The former was examined by fitting linear models to the tree mortality data; the latter, by comparing Ripley’s K -function (Ripley 1977) values to those expected under complete spatial randomness (CSR; i.e., a homogenous Poisson process). Ripley’s K -function analysis (Fig. 3) is based on the concept that if λ is the density of events per unit area, the expected number of points in a circle with radius t centered on a randomly chosen point is $\lambda K(t)$, where $K(t)$ is a function of t that depends on the spatial pattern of the points (Fortin and Dale 2005).

The statistic $\hat{K}(t)$ is an estimate of $K(t)$. Its value under CSR is $K(t) = \pi t^2$; values $\hat{K}(t) - \pi t^2 > 0$ indicate clustering, while values $\hat{K}(t) - \pi t^2 < 0$ indicate a regular

pattern (Fortin and Dale 2005). Random simulations (e.g., producing 99 point patterns where the events, dead trees, are randomly placed within the studied area) were performed to interpret the type of interaction (i.e., clustered, random, or regular pattern) and its scale (i.e., manifestation over short/long distances).

The effects of environmental conditions on the proportion of dead trees were evaluated using a binomial Generalized Linear Model (GLM; Figs. 4, 5; Appendix D). The dependent variable was the dead to total trees count ratio (i.e., mortality proportion) in each $30 \times 30 \text{ m}^2$ pixel. The independent variables were age, density, aspect, and soil depth, and all of their two-way interactions. The latter two were handled as dummy variables, representing two categories (southern vs. northern, and deep soil vs. non-deep soil). A model selection procedure (Johnson and Omland 2004), based on the Akaike Information Criterion (AIC) (Akaike 1974), was employed to select the final model (Appendix D).

To test whether the two consecutive drought events affected either the same or different areas within the forests, we have both visually compared decline magnitudes (i.e., ΔNDVI) maps (Fig. 6), and statistically tested whether a correlation existed between the ΔNDVI values (Appendix E).

An exploratory method of organizing spatiotemporal data is to develop clusters of these data (Chapman et al. 2012, Plant 2012). K-means cluster analysis, using the algorithm of Hartigan and Wong (1979), was applied to examine the spatial pattern of NDVI change through time (Fig. 7). The data for each pixel were standardized to a mean of zero and standard deviation of one (Anderson et al. 2010), to remove differences due to site quality (e.g., north-facing slopes generally have higher NDVI values than south-facing slopes) and concentrate only on the differences in the temporal sequence and direction of NDVI changes. It is important to note that no spatial information is used in the algorithm; each pixel is treated as an independent observation. The optimal number of clusters was determined as four by visually examining the plot of within-groups sums of squares as function of clusters number (Appendix F: Fig. F1) (Hothorn and Everitt 2009).

The resulting four clusters were arbitrarily labelled from 1 to 4 according to mortality level (1 is highest, and 4 is lowest). Dendrochronological sampling sites were consequently also labelled from 1 to 3, since each site was located within one of the 1–3 clusters. Results were visually evaluated in terms of clusters' spatial distribution (Fig. 7a), their average NDVI trajectories (Fig. 7b), and their association with environmental conditions and mortality rates (Appendix F: Table F1). Linear discriminant analysis was used to assess separation of the clusters (Fig. 7c).

The effects of annual rainfall on BAI and NDVI for the dendrochronological sampling sites were determined

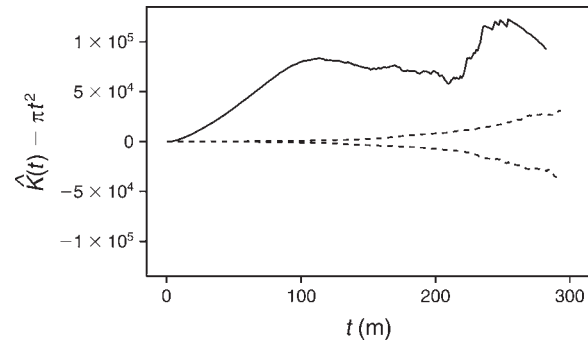


FIG. 3. Ripley's K function minus its expected value at Complete Spatial Randomness (CRS), as function of distance, for the dead *P. halepensis* trees point pattern (Appendix A: Fig. A2). Empirical values (solid line) above or below the envelope produced by 99 random simulations (dashed lines) indicate that dead trees were significantly aggregated or significantly regular, respectively. In the present case dead trees were spatially aggregated across all spatial scales. See *Materials and methods: Statistical methods*.

using linear regression (Fig. 8), based on the common period of data availability (1994–2012, excluding 2002).

Statistical analyses were conducted in R (R Development Core Team 2013). Atmospheric correction of Landsat images was done with the “landsat” package (Goslee 2011). Ripley's K -function analysis was done using package “spatstat” (Baddeley and Turner 2005). Package “MASS” (Venables and Ripley 2002) was used for linear discriminant analysis. Packages “ggplot2” (Wickham 2009) and “lattice” (Sarkar 2008) were used for visualization.

RESULTS

Spatial pattern of dead trees occurrence

A total of 8233 dead trees (Appendix A: Fig. A2) were identified within the studied forests area, giving an average density of 12.52 dead trees/ha. However, the spatial distribution of dry trees was markedly nonrandom. According to Ripley's K -function, significant clustering (“attraction”) of dead trees occurred at all spatial scales (Fig. 3). Namely, dead trees usually occurred near other dead trees, and patches of dead trees near other such patches.

Environmental determinants of mortality

The average proportion of dead trees was 5%; however, mortality was highly variable in space (Fig. 5), being either zero (in 70% of the forest area) or anywhere between 0 and 90% (in the remaining area). Mortality proportion was significantly affected by all four examined factors (Appendix D: Table D1); while three of the effects were acting in the expected direction, the fourth one (trees density) was not. Visualization of model predictions (Fig. 4) revealed that age effect on mortality was positive (higher mortality in older forest stands), density effect was negative (higher mortality in sparser stands), south-facing aspect effect was positive

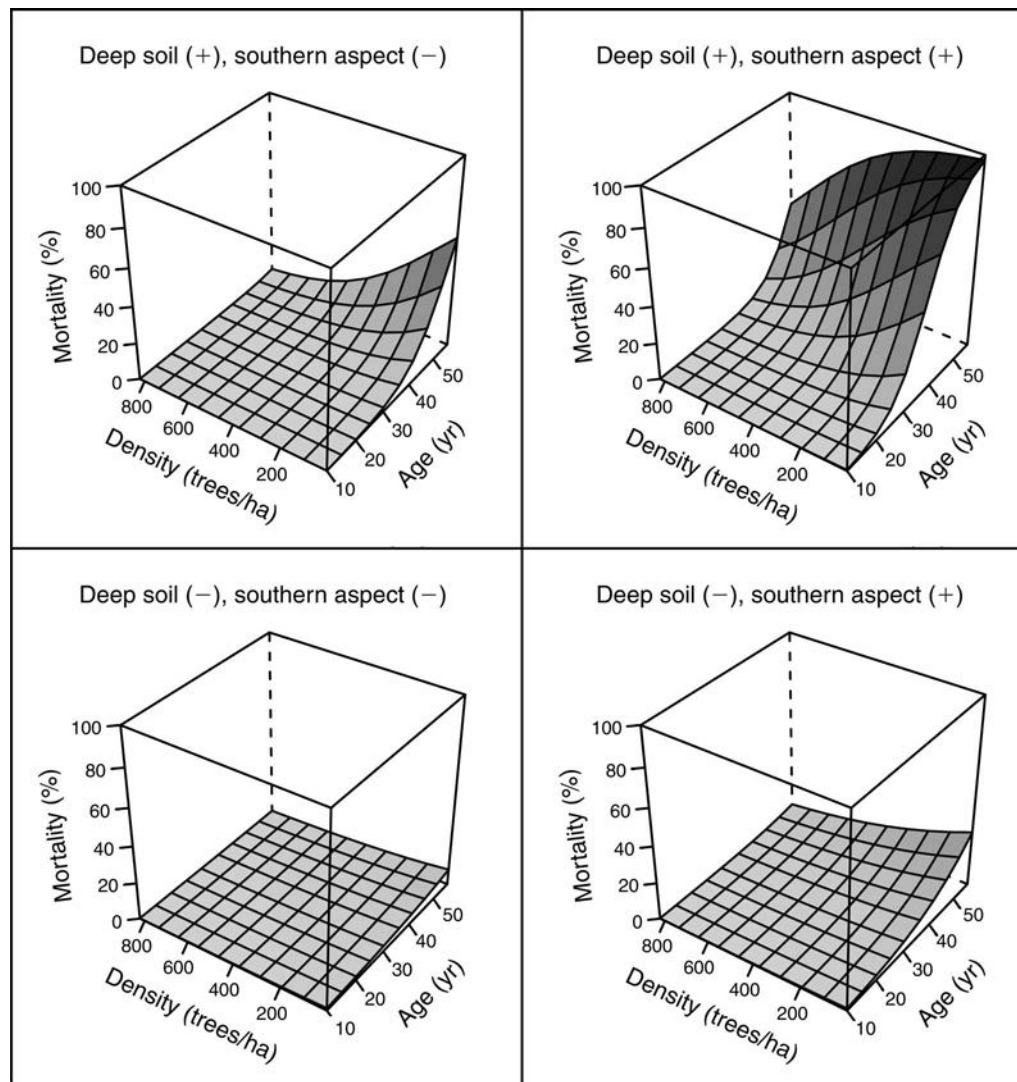


FIG. 4. Predicted mortality proportions as a function of tree density, age, topographic aspect, and soil depth, based on a Generalized Linear Model (GLM; Appendix D: Table D1).

(higher mortality on south-facing slopes), and deep soil effect was positive (higher mortality on deeper soils). The model explained 23.0% of variation in mortality proportions. While areas of relatively elevated mortality risk could be identified, the fine-grained patchiness in mortality was not captured using the examined factors (Fig. 5).

First vs. second drought effects

A weak negative correlation was found between the change in NDVI during the first ($\Delta\text{NDVI}_{\text{first}} = \text{NDVI}_{2000} - \text{NDVI}_{1998}$) and second ($\Delta\text{NDVI}_{\text{second}} = \text{NDVI}_{2011} - \text{NDVI}_{2005}$) droughts (Pearson correlation coefficient = -0.08 , $P < 0.001$; Appendix E). A visual inspection has confirmed that the two droughts affected different regions within the forest (Fig. 6). For example, the areas where $\Delta\text{NDVI}_{\text{first}} < -0.1$ and $\Delta\text{NDVI}_{\text{second}} <$

-0.1 were 30.0% and 21.1% of the entire forested area, respectively; however the two zones overlapped at only 4.5% of the forested area.

Not surprisingly, the area where NDVI had the steepest decrease during the 2005–2011 drought was associated with increased dead tree incidence in 2012. For example, average dead tree density was 40.6 trees/ha within the area where $\Delta\text{NDVI}_{\text{second}} < -0.1$, compared to 7.6 trees/ha within the area where $\Delta\text{NDVI}_{\text{second}} \geq -0.1$.

NDVI spatiotemporal clusters

Four clusters of NDVI spatiotemporal data occupied distinct geographical areas within the forest (Fig. 7a). However, differences in the NDVI trajectories among clusters could be only partially elucidated by differences in the physical and biotic characteristics of the areas they occupy.

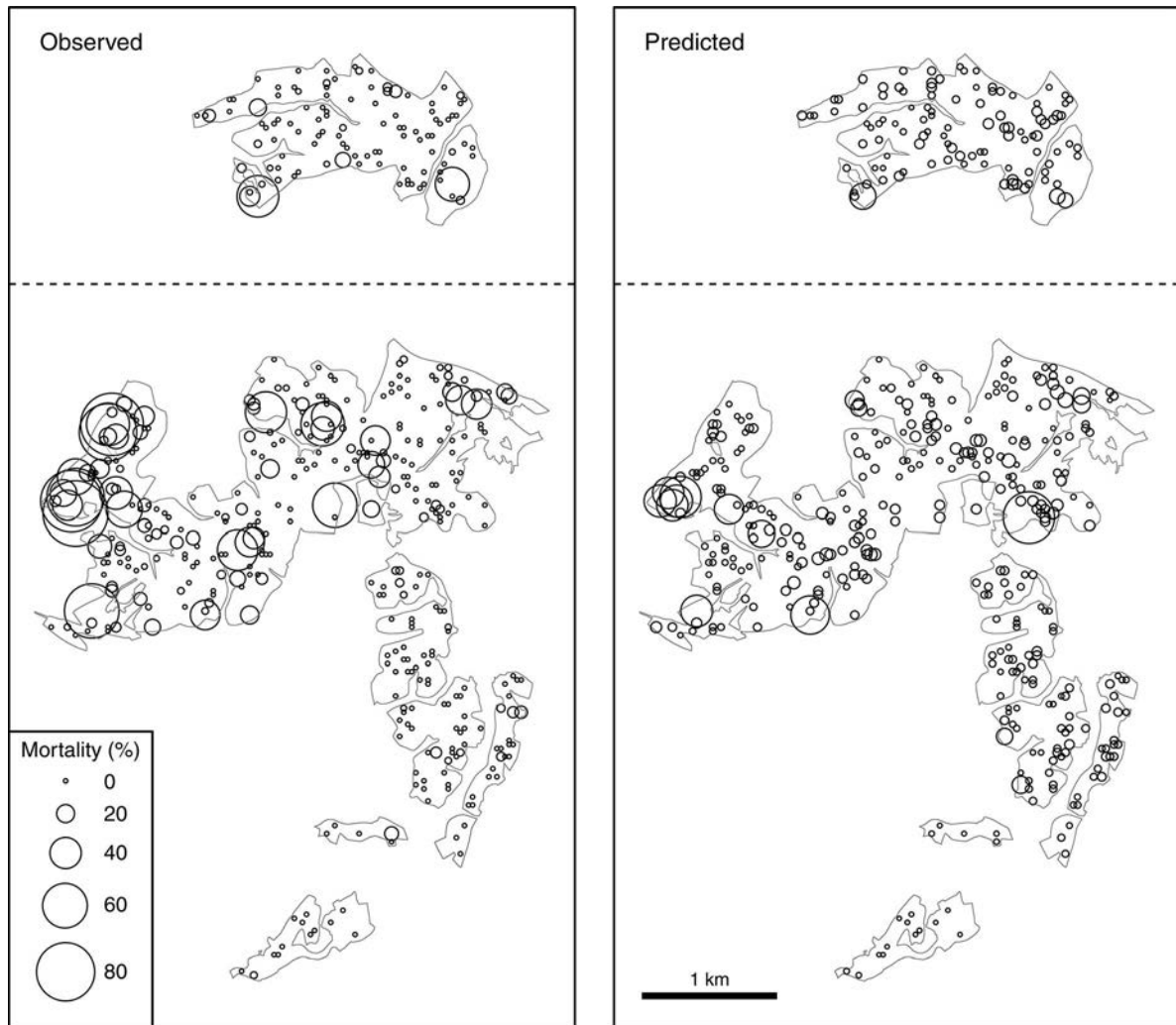


Fig. 5. Observed proportion of dead trees in Lahav and Dvira forests, and predictions based on a Generalized Linear Model (GLM; Appendix D: Table D1), in 471 randomly placed sample points.

Clusters 1–3 were characterized by NDVI decline with time (Fig. 7b) and had a similar distribution of stand ages and topographic aspects (Appendix F: Table F1). However, they differed in contemporary tree density, in deep soil occurrence, and in mortality percentages (Appendix F: Table F1), as well as in their responses to the first and second droughts (Fig. 7b). Cluster 4 occupied a relatively small part of the forest and consisted of relatively young forest stands (Appendix F: Table F1). It was distinct in the most pronounced way from clusters 1–3 (Fig. 7c), by its increasing trend of NDVI (Fig. 7b) and by its very low mortality (Appendix F: Table F1).

Cluster 1 encompassed the area most severely affected by the recent drought of 2005–2011, with average mortality of 12% (compared to ~3% in clusters 2 and 3; Appendix F: Table F1). Moreover, only cluster 1 included locations with extremely high mortality (60–90%; Fig. 5). Its area also had the lowest average NDVI

by the end of the 2005–2011 drought (Fig. 7b), and the highest proportion of cultivated areas among clusters 1–3 (Appendix F: Table F1). Cluster 2 was the least affected by either the first or second droughts, and had the highest average NDVI in 2011. Cluster 3 was the most severely affected by the 1998–2000 drought, according to the steep NDVI decline (Figs. 6 and 7b). Afterwards, NDVI in cluster 3 was relatively low and stable. Accordingly, current (2012) tree density in this cluster was lowest (Appendix F: Table F1), and included patches with very sparse tree cover.

Tree growth

The responses of tree growth to the first and second droughts according to BAI were in agreement with their responses according to NDVI (Fig. 8). Very low BAI and NDVI values were reached in 2011 in site 1 (1.17 and 0.23 cm/yr, respectively); this site also had the steepest NDVI decline during the 2005–2011 drought

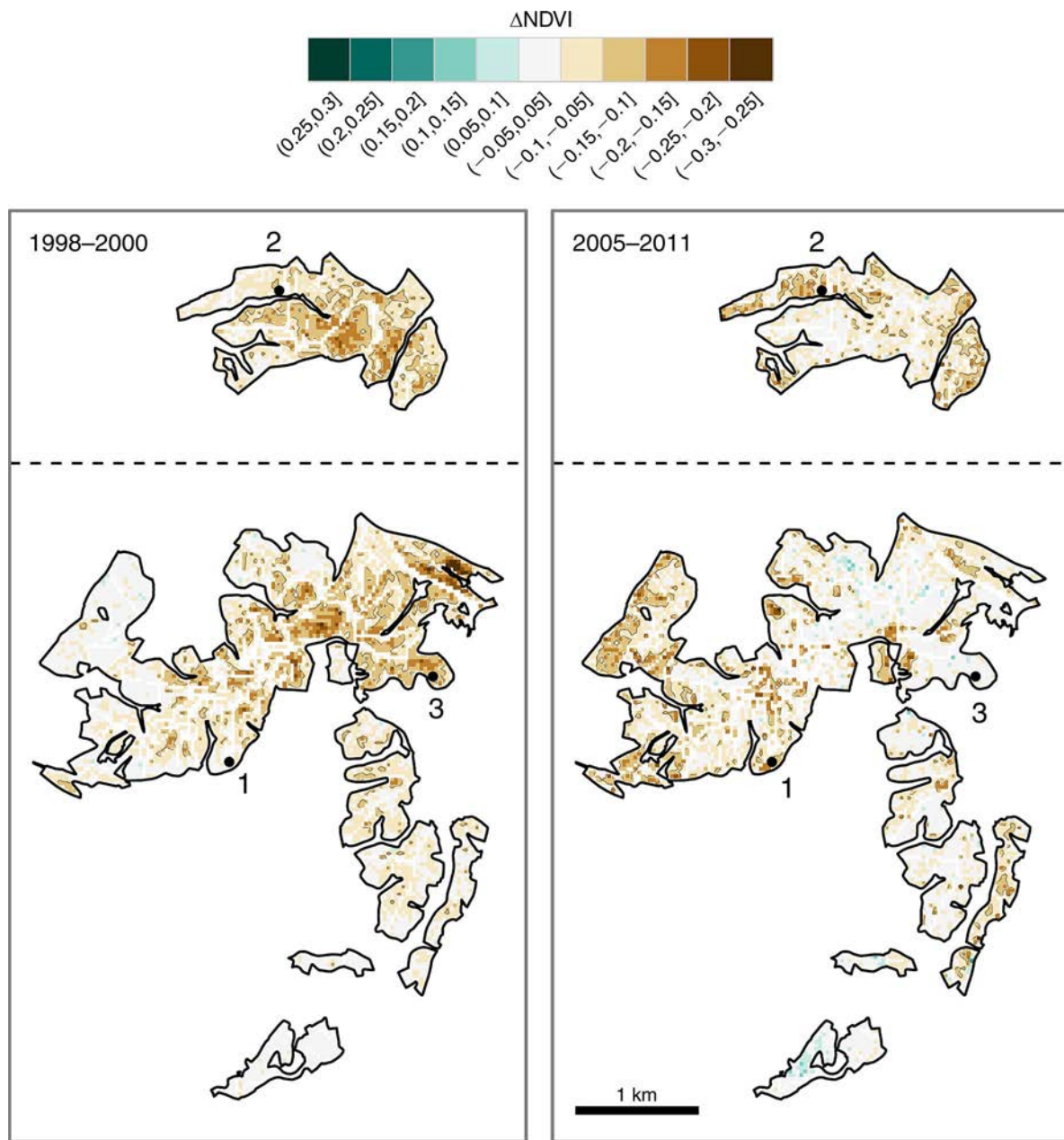


FIG. 6. NDVI (Normalized Difference Vegetation Index) difference between the beginning and the end of the first (1998–2000) and second (2005–2011) drought periods. Areas of $\Delta\text{NDVI} < -0.1$ are marked by contours. Sites where dendrochronological sampling was conducted are marked by numbered (1–3) black dots.

($\Delta\text{NDVI} = -0.16$), and substantial mortality (25%) in 2012. Sites 2 and 3 had very little recent mortality (1% and 2%), less steep NDVI declines during the 2005–2011 drought ($\Delta\text{NDVI} = -0.12$ and -0.01) and higher BAI (1.77 and 5.29 cm/yr) and NDVI (0.32 and 0.34, respectively) in 2011. According to both BAI and NDVI, the effect of the first drought was strongest in site 3, while the effect of the second drought was strongest in site 1, which is in accordance with the responses of the respective clusters the sites belong to

(Fig. 7b). Tree densities in the three sites (Appendix C) were also representative of the densities in the three respective clusters (Appendix F: Table F1), as site 3 had the lowest density (311.7 trees/ha), compared with sites 1 (373.0 trees/ha) and 2 (527.2 trees/ha).

Tree growth in all three sites closely followed annual rainfall amount; NDVI, however, was associated with rainfall to a lower and less consistent degree (Fig. 8). In site 1, substantial discrepancy between observed and predicted NDVI was reached by 2012, likely as a result

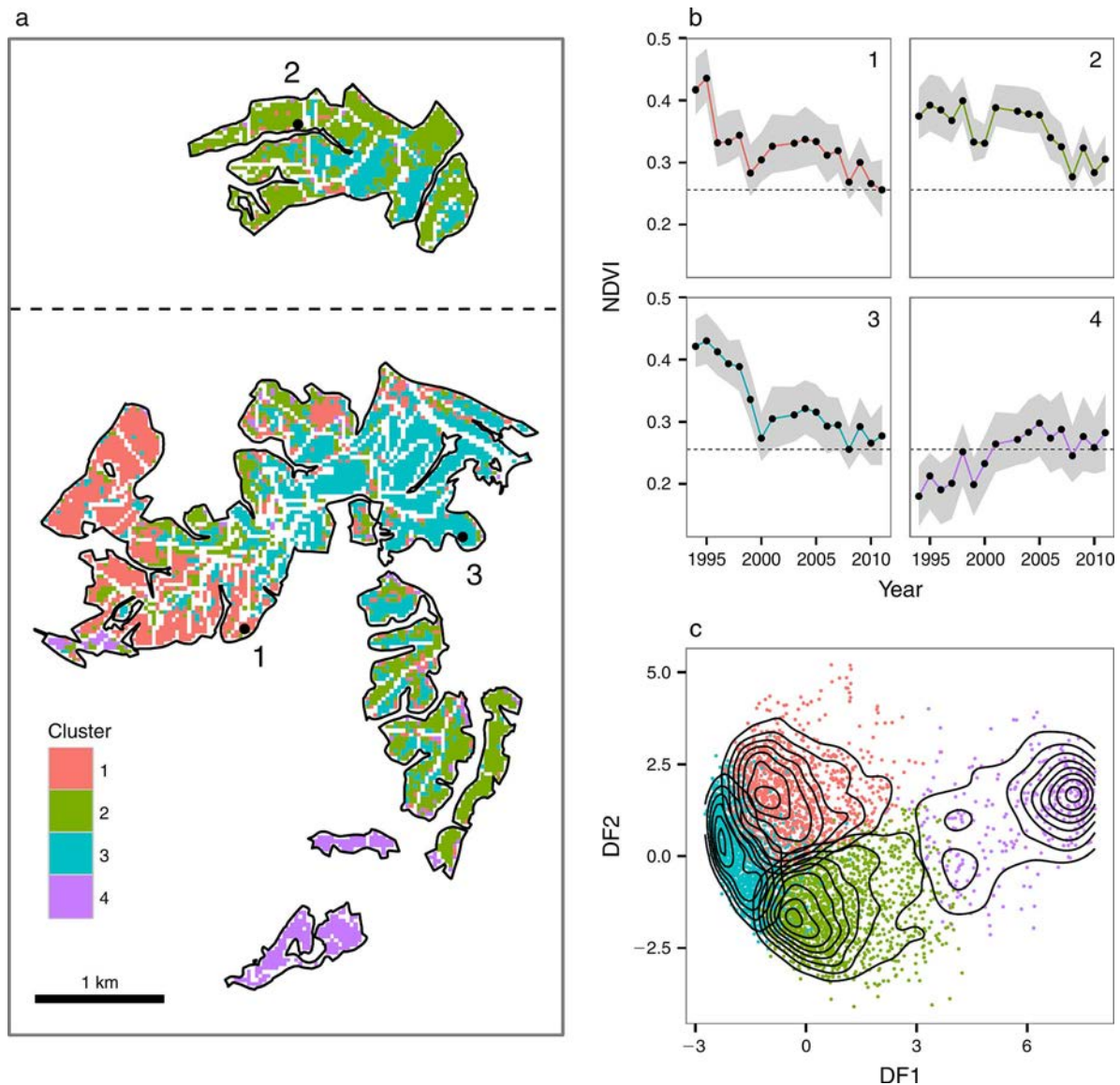


FIG. 7. Spatiotemporal cluster analysis of NDVI (Normalized Difference Vegetation Index) trajectories during 17 years between 1994 and 2011. (a) Locations of the four clusters. Sites where dendrochronological sampling took place are marked by numbered (1–3) black dots. (b) Average and 25–75% inter-quartile range of NDVI values for each cluster, as function of year. The average NDVI value in cluster 1 in 2011 is marked by a dotted line for easier comparison among panels. (c) Separation of observations in the space of the first two discriminant functions (DF1 and DF2). Contours express point density.

of the recent density reduction due to mortality. In site 3, an analogous pattern was observed for the 1998–2000 drought, i.e., a steep NDVI decline (characteristic of the “cluster 3” area, see *Results: NDVI spatiotemporal clusters*) resulting in higher than expected NDVI before 1998 and lower than expected NDVI after 2000 (Fig. 8).

DISCUSSION

Environmental effects on drought-induced mortality

This study has revealed some of the factors associated with increased probability of mortality in semiarid *P. halepensis* forests. Higher mortality was observed in

older stands and on south-facing aspects, which can be expected based on the effects of these factors on soil water availability. Older stands are composed of larger trees, which were frequently found to have higher mortality rates during drought (Floyd et al. 2009, Clifford et al. 2011). For example, mortality of *Pinus edulis* following the 1996 and 2002 severe droughts in Arizona was 2–6 fold higher for larger than smaller tree size classes (Mueller et al. 2005). Higher demands for soil water, and lower vigor due to tissue and cell senescence (Carrer and Urbinati 2004, Peñuelas 2005), may be hypothesized to increase the vulnerability of

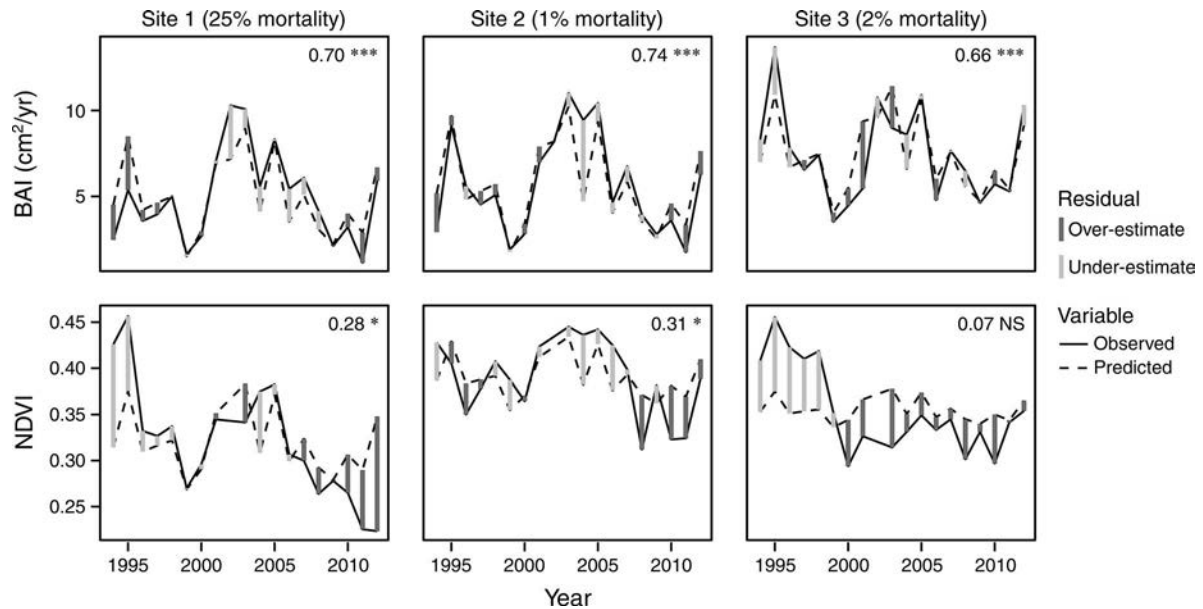


FIG. 8. Observed and predicted Basal Area Increment (BAI) and NDVI for three sites in Lahav and Dvira forests, during the period 1994–2012 (note that NDVI data were not available for 2002). Observed values (solid lines) are averages based on 28, 27, and 30 trees for BAI, and 10, 7, and 10 pixels of $30 \times 30 \text{ m}^2$ for NDVI, in sites 1, 2, and 3, respectively. The numbers in each panel denote R^2 values and significance from linear regressions of the given variable as a function of annual rainfall (* $P < 0.05$, *** $P < 0.001$, NS is not significant). Residuals from the respective models predictions (dashed lines) are shown as dark gray (overestimate) or light gray (underestimate) vertical lines.

older forest trees to drought-induced mortality (Mueller et al. 2005, Floyd et al. 2009, Linares et al. 2013).

South-facing aspects, on the other hand, receiving higher amounts of solar radiation, are subject to higher evaporative demands from the forest canopy, soil, and understory (Pigott and Pigott 1993), resulting in higher drought stress imposed on the forest trees (Huang and Anderegg 2012). Therefore, forest stands on south-facing aspects are most likely to have lower “safety margins” in terms of soil water availability, and they are indeed the first to be affected when drought occurs. The latter is true unless the trees can reduce their dependence on surface moisture by utilizing any existing deeper ground moisture pools (Sarris et al. 2007, 2013). In our case this does not appear to occur, as very high evaporation and limited rainfall may not allow deeper ground moisture pools to form at all (or cause them to become depleted very fast in case they do form during wet years and/or where soil and bedrock types permit).

The higher mortality on deeper soils quantitatively confirms previous qualitative field observations in the region (Y. Moshe, *personal observation*), while higher mortality in sparser stands was unexpected. Both results, however, are seemingly not in agreement with the prevailing view regarding the water supply–demand balance. Deeper soil should contribute to increased water supply (since soil water-holding capacity is higher), while lower tree density should theoretically decrease water demand (since soil water is divided among fewer individuals). We argue that these results

may be in fact characteristic to semiarid regions experiencing extreme drought, where the expectations of density-dependent mortality (e.g., Klos et al. 2009) on shallower soils (e.g., Brouwers et al. 2013a) may not always hold.

A widely advocated strategy for minimizing forest drought vulnerability is tree density reduction (via silvicultural thinning), in order to increase resource availability to the remaining trees within a given population (D’Amato et al. 2013, Ungar et al. 2013). Indeed, increased radial growth rates in response to thinning were consistently observed (e.g., in *P. halepensis* [Olivar et al. 2014], *Pinus ponderosa* [McDowell et al. 2006], and *Abies pinsapo* [Linares et al. 2009b]). Therefore, an association of higher mortality with higher tree density is anticipated due to presumably increased competition intensity in dense locations (Linares et al. 2010, Kerhoulas et al. 2013, Sánchez-Salguero et al. 2013). However, the latter was not steadily observed within the context of widespread forest mortality following extremely dry conditions. For example, associations of higher mortality with *lower* tree densities were observed for *P. edulis* in New Mexico (Clifford et al. 2013) and adjacent areas (Floyd et al. 2009), and for *Populus tremuloides* in Colorado (Worrall et al. 2008); no associations between mortality and density were found for *P. edulis* (Mueller et al. 2005, Clifford et al. 2011) and for mixed-conifer and *P. ponderosa* forests (Ganey and Vojta 2011) in Arizona.

Based on these patterns, it has been suggested that density dependence may be masked under prolonged and extremely limiting drought conditions, leading to mortality across all density levels (Floyd et al. 2009, Ganey and Vojta 2011), while density-dependent mortality is expressed during initial phases of a given drought event (Negron and Wilson 2003). Analogously, the latter “masking” of density-dependent processes has been suggested to vary in space, due to an interaction of density with habitat type (Bowker et al. 2012) or quality (Dwyer et al. 2010). Undoubtedly further studies are necessary to understand the environmental causes for the apparent spatial nonstationary nature of density effect on forest mortality from drought.

Deeper soils, having increased water-holding capacity, were associated with lower mortality following drought in most previous studies (Peterman et al. 2013, Vilá-Cabrera et al. 2013), contrary to the present results. However, no association between soil depth and mortality risk was observed in some cases (Brouwers et al. 2013b, Clifford et al. 2013), suggesting that soil depth effect may interact with other factors. A previous study suggested that the threshold for *P. halepensis* survival during drought is determined by the duration of the period between transpirable soil water content exhaustion and the onset of the next-season first rainfalls (Klein et al. 2014). Therefore the key to the survival of this species during extreme drought may involve maintenance of minimal transpirable soil water content during the dry season, rather than overall water-holding capacity.

In water-limited ecosystems, trees roots can penetrate the rock substrate through preferential lines, and rely on the moisture retained in rock fissures when the soil profile dries out (Herr 2008, Schwinning 2010). Access to porous bedrock types such as chalk (Schiller 1982) or to limited-infiltration soil layers (Klein et al. 2014) may therefore provide an important source of slowly depleting moisture reserves at times of drought for trees growing on shallow soils (Schiller et al. 2002, 2010, Breshears et al. 2009a, Sarris et al. 2013). Deep soils, although beneficial during normal climatic conditions due to higher water-holding capacity, may impose “hydraulic overextension” (Ogle et al. 2000, Fensham and Fairfax 2007, Allen et al. 2010), e.g., through development of a relatively shallow root system (Bellot et al. 2004, Klein et al. 2014). In addition, pines in southern Israel were found to depend on annual (mostly winter) rainfall for growth vs. multiple years of past rainfall determining growth in more humid conditions to the north (Dorman et al., *in press*). This finding suggests that shallow-rooted trees dominate within the southernmost pine populations. The combination of a shallow root system and deep soil could lead to elevated vulnerability in times of drought, when the entire soil profile dries out, while water stored in rock layers is beyond the reach of tree roots (Fensham and Fairfax 2007). We would expect the latter effect to be strongest

where evapotranspiration demand is highest, for example on southern aspects (Schiller et al. 2009), as indeed has been observed in the present study (Fig. 4).

Patchy, spatially variable, density-independent mortality; possible causes

The fine-grained spatial pattern of mortality was patchy at the whole range of relevant spatial scales; consequently the exact magnitude of mortality was largely unpredictable ($R^2 = 0.23$) to a similar degree compared with previous studies. For example, Clifford et al. (2013) could explain 14% of the spatial variation in *P. edulis* mortality in New Mexico (USA), following an extreme drought in 2002–2003 (Weiss et al. 2009); Brouwers et al. (2013a) could explain 15% of canopy dieback in southwestern Australia mediterranean forests, following an extreme drought in 2010–2011.

In some of the previous studies a division could be made between what were a posteriori identified as “high-risk” zones, where both low and high mortality levels were observed (e.g., elevation <1300 m [Linares et al. 2009a]; 2-year rainfall sum <600 mm [Clifford et al. 2013]; lower average rainfall combined with proximity to rock outcrops [Brouwers et al. 2013a, Matusick et al. 2013]; previously cultivated areas on southern aspects [present study]), in contrast to “low-risk” zones, where mortality was uniformly low. In others, no such division was apparent (Ganey and Vojta 2011). These results translate to considerable uncertainty in forecasting when and where forest mortality would occur within the landscape in future drought events, which greatly constrains management options (Breshears et al. 2011, López-Hoffman et al. 2013; see *Discussion: Implications to forest resilience following drought*).

By exploring two sequential droughts using remote sensing and dendrochronological measurements, our study further demonstrates the complexity of mortality dynamics. Not only was the spatial pattern of forest decline largely unpredicted by environmental conditions; two different parts of the forest were affected during the two drought periods (but see Mueller et al. 2005, where the opposite pattern, repeated mortality in the same locations, was observed).

Two main types of explanation, which are not mutually exclusive, may be offered for the apparently spatially autocorrelated random component in mortality. *First*, a key environmental factor (or factors), which is itself spatially autocorrelated, could be missing in the analysis (Zuur et al. 2009:177–182), thus indirectly leading to spatial “attraction” of tree mortality events. For instance, soil micro-topography (Querejeta et al. 2001, Zaady et al. 2001, Saquete Ferrandiz et al. 2006), its depth and composition (Schiller 1972, Olarieta et al. 2000), profile structure (Schiller 1977, Klein et al. 2014), and underlying lithology (Schiller 1982, Weinstein-Evron and Lev-Yadun 2000) have all been previously shown to affect development of *P. halepensis*. Since it

would be difficult to map such properties at a high resolution for extensive areas, understanding their role in forest decline from drought currently remains restricted to field sites covering limited spatial extents. However, the difference in spatial locations of affected areas in the two droughts (Fig. 6) does not support the hypothesis that the remaining variation in forest decline is exclusively related to substrate properties. If that was the case, we would expect the same locations to be affected in both drought periods, since substrate structure remains invariable within the studied time frame.

Local-scale spatial variation in rainfall amounts may also account for differences in degree of drought stress among different locations within the forest. This may be especially relevant in semiarid regions, where the limiting effect of rainfall on vegetation is relatively strong (i.e., even small changes in rainfall amount may generate large differences in forest performance [Fritts et al. 1965]), while the local-scale spatial variability in rainfall amount is relatively high (i.e., nearby locations within the landscape may receive different amounts of rainfall [Syed et al. 2003, Yakir and Morin 2011]). Finally, since the planted forests were established from foreign seed sources of undocumented origin (Schiller 2013), the potential role of adaptation to arid conditions of different genetic backgrounds (Schiller and Atzmon 2009) cannot be ruled out as an additional source of mortality variation.

Second, dead trees may elevate the mortality risk in their surroundings, so that randomly scattered initiation points expand into mortality patches by self-amplifying dynamics (Peters et al. 2004), resulting in an auto-correlated pattern. At least two mechanisms may account for such a pattern: increasing pathogens load and modification of the physical environment by dead trees. As for the first mechanism, dead or dying trees could, for example, negatively affect their proximate environment by serving as suitable hosts for diseases and parasites, thus facilitating attack on healthy trees, thereby driving a local outbreak (Allen 2007, Liu et al. 2007, Raffa et al. 2008). As for the second mechanism, the increasing water availability due to mortality may be counterbalanced, or even surpassed, by increased soil water loss due to the proliferation of herbaceous vegetation and greater solar radiation load (Rich et al. 2008, Kane et al. 2011). In other words, greater canopy openness is accompanied by increased near-ground solar radiation and associated soil temperature (Breshears et al. 1998, Royer et al. 2011), which may increase evapotranspiration from soil and understory vegetation, posing additional stress on the remaining trees. For example, in a previous study where soil evaporation in a planted *P. halepensis* forest from the semiarid region has been measured in shaded and sun-exposed areas, evaporation was found to be double, on average, in the latter (Raz-Yaseef et al. 2010).

Implications to forest resilience following drought

A previous study (Dorman et al., *in press*) has shown that, at the individual tree level, the effect of competition on tree growth in the planted *P. halepensis* forests follows a heterogeneous pattern across portions of the population having different growth rates. Specifically, while in the relatively slow-growing trees BAI was not associated with competition intensity, in the relatively fast-growing trees BAI was significantly (negatively) affected by competition. Since slow growth is associated with elevated mortality risk, it was hypothesized that mortality was not associated with higher densities. This hypothesis was supported by the present study. In other words, slow-growing individual trees (Dorman et al., *in press*) and locations of elevated mortality risk (the present study) were *not* more likely to be found under high competition intensities. Moreover, the association of higher mortality risk with *lower* tree density, and the spatially aggregated mortality pattern, imply that the performance of individual trees was not improved no matter how much competition pressure was reduced. From the point of view of forest management, we hypothesize that thinning may further improve tree growth at improved habitats, but it may not “save” predisposed stands experiencing extreme drought where patches of high (up to almost complete) mortality are initiated at unpredictable locations.

The very high agreement between BAI and annual rainfall in the semiarid forests (Fig. 8) expresses the low resistance, but high resilience, that individual *P. halepensis* trees may exhibit when facing drought. For example, the surviving trees in all three sites have quickly recovered their “usual” growth rates in 2012, following the 2005–2011 drought, even in site 1 where 25% mortality was observed. However, in order to generalize about resistance and resilience properties from individual trees to the forest ecosystem as a whole, it is essential to evaluate forest demographic trends as well (Lloret et al. 2011). Demographic information may be available from tree ring data alone (although for limited spatial extents), in cases when dead trees remain on site in datable condition (e.g., Suarez et al. 2004, Bigler et al. 2007). Otherwise, taking into account only living (surviving) trees may result in underestimation of resilience in drought-affected areas (Breda and Badeau 2008). Moreover, there is often no way of knowing the degree of removal and/or decay of wood material that took place in a given site for several decades into the past, and thus the degree of bias. Since satellite images are obtained in real time, rather than in retrospect, they may provide valuable reference information in such cases. For example, the tree density reduction in site 1, due to mortality following the 2005–2011 drought, was reflected by the lack of NDVI recovery during the relatively wet year of 2012 (Fig. 8). Similarly, the density reduction in site 3 during the 1998–2000 drought, likely due to drought-induced mortality, was indicated by the permanent NDVI decline in that time period (Fig. 8).

Substantial mortality has been observed in 2012 in the present study, and similar observations were made in the other forests of the southern region, by means of remote sensing (Dorman et al. 2013b) and field observations (local foresters, *personal communication*). Nevertheless, the systematic mapping of mortality rates has revealed that mortality was extremely low for large parts of the forests, even though the forests are located beyond the natural distribution area of the species. Thus even under such extreme climatic conditions, *P. halepensis* seems to have the potential to survive severe drought events.

Conclusions

The semiarid planted *P. halepensis* forests that we studied have recently (2005–2011) experienced the most severe drought in at least ~50 years (Fig. 2). The degree and spatial pattern of drought-induced damage were evaluated, for the first time to the best of our knowledge, simultaneously on three distinct levels of organizational complexity. The following main conclusions, directly related to forest management applications under climatic change, may change the way we think about monitoring and management of arid forest borders.

First, the association of mortality with lower tree densities does not support the notion that thinning semiarid forests will necessarily increase survival probability of the remaining trees (Ganey and Vojta 2011). Accordingly, the benefits of thinning, currently considered the main forest management tool to enhance resistance to drought (e.g., Linares et al. 2010, Vila-Cabrera et al. 2011, Ungar et al. 2013), are questionable and require further research, at least within the context of extreme drought events in semiarid ecosystems.

Second, mortality was spatially clustered, and its magnitude was largely unexplained by the physical and biotic environmental factors that can be feasibly mapped for large continuous areas. The fact that patches of substantial (up to 90%) forest cover loss may show up, apparently unpredictably, within “higher-risk” zones (e.g., older age, south-facing slopes) should be acknowledged by forest managers, especially in semiarid forests where enhanced survival probability (and not, for example, timber yield) is defined as the main management objective.

Third, it was demonstrated that the multi-perspective approach provides a more complete understanding of the studied phenomenon. While inferences based on the different methods were generally in agreement, the differences were informatively related to the different levels of organization each method addresses, making them complementary (Levin 1992). For example, dendrochronological methods account only for the portion of population present at the time of sampling, thus potentially overestimating forest resilience, while satellite remote sensing may aggregate the reflectance of

large forest canopy “portions,” thus limiting the attribution of decline to either demographic (e.g., mortality) or structural (e.g., defoliation) processes (Macfarlane et al. 2013). We therefore suggest that evaluation of forest ecosystems resilience should ultimately be based on an integration of several metrics, each suited for detecting transitions at a different level of organization, from individual trees performance (e.g., BAI), to short-term demographic trends (e.g., mortality rates) and ultimately to long-term changes in forest ecosystem functioning (e.g., remotely sensed vegetation indices).

ACKNOWLEDGMENTS

We thank David Brand, Israel Tauber, Ronen Talmor, Efrat Sheffer, Gil Siaki, Shmuel Sprintsin, and Gabriel Schiller for providing helpful information and resources. The Israeli Forest Service (KKL) willingly provided forests GIS layers and purchased the equipment and software for the dendrochronological analysis. We thank Arnon Cooper, Or Livni, Adam Wattenberg, Yoni Waitz, Ezra Ben-Moshe and Yosi Moshe for assistance in field work. This study is supported by a grant from the Chief Scientist of the Israeli Ministry of Agriculture and Rural Development and the KKL. M. Dorman acknowledges financial support from the René Karshon Foundation. D. Sarris acknowledges financial support from the Short Scientific Visit program of the European Forest Institute (Mediterranean Office); EFIMED.

LITERATURE CITED

- Akaike, H. 1974. A new look at the statistical model identification. *IEEE Transactions on Automatic Control* AC19:716–723.
- Allen, C. D. 2007. Interactions across spatial scales among forest dieback, fire, and erosion in northern New Mexico landscapes. *Ecosystems* 10:797–808.
- Allen, C. D., and D. D. Breshears. 1998. Drought-induced shift of a forest-woodland ecotone: rapid landscape response to climate variation. *Proceedings of the National Academy of Sciences USA* 95:14839–14842.
- Allen, C. D., et al. 2010. A global overview of drought and heat-induced tree mortality reveals emerging climate change risks for forests. *Forest Ecology and Management* 259:660–684.
- Anderegg, W. R. L., J. A. Berry, D. D. Smith, J. S. Sperry, L. D. L. Anderegg, and C. B. Field. 2012. The roles of hydraulic and carbon stress in a widespread climate-induced forest die-off. *Proceedings of the National Academy of Sciences USA* 109:233–237.
- Anderegg, W. R. L., J. M. Kane, and L. D. L. Anderegg. 2013a. Consequences of widespread tree mortality triggered by drought and temperature stress. *Nature Climate Change* 3:30–36.
- Anderegg, W. R. L., L. Plavcová, L. D. L. Anderegg, U. G. Hacke, J. A. Berry, and C. B. Field. 2013b. Drought’s legacy: multiyear hydraulic deterioration underlies widespread aspen forest die-off and portends increased future risk. *Global Change Biology* 19:1188–1196.
- Anderson, L. O., Y. Malhi, L. E. O. C. Aragao, R. Ladle, E. Arai, N. Barbier, and O. Phillips. 2010. Remote sensing detection of droughts in Amazonian forest canopies. *New Phytologist* 187:733–750.
- Babst, F., J. Esper, and E. Parlow. 2010. Landsat TM/ETM plus and tree-ring based assessment of spatiotemporal patterns of the autumnal moth (*Epippia autumnata*) in northernmost Fennoscandia. *Remote Sensing of Environment* 114:637–646.

- Baddeley, A., and R. Turner. 2005. spatstat: an R package for analyzing spatial point patterns. *Journal of Statistical Software* 12:1–42.
- Baguskas, S. A., S. H. Peterson, B. Bookhagen, and C. J. Still. 2014. Evaluating spatial patterns of drought-induced tree mortality in a coastal California pine forest. *Forest Ecology and Management* 315:43–53.
- Beck, P. S. A., G. P. Juday, C. Alix, V. A. Barber, S. E. Winslow, E. E. Sousa, P. Heiser, J. D. Herriges, and S. J. Goetz. 2011. Changes in forest productivity across Alaska consistent with biome shift. *Ecology Letters* 14:373–379.
- Bellot, J., F. T. Maestre, E. Chirino, N. Hernández, and J. O. de Urbina. 2004. Afforestation with *Pinus halepensis* reduces native shrub performance in a Mediterranean semiarid area. *Acta Oecologica* 25:7–15.
- Berner, L. T., P. S. A. Beck, A. G. Bunn, A. H. Lloyd, and S. J. Goetz. 2011. High-latitude tree growth and satellite vegetation indices: correlations and trends in Russia and Canada (1982–2008). *Journal of Geophysical Research-Biogeosciences* 116(G1). G01015. <http://dx.doi.org/10.1029/2010JG001475>
- Bigler, C., D. G. Gavin, C. Gunning, and T. T. Veblen. 2007. Drought induces lagged tree mortality in a subalpine forest in the Rocky Mountains. *Oikos* 116:1983–1994.
- Biondi, F., and F. Qeadan. 2008. A theory-driven approach to tree-ring standardization: defining the biological trend from expected basal area increment. *Tree-Ring Research* 64:81–96.
- Bivand, R. S., E. J. Pebesma, and V. Gomez-Rubio. 2008. Applied spatial data analysis with R. Springer, New York, New York, USA.
- Bowker, M. A., A. Muñoz, T. Martinez, and M. K. Lau. 2012. Rare drought-induced mortality of juniper is enhanced by edaphic stressors and influenced by stand density. *Journal of Arid Environments* 76:9–16.
- Breda, N., and V. Badeau. 2008. Forest tree responses to extreme drought and some biotic events: towards a selection according to hazard tolerance? *Comptes Rendus Geoscience* 340:651–662.
- Breshears, D. D., L. Lopez-Hoffman, and L. J. Graumlich. 2011. When ecosystem services crash: preparing for big, fast, patchy climate change. *Ambio* 40:256–263.
- Breshears, D. D., O. B. Myers, and F. J. Barnes. 2009a. Horizontal heterogeneity in the frequency of plant-available water with woodland intercanopy-canopy vegetation patch type rivals that occurring vertically by soil depth. *Ecohydrology* 2:503–519.
- Breshears, D. D., O. B. Myers, C. W. Meyer, F. J. Barnes, C. B. Zou, C. D. Allen, N. G. McDowell, and W. T. Pockman. 2009b. Tree die-off in response to global change-type drought: mortality insights from a decade of plant water potential measurements. *Frontiers in Ecology and the Environment* 7:185–189.
- Breshears, D. D., J. W. Nyhan, C. E. Heil, and B. P. Wilcox. 1998. Effects of woody plants on microclimate in a semiarid woodland: Soil temperature and evaporation in canopy and intercanopy patches. *International Journal of Plant Sciences* 159:1010–1017.
- Brouwers, N., G. Matusick, K. Ruthrof, T. Lyons, and G. Hardy. 2013a. Landscape-scale assessment of tree crown dieback following extreme drought and heat in a Mediterranean eucalypt forest ecosystem. *Landscape Ecology* 28:69–80.
- Brouwers, N. C., J. Mercer, T. Lyons, P. Poot, E. Veneklaas, and G. Hardy. 2013b. Climate and landscape drivers of tree decline in a Mediterranean ecoregion. *Ecology and Evolution* 3:67–79.
- Carrer, M., and C. Urbinati. 2004. Age-dependent tree-ring growth responses to climate in *Larix decidua* and *Pinus cembra*. *Ecology* 85:730–740.
- Chapman, T. B., T. T. Veblen, and T. Schoennagel. 2012. Spatiotemporal patterns of mountain pine beetle activity in the southern Rocky Mountains. *Ecology* 93:2175–2185.
- Chen, J., X. Zhu, J. E. Vogelmann, F. Gao, and S. Jin. 2011. A simple and effective method for filling gaps in Landsat ETM+ SLC-off images. *Remote Sensing of Environment* 115:1053–1064.
- Clifford, M. J., N. S. Cobb, and M. Buenemann. 2011. Long-term tree cover dynamics in a pinyon-juniper woodland: climate-change-type drought resets successional clock. *Ecosystems* 14:949–962.
- Clifford, M. J., P. D. Royer, N. S. Cobb, D. D. Breshears, and P. L. Ford. 2013. Precipitation thresholds and drought-induced tree die-off: insights from patterns of *Pinus edulis* mortality along an environmental stress gradient. *New Phytologist* 200:413–421.
- D'Amato, A. W., J. B. Bradford, S. Fraver, and B. J. Palik. 2013. Effects of thinning on drought vulnerability and climate response in north temperate forest ecosystems. *Ecological Applications* 23:1735–1742.
- Dan, J., D. H. Yaalon, H. Koyumdjisky, and Z. Raz. 1970. The soil association map of Israel. Pamphlet-Agricultural Research Organization, (Israel). *Israel Journal of Earth Sciences* 21:29–49.
- de Luis, M., K. Čufar, A. Di Filippo, K. Novak, A. Papadopoulos, G. Piovesan, C. B. K. Rathgeber, J. Raventós, M. A. Saz, and K. T. Smith. 2013. Plasticity in dendroclimatic response across the distribution range of Aleppo pine (*Pinus halepensis*). *PLoS ONE* 8:e83550.
- Dorman, M., A. Perevolotsky, D. Sarris, and T. Svoray. The effect of rainfall and competition intensity on forest response to drought: lessons learned from a dry extreme. *Oecologia*, *in press*.
- Dorman, M., T. Svoray, and A. Perevolotsky. 2012. Tree mortality in *Pinus halepensis* forests of Israel: a remote sensing approach. [In Hebrew.] *Ecology and Environment* 3:230–237.
- Dorman, M., T. Svoray, and A. Perevolotsky. 2013a. Homogenization in forest performance across an environmental gradient: the interplay between rainfall and topographic aspect. *Forest Ecology and Management* 310:256–266.
- Dorman, M., T. Svoray, A. Perevolotsky, and D. Sarris. 2013b. Forest performance during two consecutive drought periods: diverging long-term trends and short-term responses along a climatic gradient. *Forest Ecology and Management* 310:1–9.
- Dwyer, J. M., R. J. Fensham, R. J. Fairfax, and Y. M. Buckley. 2010. Neighbourhood effects influence drought-induced mortality of savanna trees in Australia. *Journal of Vegetation Science* 21:573–585.
- Fensham, R. J., and R. J. Fairfax. 2007. Drought-related tree death of savanna eucalypts: species susceptibility, soil conditions and root architecture. *Journal of Vegetation Science* 18:71–80.
- Fensham, R. J., R. J. Fairfax, and S. R. Archer. 2005. Rainfall, land use and woody vegetation cover change in semi-arid Australian savanna. *Journal of Ecology* 93:596–606.
- Floyd, M. L., M. Clifford, N. S. Cobb, D. Hanna, R. Delph, P. Ford, and D. Turner. 2009. Relationship of stand characteristics to drought-induced mortality in three Southwestern pinon-juniper woodlands. *Ecological Applications* 19:1223–1230.
- Fortin, M. J., and M. R. T. Dale. 2005. Spatial analysis: a guide for ecologists. Cambridge University Press, Cambridge, UK.
- Fritts, H. C., D. G. Smith, J. W. Cardis, and C. A. Budelsky. 1965. Tree-ring characteristics along a vegetation gradient in northern Arizona. *Ecology* 46:393–401.
- Fu, P. D., and P. M. Rich. 2002. A geometric solar radiation model with applications in agriculture and forestry. *Computers and Electronics in Agriculture* 37:25–35.
- Galiano, L., J. Martínez-Vilalta, and F. Lloret. 2011. Carbon reserves and canopy defoliation determine the recovery of Scots pine 4 yr after a drought episode. *New Phytologist* 190:750–759.

- Ganey, J. L., and S. C. Vojta. 2011. Tree mortality in drought-stressed mixed-conifer and ponderosa pine forests, Arizona, USA. *Forest Ecology and Management* 261:162–168.
- Garrity, S. R., C. D. Allen, S. P. Brumby, C. Gangodagamage, N. G. McDowell, and D. M. Cai. 2013. Quantifying tree mortality in a mixed species woodland using multitemporal high spatial resolution satellite imagery. *Remote Sensing of Environment* 129:54–65.
- Girard, F., M. Vennetier, F. Guibal, C. Corona, S. Ouarmim, and A. Herrero. 2012. *Pinus halepensis* Mill. crown development and fruiting declined with repeated drought in Mediterranean France. *European Journal of Forest Research* 131:919–931.
- Girard, F., M. Vennetier, S. Ouarmim, Y. Caraglio, and L. Misson. 2011. Polycyclism, a fundamental tree growth process, decline with recent climate change: the example of *Pinus halepensis* Mill. in Mediterranean France. *Trees-Structure and Function* 25:311–322.
- Gitlin, A. R., C. M. Stultz, M. A. Bowker, S. Stumpf, K. L. Paxton, K. Kennedy, A. Munoz, J. K. Bailey, and T. G. Whitham. 2006. Mortality gradients within and among dominant plant populations as barometers of ecosystem change during extreme drought. *Conservation Biology* 20:1477–1486.
- Goslee, S. C. 2011. Analyzing remote sensing data in R: The landsat package. *Journal of Statistical Software* 43:1–25.
- Hall, J. K., and R. L. Cleave. 1988. The DTM project. *Geological Survey of Israel* 6:1–7.
- Hargreaves, G. H. 1994. Defining and using reference evapotranspiration. *Journal of Irrigation and Drainage Engineering-ASCE* 120:1132–1139.
- Hartigan, J. A., and M. A. Wong. 1979. A K-means clustering algorithm. *Applied Statistics* 28:100–108.
- Herr, N. 2008. Rock-soil system and water regime dynamics in the habitat as the main ecological factors of *Quercus ithaburensis* and *Quercus calliprinos* in Alonim-Menashe region. Dissertation. Hebrew University of Jerusalem, Jerusalem, Israel.
- Hicke, J. A., and M. J. B. Zeppel. 2013. Climate-driven tree mortality: insights from the piñon pine die-off in the United States. *New Phytologist* 200:301–303.
- Hothorn, T., and B. S. Everitt. 2009. A handbook of statistical analyses using R. Second edition. Taylor and Francis, London, UK.
- Huang, C.-Y., and W. R. L. Anderegg. 2012. Large drought-induced aboveground live biomass losses in southern Rocky Mountain aspen forests. *Global Change Biology* 18:1016–1027.
- Johnson, J. B., and K. S. Omland. 2004. Model selection in ecology and evolution. *Trends in Ecology and Evolution* 19:101–108.
- Kane, J. M., K. A. Meinhardt, T. Chang, B. L. Cardall, R. Michalet, and T. G. Whitham. 2011. Drought-induced mortality of a foundation species (*Juniperus monosperma*) promotes positive afterlife effects in understory vegetation. *Plant Ecology* 212:733–741.
- Kerhoulas, L. P., T. E. Kolb, M. D. Hurteau, and G. W. Koch. 2013. Managing climate change adaptation in forests: a case study from the U.S. Southwest. *Journal of Applied Ecology* 50:1311–1320.
- Kharuk, V. I., S. T. Im, P. A. Oskorbin, I. A. Petrov, and K. J. Ranson. 2013. Siberian pine decline and mortality in southern Siberian mountains. *Forest Ecology and Management* 310:312–320.
- Klein, T., E. Rotenberg, E. Cohen-Hilaleh, N. Raz-Yaseef, F. Tatarinov, Y. Preisler, J. Ogée, S. Cohen, and D. Yakir. 2014. Quantifying transpirable soil water and its relations to tree water use dynamics in a water-limited pine forest. *Ecohydrology* 7:409–419.
- Klos, R. J., G. G. Wang, W. L. Bauerle, and J. R. Rieck. 2009. Drought impact on forest growth and mortality in the southeast USA: an analysis using Forest Health and Monitoring data. *Ecological Applications* 19:699–708.
- le Polain de Waroux, Y., and E. F. Lambin. 2012. Monitoring degradation in arid and semi-arid forests and woodlands: the case of the argan woodlands (Morocco). *Applied Geography* 32:777–786.
- Levin, S. A. 1992. The problem of pattern and scale in ecology: the Robert H. MacArthur award lecture. *Ecology* 73:1943–1967.
- Linares, J. C., J. J. Camarero, and J. A. Carreira. 2009a. Interacting effects of changes in climate and forest cover on mortality and growth of the southernmost European fir forests. *Global Ecology and Biogeography* 18:485–497.
- Linares, J. C., J. J. Camarero, and J. A. Carreira. 2009b. Plastic responses of *Abies pinsapo* xylogenesis to drought and competition. *Tree Physiology* 29:1525–1536.
- Linares, J. C., J. J. Camarero, and J. A. Carreira. 2010. Competition modulates the adaptation capacity of forests to climatic stress: insights from recent growth decline and death in relict stands of the Mediterranean fir *Abies pinsapo*. *Journal of Ecology* 98:592–603.
- Linares, J. C., L. Taiqui, G. Sangüesa-Barreda, J. Ignacio Seco, and J. Julio Camarero. 2013. Age-related drought sensitivity of Atlas cedar (*Cedrus atlantica*) in the Moroccan Middle Atlas forests. *Dendrochronologia* 31:88–96.
- Liphshitz, N., and G. Biger. 2001. Past distribution of Aleppo pine (*Pinus halepensis*) in the mountains of Israel (Palestine). *Holocene* 11:427–436.
- Liu, D., M. Kelly, P. Gong, and Q. Guo. 2007. Characterizing spatial-temporal tree mortality patterns associated with a new forest disease. *Forest Ecology and Management* 253:220–231.
- Lloret, F., E. G. Keeling, and A. Sala. 2011. Components of tree resilience: effects of successive low-growth episodes in old ponderosa pine forests. *Oikos* 120:1909–1920.
- Lloyd, A. H., A. G. Bunn, and L. Berner. 2011. A latitudinal gradient in tree growth response to climate warming in the Siberian taiga. *Global Change Biology* 17:1935–1945.
- Lopatin, E., T. Kolstrom, and H. Specker. 2006. Determination of forest growth trends in Komi Republic (northwestern Russia): combination of tree-ring analysis and remote sensing data. *Boreal Environment Research* 11:341–353.
- López-Hoffman, L., D. D. Breshears, C. D. Allen, and M. L. Miller. 2013. Key landscape ecology metrics for assessing climate change adaptation options: rate of change and patchiness of impacts. *Ecosphere* 4:art101.
- Macfarlane, W. W., J. A. Logan, and W. R. Kern. 2013. An innovative aerial assessment of Greater Yellowstone Ecosystem mountain pine beetle-caused whitebark pine mortality. *Ecological Applications* 23:421–437.
- Matusick, G., K. X. Ruthrof, N. C. Brouwers, B. Dell, and G. S. J. Hardy. 2013. Sudden forest canopy collapse corresponding with extreme drought and heat in a mediterranean-type eucalypt forest in southwestern Australia. *European Journal of Forest Research* 132:497–510.
- Matyas, C. 2010. Forecasts needed for retreating forests. *Nature* 464:1271.
- McDowell, N. G., H. D. Adams, J. D. Bailey, M. Hess, and T. E. Kolb. 2006. Homeostatic maintenance of ponderosa pine gas exchange in response to stand density changes. *Ecological Applications* 16:1164–1182.
- McDowell, N. G., D. J. Beerling, D. D. Breshears, R. A. Fisher, K. F. Raffa, and M. Stitt. 2011. The interdependence of mechanisms underlying climate-driven vegetation mortality. *Trends in Ecology and Evolution* 26:523–532.
- McDowell, N. G., R. A. Fisher, C. Xu, J. C. Domec, T. Hölttä, D. S. Mackay, J. S. Sperry, A. Boutz, L. Dickman, and N. Gehres. 2013a. Evaluating theories of drought-induced vegetation mortality using a multimodel-experiment framework. *New Phytologist* 200:304–321.

- McDowell, N., W. T. Pockman, C. D. Allen, D. D. Breshears, N. Cobb, T. Kolb, J. Plaut, J. Sperry, A. West, D. G. Williams, and E. A. Yépez. 2008. Mechanisms of plant survival and mortality during drought: why do some plants survive while others succumb to drought? *New Phytologist* 178:719–739.
- McDowell, N. G., M. G. Ryan, M. J. B. Zeppel, and D. T. Tissue. 2013b. Improving our knowledge of drought-induced forest mortality through experiments, observations, and modeling. *New Phytologist* 200:289–293.
- Michaelian, M., E. H. Hogg, R. J. Hall, and E. Arsenault. 2011. Massive mortality of aspen following severe drought along the southern edge of the Canadian boreal forest. *Global Change Biology* 17:2084–2094.
- Mora, C., et al. 2013. The projected timing of climate departure from recent variability. *Nature* 502:183–187.
- Muller, R. C., C. M. Scudder, M. E. Porter, R. T. Trotter, C. A. Gehring, and T. G. Whitham. 2005. Differential tree mortality in response to severe drought: evidence for long-term vegetation shifts. *Journal of Ecology* 93:1085–1093.
- Negron, J. F., and J. L. Wilson. 2003. Attributes associated with probability of infestation by the pinon ips, *Ips confusus* (Coleoptera: Scolytidae), in pinon pine, *Pinus edulis*. *Western North American Naturalist* 63:440–451.
- Ogle, K., T. G. Whitham, and N. S. Cobb. 2000. Tree-ring variation in pinyon predicts likelihood of death following severe drought. *Ecology* 81:3237–3243.
- Olarieta, J. R., A. Uson, R. Rodriguez, M. Rosa, R. Blanco, and M. Antunez. 2000. Land requirements for *Pinus halepensis* Mill. growth in a plantation in Huesca, Spain. *Soil Use and Management* 16:88–92.
- Olivar, J., S. Bogino, C. Rathgeber, V. Bonnesoeur, and F. Bravo. 2014. Thinning has a positive effect on growth dynamics and growth-climate relationships in Aleppo pine (*Pinus halepensis*) trees of different crown classes. *Annals of Forest Science* 71:395–404.
- Osem, Y., H. Yavlovich, N. Zecharia, N. Atzman, Y. Moshe, and G. Schiller. 2013. Fire-free natural regeneration in water limited *Pinus halepensis* forests: a silvicultural approach. *European Journal of Forest Research* 132:679–690.
- Osem, Y., E. Zangy, E. Bney-Moshe, Y. Moshe, N. Karni, and Y. Nisan. 2009. The potential of transforming simple structured pine plantations into mixed Mediterranean forests through natural regeneration along a rainfall gradient. *Forest Ecology and Management* 259:14–23.
- Peñuelas, J. 2005. Plant physiology: a big issue for trees. *Nature* 437:965–966.
- Perevolotsky, A., and E. Sheffer. 2009. Forest management in Israel—the ecological alternative. *Israel Journal of Plant Sciences* 57:35–48.
- Peterman, W., R. H. Waring, T. Seager, and W. L. Pollock. 2013. Soil properties affect pinyon pine-juniper response to drought. *Ecohydrology* 6:455–463.
- Peters, D. P. C., R. A. Pielke, B. T. Bestelmeyer, C. D. Allen, S. Munson-McGee, and K. M. Havstad. 2004. Cross-scale interactions, nonlinearities, and forecasting catastrophic events. *Proceedings of the National Academy of Sciences USA* 101:15130–15135.
- Pettorelli, N., J. O. Vik, A. Mysterud, J.-M. Gaillard, C. J. Tucker, and N. C. Stenseth. 2005. Using the satellite-derived NDVI to assess ecological responses to environmental change. *Trends in Ecology and Evolution* 20:503–510.
- Pigott, C. D., and S. Pigott. 1993. Water as a determinant of the distribution of trees at the boundary of the Mediterranean zone. *Journal of Ecology* 81:557–566.
- Plant, R. E. 2012. Spatial data analysis in ecology and agriculture using R. Taylor and Francis, London, UK.
- Querejeta, J. I., A. Roldan, J. Albaladejo, and V. Castillo. 2001. Soil water availability improved by site preparation in a *Pinus halepensis* afforestation under semiarid climate. *Forest Ecology and Management* 149:115–128.
- R Development Core Team. 2013. R: A language and environment for statistical computing. R Foundation for Statistical Computing, Vienna, Austria.
- Raffa, K. F., B. H. Aukema, B. J. Bentz, A. L. Carroll, J. A. Hicke, M. G. Turner, and W. H. Romme. 2008. Cross-scale drivers of natural disturbances prone to anthropogenic amplification: the dynamics of bark beetle eruptions. *BioScience* 58:501–517.
- Raz-Yaseef, N., E. Rotenberg, and D. Yakir. 2010. Effects of spatial variations in soil evaporation caused by tree shading on water flux partitioning in a semi-arid pine forest. *Agricultural and Forest Meteorology* 150:454–462.
- Raz-Yaseef, N., D. Yakir, G. Schiller, and S. Cohen. 2012. Dynamics of evapotranspiration partitioning in a semi-arid forest as affected by temporal rainfall patterns. *Agricultural and Forest Meteorology* 157:77–85.
- Rich, P. M., D. D. Breshears, and A. B. White. 2008. Phenology of mixed woody-herbaceous ecosystems following extreme events: net and differential responses. *Ecology* 89:342–352.
- Ripley, B. D. 1977. Modelling spatial patterns. *Journal of the Royal Statistical Society Series B-Methodological* 39:172–212.
- Royer, P. D., N. S. Cobb, M. J. Clifford, C.-Y. Huang, D. D. Breshears, H. D. Adams, and J. Camilo Villegas. 2011. Extreme climatic event-triggered overstorey vegetation loss increases understorey solar input regionally: primary and secondary ecological implications. *Journal of Ecology* 99:714–723.
- Rozas, V., and J. M. Olano. 2013. Environmental heterogeneity and neighbourhood interference modulate the individual response of *Juniperus thurifera* tree-ring growth to climate. *Dendrochronologia* 31:105–113.
- Sánchez-Salguero, R., J. J. Camarero, M. Dobbertin, Á. Fernández-Cancio, A. Vilà-Cabrera, R. D. Manzanedo, M. A. Zavala, and R. M. Navarro-Cerrillo. 2013. Contrasting vulnerability and resilience to drought-induced decline of densely planted vs. natural rear-edge *Pinus nigra* forests. *Forest Ecology and Management* 310:956–967.
- Saquejo Ferrandiz, A., M. J. Lledo Solbes, A. Escarre Esteve, M. A. Ripoll Morales, and E. De-Simon Navarrete. 2006. Effects of site preparation with micro-basins on *Pinus halepensis* Mill. afforestations in a semiarid ombroclimate. *Annals of Forest Science* 63:15–22.
- Sarkar, D. 2008. Lattice: multivariate data visualization with R. Springer, New York, New York, USA.
- Sarris, D., D. Christodoulakis, and C. Korner. 2007. Recent decline in precipitation and tree growth in the eastern Mediterranean. *Global Change Biology* 13:1187–1200.
- Sarris, D., R. Siegwolf, and C. Koerner. 2013. Inter- and intra-annual stable carbon and oxygen isotope signals in response to drought in Mediterranean pines. *Agricultural and Forest Meteorology* 168:59–68.
- Schiller, G. 1972. Ecological factors affecting the growth of Aleppo pine in the southern Judean hills. Leaflet No. 44. [In Hebrew.] Agricultural Research Organization, Forest Division, Ilanot, Israel.
- Schiller, G. 1977. Interrelations between site factors and performance of Aleppo pine in the Sha'ar ha'Gay forest. [Hebrew with English summary.] *La-Yaaran* 27:13–23.
- Schiller, G. 1982. Significance of bedrock as a site factor for Aleppo pine. *Forest Ecology and Management* 4:213–223.
- Schiller, G. 2000. Ecophysiology of *Pinus halepensis* Mill. and *P. brutia* Ten. Pages 51–65 in G. Ne'eman and L. Traubaud, editors. *Ecology, biogeography and management of Pinus halepensis and P. brutia forest ecosystems in the Mediterranean Basin*. Backhuys, Leiden, The Netherlands.
- Schiller, G. 2013. Degeneration and premature mortality of *Pinus halepensis* in Israel following seeds importation from foreign ecosystems. [In Hebrew.] *Ecology and Environment* 4:167–175.

- Schiller, G., and N. Atzmon. 2009. Performance of Aleppo pine (*Pinus halepensis*) provenances grown at the edge of the Negev desert: a review. *Journal of Arid Environments* 73:1051–1057.
- Schiller, G., E. D. Ungar, S. Cohen, and N. Herr. 2010. Water use by Tabor and Kermes oaks growing in their respective habitats in the Lower Galilee region of Israel. *Forest Ecology and Management* 259:1018–1024.
- Schiller, G., E. D. Ungar, S. Cohen, Y. Moshe, and N. Atzmon. 2009. Aspect effect on transpiration of *Pinus halepensis* in Yatir forest. [In Hebrew.] *Yaar* 11:14–19.
- Schiller, G., E. D. Ungar, and Y. Cohen. 2002. Estimating the water use of a sclerophyllous species under an East-Mediterranean climate: I. Response of transpiration of *Phillyrea latifolia* L. to site factors. *Forest Ecology and Management* 170:117–126.
- Schiller, G., E. D. Ungar, and A. Genizi. 2005. Is tree fate written in its tree rings? Characterization of trees in Kramim forest following the 1998/99 dry winter. [In Hebrew.] *Yaar* 7:18–25.
- Schwinning, S. 2010. The ecohydrology of roots in rocks. *Ecohydrology* 3:238–245.
- Shafran-Nathan, R., T. Svoray, and A. Perevolotsky. 2013. Continuous droughts' effect on herbaceous vegetation cover and productivity in rangelands: results from close-range photography and spatial analysis. *International Journal of Remote Sensing* 34:6263–6281.
- Shimazaki, M., T. Sasaki, K. Hikosaka, and T. Nakashizuka. 2011. Environmental dependence of population dynamics and height growth of a subalpine conifer across its vertical distribution: an approach using high-resolution aerial photographs. *Global Change Biology* 17:3431–3438.
- Stimson, H. C., D. D. Breshears, S. L. Ustin, and S. C. Kefauver. 2005. Spectral sensing of foliar water conditions in two co-occurring conifer species: *Pinus edulis* and *Juniperus monosperma*. *Remote Sensing of Environment* 96:108–118.
- Suarez, M. L., L. Ghermandi, and T. Kitzberger. 2004. Factors predisposing episodic drought-induced tree mortality in *Nothofagus*-site, climatic sensitivity and growth trends. *Journal of Ecology* 92:954–966.
- Svoray, T., and A. Karnieli. 2011. Rainfall, topography and primary production relationships in a semiarid ecosystem. *Ecohydrology* 4:56–66.
- Syed, K. H., D. C. Goodrich, D. E. Myers, and S. Sorooshian. 2003. Spatial characteristics of thunderstorm rainfall fields and their relation to runoff. *Journal of Hydrology* 271:1–21.
- Tucker, C. J. 1979. Red and photographic infrared linear combinations for monitoring vegetation. *Remote Sensing of Environment* 8:127–150.
- Ungar, E. D., E. Rotenberg, N. Raz-Yaseef, S. Cohen, D. Yakir, and G. Schiller. 2013. Transpiration and annual water balance of Aleppo pine in a semiarid region: implications for forest management. *Forest Ecology and Management* 298:39–51.
- Vacchiano, G., M. Garbarino, E. Borgogno Mondino, and R. Motta. 2012. Evidences of drought stress as a predisposing factor to Scots pine decline in Valle d'Aosta (Italy). *European Journal of Forest Research* 131:989–1000.
- Venables, W. N., and B. D. Ripley. 2002. Modern applied statistics with S. Springer, New York, New York, USA.
- Vicente-Serrano, S. M., T. Lasanta, and C. Gracia. 2010. Aridification determines changes in forest growth in *Pinus halepensis* forests under semiarid Mediterranean climate conditions. *Agricultural and Forest Meteorology* 150:614–628.
- Vila-Cabrera, A., J. Martinez-Vilalta, L. Galiano, and J. Retana. 2013. Patterns of forest decline and regeneration across Scots pine populations. *Ecosystems* 16:323–335.
- Vila-Cabrera, A., J. Martinez-Vilalta, J. Vayreda, and J. Retana. 2011. Structural and climatic determinants of demographic rates of Scots pine forests across the Iberian Peninsula. *Ecological Applications* 21:1162–1172.
- Volcani, A., A. Karnieli, and T. Svoray. 2005. The use of remote sensing and GIS for spatio-temporal analysis of the physiological state of a semi-arid forest with respect to drought years. *Forest Ecology and Management* 215:239–250.
- Weinstein-Evron, M., and S. Lev-Yadun. 2000. Palaeoecology of *Pinus halepensis* in Israel in the light of palynological and archaeobotanical data. Pages 119–130 in G. Ne'eman and L. Traubaud, editors. *Ecology, biogeography and management of *Pinus halepensis* and *P. brutia* forest ecosystems in the Mediterranean Basin*. Backhuys, Leiden, The Netherlands.
- Weiss, J. L., C. L. Castro, and J. T. Overpeck. 2009. Distinguishing pronounced droughts in the southwestern United States: seasonality and effects of warmer temperatures. *Journal of Climate* 22:5918–5932.
- Wickham, H. 2009. *ggplot2: elegant graphics for data analysis*. Springer, New York, New York, USA.
- Worrall, J. J., L. Egeland, T. Eager, R. A. Mask, E. W. Johnson, P. A. Kemp, and W. D. Shepperd. 2008. Rapid mortality of *Populus tremuloides* in southwestern Colorado, USA. *Forest Ecology and Management* 255:686–696.
- Wulder, M. A., S. M. Ortlepp, J. C. White, and S. Maxwell. 2008. Evaluation of Landsat-7 SLC-off image products for forest change detection. *Canadian Journal of Remote Sensing* 34:93–99.
- Yakir, H., and E. Morin. 2011. Hydrologic response of a semiarid watershed to spatial and temporal characteristics of convective rain cells. *Hydrology and Earth System Sciences* 15:393–404.
- Yuhas, A. N., and L. A. Scuderi. 2009. MODIS-derived NDVI characterisation of drought-induced evergreen dieoff in western North America. *Geographical Research* 47:34–45.
- Zaady, E., M. Shachak, and Y. Moshe. 2001. Ecological approach for afforestation in arid regions of the northern Negev Desert, Israel. Pages 219–238 in D. K. Vajpeyi, editor. *Deforestation, environment, and sustainable development: a comparative analysis*. Praeger, Westport, Connecticut, USA.
- Zuur, A. F., E. N. Ieno, N. J. Walker, A. A. Saveliev, and G. M. Smith. 2009. *Mixed effects models and extensions in ecology with R*. Springer-Verlag, New York, New York, USA.

SUPPLEMENTAL MATERIAL

Ecological Archives

Appendices A–F are available online: <http://dx.doi.org/10.1890/14-0698.1.sm>

4 Concluding discussion

4.1 Observing forest response to drought – from patterns to processes

Water is an essential resource for all forest trees, while in many parts of the world water availability is the main limiting factor for tree growth and survival (Boisvenue & Running, 2006). The Mediterranean region is an example of such an environment (Pigott & Pigott, 1993; Zavala *et al.*, 2000). Tree responses to shortage in water availability (i.e., drought) range from short-term *physiological* responses, such as reduction in photosynthetic rate due to stomatal closure, through *structural* responses, such as reduction in annual growth rate and defoliation, up to *demographic* responses, such as reduced recruitment and increased mortality. Although the three types of responses are interconnected – for example, reduced tree growth rate may be a predisposing factor for mortality (Suarez *et al.*, 2004; Bigler *et al.*, 2007; Vila-Cabrera *et al.*, 2011) – it is essential to explicitly define the distinctions when discussing (a) which traits are being measured using a given method, and (b) in what way is response to drought according to the given trait related to long-term resistance and resilience to drought of the forest ecosystem.

Overcoming drought stress involves spending more resources by the tree, for example for growing new leaves following defoliation (Galiano *et al.*, 2011) or constructing new xylem to compensate for hydraulic failure (Brodrribb *et al.*, 2010). Radial growth rate of the tree trunk is a valuable structural trait for monitoring a tree's physiological state over time, since its carbon-allocation priority is relatively low (Hanson & Weltzin, 2000), i.e. under limiting conditions radial growth is among the first traits to be affected (Borghetti *et al.*, 1998; Klein *et al.*, 2005). As stress continues, the ability of the tree to survive diminishes. At a certain point irreversible damage occurs, which the tree no longer can withstand, and it dies. For example, respiration may no longer

be supported as carbon reserves diminish, desiccation can take place as a result of water transport cessation or the tree may suffer lethal damage from insects because defensive compounds can no longer be produced (McDowell *et al.*, 2011).

Tree growth data (Section 3.3) from the arid part of the climatic gradient (~300 mm of average annual rainfall) have indeed shown that *P. halepensis* trees have experienced substantial growth reductions during the two recent drought periods of 1998-2000 and 2005-2011. The very low growth rates (for example, 2.4 cm and 2.8 cm² yr⁻¹ in 1999 and 2011, respectively, compared to a 30-year average of 6.5 cm² yr⁻¹) and substantial proportions of missing rings (18% in 2011) express the extreme stress the trees have experienced as a result of the highly limiting water availability conditions.

At the same time, drought stress reduces the water (Baquedano & Castillo, 2006) and chlorophyll (Baquedano & Castillo, 2007) content of leaves, as well as the length of newly produced leaves (Korner *et al.*, 2005) and overall leaf area (Carnicer *et al.*, 2011). In this study, remotely-sensed NDVI served as an inclusive indicator of forest canopy state, since it is positively associated with canopy-related traits (Myneni *et al.*, 1995; Pettorelli *et al.*, 2005). However, tree mortality obviously also involves the gradual reduction of green biomass in the canopy of the respective dying tree (to zero, eventually).

NDVI decline over time could thus be interpreted as either structural (i.e. desiccation of needles and defoliation) change alone, or as a combination of structural and subsequent demographic (i.e. tree mortality) changes within the respective forest patch the satellite observes. Persistent decline, with limited recovery after drought stress has been relieved (Section 3.1) was observed in the dry part of the climatic gradient (<350 mm of average annual rainfall) and supports the latter scenario. Additional information is necessary, however, to interpret the observed NDVI decline pattern in terms of structural and demographic processes.

Observations of tree mortality (Sections 3.2 and 3.4) indeed confirmed that demographic changes took place as a result of the drought, in addition to structural ones, although the intensity of the former was highly variable in space. For example,

in Lahav and Dvira forests, NDVI decline during the drought of 2005-2011 was observed in 86% of the forested area, while mortality following the drought was limited to only 30% of the area (Section 3.4). Moreover, mortality was highly variable among different locations (2-90% dead trees) within that latter area where it was observed.

4.2 Environmental determinants of forest mortality

The highest sensitivity to drought was observed in forests occupying the arid part of the studied climatic gradient (<350 mm of average annual rainfall). In addition to the observed forest greenness decline (Sections 3.1 and 3.2) and substantial mortality (Section 3.4), trees growing in that region immediately (same-year) and strongly (90% of growth rate variation explained by annual rainfall) responded to the annual rainfall amount reduction (Section 3.3). This pattern suggests that no "buffering", in terms of water availability for the trees, takes place in such dry settings. This is in agreement with previous knowledge regarding annual water balance in planted *P. halepensis* forests in that region (Raz-Yaseef *et al.*, 2010, 2012; Ungar *et al.*, 2013; Klein *et al.*, 2014). The latter studies showed that the majority of annual rainfall is lost to the atmosphere during the same year, which is likely reflected in a very limited potential for carried-over moisture over multi-annual time scales.

The mild response to drought at the humid edge of the climatic gradient, as well as a weaker and more lagged relation between tree growth and rainfall amounts, suggest that sensitivity of *P. halepensis* forests to drought in this region is relatively weak. Divergence was thus observed along the climatic gradient, both in long-term forest greenness trend (<540 mm – decrease; >540 mm – increase) and in time-scale of dominant response to rainfall variation (<500 mm – annual; >500 mm – multi-annual). These thresholds identify the transition zone southwards of which planted *P. halepensis* forests are probably not sustainable, given the climatic conditions and management practices experienced during 1983-2012.

On the local spatial scale (Section 3.4), higher mortality was observed under locally drier conditions (south-facing aspects) coinciding with higher moisture demands (older forest stands). It was also demonstrated that although forest performance becomes most highly homogeneous in the dry region during drought (Section 3.2), the locally drier habitats (which suffer substantial mortality) still reach the lowest absolute performance levels, supporting a nonlinear (i.e. threshold-related) tree mortality risk behavior. Counter intuitively, deeper soils were identified as a risk-factor to drought-induced mortality (Section 3.4), supposedly due to the fact that under prolonged drought they impose limited root access to the bedrock layers, where residual moisture may sustain tree survival after the entire soil profile dries out (Schiller 1982). In addition, competition intensity had no negative effect on either tree survival probability (Section 3.4) or the growth rate of inferior trees (Section 3.3). This result, combined with similar ones obtained for other drought-induced forest mortality events (Worrall *et al.*, 2008; Floyd *et al.*, 2009; Clifford *et al.*, 2013), suggests a potential role for self-amplifying mechanisms in tree mortality (Section 3.4), and casts doubt on the generally held view that forest thinning could reduce tree mortality risk.

5 References

- Adams HD, Guardiola-Claramonte M, Barron-Gafford GA et al. (2009) Temperature sensitivity of drought-induced tree mortality portends increased regional die-off under global-change-type drought. *Proceedings of the National Academy of Sciences of the United States of America*, **106**, 7063–7066.
- Adams HD, Luce CH, Breshears DD et al. (2012) Ecohydrological consequences of drought-and infestation-triggered tree die-off: insights and hypotheses. *Ecohydrology*, **5**, 145–159.
- Allen CD, Macalady AK, Chenchouni H et al. (2010) A global overview of drought and heat-induced tree mortality reveals emerging climate change risks for forests. *Forest Ecology and Management*, **259**, 660–684.
- Anderegg WRL, Berry JA, Smith DD, Sperry JS, Anderegg LDL, Field CB (2012) The roles of hydraulic and carbon stress in a widespread climate-induced forest die-off. *Proceedings of the National Academy of Sciences of the United States of America*, **109**, 233–237.
- Anderson RG, Canadell JG, Randerson JT et al. (2010a) Biophysical considerations in forestry for climate protection. *Frontiers in Ecology and the Environment*, **9**, 174–182.
- Anderson LO, Malhi Y, Aragao LEOC, Ladle R, Arai E, Barbier N, Phillips O (2010b) Remote sensing detection of droughts in Amazonian forest canopies. *New Phytologist*, **187**, 733–750.
- Baquedano FJ, Castillo FJ (2006) Comparative ecophysiological effects of drought on seedlings of the Mediterranean water-saver *Pinus halepensis* and water-spenders *Quercus coccifera* and *Quercus ilex*. *Trees-Structure and Function*, **20**, 689–700.
- Baquedano FJ, Castillo FJ (2007) Drought tolerance in the Mediterranean species *Quercus coccifera*, *Quercus ilex*, *Pinus halepensis*, and *Juniperus phoenicea*. *Photosynthetica*, **45**, 229–238.
- Beck PSA, Juday GP, Alix C et al. (2011) Changes in forest productivity across Alaska consistent with biome shift. *Ecology Letters*, **14**, 373–379.
- Berner LT, Beck PSA, Bunn AG, Goetz SJ (2013) Plant response to climate change along the forest-tundra ecotone in northeastern Siberia. *Global change biology*, **19**, 3449–3462.
- Bigler C, Gavin DG, Gunning C, Veblen TT (2007) Drought induces lagged tree mortality in a subalpine forest in the Rocky Mountains. *Oikos*, **116**, 1983–1994.
- Birdsey R, Pan Y (2011) Ecology: Drought and dead trees. *Nature Climate Change*, **1**, 444–445.
- Boisvenue C, Running SW (2006) Impacts of climate change on natural forest productivity - evidence since the middle of the 20th century. *Global Change Biology*, **12**, 862–882.

- Borghetti M, Cinnirella S, Magnani F, Saracino A (1998) Impact of long-term drought on xylem embolism and growth in *Pinus halepensis* Mill. *Trees (Berlin)*, **12**, 187–195.
- Breshears DD, Cobb NS, Rich PM et al. (2005) Regional vegetation die-off in response to global-change-type drought. *Proceedings of the National Academy of Sciences of the United States of America*, **102**, 15144–15148.
- Breshears DD, Myers OB, Meyer CW et al. (2009) Tree die-off in response to global change-type drought: mortality insights from a decade of plant water potential measurements. *Frontiers in Ecology and the Environment*, **7**, 185–189.
- Brodrribb TJ, Bowman D, Nichols S, Delzon S, Burlett R (2010) Xylem function and growth rate interact to determine recovery rates after exposure to extreme water deficit. *New Phytologist*, **188**, 533–542.
- Carnicer J, Coll M, Ninyerola M, Pons X, Sanchez G, Penuelas J (2011) Widespread crown condition decline, food web disruption, and amplified tree mortality with increased climate change-type drought. *Proceedings of the National Academy of Sciences of the United States of America*, **108**, 1474–1478.
- Clifford MJ, Cobb NS, Buenemann M (2011) Long-term tree cover dynamics in a pinyon-juniper woodland: climate-change-type drought resets successional clock. *Ecosystems*, **14**, 949–962.
- Clifford MJ, Royer PD, Cobb NS, Breshears DD, Ford PL (2013) Precipitation thresholds and drought-induced tree die-off: insights from patterns of *Pinus edulis* mortality along an environmental stress gradient. *New Phytologist*, **200**, 413–421.
- Coll M, Penuelas J, Ninyerola M, Pons X, Carnicer J (2013) Multivariate effect gradients driving forest demographic responses in the Iberian Peninsula. *Forest Ecology and Management*, **303**, 195–209.
- Dorman M, Svoray T, Perevolotsky A, Sarris D (2013a) Forest performance during two consecutive drought periods: Diverging long-term trends and short-term responses along a climatic gradient. *Forest Ecology and Management*, **310**, 1–9.
- Dorman M, Svoray T, Perevolotsky A (2013b) Homogenization in forest performance across an environmental gradient – The interplay between rainfall and topographic aspect. *Forest Ecology and Management*, **310**, 256–266.
- Dorman M, Perevolotsky A, Sarris D, Svoray T (2015a) The effect of rainfall and competition intensity on forest response to drought: Lessons learned from a dry extreme. *Oecologia*, **177**, 1025–1038.
- Dorman M, Svoray T, Perevolotsky A, Moshe Y, Sarris D (2015b) What determines tree mortality in dry environments? A multi-perspective approach. *Ecological Applications*, **25**, 1054–1071.
- Floyd ML, Clifford M, Cobb NS, Hanna D, Delph R, Ford P, Turner D (2009) Relationship of stand characteristics to drought-induced mortality in three Southwestern pinon-juniper woodlands. *Ecological Applications*, **19**, 1223–1230.
- Galiano L, Martinez-Vilalta J, Lloret F (2011) Carbon reserves and canopy defoliation determine the recovery of Scots pine 4 yr after a drought episode. *New*

- Phytologist*, **190**, 750–759.
- Gamfeldt L, Snäll T, Bagchi R et al. (2013) Higher levels of multiple ecosystem services are found in forests with more tree species. *Nature communications*, **4**, 1340.
- Garrity SR, Allen CD, Brumby SP, Gangodagamage C, McDowell NG, Cai DM (2013) Quantifying tree mortality in a mixed species woodland using multitemporal high spatial resolution satellite imagery. *Remote Sensing of Environment*, **129**, 54–65.
- Gaylord ML, Kolb TE, Pockman WT et al. (2013) Drought predisposes pinon–juniper woodlands to insect attacks and mortality. *New Phytologist*, **198**, 567–578.
- Gitlin AR, Sthultz CM, Bowker MA et al. (2006) Mortality gradients within and among dominant plant populations as barometers of ecosystem change during extreme drought. *Conservation Biology*, **20**, 1477–1486.
- Gomez-Aparicio L, Garcia-Valdes R, Ruiz-Benito P, Zavala MA (2011) Disentangling the relative importance of climate, size and competition on tree growth in Iberian forests: implications for forest management under global change. *Global Change Biology*, **17**, 2400–2414.
- Hanson PJ, Weltzin JF (2000) Drought disturbance from climate change: response of United States forests. *Science of the Total Environment*, **262**, 205–220.
- Hicke JA, Zeppel MJB (2013) Climate-driven tree mortality: insights from the piñon pine die-off in the United States. *New Phytologist*, **200**, 301–303.
- Hoerling M, Eischeid J, Perlitz J, Quan X, Zhang T, Pegion P (2012) On the increased frequency of Mediterranean drought. *Journal of Climate*, **25**, 2146–2161.
- Hoffmann WA, Marchin RM, Abit P, Lau OL (2011) Hydraulic failure and tree dieback are associated with high wood density in a temperate forest under extreme drought. *Global Change Biology*, **17**, 2731–2742.
- Jactel H, Petit J, Desprez-Loustau M, Delzon S, Piou D, Battisti A, Koricheva J (2012) Drought effects on damage by forest insects and pathogens: a meta-analysis. *Global Change Biology*, **18**, 267–276.
- Kharuk VI, Im ST, Oskorbin PA, Petrov IA, Ranson KJ (2013) Siberian pine decline and mortality in southern siberian mountains. *Forest Ecology and Management*, **310**, 312–320.
- Klein T, Hemming D, Lin TB, Grunzweig JM, Maseyk K, Rotenberg E, Yakir D (2005) Association between tree-ring and needle delta C-13 and leaf gas exchange in *Pinus halepensis* under semi-arid conditions. *Oecologia*, **144**, 45–54.
- Klein T, Di Matteo G, Rotenberg E, Cohen S, Yakir D (2013) Differential ecophysiological response of a major Mediterranean pine species across a climatic gradient. *Tree physiology*, **33**, 26–36.
- Klein T, Rotenberg E, Cohen-Hilaleh E et al. (2014) Quantifying transpirable soil water and its relations to tree water use dynamics in a water - limited pine forest. *Ecohydrology*, **7**, 409–419.
- Koepke DF, Kolb TE, Adams HD (2010) Variation in woody plant mortality and dieback from severe drought among soils, plant groups, and species within a

- northern Arizona ecotone. *Oecologia*, **163**, 1079–1090.
- Korner C, Sarris D, Christodoulakis D (2005) Long-term increase in climatic dryness in the East-Mediterranean as evidenced for the island of Samos. *Regional Environmental Change*, **5**, 27–36.
- Levin SA (1992) The problem of pattern and scale in ecology: the Robert H. MacArthur award lecture. *Ecology*, **73**, 1943–1967.
- Linares JC, Camarero JJ, Carreira JA (2010a) Competition modulates the adaptation capacity of forests to climatic stress: insights from recent growth decline and death in relict stands of the Mediterranean fir *Abies pinsapo*. *Journal of Ecology*, **98**, 592–603.
- Linares JC, Camarero JJ, Bowker MA, Ochoa V, Carreira JA (2010b) Stand-structural effects on *Heterobasidion abietinum*-related mortality following drought events in *Abies pinsapo*. *Oecologia*, **164**, 1107–1119.
- Lloyd AH, Bunn AG, Berner L (2011) A latitudinal gradient in tree growth response to climate warming in the Siberian taiga. *Global Change Biology*, **17**, 1935–1945.
- De Luis M, Čufar K, Di Filippo A et al. (2013) Plasticity in dendroclimatic response across the distribution range of Aleppo pine (*Pinus halepensis*). *PloS one*, **8**, e83550.
- Macfarlane WW, Logan JA, Kern WR (2013) An innovative aerial assessment of Greater Yellowstone Ecosystem mountain pine beetle-caused whitebark pine mortality. *Ecological Applications*, **23**, 421–437.
- Mathisen IE, Mikheeva A, Tutubalina OV, Aune S, Hofgaard A (2014) Fifty years of tree line change in the Khibiny Mountains, Russia: advantages of combined remote sensing and dendroecological approaches. *Applied Vegetation Science*, **17**, 6–16.
- Matyas C (2010) Forecasts needed for retreating forests. *Nature*, **464**, 1271–1271.
- McDowell N, Pockman WT, Allen CD et al. (2008) Mechanisms of plant survival and mortality during drought: why do some plants survive while others succumb to drought? *New Phytologist*, **178**, 719–739.
- McDowell NG, Allen CD, Marshall L (2010) Growth, carbon-isotope discrimination, and drought-associated mortality across a *Pinus ponderosa* elevational transect. *Global Change Biology*, **16**, 399–415.
- McDowell NG, Beerling DJ, Breshears DD, Fisher RA, Raffa KF, Stitt M (2011) The interdependence of mechanisms underlying climate-driven vegetation mortality. *Trends in Ecology & Evolution*, **26**, 523–532.
- McDowell NG, Ryan MG, Zeppel MJB, Tissue DT (2013a) Improving our knowledge of drought-induced forest mortality through experiments, observations, and modeling. *New Phytologist*, **200**, 289–293.
- McDowell NG, Fisher RA, Xu C et al. (2013b) Evaluating theories of drought-induced vegetation mortality using a multimodel–experiment framework. *New Phytologist*, **200**, 304–321.
- Michaelian M, Hogg EH, Hall RJ, Arsenault E (2011) Massive mortality of aspen following severe drought along the southern edge of the Canadian boreal forest. *Global Change Biology*, **17**, 2084–2094.

- Mueller RC, Scudder CM, Porter ME, Trotter RT, Gehring CA, Whitham TG (2005) Differential tree mortality in response to severe drought: evidence for long-term vegetation shifts. *Journal of Ecology*, **93**, 1085–1093.
- Myneni RB, Hall FG, Sellers PJ, Marshak AL (1995) The interpretation of spectral vegetation indexes. *Geoscience and Remote Sensing, IEEE Transactions on*, **33**, 481–486.
- Osem Y, Zangy E, Bney-Moshe E, Moshe Y, Karni N, Nisan Y (2009) The potential of transforming simple structured pine plantations into mixed Mediterranean forests through natural regeneration along a rainfall gradient. *Forest Ecology and Management*, **259**, 14–23.
- Osem Y, Yavlovich H, Zecharia N, Atzmon N, Moshe Y, Schiller G (2013) Fire-free natural regeneration in water limited *Pinus halepensis* forests: a silvicultural approach. *European Journal of Forest Research*, **132**, 679–690.
- Parmesan C (2006) Ecological and evolutionary responses to recent climate change. *Annual Review of Ecology, Evolution, and Systematics*, 637–669.
- Pasho E, Julio Camarero J, de Luis M, Vicente-Serrano SM (2011) Impacts of drought at different time scales on forest growth across a wide climatic gradient in north-eastern Spain. *Agricultural and Forest Meteorology*, **151**, 1800–1811.
- Penuelas J, Sardans J, Estiarte M et al. (2013) Evidence of current impact of climate change on life: A walk from genes to the biosphere. *Global Change Biology*, **19**, 2303–2338.
- Pettorelli N, Vik JO, Mysterud A, Gaillard J-M, Tucker CJ, Stenseth NC (2005) Using the satellite-derived NDVI to assess ecological responses to environmental change. *Trends in Ecology & Evolution*, **20**, 503–510.
- Pigott CD, Pigott S (1993) Water as a determinant of the distribution of trees at the boundary of the Mediterranean zone. *Journal of Ecology*, **81**, 557–566.
- Raz-Yaseef N, Yakir D, Rotenberg E, Schiller G, Cohen S (2010) Ecohydrology of a semi-arid forest: partitioning among water balance components and its implications for predicted precipitation changes. *Ecohydrology*, **3**, 143–154.
- Raz-Yaseef N, Yakir D, Schiller G, Cohen S (2012) Dynamics of evapotranspiration partitioning in a semi-arid forest as affected by temporal rainfall patterns. *Agricultural and Forest Meteorology*, **157**, 77–85.
- Rotenberg E, Yakir D (2010) Contribution of semi-arid forests to the climate system. *Science*, **327**, 451–454.
- Royer PD, Cobb NS, Clifford MJ, Huang C-Y, Breshears DD, Adams HD, Camilo Villegas J (2011) Extreme climatic event-triggered overstorey vegetation loss increases understorey solar input regionally: primary and secondary ecological implications. *Journal of Ecology*, **99**, 714–723.
- Sarris D, Siegwolf R, Koerner C (2013) Inter- and intra-annual stable carbon and oxygen isotope signals in response to drought in Mediterranean pines. *Agricultural and Forest Meteorology*, **168**, 59–68.
- Schiller G, Atzmon N (2009) Performance of Aleppo pine (*Pinus halepensis*) provenances grown at the edge of the Negev desert: A review. *Journal of Arid Environments*, **73**, 1051–1057.
- Schiller G, Ungar ED, Genizi A (2005) Is tree fate written in its tree rings?

- Characterization of trees in Kramim forest following the 1998/99 dry winter. *Yaar*, 18–25. (In Hebrew).
- Schiller G, Ungar ED, Cohen S, Moshe Y, Atzmon N (2009) Aspect effect on transpiration of *Pinus halepensis* in Yatir forest. *Yaar*, **11**, 14–19. (In Hebrew).
- Stocker TF, Qin D, Plattner GK et al. (2013) IPCC, 2013: Climate Change 2013: The Physical Science Basis. Contribution of Working Group I to the Fifth Assessment Report of the Intergovernmental Panel on Climate Change.
- Suarez ML, Ghermandi L, Kitzberger T (2004) Factors predisposing episodic drought-induced tree mortality in *Nothofagus* - site, climatic sensitivity and growth trends. *Journal of Ecology*, **92**, 954–966.
- Ungar ED, Rotenberg E, Raz-Yaseef N, Cohen S, Yakir D, Schiller G (2013) Transpiration and annual water balance of Aleppo pine in a semiarid region: Implications for forest management. *Forest Ecology and Management*, **298**, 39–51.
- Vila-Cabrera A, Martinez-Vilalta J, Vayreda J, Retana J (2011) Structural and climatic determinants of demographic rates of Scots pine forests across the Iberian Peninsula. *Ecological Applications*, **21**, 1162–1172.
- Walther G-R, Post E, Convey P et al. (2002) Ecological responses to recent climate change. *Nature*, **416**, 389–395.
- Williams AP, Allen CD, Millar CI, Swetnam TW, Michaelsen J, Still CJ, Leavitt SW (2010) Forest responses to increasing aridity and warmth in the southwestern United States. *Proceedings of the National Academy of Sciences of the United States of America*, **107**, 21289–21294.
- Williams AP, Allen CD, Macalady AK et al. (2013) Temperature as a potent driver of regional forest drought stress and tree mortality. *Nature Climate Change*, **3**, 292–297.
- Worrall JJ, Egeland L, Eager T, Mask RA, Johnson EW, Kemp PA, Shepperd WD (2008) Rapid mortality of *Populus tremuloides* in southwestern Colorado, USA. *Forest Ecology and Management*, **255**, 686–696.
- Zavala MA, Espelta JM, Retana J (2000) Constraints and trade-offs in Mediterranean plant communities: The case of holm oak-Aleppo pine forests. *Botanical Review*, **66**, 119–149.

6 Supplementary material

6.1 Supplementary material for Section 3.1

Table S1 – Root Mean Square Error (RMSE) values of Leave-One-Out Cross Validation (LOOCV) when interpolating annual rainfall of 26 years using 8 different methods: Universal Kriging (UK) with 7 combinations of 3 predictors, elevation ("elev"), distance from the Mediterranean sea ("sea") and latitude ("y"), and Ordinary Kriging (OK). Each table cell contains the RMSE value of LOOCV when using a given method and interpolating annual rainfall data from 96 meteorological stations, for a given year. The bottom row shows mean RMSE values of a given method among all 26 years.

Year	UK elev+sea +y	UK elev+sea	UK elev+y	UK sea+y	UK elev	UK sea	UK y	OK
1986	45.8	48.0	48.2	49.1	48.2	50.1	49.9	50.3
1987	77.3	79.4	76.3	75.6	75.4	76.5	76.7	78.8
1988	81.2	82.3	79.1	78.8	76.8	77.9	84.6	84.1
1989	48.7	48.5	49.1	49.6	47.9	49.5	53.2	52.8
1990	58.0	58.1	60.0	62.4	57.8	62.2	64.8	64.1
1991	50.8	50.8	51.9	54.9	51.3	54.7	55.5	55.3
1992	115.1	117.8	110.9	117.4	107.1	117.9	113.6	112.5
1993	64.0	63.4	63.3	72.1	62.7	71.3	75.3	77.0
1994	45.9	45.4	46.3	52.3	45.5	51.3	55.1	55.4
1995	74.5	74.3	75.1	76.5	74.3	76.0	79.5	78.3
1996	57.8	57.8	58.6	62.4	64.5	62.6	64.5	68.6
1997	58.9	58.2	63.8	59.7	59.3	58.9	63.8	63.8
1998	531.6	63.5	61.4	249.6	59.8	63.1	66.5	64.8
1999	37.0	36.6	36.7	38.7	37.3	39.5	41.2	44.3
2000	507.8	55.2	52.5	370.8	50.4	55.5	59.5	56.5
2001	316.7	317.7	57.0	60.8	57.0	58.9	61.7	62.0
2002	1426.7	1067.0	62.1	95.7	62.0	72.1	70.5	71.4
2003	286.3	72.2	67.3	85.7	67.5	84.6	88.8	90.8
2004	446.3	54.5	59.0	58.6	59.8	58.1	63.5	71.4
2005	89.1	79.6	53.1	59.0	53.1	59.0	61.7	61.9
2006	53.7	56.8	52.9	56.9	52.8	58.3	59.2	61.0
2007	52.6	51.9	63.5	53.1	63.0	53.0	54.9	56.0
2008	35.8	37.0	36.8	40.7	38.2	41.0	43.8	46.1
2009	52.1	48.5	47.9	54.3	46.2	51.8	51.4	52.7
2010	48.7	49.3	48.1	54.6	47.0	53.5	53.5	53.0
2011	51.3	50.3	48.4	49.0	48.7	48.1	49.8	51.1
Average	181.3	108.6	58.8	82.2	58.2	61.8	63.9	64.8



Figure S1 – A view of Lahav forest, a planted *Pinus halepensis* forest in southern Israel (average annual rainfall of 280 mm in 1985-2011). Location of Lahav forest within the studied area is shown in Fig. S2. There are dead trees in the lower part of the picture and in the back, near the watch tower. The photograph also shows, from a different angle, the Lahav forest site, one of three sites where dendrochronological sampling took place (marked by arrow) (Photo: Michael Dorman, October 2011).

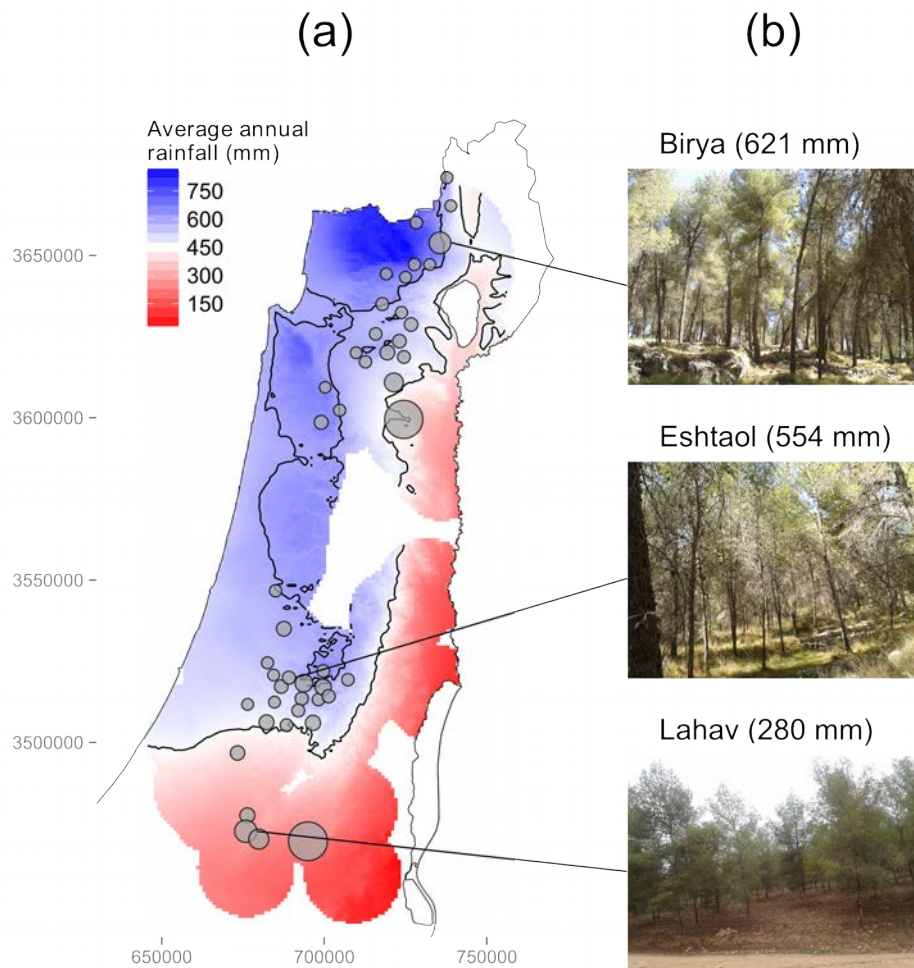


Figure S2 – (a) A map of average annual rainfall during 1985-2011 (background color) and locations of the centroids of the studied forests (grey circles). Rainfall amount values were obtained by spatial interpolation of data from 96 meteorological stations (shown as black points in Fig. 1), by using Universal Kriging with elevation as a covariate. Interpolation was applied using a 1000-m grid and only within 15 km of the nearest meteorological station. Circle size is proportional to forest size, ranging between 11 and 656 pixels of $90 \times 90 \text{ m}^2$. Thin lines mark international borders and coastlines of the Sea of Galilee and the Dead Sea. Thick lines show the 450 mm and the 600 mm isohyets. Universal Transverse Mercator (UTM) zone 36N coordinates (m) are shown on the axes. (b) Photographs of the three dendrochronological sampling sites in Biryia, Eshtaol and Lahav forests (Photos: M.D. 2011-2012). A view from a different angle of the Lahav forest site is shown in Fig. S1.

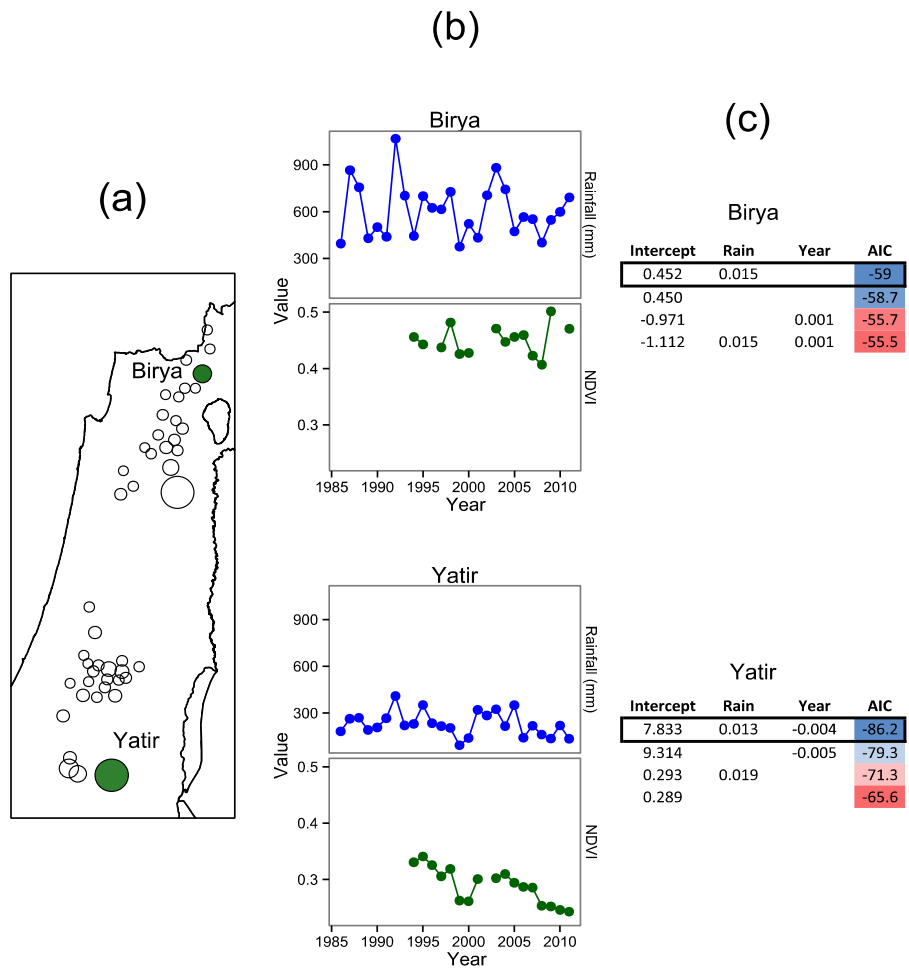


Figure S3 – An example of the input data and the model selection procedure for two of the 46 forests used in this study. These two forests – Biry and Yatir – are the largest in the humid and arid regions receiving on average 621 and 236 mm annual rainfall, respectively (during 1985-2011). (a) Locations of the forests. (b) Annual rainfall and NDVI as function of year in each forest, (c) Ranking of the four alternative linear regression models of NDVI: the full model $NDVI_t = \beta_0 + \beta_1 \times t + \beta_2 \times Rain_t + \varepsilon$ and the three simplified nested models each of which lacked one or both of the predictors, t and $Rain_t$. According to AIC, the model lacking the t effect best describes the NDVI pattern in Biry, while the full model best describes the NDVI pattern in Yatir. Therefore the estimated values of the year (t) effect were 0 for Biry -0.004 for Yatir; the values of the rainfall ($Rain_t$) effect were 0.015 for Biry and 0.013 for Yatir. The negative value of the year effect in Yatir expresses NDVI decline with time in that location, while absence of a year effect in Biry expresses temporal stability of NDVI. The same model selection procedure was repeated for the 46 forests in (a). The estimated values of the year and rainfall effects for each forest were then summarized in Fig. 2.

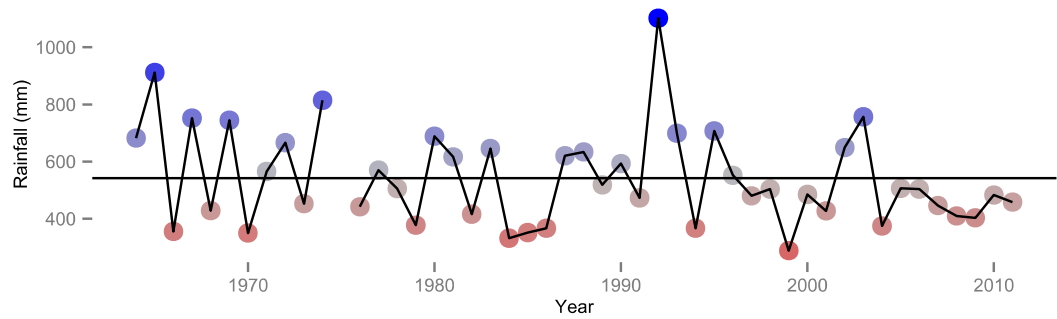
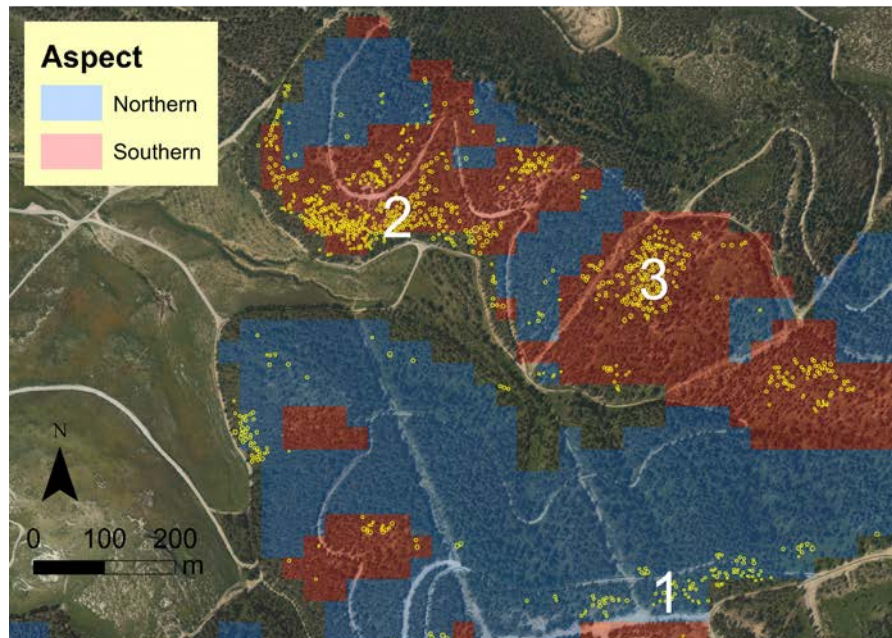


Figure S4 – Annual rainfall amount at Bet-Dagan (central Israel; coordinates on Fig. 1: 671333, 3542699 UTM zone 36N) during 1964-2011. A horizontal line marks the average annual rainfall (542 mm). Point colors are proportional to the magnitude of deviation from the average (red = below average, blue = above average). Rainfall for 1975 is missing.

6.2 Supplementary material for Section 3.2

(a)



(b)



(c)



(d)



(e)



Figure S1 – Zoom-in view (a) of the area within Lahav forest which is marked by a black dashed rectangle in Fig. 5. Two patches of tree mortality are further magnified (b, c). Photographs show how these mortality patches appear from the ground (d, e). Locations of the photographer (1) and of the two mortality patches (2, 3) are marked on all panels for orientation. The background in panels (a), (b) and (c) is an aerial photograph from winter 2011/12; yellow circles mark the locations of dead trees, manually identified on the aerial photograph. Semi-transparent blue and red colors mark northern and southern aspects, respectively, in (a). Note the difference in dead tree frequency between the opposite northern and southern aspects, seen in the lower and upper parts of panel (a), respectively. The difference in tree canopy condition among aspects is also evident from ground-view, seen in the front (what appears to be near – the northern aspect) and in the back (what appears to be far – the southern aspect) in panels (d, e). (Photographs: Dimitrios Sarris, August 2012).

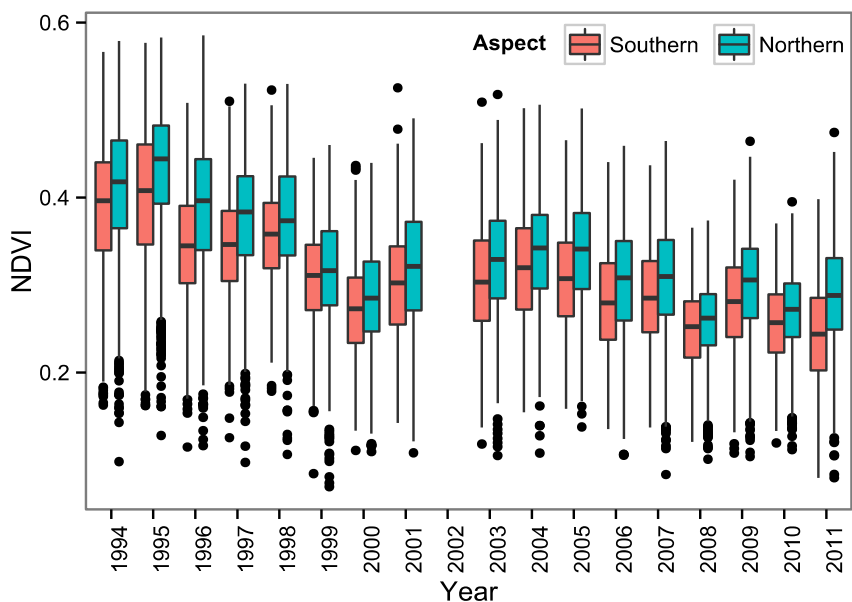


Figure S2 – Box and whiskers plot of NDVI, among $30 \times 30 \text{ m}^2$ pixels located on southern and northern aspects in Lahav forest, during the period 1994-2011. The upper and lower "hinges" correspond to the 25 and 75% quartiles. The upper whiskers extend from the hinge to the highest value that is within 1.5 of the 25-75% inter-quartile range. Data beyond the end of the whiskers are outliers and plotted as points.

6.3 Supplementary material for Section 3.3

Table S1 – Temporal trends (1966-2012) of P, T_{\min} and T_{\max} , at seasonal to annual scales, in three regions. Values are slopes (mm or $^{\circ}\text{C}$ per year) and significance (indicated by asterisks) based on linear regression of a given variable as function of year. Significant ($p < 0.05$) trends are printed in bold.

Variable	Period	South ^a	Center	North
P	Winter	0.173	-0.021	-0.469
	Spring	-0.761	-1.219*	-1.665*
	Fall ^b	-0.122	-0.345	0.064
	Annual	-0.705	-1.588	-2.033
T_{\min}	Winter	0.031**	0.02	0.022
	Spring	0.025**	0.019*	0.025**
	Summer	0.051***	0.036***	0.046***
	Fall	0.044***	0.028***	0.022*
	Annual	0.037***	0.026***	0.029***
T_{\max}	Winter	0.026	0.03	0.028
	Spring	0.026*	0.022	0.028*
	Summer	0.054***	0.040***	0.034***
	Fall	0.034***	0.030**	0.030**
	Annual	0.035***	0.030***	0.029***

^a Abbreviations: *** $p < 0.001$, ** $p < 0.01$, * $p < 0.05$

^b The trend of summer P is not shown since rainfall amounts in that season are negligible (Table 2)

Table S2 – Frequency of cores having at least one missing ring, and cores where missing ring positions were identified by cross-dating, in the three climatic regions.

	South	Center	North
≥1 missing rings	21.1%	4.4%	6.1%
Identified – 1999	0.6%	0.0%	0.0%
Identified – 2011	17.9%	2.8%	0.0%

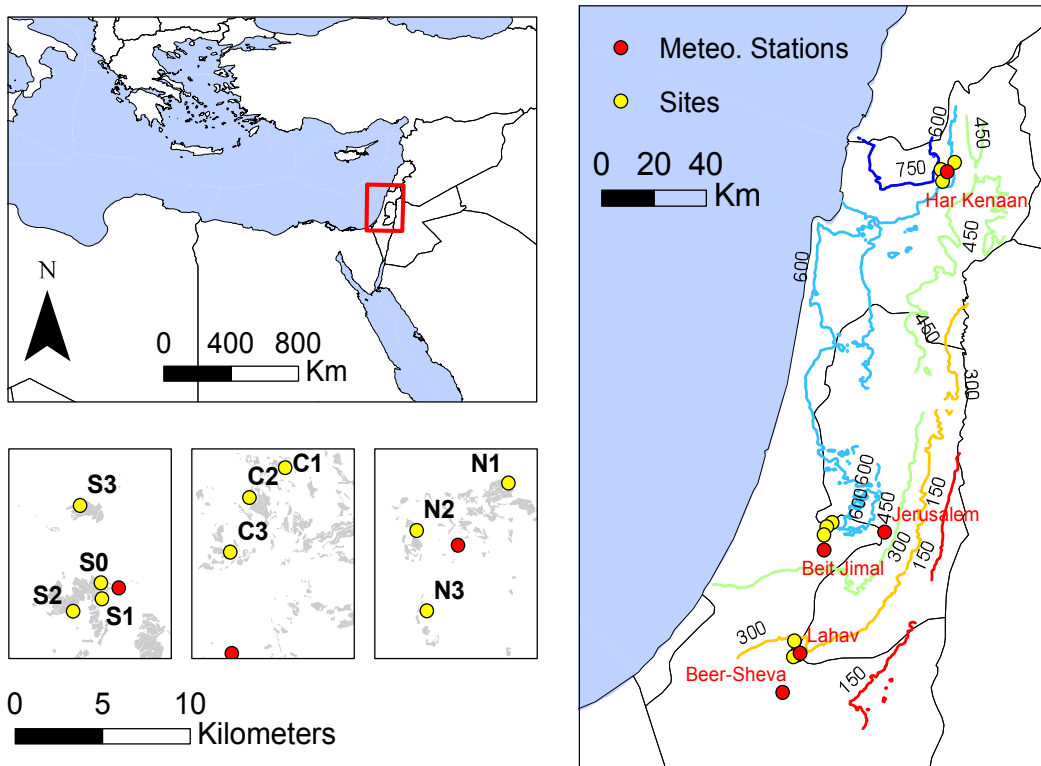


Figure S1 – Location of the sampled sites and meteorological stations. The three main meteorological stations were Har Kenaan, Beit Jimal and Lahav for the north, center and south regions, respectively. The two additional stations were Jerusalem and Beer-Sheva for the center and south regions, respectively. Contour lines refer to average annual rainfall amount (mm) for the period 1985–2011; data are based on interpolation from 96 meteorological stations (see Section 3.1). Grey polygons in the three small maps indicate planted *Pinus halepensis* forests.

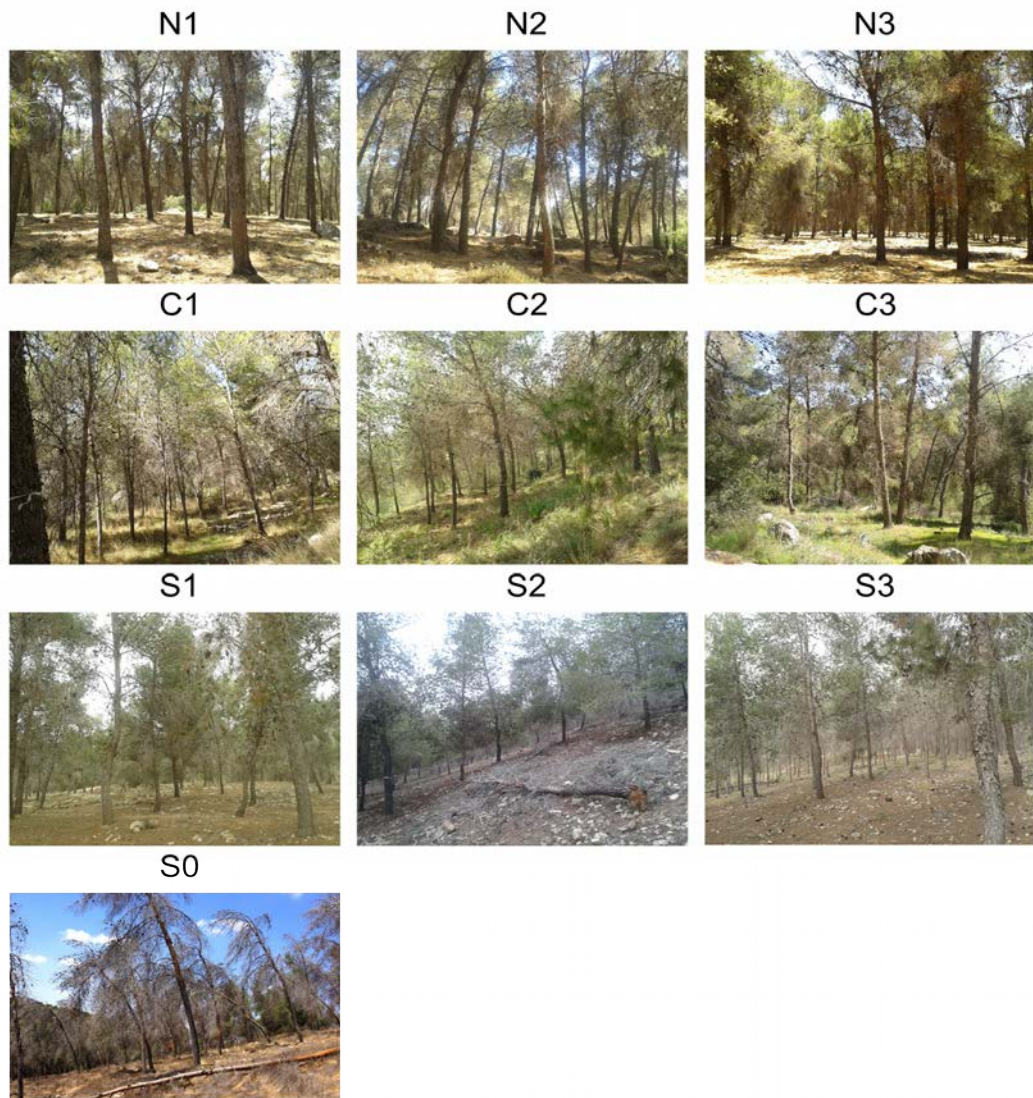


Figure S2 – Ground photographs of the ten study sites, taken at the time of sampling (fall 2012 – spring 2013).

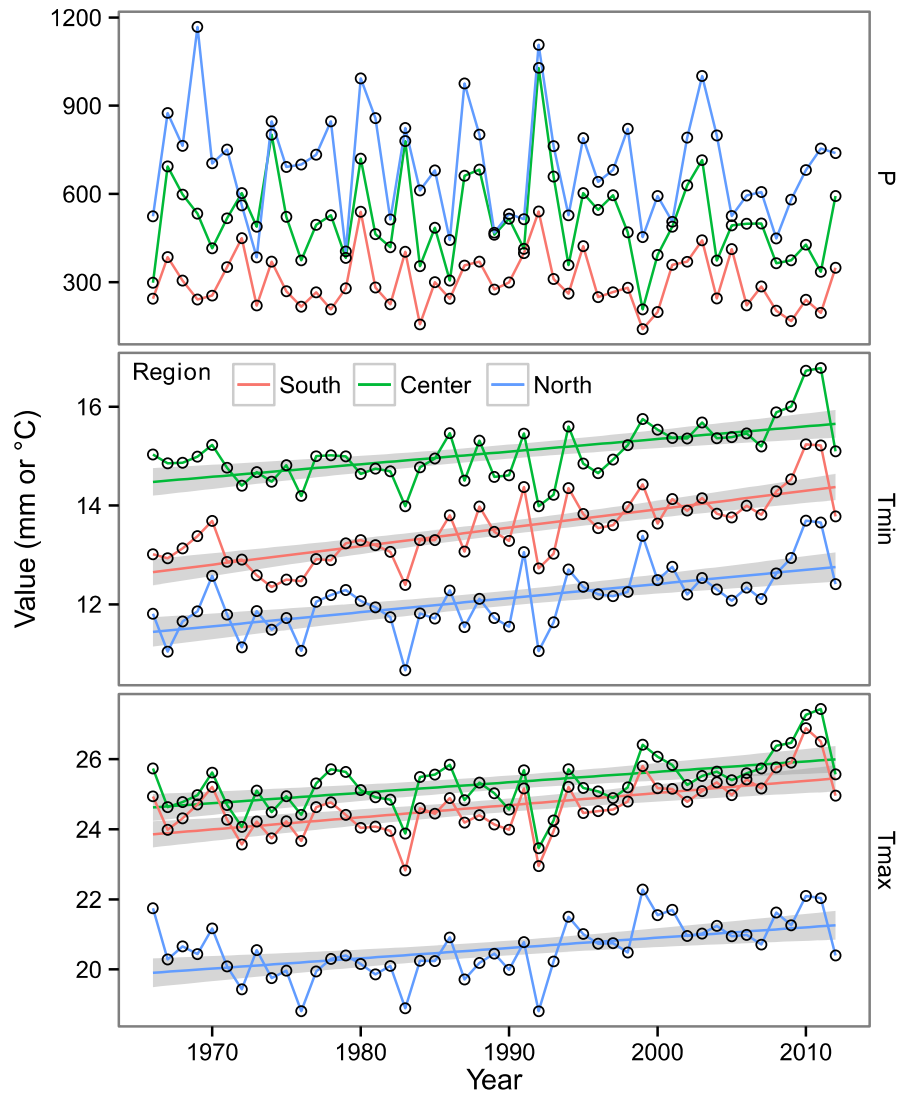


Figure S3 – Annual precipitation (P), minimum temperature (T_{\min}) and maximum temperature (T_{\max}) in the three regions during 47 seasons (1966-2012). Linear regression lines with 95% confidence intervals are shown for variable/region combinations where significant temporal trends were observed ($p < 0.001$) (Table S1).

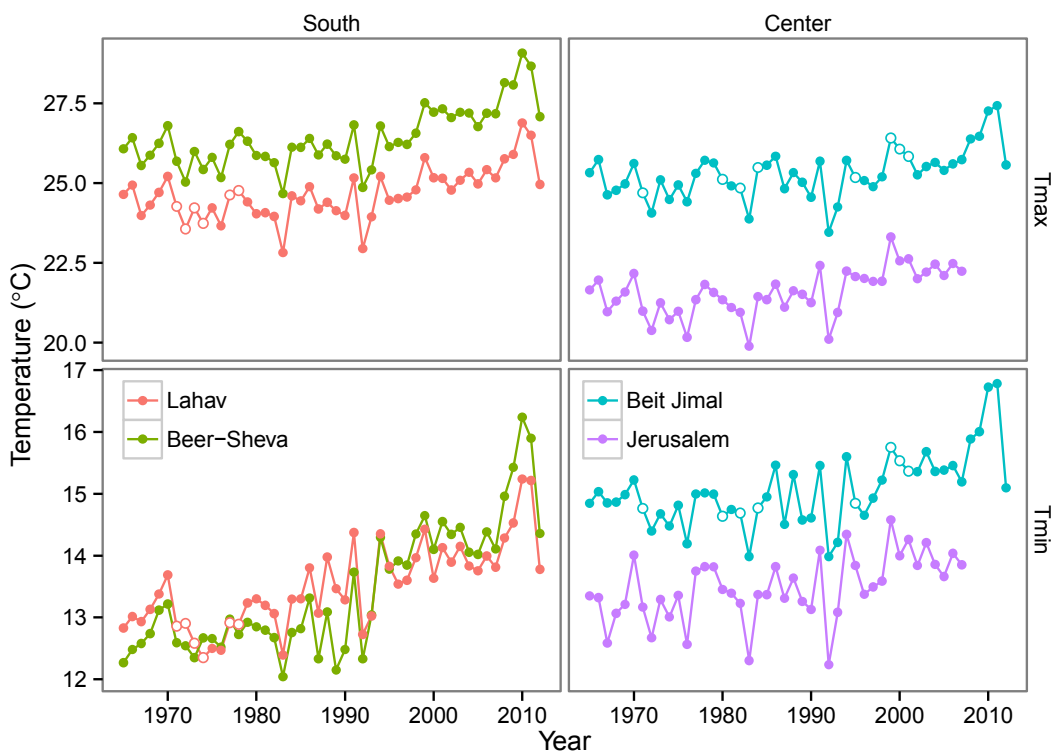


Figure S4 – Average annual temperature at predicted (Lahav and Beit Jimal) and predictor (Beer-Sheva and Jerusalem) stations in the south and center regions (Fig. S1). Predicted-station values were averaged after interpolating missing values according to those from the predictor stations (Fig. S5). Years when more than 10% of daily values were missing (prior to interpolation) are indicated by empty circles.

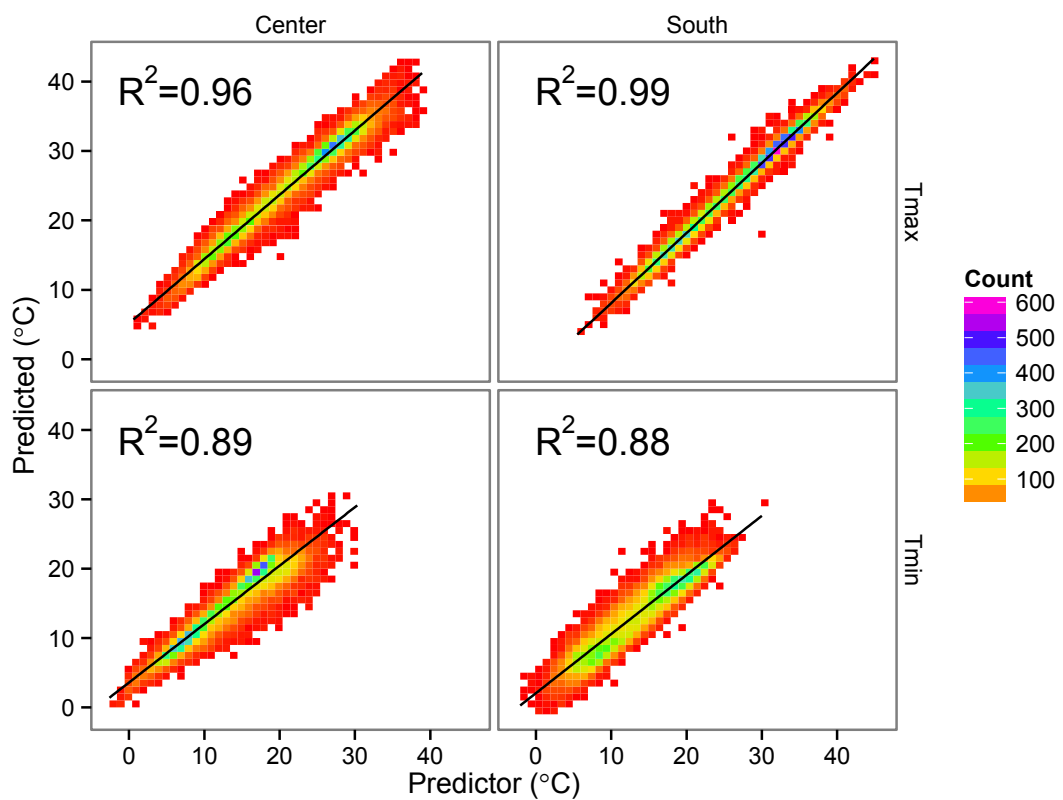


Figure S5 – Agreement between predictor and predicted stations in their daily T_{\min} and T_{\max} values. Predicted stations were Lahav and Beit Jimal and predictor stations were Beer-Sheva and Jerusalem, for the south and center regions, respectively (Fig. S1). Pixel colors express day counts within a given 1×1 $^{\circ}\text{C}$ combination. Black lines are linear regression fits; R^2 values of the regressions appear on each panel.

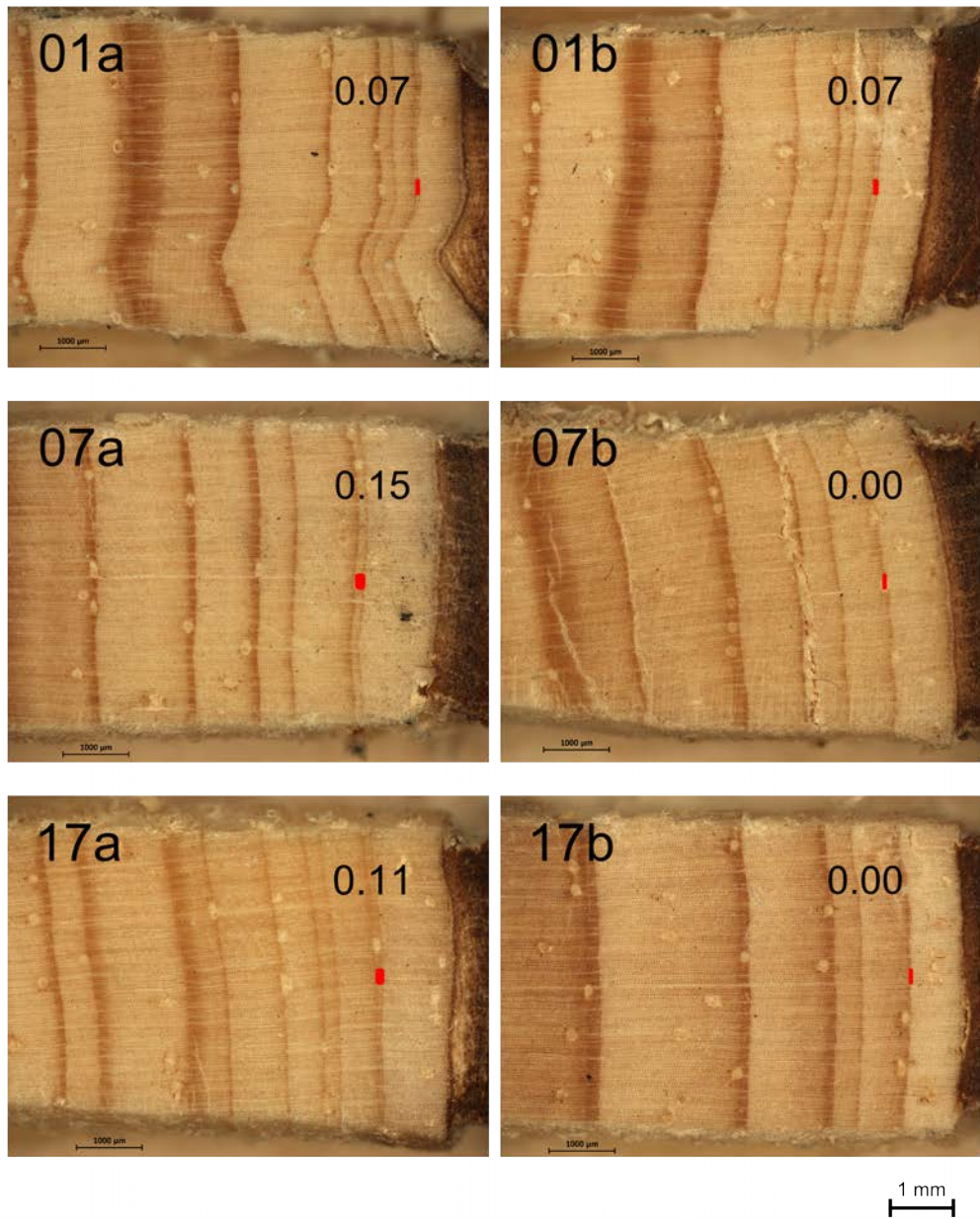


Figure S6 – Zoom-in photographs of the last several millimeters in six cores (from three trees) from site S2, exhibiting very little growth in 2011. Core identification code is composed of a tree number (1–30) and core number ("a" or "b"). The position of the 2011 tree-ring is indicated by a red line; the number above it is the tree-ring width (TRW; mm). Tree "01" exhibited a very narrow ring in 2011. Trees "07" and "17" exhibited incomplete ring formation in 2011, i.e., very low growth in one side ("a") of their trunk and zero growth (i.e., missing ring) in the other side ("b"). See Section 6.5 for additional images.

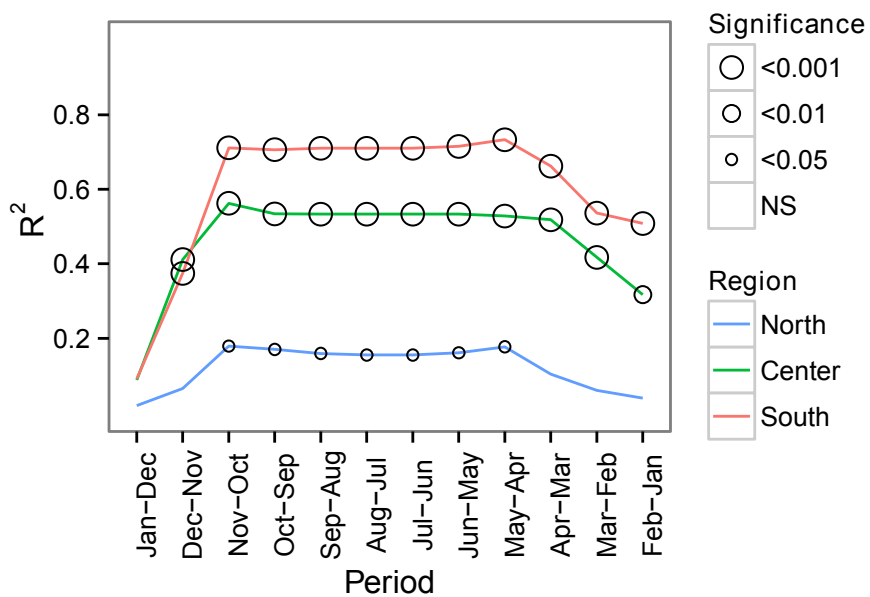


Figure S7 – R^2 values from linear regression of tree growth (BAI) as function of rainfall amount, for different annual 12-month integration periods, per region. Significant effects of rainfall are marked by empty circles, with circle size proportional to significance level.

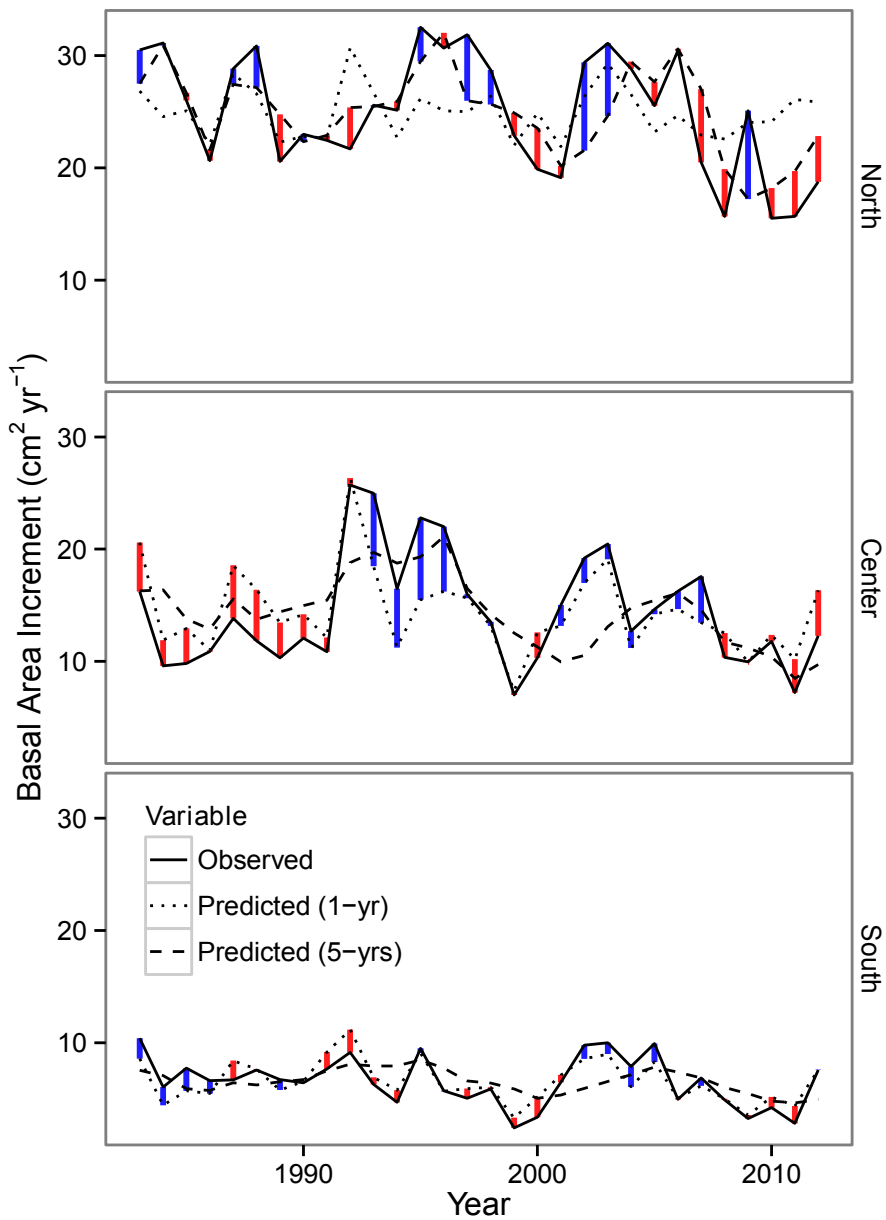


Figure S8 – Observed (solid lines) and predicted (dotted and dashed lines) BAI in three regions. Predictions are based on the linear regression models, with BAI treated as a function of rainfall amount during 1983–2012, with the independent variable being either annual rainfall (dotted lines) or 5-year rainfall (dashed lines). Residuals are shown as vertical lines. They refer to the best model describing BAI variation (Fig. 3), which was either based on annual rainfall (south and center) or 5-year rainfall (north).

6.4 Supplementary material for Section 3.4

Appendix A – Data sources and final products for mapping tree mortality and environmental conditions in Lahav and Dvira forests

Table A1 – Image identification code, acquisition date, number of control points, and Root Mean Square Error (RMSE) in georeferencing, for 10 historical aerial photographs used to map cultivated areas in 1945. Rows in the table are ordered according to images order in space, from left to right (i.e. west to east) and then top to bottom (i.e. north to south; see Fig. A4).

Forest	Image ID	Date	Control points	RMSE (m)
Dvira	ps21-5140	28.1.1945	25	3.70
	ps13-6032	5.1.1945	21	3.94
	ps13-6033	5.1.1945	21	4.00
Lahav	ps13-5154	5.1.1945	22	4.58
	ps13-5152	5.1.1945	21	4.15
	ps29-6071	14.3.1945	25	4.54
	ps29-6069	14.3.1945	27	2.43
	ps13-5137	5.1.1945	22	4.41
	ps13-5138	5.1.1945	23	3.08
	ps13-5139	5.1.1945	24	4.36

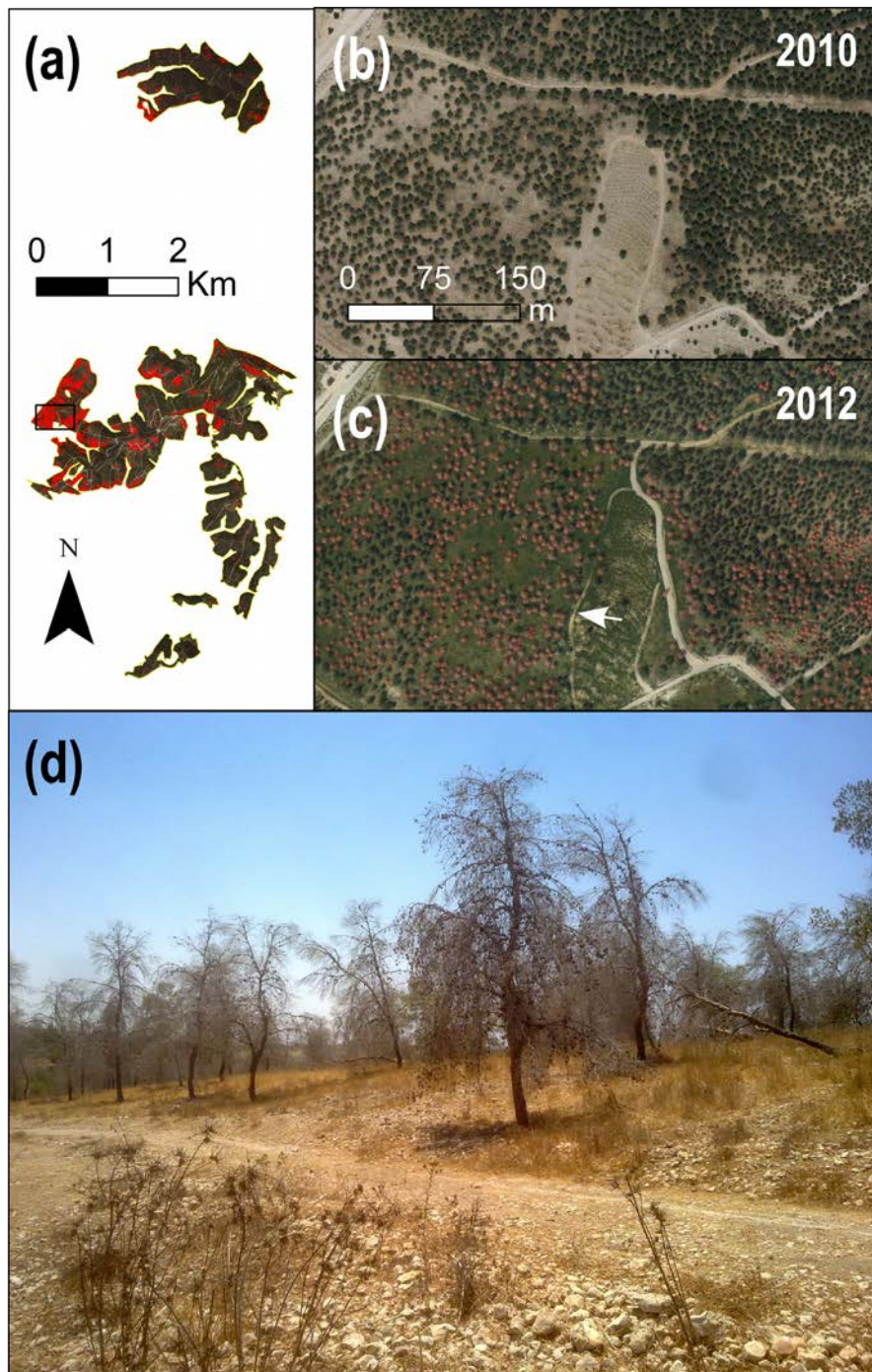


Figure A1 – An example of a high-mortality location in Lahav forest is marked by a black rectangle in (a). Aerial photographs of that area from summer 2010 and winter 2012 are shown in (b) and (c), respectively. Dead trees (distinguishable by their gray/reddish color on the 2012 image) were marked by red circles in (a) and (c). A ground photograph of the location marked by a white arrow in (c) is shown in (d). (Photo: Michael Dorman, summer 2012).

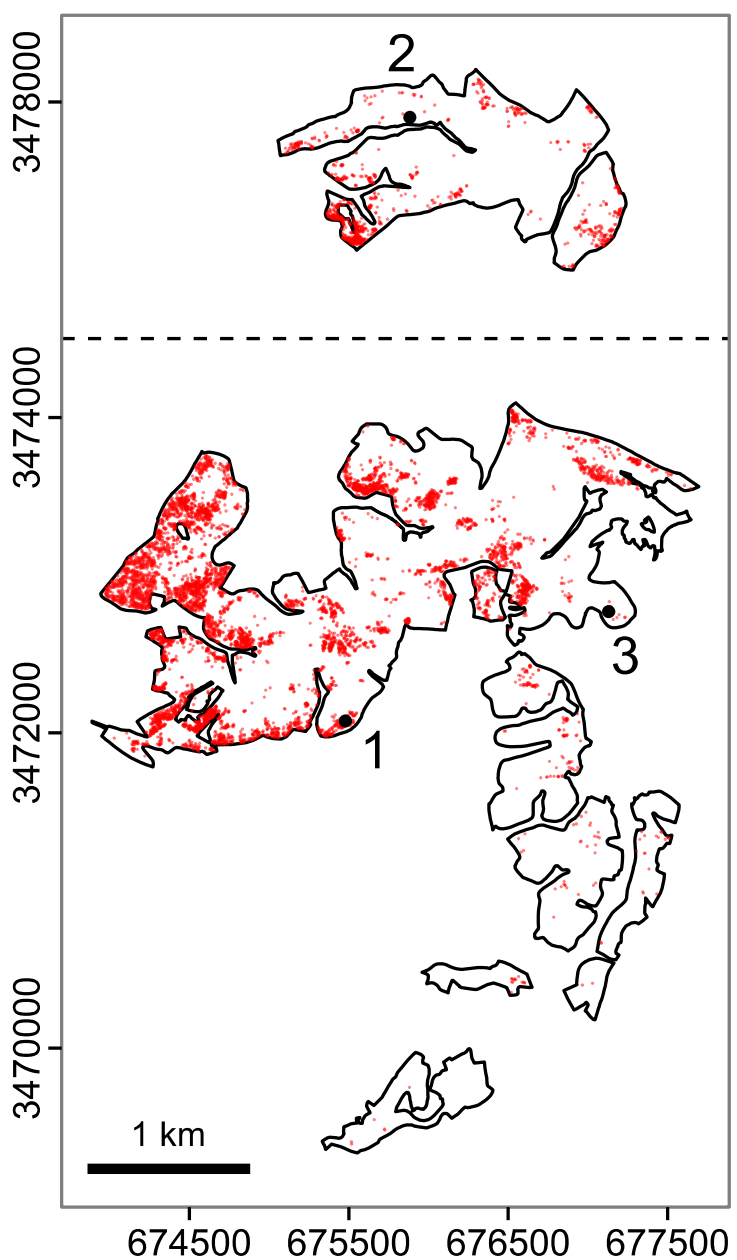


Figure A2 – Dead trees locations in Lahav and Dvira forests. Each dead tree identified on the aerial photograph (see Fig. A1) is marked by a red dot. Sites where dendrochronological sampling took place are marked by numbered (1-3) black dots. Universal Transverse Mercator (UTM) zone 36N coordinates (m) are shown on the axes.

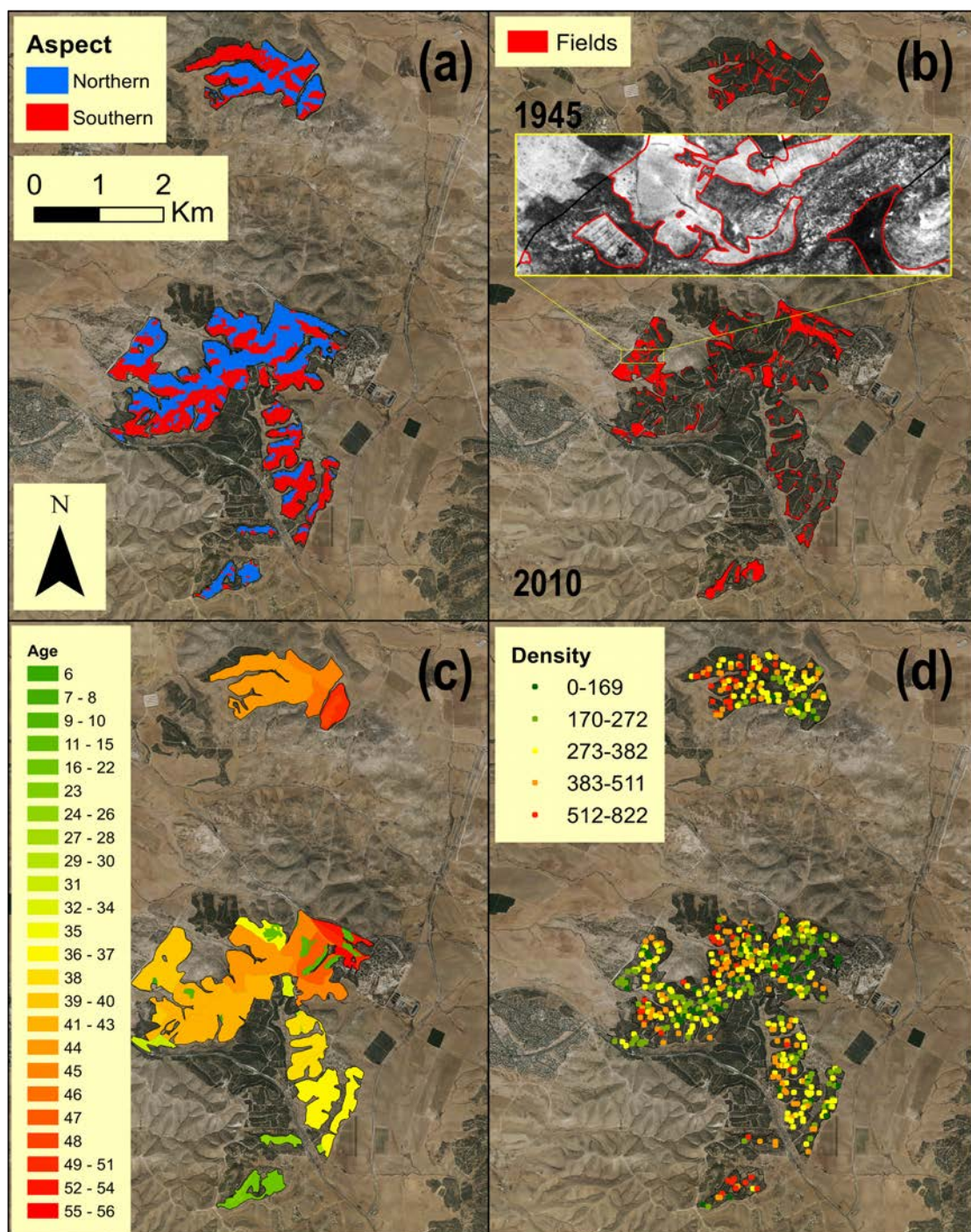


Figure A3 – Environmental conditions in Lahav and Dvira forests: (a) topographic aspect, (b) previously cultivated areas, (c) forest age (in 2012), (d) tree density (trees ha^{-1}). The background is an aerial photograph from 2010.

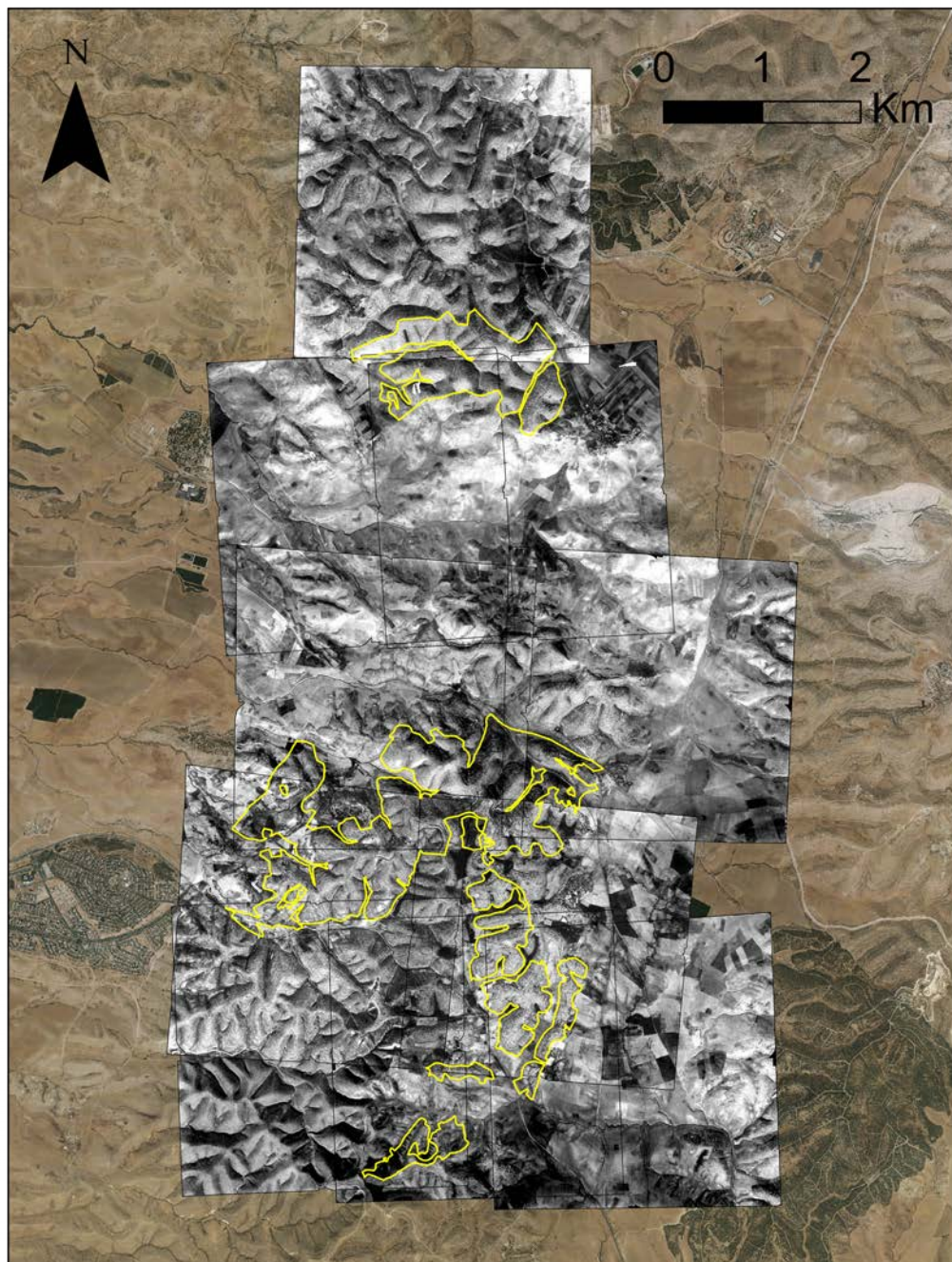


Figure A4 – A mosaic of 10 aerial photographs taken in 1945 (Table A1) used to delineate previously cultivated areas (Fig. A3). The background is an aerial photograph from 2010. The area that is presently (2012) covered by a *Pinus halepensis* planted forest is marked in yellow. Note that no tree cover is visible in 1945, since the first plantings were in 1956; beforehand most of the area was either agriculturally cultivated (where soil depth was sufficient) or grazed.

Appendix B – List of Landsat satellite images and derived NDVI maps

Table B1 – List of Landsat-5 TM (L5 TM) and Landsat-7 ETM+ (L7 ETM+) satellite images used in the study. All images were of the 174/038 (path/row) scene location and had zero cloud cover within the studied area.

Year	Satellite	Date
1994	L5 TM	4.10
1995	L5 TM	7.10
1996	L5 TM	23.9
1997	L5 TM	10.9
1998	L5 TM	15.10
1999	L5 TM	2.10
2000	L5 TM	4.10
2001	L7 ETM+	13.9
2002	-	-
2003	L5 TM	11.9
2004	L5 TM	29.9
2005	L5 TM	16.9
2006	L5 TM	19.9
2007	L5 TM	22.9
2008	L5 TM	8.9
2009	L5 TM	27.9
2010	L5 TM	16.10
2011	L5 TM	17.9
2012	L7 ETM+	27.9

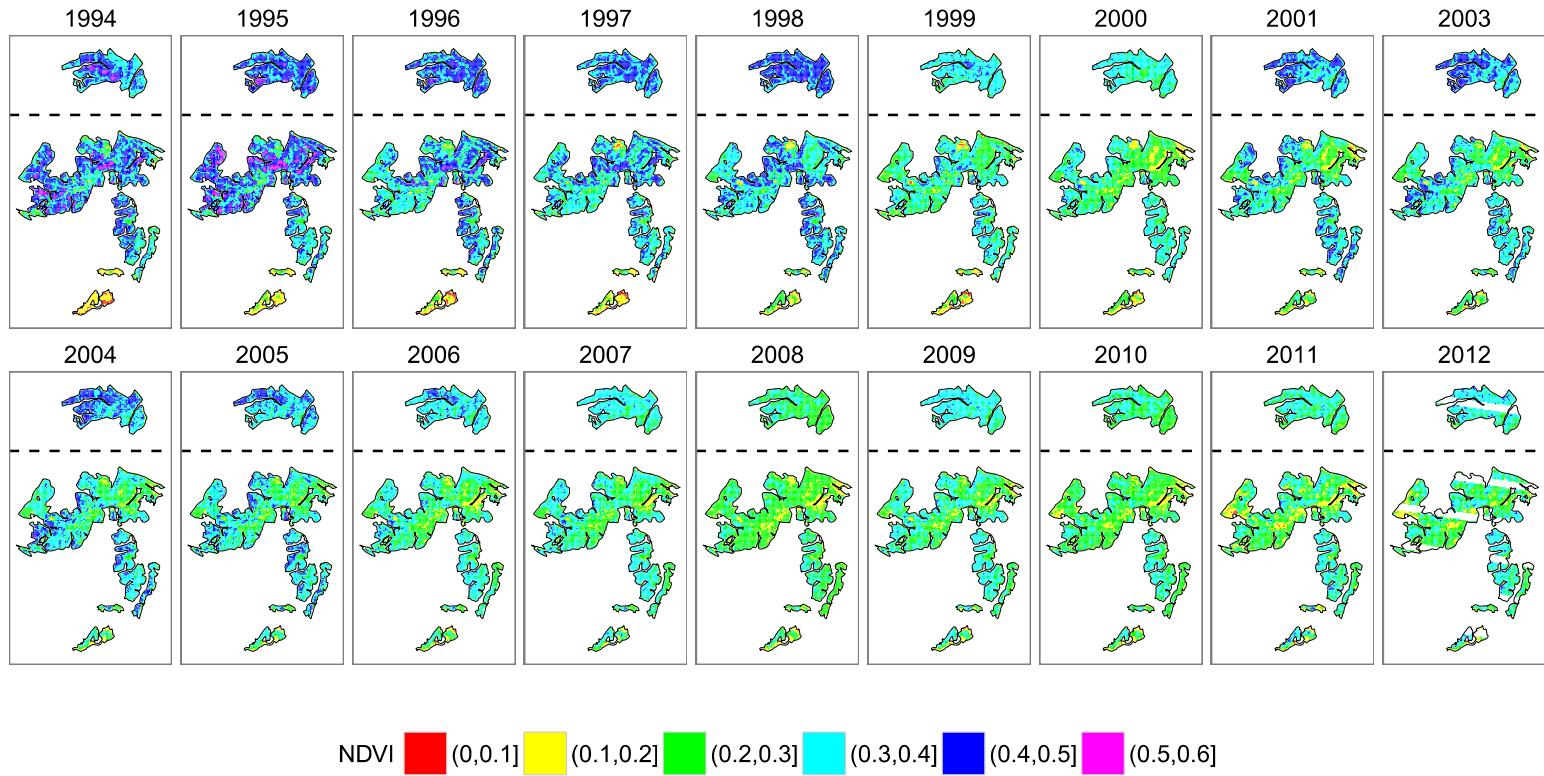


Figure B1 – NDVI in Lahav and Dvira forests in 18 years during the period 1994-2012. Note that an NDVI image for the year 2002 was not available (Table B1). Note that the 2012 image has 22.4% of missing data, due to the Scan Line Corrector (SLC) failure in the Landsat-7 satellite which occurred in 2003.

Appendix C – Structural characteristics of the 3 sites where dendrochronological sampling took place

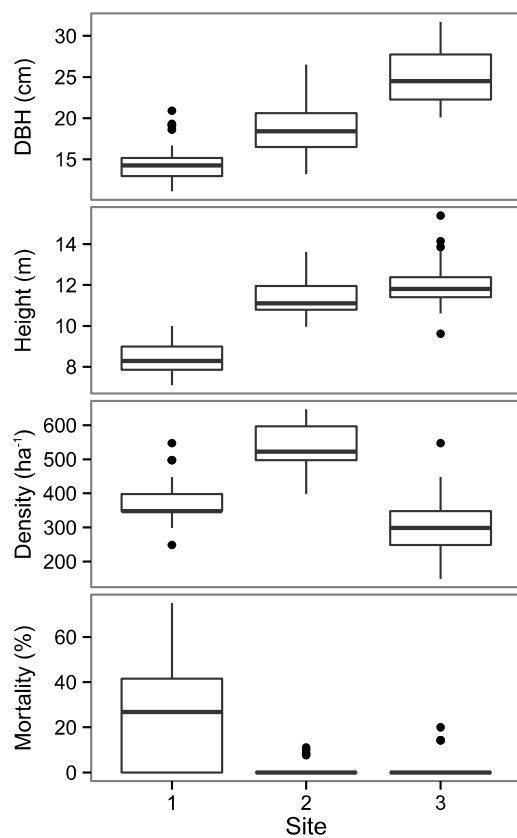


Figure C1 – Tree Diameter at Breast Height (DBH), height, density and mortality in the 3 sites where dendrochronological sampling took place (n=30 in each site). Boxplots show the distribution of observed values among either the sampled trees (DBH, height) or those in the 8-m-radius circles around them (density, mortality). Density measurements express both living and standing dead trees, while mortality measurements express percentage of the dead trees. The upper and lower "hinges" correspond to the 25% and 75% quartiles. The upper whiskers extend from the hinge to the highest value that is within 1.5 of the 25–75% inter-quartile range. Data beyond the end of the whiskers are outliers and plotted as points.

Appendix D – Generalized Linear Mixed-Effects Model of mortality proportion

Table D1 – Estimates, standard errors and P-values for the fixed effects in the final Generalized Linear Model (GLM) describing mortality proportion as function of environmental conditions.

	Estimate	Std. Error	P
Intercept	-4.653	0.614	<0.001
Age	0.041	0.013	0.002
Southern aspect	-0.436	0.813	0.592
Density	-0.025	0.004	<0.001
Deep soil	-3.718	1.308	0.004
Age × Southern aspect	0.035	0.019	0.064
Age × Deeper soil	0.116	0.031	<0.001
Southern aspect × Deeper soil	1.786	0.312	<0.001
Density × Deeper soil	-0.025	0.008	0.001

Appendix E – Correlation between forest responses to the first and second droughts

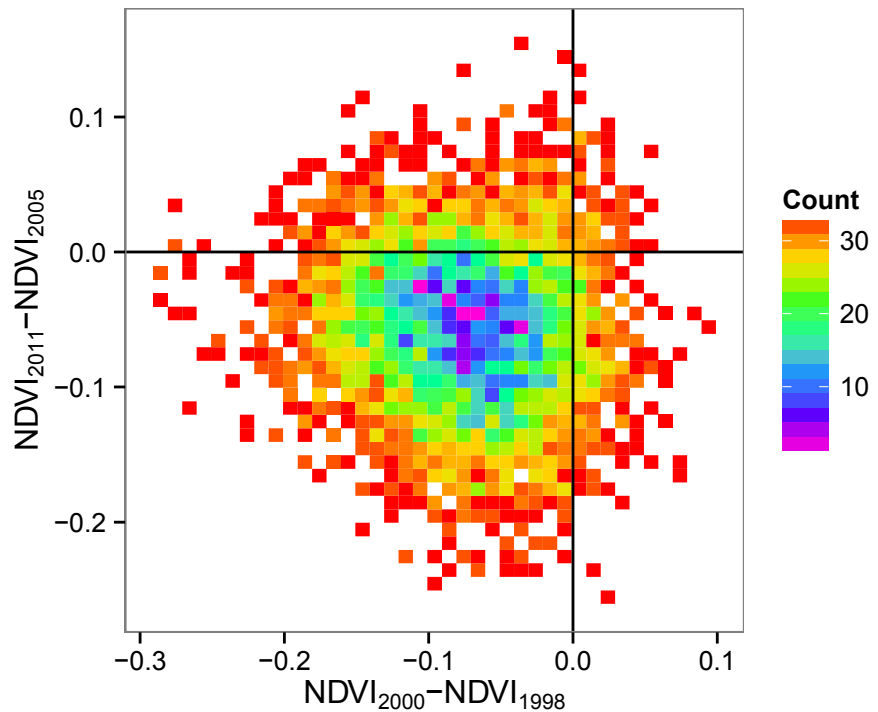


Figure E1 – Correlation between first ($\Delta\text{NDVI}_{\text{first}} = \text{NDVI}_{2000} - \text{NDVI}_{1998}$) and second ($\Delta\text{NDVI}_{\text{second}} = \text{NDVI}_{2011} - \text{NDVI}_{2005}$) drought effects. Colors express the pixels count within a given 0.01×0.01 ΔNDVI combination. A weak negative correlation was found between the effects of both droughts (Pearson correlation coefficient = -0.08 , $p < 0.001$). Note that the correlation coefficient was calculated based on raw data, while aggregation to 0.01×0.01 ΔNDVI combinations is shown for easier interpretation.

Appendix F – Additional details regarding cluster analysis of NDVI spatiotemporal data

Table F1 – Biotic and physical characteristics in four zones within the forest (Fig. 7), obtained by spatiotemporal clustering of NDVI data. Values for age, density and mortality are average \pm one standard error.

Cluster	Proportion (%)	Age (in 2012)	Density (trees ha ⁻¹)	Southern aspect (%)	Deeper soil (%)	Mortality (%)
1	24	40.6 \pm 0.7	329.6 \pm 11.7	47.3	16.1	12.0 \pm 2.0
2	36	41.5 \pm 0.3	372.7 \pm 10.2	61.5	5.3	3.2 \pm 0.7
3	32	42.0 \pm 0.8	283.2 \pm 9.5	51.0	2.6	2.7 \pm 0.7
4	8	29.9 \pm 1.3	420.5 \pm 29.7	51.4	29.7	1.5 \pm 0.6

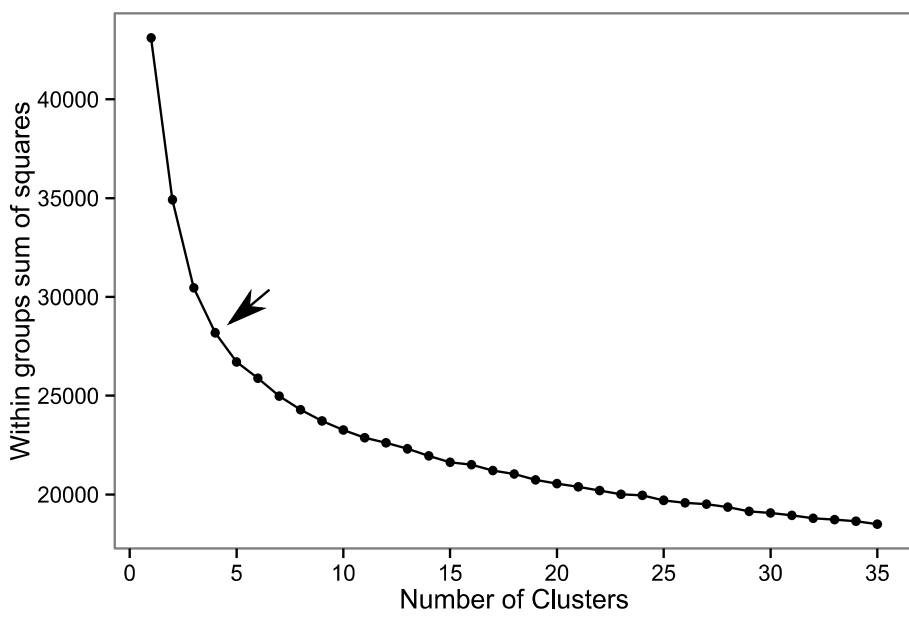


Figure F1 – Within groups' sum of squares as function of number of clusters, in K-means clustering of spatiotemporal NDVI data. The arrow marks the visually determined optimal number of clusters (four), located where the curve starts to bend (i.e. where increasing the number of clusters does not substantially reduce within-cluster variability).

6.5 Additional figures regarding missing tree rings



Figure 2 – Photographs of the last (i.e., closest to bark) ~2.5-cm lengths of 60 cores (from 30 trees) in site S2. Core identification code is composed of a tree number (1–30) and core number ("a" or "b"). The position of the 2011 tree-ring is indicated by a red line; the number above it is the tree-ring width (TRW; mm). Cases where TRW was not available because of undetermined ring position are marked "NA".

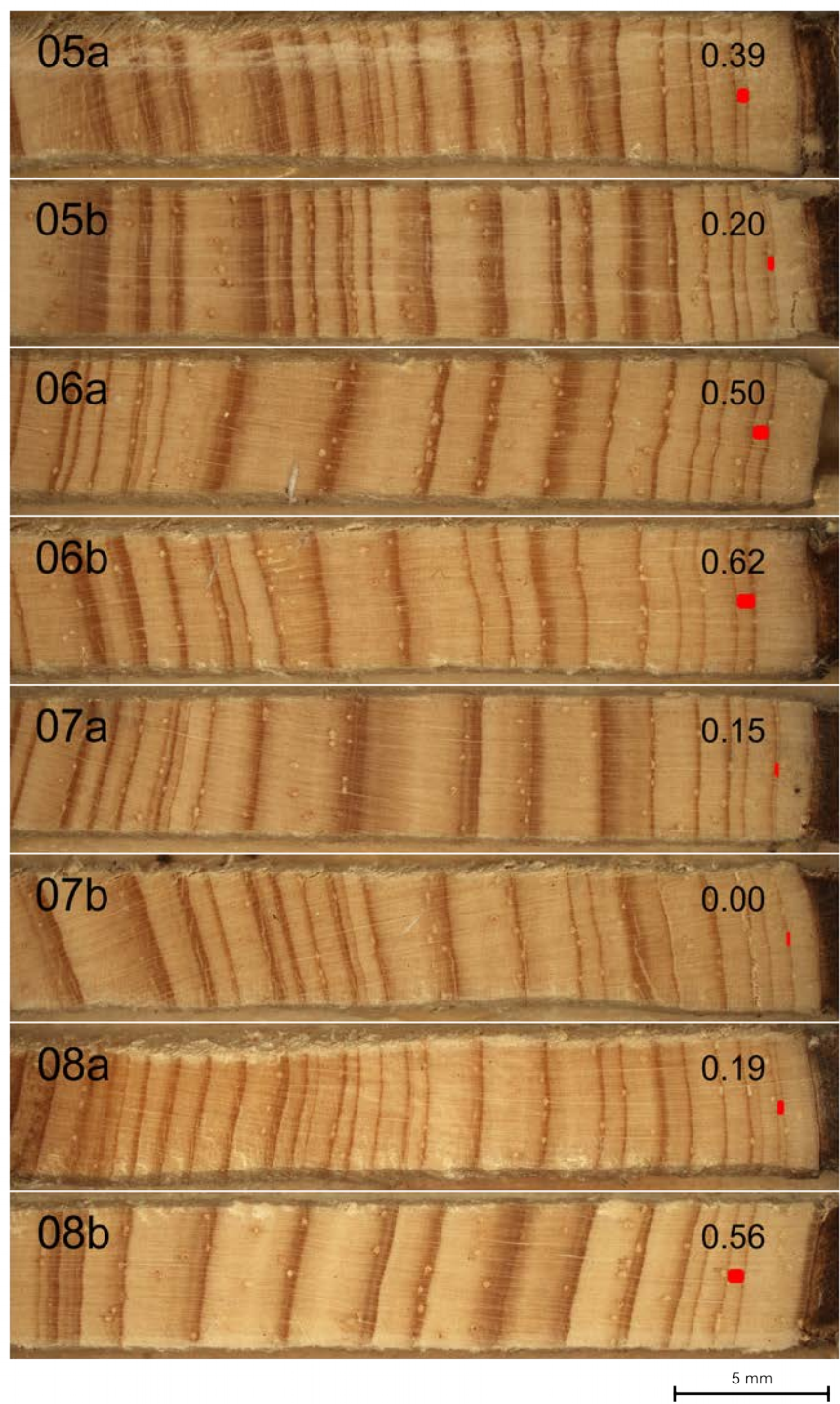


Figure 2 (continued).

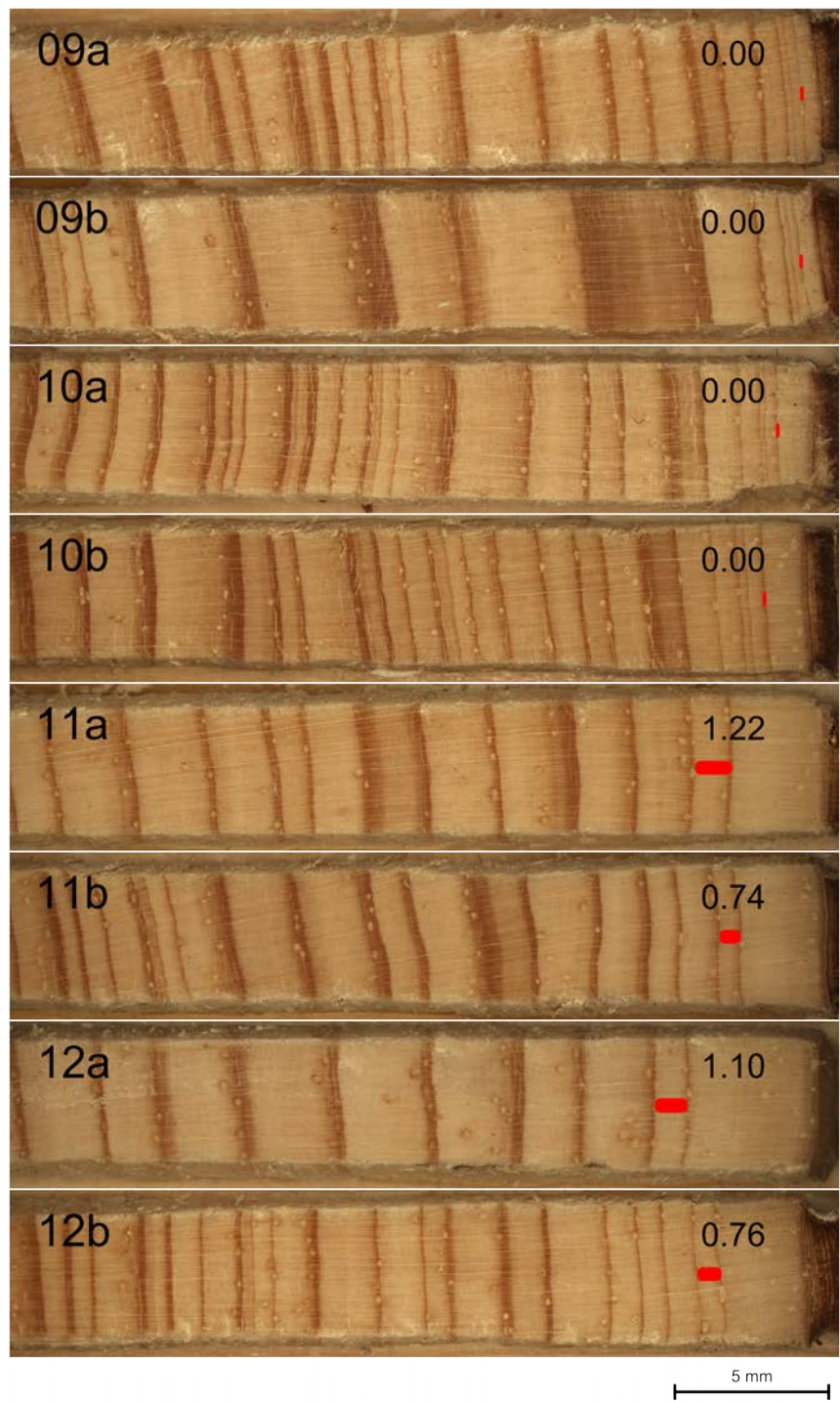


Figure 2 (continued).

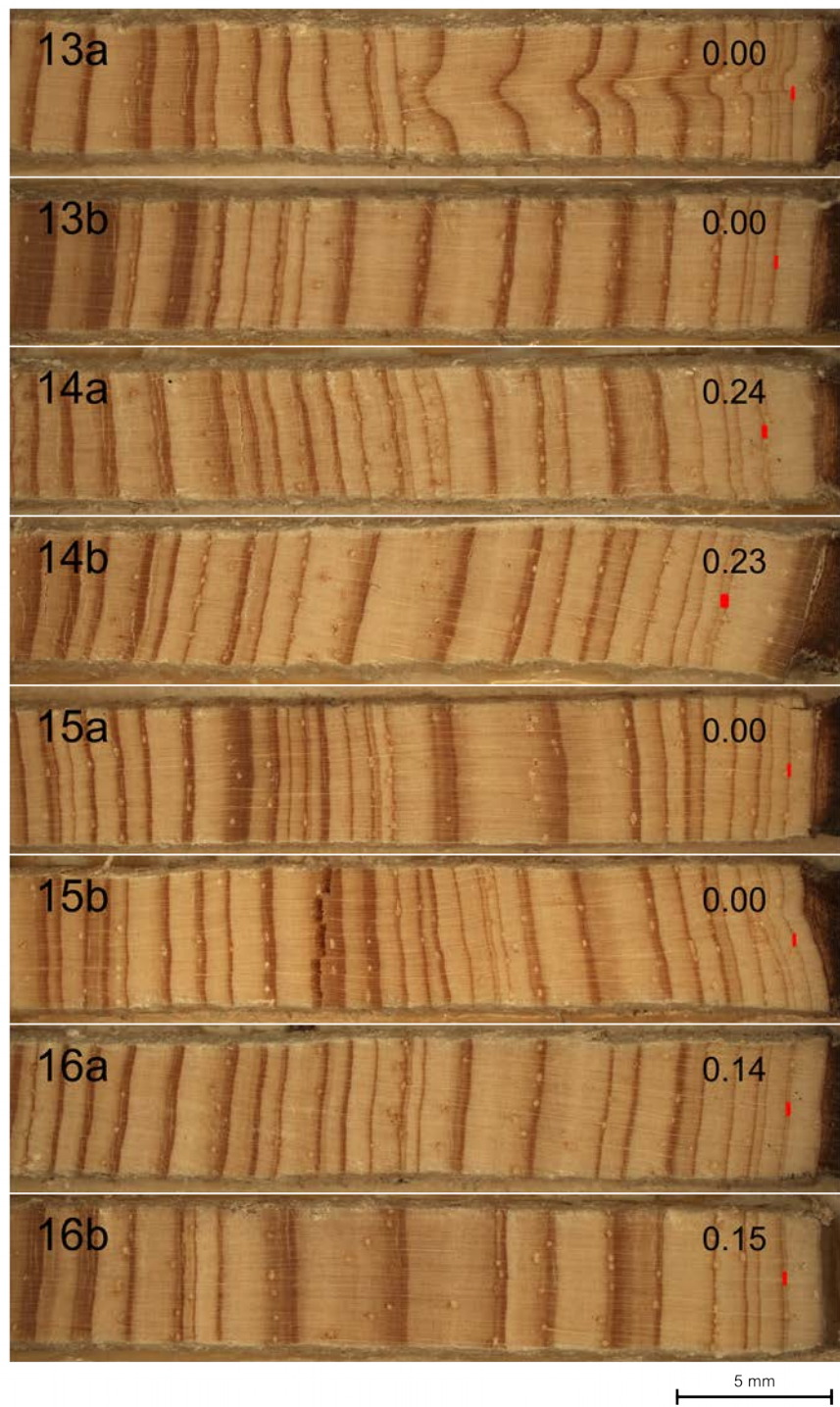


Figure 2 (continued).

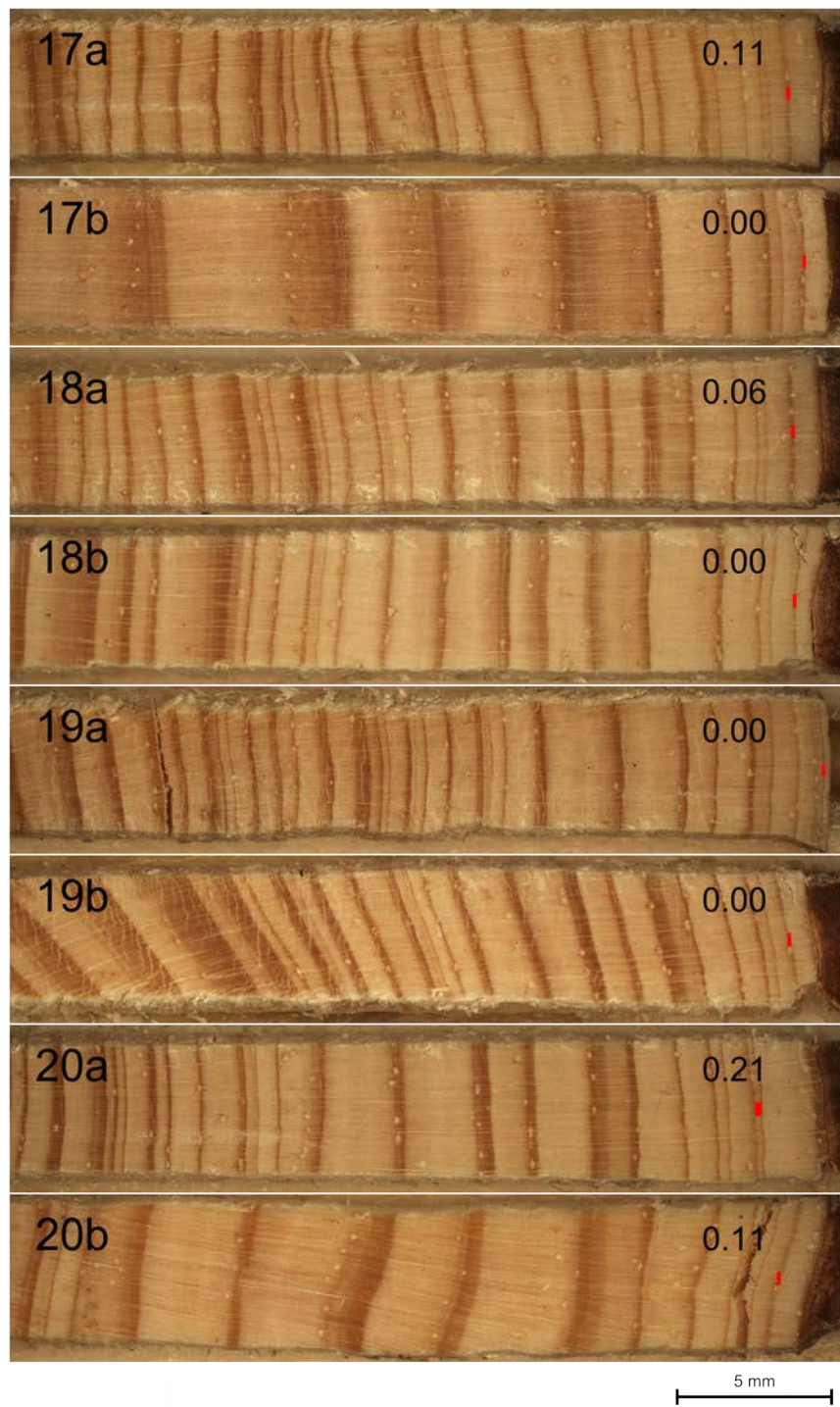


Figure 2 (continued).

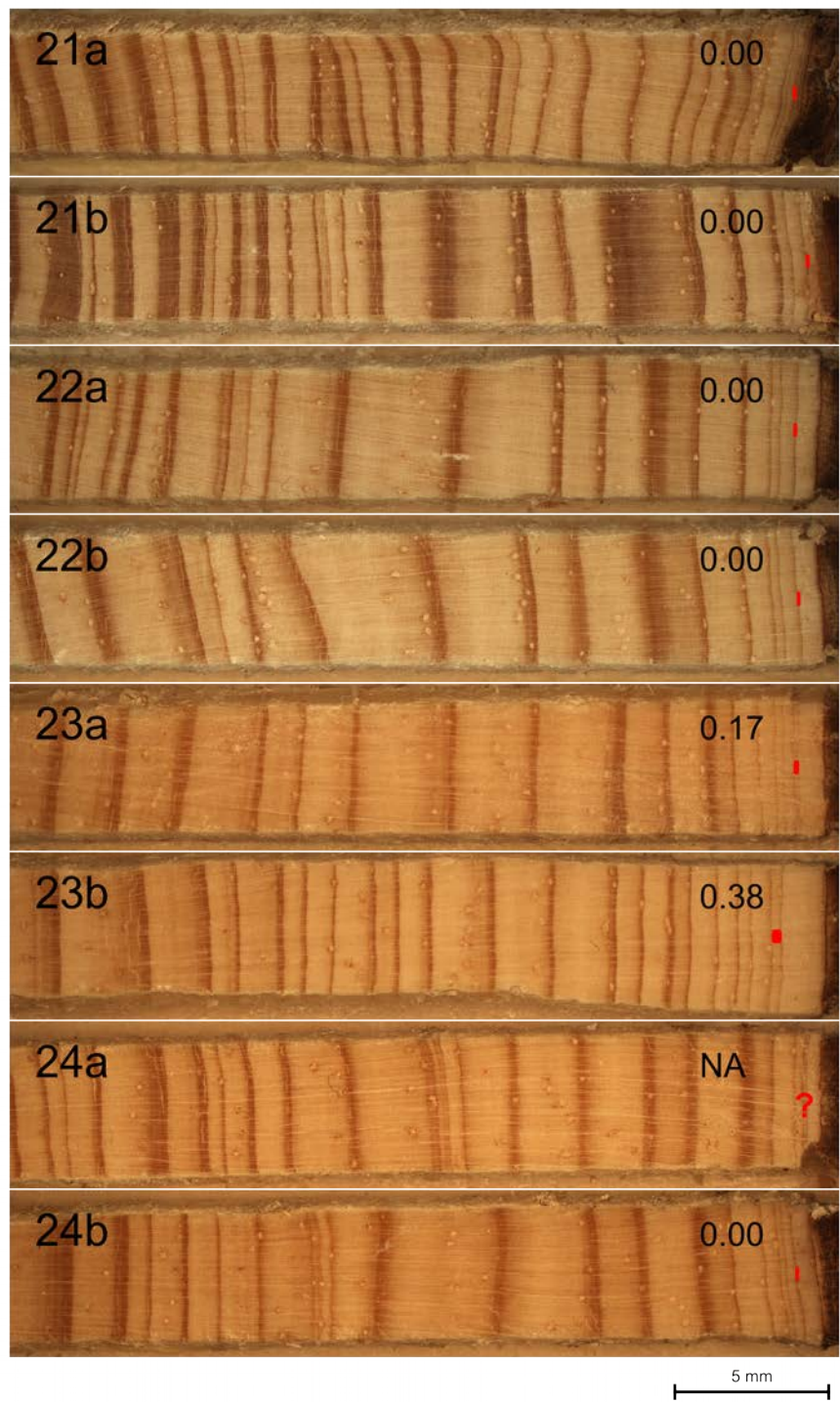


Figure 2 (continued).

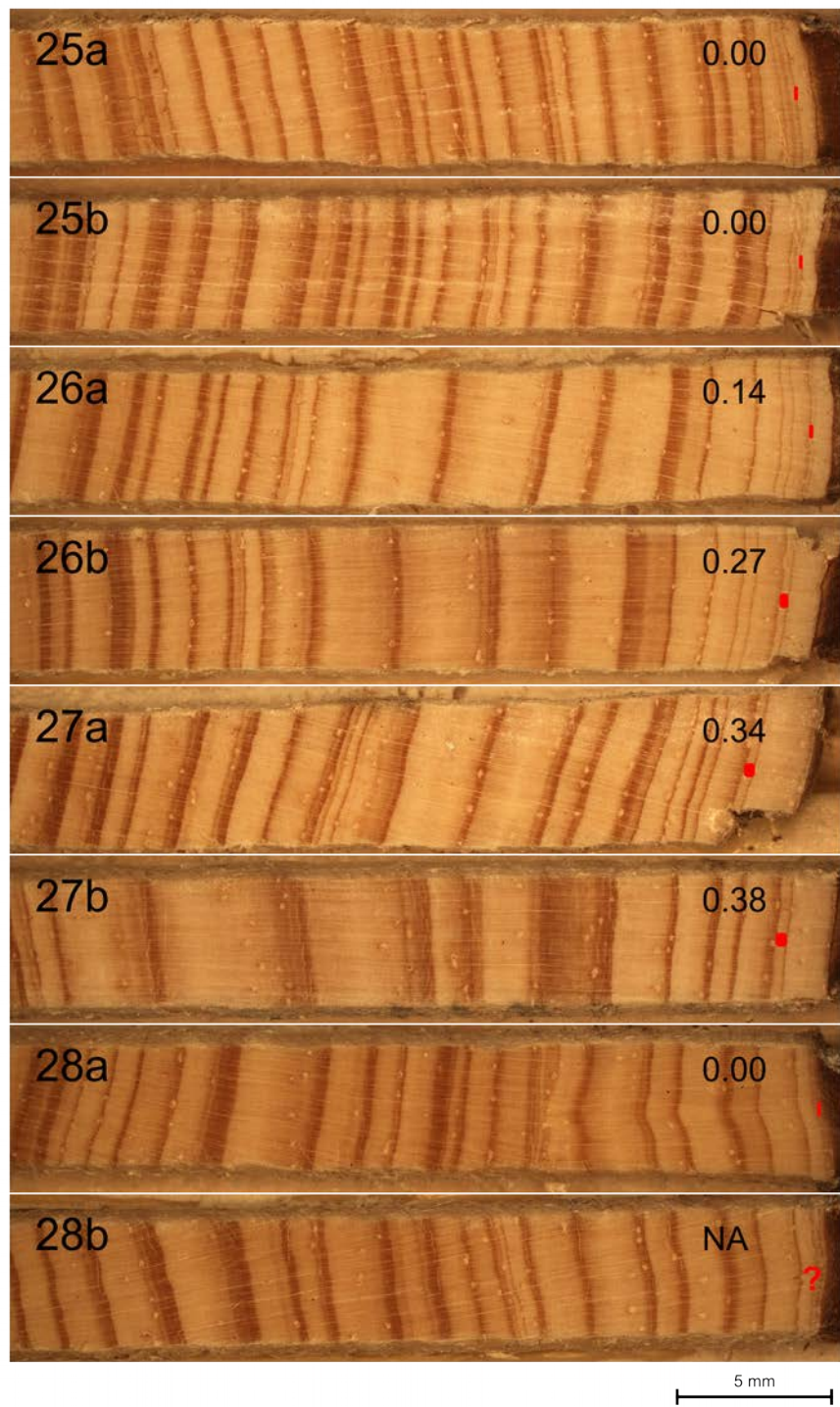


Figure 2 (continued).

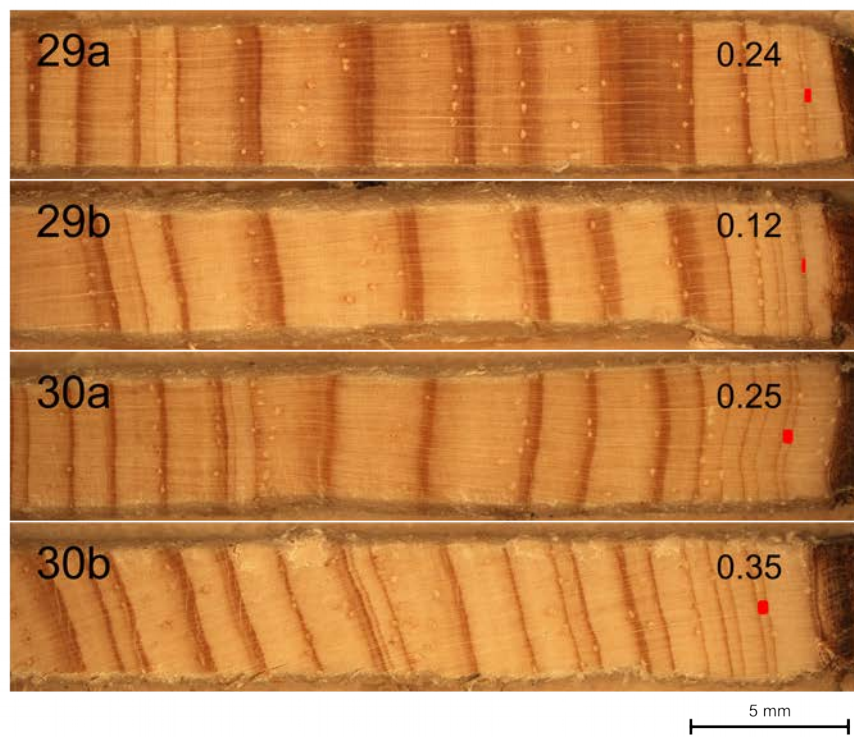


Figure 2 (continued).

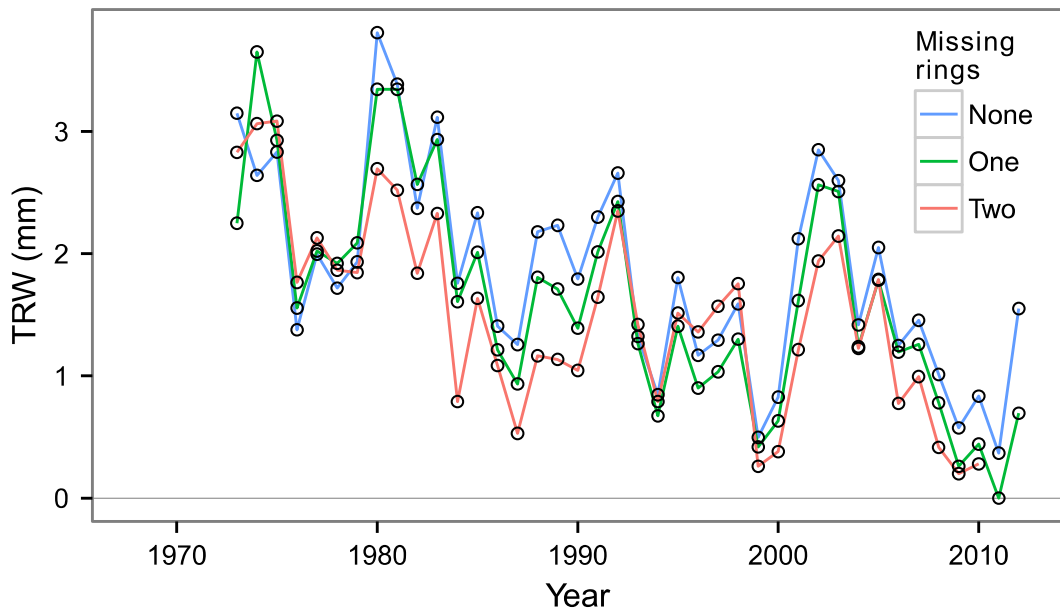


Figure 3 – Average tree-ring width (TRW) as function of year in site S2. There were three groups of cores: no missing rings ($n = 37$); one missing ring ($n = 21$); and two missing rings ($n = 2$). All individual missing rings were identified as referring to 2011 (Figure 2); they were interpolated by adding zero growth (0 mm) in the corresponding position, which resulted in perfect matching of the chronologies. In the two cores from which two rings were missing, the positions could not be unambiguously resolved, although, in light of this figure it is likely that they occurred in two out of the last three years of measurements (2010–2012).

תמותה כתוצאה מיובש בিירות נטוועים של ארון

ירושלים: מחקר מרובה קני מידה

**מחקר לשם מילוי חלקו של הדרישות לקבלת תואר "דוקטור
לפילוסופיה"**

מאთ

邁可爾·多爾曼

הוגש לסינאט אוניברסיטה בן גוריון בנגב

11/11/14

י"ח חשוון תשע"ה

באר שבע

תמותה כתוצאה מיובש בিירות נטוועים של ארון ירושלים: מחקר מרובה קני מידת

**מחקר לשם מילוי חלקו של הדרישות לקבלת תואר "דוקטור
לפילוסופיה"**

מאთ

מייכאל דורמן

הוגש לסינאט אוניברסיטה בן גוריון בנגב

11/11/14

י"ח חשוון תשע"ה

באר שבע

תמותה כתוצאה מיובש בিירות נטוועים של ארון

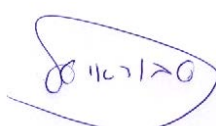
ירושלים: מחקר מרובה קני מידת

**מחקר לשם מילוי חלקו של הדרישות לקבלת תואר "דוקטור
לפילוסופיה"**

מאת

邁克爾 דורמן

הוגש לסינאט אוניברסיטה בן גוריון בנגב



אישור המנהחים

אישור דיקן בית הספר ללימודים מחקר מתקדמים

11/11/14

י"ח חשוון תשע"ה

באר שבע

העבודה נעשתה בהדרכת:

פרופ' טל סבורי ופרופ' אבי פרבולוצקי

במחלקה לגיאוגרפיה ופיתוח סביבתי,

הפקולטה למדעי הרוח והחברה

תקציר

מבוא

מערכות יער מתפקדות תחת תנאי עקה גוברים כתוצאה משינוי אקלים גלובליים אשר עשויים להוביל לתמונות יער בהיקף נרחב. אף עם פי כו, גורמים הקובעים מתי והיכן יתרחשו אירועי תמותה אינם מובנים דיימ. לדוגמה, ההיבטים הבאים של תגובה יער לבצורת שירותים באירועים משמעותית:

1. תגובה לבצורות חוזרות ונשנות לאורך גרדיאנט אקלימי
2. קני-מידה עיתתיים של השפעת שונות אקלימית על קצב גידול העץ, והשינוי המרחבית-עתיתם שלהם בהתייחס לתנאי איזון מים
3. השפעות סביבתיות מקומיות, בפרט של עצמת תחרות, על קצב גידול העצים וסיכון תמותה

תצלויות נוספות, אם כן, נחוצות על מנת לתעד אירועי הידדרות בתפקיד העיר, להבין את הגורמים להם, ולפתח תכניות ממשק בר-קיימא. מכשול מרכזי בפני השגת מטרות אלה הוא העובדה שתמונות עצים הינה לרוב בעלי דפוס כתמי על-פני מספר קני מידת מרחבים ומאופיינת בדינמיקה עיתתית ארכט-טוחה. המחקר בתחום נדרש לשלב שיטות ומקורות מידע מגוונים, מספר דיסציפלינות מדעיות, על-מנת לתפות דפוסים אינפורטטיביים רלוונטיים רבים ככל הנitin, אולם עד כה הדבר נעשה לעיתים רוחוקות בלבד.

ההידוש של המחקר הנוכחי, לעומת זאת, מתקנים קודמים, הנ שוני מישורים עיקריים.ראשית, היירות הנחקרים (יערות טבעיים של אורן ירושלים – *Pinus halepensis* – בישראל) פרושים על-פני גרדיאנט אקלימי רחב, אולם מהווים מערכת אקוולוגית הומוגנית יחסית, מעשה ידי אדם (יערות חד-מינים וחד-גילאים), מצב אשר למעשה מיצמצם את השפעת הרכב המינים של העיר על תגובה לבצורת וمبודד את השפעת הגרדיינט האקלימי. בנוסף, היירות חוו לאחרונה רצף חסר תקדים של אירועי בצורת, ותמונות עציםמשמעותית כתוצאה לכך. שנית, גישה מרובת-פרשפטיות ננקטה על מנת לחתם מבט מקיף יותר של הדפוסים הקשורים בפגיעה הבצורת בעיר. ביצועי העיר נצפו סימולטנית בשלהי קני מידת נפרדים, על-ידי שילוב של: (1) סדרות זמן של נקודתי של מיקום עצים מתים, מתצלום אוויר ברזולציה גבוהה; ו-(2) סדרת זמן של תוספת שטח עצה (BAI), מניתוח דגימות של טבעות עצים.

שיטות

בקנה מידת אזורי, סדרות זמן של נתוני כמות משקעים שעברו אינטראפלציה מרחבית ונתוני חישה מרוחק שימשו להערכת התנאים הסביבתיים אליהם חשופים היערות ותגבותיהם לתנאים אלה, בהתאם. מצב חוף היער הוערך בעזרת נתוני NDVI, אשר התקבלו מהדמאות לויאין Landsat לתקופה 1994-2011. על מנת להרחיב את הפרספקטיב של המחקר, ביצועי היער נדגוו לכל אורך הגראדיאנט האקלימי ביערות נטוועים של אורה ירושלים בישראל (~250 עד ~750 מ"מ כמות משקעים سنوية ממוצעת). כמו כן, בעזרת נתוני מיפוי טופוגרפי נחקרה האינטראקטיה בין השפעת גורמי סביבה מקומיים ואזוריים בהשפעתם על ביצועי יער בעת בוצרת.

על מנת להעריך את המאפיינים העיתויים של השפעת תנאים אקלימים על קצב גידול העץ, כמו גם את ההשפעה המוסחת של תחרות בין עצים שכנים על תגובה לבוצרת,TeVות עצים נדגוו בשלושה אזורים לאורך הגראדיאנט האקלימי (~300, ~500 ו-~700 מ"מ). מהלכי קצב גידול אזוריים נבנו, ונבחנו בהתאם לנוטונים אקלימיים מפורטים עבור התקופה 1983-2012. בנוסף, עוצמת תחרות הוערכה לכל אחד מהעצים במדגם, על מנת לבחון את ההשפעה המוסחת של תחרות על הירידה בקצב הגדלוב בזמן בוצרת (2011) וההתאוששות שלאחר מכן (2012).

בקנה מידת מקומי, הערכה של תמותת עצים, והגורמיים המשפיעים עליה, בוצעה בשני יענות אורה ירושלים מייצגים מסביבה צחי-צחיחה (~300 מ"מ). דפוס נקודתי ממוקף של עצים מותים התקבל מפענוח של צילום אווריר ברזולוציה גבוהה משנת 2012, בעוד שתנאי הסביבה אופינו באופן מפורש מבחינה מרחבית בעזרת שרגג גבהים דיגיטלי – DEM, צילומי אווריר היסטוריים ונתונים של קק"ל. נתוני NDVI מלויאין Landsat לתקופה 1994-2012 ונתוני קצב גידול מדיגוםTeVות עצים שימושו כמקורות מידע משלימים בניתוח זה.

תוצאות

שאלות המחקר העיקריות והפתרונות המתיחסות לכל שאלה, בהתאם, מפורטים להלן:

1. כיצד ביצועי היער הגיבו לשתי תקופות בוצרת עוקבות לאורך הגראדיאנט האקלימי

(פרק 3.1): שלושה סוגים תגובה הוגדרו:

1. ביצועים יציבים עם קוולציה נמוכה לדפוס המשקעים באזור החל (מעל 500 מ"מ)

2. ירידת מתונה בביצועים עם קוולציה גבוהה לכמות משקעים באזור האמצעי (~350-500 מ"מ)

3. ירידת חדה בביצועים עם קוולציה גבוהה לכמות משקעים באזור היבש (~350 מ"מ)

- .2. האם התגובה לבצורת השניה נבדלה מהתגובה לבצורת הראשונה, ובאיזה אופן הבדלים השתנו לאורך הגדריאנט האקלימי (פרק 3.1)? ? תגובת היערות לבצורת הראשונה הייתה שלילית באופן הומוגני לאורך הגדריאנט האקלימי. התגובה לבצורת השנייה נבדלה בין האזוריים, והייתה שלילית באזוריים היבש והאמצעי (מתחת ל-500 מ"מ) וקרובה לאפס באזורי הלח.
- .3. כיצד כמות המשקעים השנתית השפיעה על ההבדל בביטויים בין מפנים צפוניים ודרומיים בשנה נתונה, וכייזד השפעה זו משתנה לאורך הגדריאנט האקלימי (פרק 3.2)? השפעת המפנה על ביצועי העיר נמצאה בהתאם, באופן לינארי, עם כמות המשקעים באזורי היבש (השפעה חזקה יותר של מפנה בשנים גשומות), אבל לא באזוריים האמצעיים והמלח.
- .4. כיצד פרק הזמן של תנאי אקלים אליו העצים מגיבים באופן מרבי משתנה למרחב, ככלומר באזוריים שונים לאורך הגדריאנט האקלימי, ובזמן, ככלומר בתקופה לחיה חסית לעומת תקופה יבשה מאוד (פרק 3.3)? קנה מידת המשפעו ביותר של כמות משקעים על קצב גידול היה שנתי בתנאים יבשים (מתחת ל-500 מ"מ) הן בזמן והן למרחב, ורובה שנתי בתנאים לחים יותר.
- .5. באיזו מידת תחרות בין עצים שכנים מוסתת את הרידת בקצב גידול כתוצאהה מבצורת ואת התואשותה בשנה גשומה לאחר מכון, והאם השפעות אלה משתנות לאורך הגדריאנט האקלימי (פרק 3.3)? לא נמצא הבדל מהותי באופי השפעת התחרות בין האזוריים. נראה שעוצמת תחרות קובעת את הסף העליון של קצב הגדל, ולמן השונות בקצב גידול בין עצים גדלה ככל שעוצמת התחרות פוחתת.
- .6. מהו הדפוס המרחבי של העצים המתים בעקבות ביצות חריפה (מקובץ, אקראי, רגולרי) (פרק 3.4)? הדפוס המרחבי של עצים מתים היה מוקבץ לאורך כל טווח קני מידת המרחביים.
- .7. כיצד גורמי סבירה ביוטית (גיל, צפיפות) ואביוטית (مفנה, עומק קרקע) משפיעים על סיכוי תמותת העצים (פרק 3.4)? תמותה רבה יותר, באופן מובהק, נפתחה בגלaliasים מבודדים, צפיפות נמוכה, מפנים דרומיים וקרקעות עמוקות. יחד עם זאת, לא ניתן היה לחזות באופן מלא את מקום כתמי התמותה בתוך אורי "סיכון גבוה" בעורת הגורמים הסביבתיים שנבדקו.
- .8. באיזה אופן השטח המיעור מתחלק לאזוריים נבדלים של מהלך ביצועים ייחודי בעבר? האם אזוריים אלה נמצאים בהתאם עם גורמים סביבתיים ועם אחוז תמותת עצים (פרק 3.4)? שני אזוריים נפרדים של העיר הושפעו במהלך שתי תקופות בצורת אחרונות. יחד עם זאת, הבדלים בין אזוריים בעלי מהלך ביצועים ייחודי בעבר ייחסו באופן חלקו בלבד להבדלים בתנאים הפיזיים והביוטיים באותו האזוריים.

הרגישות הגבוהה ביותר לבוצרת נפתחה ביערות אשר נמצאים בחלקו היבש של הגראדיאנט האקלימי הנחקר (מתחת ל-350 מ"מ). בנוסף לירידה בכמות ביומסה ירוכה ותמותה ממשמעותית, נפתחה תוגבה מידית (באותה שנה) וחזקה (90% של השונות בקצב גידול מוסברת על-ידי כמות משקעים) של העצים לכמות המשקעים הפחותה. דפוס זה מצביע על העדר "בופר", מבחינת מים זמינים עבור העצים, בתנאים יבשים כגון אלה. תוצאה זו נמצאת בהתאם עם מחקרים קודמים שנערכו באזורה, אשר הראו ש מרבית כמות המשקעים השנתית אובדת לאטמוספירה במהלך אותה השנה, מה שככל הנראה מביא לפוטנציאל מוגבל מאוד של מים זמינים המועברים משנה לשנה, בקני מידה רב-שנתיתם.

התוגבה המתונה לבוצרת חלק החלק של הגראדיאנט האקלימי, כמו גם המתואם החלש יותר, המתקיים בקני מידה ארוכים יותר, בין קצב גידול העצים לבין כמות המשקעים, מצביעים על כך שהרגישות של יערות אורך ירושלים לבוצרת באזורה זה נמוכה יחסית. "התפלגות" בתוגבות היערות לבוצרת נפתחה, אם כן, לאורך הגראדיאנט האקלימי, הן מבחינת מגמה ארוכת-טוח של כמות ביומסה ירוכה (מתחת ל-540 מ"מ – ירידה ; מעל 540 מ"מ – עלייה) והן מבחינת קנה המידה העיתוי של התוגבה הדומיננטית לשונות בכמות המשקעים (מתחת ל-500 מ"מ – שנתי ; מעל 500 מ"מ – רב-שנתי). ספירים אלו תוחמים את אזור המעבר שמדרומים לו יערות אורך ירושלים נטוועים ככל הנראה אינם בריא-קיימה, בהינתן התנאים האקלימיים והמשק שהיערות חוו במהלך 1983-2012.

בקנה מידה מקומי, תמותה רבה יותר נפתחה תחת תנאי סביבה יבשים יחסית (מפנים דרומיים) במקביל לדרישה גבוהה יותר למים (עצים בגיל מבוגר). כמו כן הוגם כי למרות ההומוגניות הרבה יותר בביצועי עיר בעת בוצרת, עצים אשר נמצאים בבתי גידול יבשים יחסית, באופן מקומי, בכל זאת מגיעים לרמת ביצועים נמוכות יותר באופן מוחלט (וחווים סיכון תמורה גבוהים יותר). נמצא זה תומך בהתנגדות לא-lienaria (כלומר, תלויות-סף) של תמותה עצים. באופן המנוגד לאינטואיציה, קרקיוטות עמוקות זוהו כגורם סיכון לתמורה כתוצאה מבוצרת. הסיבה לכך היא שבזמן עקט יושב ממושכת קרקע عمוקה מביאה ככל הנראה לגישה מוגבלת של מערכת השורשים לשכבות הסלע, היכן שלוחות קרקע שיורית עשויה לתמוך בהישרדות העצים לאחר שפרופיל הקרקע כולו התיבש. בנוסף, לעוצמת תחרות לא הייתה השפעה שלילית על הישרדות העצים ועל קצב הגידול של עצים נוחות. תוצאה זו, בצירוף דפוס התמורה הכתמי במרחב, מצביעים על כך שתהליכי שmagvirim את עצם עשויים לשחק תפקיד משמעותי ממשמעותם בתמורה עצים ומטיילים ספק בדעת הרוחות שدليل העיר עשוי בהכרח להפחית את סיכון התמורה.

עבודת דוקטורט זו הדגימה שימוש של מספר מקורות מידע (חישה מרוחק מלווין, צילום אוויר וניטוח טבעות עצים) יכול להביא להבנה שלמה יותר של השונות המרחבית-עיתית בזקי בוצרת ליערות. בעוד המשקנות הנbowות מהשיטות השונות נמצאו באופן כללי בהסכמה, ההבדלים היו קשורים באופן אינפורטטיבי לרמות הארגון השונות שכל שיטה מתאפישת אליהן, מה שהופך

את השיטות למשלים זו את זו. לדוגמה, ניתוח טבעות עצים מתייחס לחלק קטן של האוכלוסייה אשר זמין לדיגום, ובכך בפוטנציה מעריך יתר על המידה את הגמישות (resilience), בעוד שחייב מרוחוק מלוויין עשויה לקבץ את אותות החזר של "חלקים" גדולים מחופת העיר, מה ש מגביל את השיווק של ירידה בתפקיד העיר לתהליכי דמוגרפיים (כגון תמותה) או מבנים (כגון נסירת עליים). لكن מוצע שהערכה של גמישות מערכות יער בתגובה לבצורת צרייכים בסופו של דבר להתבסס על אינטגרציה של מספר מודדים, שככל אחד מהם מתאים לזהות מגמות שינוי ברמות ארגון שונות.